DEVELOPMENT AND APPLICATION OF DROUGHT FORECASTING MODELS FOR NIGERIA SUDANO SAHELIAN REGION

BY

Babatunde Korode ADEOGUN

Department of Water Res. and Envtal. Engineering
Faculty of Engineering
Ahmadu Bello University, Zaria Nigeria

SEPTEMBER, 2014

DEVELOPMENT AND APPLICATION OF DROUGHT FORECASTING MODELS FOR NIGERIA SUDANO SAHELIAN REGION

BY

Babatunde Korode ADEOGUN
B.Sc, (UNAAB); MSc., (ABU)
Ph.D./ENG/00605/2008-2009

A DISSERTATION SUBMITTED TO THE SCHOOL OF POSTGRUADUATE STUDIES, AHMADU BELLO UNIVERSITY, ZARIA

IN PARTIAL FULFILMENT OF THE REQUIREMENTS FOR THE AWARD

OF

DOCTOR OF PHILOSOPHY DEGREE IN WATER RESOURCES AND ENVIRONMENTAL ENGINEERING

DEPARTMENT OF WATER RESOURCES AND ENVIRONMENTAL ENGINEERING, FACULTY OF ENGINEERING,
AHMADU BELLO UNIVERSITY, ZARIA

NIGERIA

SEPTEMBER, 2014

DECLARATION

I declare that this dissertation entitled "Development and Application of Drought Forecasting Models for Nigeria Sudano Sahelian Region" is a result of my original work carried out by me in the Department of Water Resources and Environmental Engineering, Ahmadu Bello University, Zaria, under the supervision of Dr J. A Otun, Dr. A Ismail and Prof. C A Okuofu.

The information derived from the literature has been duly acknowledged in the text and a list of references provided. No part of this thesis was previously presented for another degree or diploma at this or any other university.

ADEOGUN, Babatunde Korode	_____	_____
Name of student	Signature	Date

CERTIFICATION

This dissertation entitled "Development and Application of Drought Forecasting Models for Nigeria Sudano Sahelian Region" by ADEOGUN, Babatunde Korode meets the regulations governing the award of the degree of Doctor of Philosophy (Ph.D) of Ahmadu Bello University, Zaria, and is approved for its contribution to knowledge and literary presentation.

Chairman, Supervisory committee Dr J. A. Otun	Signature	Date
Member, Supervisory committee Dr A. Ismail	Signature	Date
Member, supervisory committee Prof C.A. Okuofu	Signature	Date
Head of Department Dr D.B. Adie	Signature	Date
Dean, Postgraduate School Prof. A.A. Joshua	Signature	Date

DEDICATION

I dedicate this research work to the memory of my late mother, Mrs. Winifred Gbeyinsola Adeogun, who longed for an accomplishment like this. However, like our Lord's Prayer: Thy wish be done on earth. Glory be to God in heaven.

ACKNOWLEDGMENTS

I thank Almighty God for the favour, gift of life and grace to be able to start and complete this course of study. I wish to acknowledge the support and counsels of my supervisors; Dr. J. A. Otun, Dr Abubakar Ismail and Prof. C.A. Okuofu for the wealth of knowledge I enjoyed from you all , I place my appreciation on record.

I wish to profoundly thank Dr. D.B. Adie, Head of Department, Water Resources and Environmental Engineering, ABU Zaria, for his valuable constructive contribution to the work. I appreciate valuable suggestions of Dr. M.A Ajibike and also, I would not forget the efforts of my colleagues: Dr. S.B. Igboro, Dr. (Mrs) F.B. Ibrahim, Engr. S.A. Abudullahi and Engr. Ismail Sanni, who had given their expertise at one point or the other during the period of investigation. I would like to express my gratitude to all the staff of Water Resources and Environmental Engineering for their concern and love during this study. Worthy of appreciation is the assistance of Mallam Asara for his worthy training on the application of Geographic Information System (GIS).

This thesis would not be complete without showing due appreciation to my darling wife, Barrister (Mrs) Olaronke F. Adeogun and my baby, Miss Oluwaromilola, O. Adeogun, for their understanding whenever I' m away from home. I thank my parent, brothers and sister, for their words of encouragement. It is not possible to thank them enough for their long-term support, direct help and last minute patience.

Lastly, I appreciate and acknowledge the dissertation completion grant from the ABU MacArthur Foundation.

ABSTRACT

Drought is a creeping natural phenomenon affecting the arid and semi arid regions, including Nigerian Sudano-Sahelian Region. This research investigated droughts in Nigeria Sudano-Sahelian Region and developed forecasting models for drought monitoring and management in the region using well analysed meteorological data and imageries. The meteorological data consists of temperature and rainfall data, both from 1979 to 2008, collected from Nigeria Meteorological Organisation (NIMET), Oshodi, Lagos. The Imageries consist of Normalized Difference Vegetation Index (NDVI) spanning 1981 to 2011, obtained from National Aeronautics and Space Administration (NASA) and SPOT – Vegetation Programme of Vision on Technology (VITO), websites. Standardized Precipitation Index (SPI) at different time scales were extracted from the rainfall record and compared to determine the most suitable one for real time and early warning tool for drought forecasting and, it was discovered that SPI_1 reflected nearly all droughts from near normal condition to very severe dry condition. As a result, SPI_1 was chosen for modelling but, it was compared with monthly NDVI anomaly to select the better one. The results indicated that drought episodes detected by NDVI anomaly lagged some months behind the corresponding ones identified by SPI_1. Hence SPI_1 was modelled, based on Auto Regressive Moving Average/Seasonal Auto Regressive Moving Average (ARIMA/SARIMA), to simulate drought occurrence at each station. Multiplicative SARIMA model found suitable for SPI_1 forecasting at Sokoto, Nguru, Potiskum, Kano and Gusau Stations was $(011)x(011)_{12}$ while SARIMA model $(1,1,1)x(1,1,1)_{12}$ was found suitable for SPI_1 forecasting in Katsina and Maiduguri Stations. The multiplicative SARIMA temperature models developed for Sokoto, Nguru, Potiskum, Kano and Gusau Stations was SARIMA $(2,1,1)x(2,1,1)_{12}$ while SARIMA $(3,1,1)x(3,1,1)_{12}$ was found most

suitable for Katsina and Maiduguri Stations. Drought analysis in the region showed that the region had been exposed to droughts of different severity and magnitudes although, the level of risk varies from one location to another. The region had been classified into high drought risk zone consisting of Sokoto, Katsina, Damaturu and Nguru Stations, both in Yobe, and Maiduguri. Moderate risk zone included Guzau, Kano and Dutse while parts of Bauchi and Gombe States were identified as low risk zone. A drought management plan was proposed for the study area based on the developed forecasting models. The plan has three phases of drought emergence watch, warning and emergency.

TABLE OF CONTENTS

	Title page	i
	Declaration	ii
	Certification	iii
	Dedication	iv
	Acknowledgement	v
	Abstract	vi
	Table of Contents	viii
	List of Figures	xiii
	List of Tables	xx
	List of Appendices	xxi
1.0	**INTRODUCTION**	1
1.1	**Background**	1
1.2	**Statement of Research Problem**	3
1.3	**Justification**	4
1.4	**Aim and Objectives**	4
1.5	**Study Limitations**	5
2.0	**LITERATURE REVIEW**	6
2.1	General Overview	6
2.2	Historic Drought Episodes in Nigeria	6
2.3	National Response to Drought	7
2.4	Drought Definitions	8
2.4.1	Conceptual Definition of Drought	9

2.4.2 Operational Definition of Drought 9

2.5 Classification of Drought 9

2.5.1 Meteorological Drought 10

2.5.2 Agricultural Drought 10

2.5.3 Hydrological Drought 10

2.5.4 Socio-economy Drought 10

2.6 Drought Time Scales 11

2.7 Drought Parameters 11

2.8 Drought Variables 12

2.9 Drought Indices And Their Application In Drought Assessment 13

2.9.1 Palmer Drought Severity Index 13

2.9.2 Standardized Precipitation Index 14

2.9.3 Crop Moisture Index 16

2.9.4 Surface Water Supply Index 16

2.9.5 Effective Drought Index 17

2.9.6 Deciles 18

2.9.7 Percent Normal 18

2.10 Satellite Based Drought Indices For Drought Analysis 18

2.10.1 NDVI from Various Sensors 19

2.11 Drought Forecasting Using Models 21

2.12 Relationship Between Climate Change and Drought 22

2.12.1 Changing Climate: The Ocean Connection 23

2.13 Downscaling Of General Circulation Models To Local Scenerios 23

2.13.1 Types of Scenarios 24

2.14 Drought Early Warning Systems 25

3.0 MATERIALS AND METHODS **26**

3.1 Materials 26

3.1.1 Study Area 26

3.1.2 Satellite Imagery 27

3.1.3 Preparation of Map of the Study Area 27

3.1.4 Data Acquisition 28

3.1.5 Data Extraction and Processing 29

3.1.6 Processing of Meteorological Data 31

3.2 Methods 32

3.2.1 Analysis of Drought in the NSSR using NDVI Anomalies 32

3.2.2 Analysis of drought in the NSSR using Standard Precipitation Index 33

3.2.3 Temperature and Rainfall Analysis 35

3.2.4 Comparison of SPI and NDVI Anomalies 35

3.2.5 Degree of Spatial Drought Occurrence Analysis 35

3.2.6 Seasonal Drought Pattern Analysis 36

3.2.7 Development of Predictive Models for Drought Management in NSSR 36

3.2.8 Model Validation and Forecasting 39

3.2.9 Performance Criteria 40

3.2.10 Developing a Drought Management Plan for NSSR 40

4.0 RESULTS AND DISCUSSION **41**

4.1 Digitization of Nigerian Sudano-Sahelian Region 41

4.2 Data Extraction and Processing 41

4.2.1 Imageries Similarity Test 42

4.2.2 Validation of Imageries 42

4.3 Processing of Meteorological Data 43

4.3.1 Homogeneity Test 43

4.3.2 Distribution Test 46

4.4 Drought Analysis In NSSR Region Based On Percent NDVIAnomalies 48

4.5 Drought Analysis In NSSR Stations Based On Percent NDVI Anomalies 52

4.6 Drought Analysis In NSSR Based on SPI 60

4.7 Temperature and Rainfall Analysis 63

4.8 Comparison of Annual Accumulated Negative SPI_1 and Annual Accumulated Negative Percent Monthly NDVI Anomalies 64

4.9 Comparison of SPI_1 And NDVI Drought Events 66

4.9.1 Comparison of Very Severe Drought Events 66

4.9.2 Comparison of Severe Drought Events 68

4.9.3 Comparison of Moderate Drought Events 68

4.10 Analysis of Degree of Spatial Drought Occurrence 71

4.11 Analysis of Seasonal Drought Trend In NSSR 75

4.12 Analysis of Stochastic Models For Drought Management In NSSR 79

4.12.1 SPI_1 Model Identification 79

4.12.2 Parameter Estimation and Diagnostic Checking 87

4.12.3 Temperature Model Identification 90

4.12.4 Parameters Estimation and Diagnostic Checking 97

4.13 Model Validation 100

4.14 Performance Criteria 103

4.15 Drought Forecasting Using Models 103

4.16 Comparison of Model Forecasts And Nigerian Meteorological Agency Climate Predictions 111

4.17 Proposed Drought Management Plan For NSSR 112

5.0 SUMMARY, CONCLUSIONS AND RECOMMENDATIONS 117

5.1 Summary 117

5.1.1 Areas of Contribution to Knowledge 119

5.2 Conclusions 119

5.3 Recommendations 120

REFERENCES 122

APPENDIX A 130

APPENDIX B 133

APPENDIX C 136

APPENDIX D 139

APPENDIX E 142

APPENDIX F 156

APPENDIX G 161

APPENDIX H 177

APPENDIX I 188

APPENDIX J 193

APPENDIX K 209

APPENDIX L 213

APPENDIX M 217

LIST OF FIGURES

Figure 2.1: Definition Sketch of Drought Parameters 11

Figure 3.1 Map of Nigeria Showing the Sudano-Sahelian Region and the Synoptic Stations Used in the Study 26

Figure 3.2 Administrative Map of Nigeria 28

Figure: 4.1 Digitized Study Area: Nigeria Sudano Sahelian Region 41

Figure 4.2: Similarity Test for NASA and VITO Imageries 42

Figure 4.3: Validation of imageries using phonological metric 43

Figure 4.4a: Cumulative precipitation for Sokoto Station vs other stations (1979-2008) 44

Figure 4.4b: Cumulative precipitation for Katsina Station vs other stations (1979-2008) 44

Figure 4.4c: Cumulative temperature for Sokoto Station vs other stations (1979-2008) 45

Figure 4.4d: Cumulative temperature for Katsina Station vs other stations (1979-2008) 45

Figure 4.5a: Empirical cumulative distribution function (cdf) for Sokoto Station precipitation data Series (1979 2008) 46

Figure 4.5b: Empirical cumulative distribution function (cdf) for Katsina Station precipitation data Series (1979-2008) 47

Figure 4.5c: Empirical cumulative distribution function (cdf) for Sokoto Station temperature data Series (1979-2008) 47

Figure 4.5d: Empirical cumulative distribution function (cdf) for Katsina Station temperature data Series (1979-2008) 48

Figure 4.6a: NSSR Percent Dekadel Anomaly Trend 48

Figure 4.6b: NSSR Percent Monthly Anomaly Trend 49

Figure 4.6c: NSSR Percent Wet Season Average NDVI Anomaly Trend 49

Figure 4.6d: NSSR Percent Dry Season Average NDVI Anomaly Trend 49

Figure 4.6e: NSSR Percent Annual Average NDVI Anomaly 50

Figure 4.7a: Sokoto Station Percent Dekadel NDVI Anomaly Trend 52

Figure 4.7b: Katsina Station Percent Dekadel NDVI Anomaly Trend 52

Figure 4.7c: Nguru Station Percent Dekadel NDVI Anomaly Trend 53

Figure 4.7d: Potiskum Station Percent Dekadel NDVI Anomaly Trend 53

Figure 4.7e: Maiduguri Station Percent Dekadel NDVI Anomaly Trend 54

Figure 4.7f: Kano Station Percent Dekadel NDVI Anomaly Trend 54

Figure 4.7g: Gusau Station Percent Dekadel NDVI Anomaly Trend 54

Figure 4.8a: Sokoto Station Percent Monthly NDVI anomalies 55

Figure 4.8b: Katsina Station Percent Monthly NDVI anomalies 55

Figure 4.8c: Nguru Station Percent Monthly NDVI anomalies 55

Figure 4.8d: Potiskum Station Percent Monthly NDVI anomalies 56

Figure 4.8e: Maiduguri Station Percent Monthly NDVI anomalies 56

Figure 4.8f: Kano Station Percent Monthly NDVI anomalies 56

Figure 4.8g: Gusau Station Percent Monthly NDVI anomalies 57

Figure 4.9a: Sokoto Station percent annual NDVI anomalies 57

Figure 4.9b: Katsina Station percent annual NDVI anomalies 57

Figure 4.9c: Nguru Station percent annual NDVI anomalies 58

Figure 4.9d: Potiskum Station percent annual NDVI anomalies 58

Figure 4.9e: Maiduguri Station percent annual NDVI anomalies 58

Figure 4.9f: Kano Station percent annual NDVI anomalies 59

Figure 4.9g: Gusau Station percent annual NDVI anomalies 59

Figure 4.10a: NSSR SPI_1 Time Series 61

Figure 4.10b: NSSR SPI_3 Time Series 61

Figure 4.10c: NSSR SPI_6 Time Series 61

Figure 4.0d: NSSR SPI_12 Time Series 62

Figure 4.10e: NSSR SPI_24 Time Series 62

Figure 4.11: Annual monthly mean temperature (1979-2008) 63

Figure 4.12: Annual rainfall (1979-2008) 64

Figure 4.13: Annual accumulated negative SPI_1 (1979-2008) 65

Figure 4.14: Annual accumulated negative percent monthly NDVI anomalies 65

Figure 4.15a: Spatial distribution of average dekadel NDVI anomaly (September, 1984) 72

Figure 4.15b: Spatial distribution of average dekadel NDVI anomaly (September, 1994) 73

Figure 4.15c: Spatial distribution of average dekadel NDVI anomaly (September, 2004) 73

Figure 4.15d: Drought risk map based on NDVI anomalies 74

Figure 4.16a: Sokoto Station Seasonal Drought Pattern 75

Figure 4.16b: Nguru Station Seasonal Drought Pattern 75

Figure 4.16c: Katsina Station Seasonal Drought Pattern 76

Figure 4.16d: Maiduguri Station Seasonal Drought Pattern 76

Figure 4.16e: Guzau Station Seasonal Drought Pattern 77

Figure 4.16f: Kano Station Drought Pattern 77

Figure 4.16g: Potiskum Station Drought Pattern 78

Figure 4.17a: ACF plot for selecting relevant models for NSSR SPI_1 series 80

Figure 4.17b: PACF plot for selecting relevant models for NSSR SPI_1 series 80

Figure 4.18a: Comparison of computed NSSR SPI_1 with forecasted SPI_1 using SARIMA $(2,0,2)x(2,1,2)_{12}$ 83

Figure 4.18b: Comparison of computed Sokoto Station SPI_1 with forecasted SPI_1 using SARIMA $(0,1,1)x(0,1,1)_{12}$ 83

Figure 4.18c: Comparison of computed Katsina Station SPI_1 with forecasted SPI_1 using SARIMA $(1,1,1)x(1,1,1)_{12}$ 84

Figure 4.18d: Comparison of computed Nguru Station SPI_1 with forecasted SPI_1 using SARIMA $(0,1,1)x(0,1,1)_{12}$ 84

Figure 4.18e. Comparison of computed Potiskum Station SPI_1 with forecasted SPI_1 using SARIMA $(0,1,1)x(0,1,1)_{12}$ 85

Figure 4.18f. Comparison of computed Maiduguri Station SPI_1 with forecasted SPI_1 using SARIMA $(1,1,1)x(1,1,1)_{12}$ 85

Figure 4.18g. Comparison of computed Kano Station SPI_1 with forecasted SPI_1 using SARIMA $(0,1,1)x(0,1,1)_{12}$ 86

Figure 4.18h. Comparison of computed Gusau Station SPI_1 with forecasted SPI_1 using SARIMA $(0,1,1)x(0,1,1)_{12}$ 86

Figures 4.19a: Partial Autocorrelation function (PACF) of SPI_1 model for Sokoto Station 88

Figures 4.19b: Partial Autocorrelation function (PACF) of SPI_1 model for Sokoto Station 88

Figures 4.19c: Normal Probability Plot of SPI_1 model for Sokoto Station 89

Figures 4.19d: Normal Probability Plot of SPI_1 model for Sokoto Station 89

Figure 4.20a: ACF plot for selecting relevant models for transformed NSSR temperature series 90

Figure 4.20b: PACF plot for selecting relevant models for transformed NSSR temperature series 90

Figure 4.21a: Comparison of NSSR Observed and predicted Transformed Temperature using SARIMA $(2,1,1)x(2,1,1)_{12}$ 93

Figure 4.21b: Comparison of Sokoto Station Observed and predicted Transformed Temperature using SARIMA $(2,1,1)x(2,1,1)_{12}$ 93

Figure 4.21c: Comparison of Katsina Station Observed and predicted Transformed Temperature using SARIMA $(3,1,1)x(3,1,1)_{12}$ 94

Figure 4.21d: Comparison of Nguru Station Observed and predicted Transformed Temperature using SARIMA $(2,1,1)x(2,1,1)_{12}$ 94

Figure 4.21e: Comparison of Potiskum Station Observed and predicted Transformed Temperature using SARIMA $(2,1,1)x(2,1,1)_{12}$ 95

Figure 4.21f: Comparison of Maiduguri Observed and predicted Transformed Temperature using SARIMA $(3,1,1)x(3,1,1)_{12}$ 95

Figure 4.21g: Comparison of Kano Station Observed and predicted Transformed Temperature using SARIMA $(2,1,1)x(2,1,1)_{12}$ 96

Figure 4.21h: Comparison of Gusau Station Observed and predicted Transformed Temperature using SARIMA $(2,1,1)x(2,1,1)_{12}$ 96

Figures 4.22a: Autocorrelation Function (ACF) of temperature model for Sokoto Station 99

Figures 4.22b: Partial Autocorrelation Function (PACF) of temperature model for Sokoto Station 99

Figures 4.22 c: Residuals Histograms of temperature model for Sokoto Station 99

Figures 4.22 d: Normal Probability Plot of temperature model for Sokoto Station 100

Figure 4.23a: 12 months NSSR SPI_1 forecast 103

Figure 4.23b: 12 months Sokoto Station SPI_1 forecast 104

Figure 4.23c: 12 months Katsina Station SPI_1 forecast 104

Figure 4.23d: 12 months Nguru Station SPI_1 forecast 105

Figure 4.23e: 12 months Potiskum Station SPI_1 forecast 105

Figure 4.23f: 12 months Maiduguri Station SPI_1 forecast 106

Figure 4.23g: 12 months Kano StationSPI_1 forecast 106

Figure 4.23h: 12 months Gusau Station SPI_1 forecast 107

Figure 4.24a: NSSR transformed temperature forecast 107

Figure 4.24b: Sokoto Station transformed forecast 108

Figure 4.24c: Katsina Station transformed temperature forecast 108

Figure 4.24d: Nguru Station transformed temperature forecast 109

Figure 4.24e: Potiskum transformed temperature forecast 109

Figure 4.24f: Maiduguri Station transformed temperature forecast 110

Figure 4.24g: Kano Station transformed temperature forecast 110

Figure 4.24h: Gusau Station transformed temperature forecast 111

LIST OF TABLES

Table 2.1: Classes for wet and dry periods 15

Table 2.2: Standardized Precipitation Index 16

Table 2.3: Drought Risk Classification Using NDVI Anomalies 21

Table 4.1: Comparison of very severe drought events based on SPI_1 and percent monthly NDVI anomalies 67

Table 4.2: Comparison of severe drought events based on SPI_1 and percent monthly NDVI anomalies 69

Table 4.3: Comparison of moderate drought events based on SPI_1 and percent monthly NDVI anomalies 70

Table 4.4: Statistical Analysis of NSSR and Synoptic Stations NDVI 71

Table 4.5: Comparison of Goodness of Fit Statistics and Statistical Parameters of SPI_1 Models 82

Table 4.6: SPI_1 Model Parameters 87

Table 4.7: Comparison of Goodness of Fit Statistics and Statistical Parameters of Monthly Mean Temperature Models 92

Table 4.8: Temperature Model Parameters 97

Table 4.9: Validation of SARIMA Model for Sokoto Station SPI_1 101

Table 4.10: Validation of SARIMA Model for Katsina Station SPI_1 101

Table 4.11: Validation of SARIMA Model for Gusau Station SPI_1 101

Table 4.12 Validation of SARIMA Model for Sokoto Station transformed temperature 102

Table 4.13 Validation of SARIMA Model for Katsina Station transformed temperature 102

Table 4.14: Validation of SARIMA Model for Gusau Station transformed temperature 102

LIST OF APPENDICES

APPENDIX A: Cumulative precipitation for Station vs other stations (1979-2008) 130

APPENDIX B: Cumulative temperature for Station vs other stations (1979-2008) 133

APPENDIX C: Empirical cumulative distribution function (cdf) for precipitation data Series (1979-2008) 136

APPENDIX D: Empirical cumulative distribution function (cdf) for temperature data Series (1979-2008) 139

APPENDIX E: SPI_1 to SPI_24 Time Series 142

APPENDIX F: SPI_1 Autocorrelation Function (ACF) and Partial Autocorrelation Function (PACF 156

APPENDIX G: Results of SPI_1 Series SARIMA Models and Parameters 161

APPENDIX H: SPI_1 ACF & PACF Of Residual Plots, Distribution Histogram and Normal Distribution Plots 177

APPENDIX I: ACF and PACF plots for transformed temperature data 188

APPENDIX J:Temperature Series Sarima Models and Parameters 193

APPENDIX K: Temperature Model ACF & PACF of Residual Plots, Distribution Histogram and Normal Distribution Plots 209

APPENDIX L: SPI Forecasts using Selected SPI_1Models 213

APPENDIX M: Temperature Forecasts using Selected Temperature Models 217

CHAPTER ONE

INTRODUCTION

1.1 BACKGROUND

Drought is a dry condition and "natural creeping phenomenon", which makes its onset and end difficult to determine. Its progress is insidious and its effects can be devastating especially in arid and semi-arid regions. Drought is one of the most important weather – related natural disaster which is often aggravated by human activities. Since it affects very large areas for months and years, it has serious adverse impacts on regional food production, human life expectancy, and the economic performance of vast regions or several countries. Borno State for example is one of the most affected land areas of Nigeria that has suffered a fifteen-year drought spanning between 1960 and 1999, according to Fidelis (2003) who studied spatial distribution of drought in sub-saharan region of Nigeria. The persistent drought has indeed, a number of times caused famine in Northern Nigeria, especially during the drought episode of 1972-1973, during which thousands of animals died and farm yields dropped by up to 60% (Fidelis, 2003). It is estimated that 4 billion people will live under conditions of severe water stress by the year 2025, with conditions being particularly severe in Africa, the Middle East, and South Asia (Diwan, 2002). In order to minimize or avert disasters resulting from drought, it is important to put in place a drought management action-plan that details processes to be followed for drought monitoring, forecasting, impact assessment and response.

There are various drought indices used to assess drought conditions but, each has one limitation or another. For example, the Palmer (1965) Index is applicable within the United

States but has little acceptance elsewhere (Kogan, 1990; Smith et. al., 1993). In this regards, Mckee et. al.(1993) and Shafer and Dezman (1982) produced linear models such as Standardized Precipitation Index (SPI) and Surface Water Supply Index (SWSI), respectively to analyze drought. Recently, a school of thought has it that effective drought analysis and management should be based on robust and non-linear models, like Geographical Information System (GIS) models, that could incorporate many climatic features, since drought is caused by many factors such as delay in onset of rainfall, high temperature and evapotranspiration and so on. In combination with the data used for analysis in the other methods, GIS incorporates other non-convectional information such as the satellite imagery at high resolution, which can be used for detailed monitoring, damage assessment and long term relief management (Jeyaseelan and Chandrasekar, 2002). Besides, the GIS approach produces a GIS-generated map which is user friendly, robust and has a robust database system which makes features such as query, drought trends, patterns and modelling possible from which comprehensive assessment and prediction can be inferred. Moreover, satellite images are often the only information available in real-time for arid and semi –arid regions of Africa, which are often subject to drought and poor crop conditions, and where timely and reliable ground information is often difficult to obtain (FAO, 1999)

The incessant droughts in the region necessitate a detailed study to know the periodicity and intensity of droughts in order to develop strategies for mitigating the impact. This study is an attempt to apply GIS to imageries and ground based data analyses with the aim of developing predictive models for drought management in the Nigerian Sudano-Sahelian Region (NSSR).

1.2 STATEMENT OF RESEARCH PROBLEM

Drought has been a threat to the human race since time immemorial. The Nigerian Sudano-Sahelian Region (NSSR) had witnessed recurrent, severe and prolonged drought events, some lasting several years. According to Medugu (2007), the zone started the 20th century with a prolonged drought of 1903 culminating in that of 1911-1914. Other droughts included those of 1919; 1924; 1935 and 1951-1954. Since then, other drought episodes with considerable adverse impact on the environment and socio-economic activities are those of 1972-1973 and 1984-1985. The recurrent droughts had caused famine in Northern Nigeria severally, especially during the drought episode of 1972-1973, during which thousands of animals died and farm yields dropped by up to 60% (Fidelis, 2003).

There have been several coordinated efforts by the government at the national level to mitigate the adverse effects of drought. For instance, the Federal Ministry of Environment (FMEnv) has a Department devoted to drought and desertification. Part of the department's mandate is to ensure natural utilization, management and conservation of national resources in the country's dry lands as well as effective management of the effect of drought. The department also strengthens cooperation with other countries and international organizations combating desertification and mitigating the effects of drought. From these mandates, it is clear that the focus of the FMEnv is on managing the effects of drought and mitigation and not drought management (EC Report, 2006). This has been the government attitude to drought hitherto.

There is lack of real time and early drought warning systems to manage drought in the country. Medugu (2007) called for the development of a national drought forecasting and

early warning system to manage the frequent droughts in the Nigerian Sudano-Sahelian Region (NSSR).

To address the above problems, this research aims at developing predictive modelling tools for drought forecasting, monitoring and management in the NSSR.

1.3 JUSTIFICATION

The benefits to be realized from the study justify the rationale for embarking on it. Drought risk zones in the Sudano-Sahelian Region of Nigeria will be identified. This will aid directing necessary response to the identified drought hot spots. Management of drought is centered of the use of a system that predict drought early to aid early preparedness. This study aims at developing forecasting models which will be useful for effective management of the incessant drought problems in the Sudano-Sahelian Region of Nigeria.

Consequently, the adverse impact of drought will be reduced since the developed forecasting models will aid early preparedness and effective drought management. Besides, the study will update information on drought in the study area and, this will be useful for further investigations.

1.4 AIM AND OBJECTIVES

The aim of this research is to develop stochastic models for drought forecasting to aid effective drought management in the NSSR.

The objectives of the study reported herein are to:

i. identify drought risk zones in the study area.
ii. classify the region into drought risk zones.

iii. identify a suitable drought index for drought analysis and forecasting

iv. develop a suitable drought management plan for NSSR

v. recommend suitable drought mitigation measures based on the study.

1.5 STUDY LIMITATIONS

The remotely sensed imagery used as drought index is Normalized Difference Vegetation Index (NDVI) which is readily available for a period of more than thirty years. Other available remotely sensed imageries, such as Rainfall Estimates (RFE) have short period of records of about fifteen years. This short period for drought analysis would not yield reasonable hydrological assessment hence, ground based rainfall data were used to derive Standardized Precipitation Index (SPI) for drought analysis in this study.

CHAPTER TWO

LITERATURE REVIEW

2.1 GENERAL OVERVIEW

Drought, exacerbated by climate change, represents one of the greatest environmental challenges of our times, especially in arid and semi-arid regions. The Sudano-Sahelian Region of Nigeria is not an exception to the threat of persistent drought which has severely and severally caused famine in Northern Nigeria. For instance, the drought episode of 1972 -1973 resulted in the death of thousands of animals and reduction in farm yields by up to 60% in the region (Okorie, 2003). As a result of the historic adverse impacts of drought on socio-economy and environment, many researches in the literature are directed at analyzing drought phenomenon so as to gain in-dept knowledge to aid better assessment and prediction of its occurrence and hence enable prompt response, mitigation strategies and preparedness plans geared towards its effective management.

Therefore, this chapter evaluates past investigations on drought and also, trends in drought analysis methods are discussed so as to reflect the state of the art on the subject.

2.2 HISTORIC DROUGHT EPISODES IN NIGERIA

Historically, droughts have been occurring in the NSSR since time immemorial. Oladipo (1992) reported that many historical droughts have occurred in the Northern region of Nigeria. Using the translations from Arabic chronicles, there are indications that the Sahelian zone of Nigeria was affected by droughts and famine at about 1681-1687 and 1738-1756. Also, recurring severe drought events of over a 12-year period, between 1828 and 1839, were experienced around Kano and Maiduguri (Otun, 2005). According to him,

the droughts of the 1840s were called Darara (Hausa), while those that occurred in the 1850s were referred to as Bamga-Bamga.

The moderate to severe drought of 1902-1904, referred to as Izenere (sale of children), appeared across the entire northern region (Oguntoyinbo and Richards, 1977; Apeldoorn, 1981). Other drought incidences documented in the 1990s in locations north of latitude 11^{o} N in Nigeria include that of 1913-16, 1942-45, 1971-73, and 1983-84 (FGN 1998). These drought episodes caused massive famines. Each time drought occurs in Nigeria, the area that usually receives very severe impacts includes all areas north of 11^{o} N parallel (mainly around Sokoto, Zamfara, Katsina, Kano, Jigawa, Yobe, and Borno, states) (Akeh *et. al.,* 2001)

Otun (2005) reported that the effects of the 1971-73 severe drought and the 1983-84 localized droughts on agricultural production prompted the Federal Government of Nigeria (FGN) through its various relevant agencies, to put in place some institutional arrangements and schemes to minimize drought impacts.

2.3 NATIONAL RESPONSE TO DROUGHT

The response of the Federal Government of Nigeria to drought is worrisome and abounds in the literature. Otun (2005) reported that the response of government to droughts, especially during the 1972-73 episodes, were only on an ad hoc basis. They immediately provided relief packages that consisted of the provision of subsidized food, making water available in water tanks and through sinking of boreholes and wells and the provision of medicare. In addition, The Federal government of Nigeria also developed and executed many large-scale

dam construction and irrigation projects within the region in the 70s as a mitigation strategy to combat drought in the region (Otun, 2005).

It is only recently after more than twenty years, that a drought policy is being prepared with the creation of a Department of Drought and Desertification in the Federal Ministry of Environment. The department strengthens cooperation with other countries and international organizations combating desertification and mitigating the effects of drought. From these mandates, it is clear that the focus of the FMEnv is on managing the effects of drought and mitigation and not drought management (EC Report, 2006). The approach of the government to drought planning and mitigation can be best described as being uncoordinated, piecemeal and basically consists of ad hoc measures.

Also, government at the national level mitigates the adverse effects of drought by establishing National Emergency Management Agency (NEMA) in 1999, via Act 12 as amended by Act 50 of 1999, to manage disasters in Nigeria. The National Emergency Management Authority was established with a sole mandate to give attention and support to victims of any disasters in the country. In drought-induced disaster for example, NEMA fulfills her mandate by providing full emergency relief materials to the victims but, no attention is given to the cause, in this case drought. In addition, Nigeria has in place a Drought Preparedness Plan (2005) which contains a number of adaptation strategies in some of its specific objectives (Oladipo, 2010).

2.4 DROUGHT DEFINITIONS

Drought can be defined as a normal, recurrent feature of climate and comes in virtually all-climatic zones with varying characteristics from one region to another. According to Okorie

(2003), drought is a temporary aberration: it differs from aridity, which is restricted to low rainfall regions and is a permanent feature of climate. It mostly originates from a deficiency of precipitation over a long period of time, usually a season or more. He further noted that the deficiency results in a water shortage for some human activities, groups or environmental sectors. According to him, It has scores of many definitions though, there are two main kinds of drought definitions: conceptual and operational.

2.4.1 Conceptual Definition of Drought

Conceptual definitions help people to understand the concept of drought which Okorie (2003) defined as a protracted period of deficient precipitation resulting in extensive damage to crops and consequently, loss of yield.

2.4.2 Operational Definition of Drought

Operational definitions help people to identify the beginning, end and degree of severity of a drought. In order to determine the degree of drought, operational definition specifies the degree of departure from an average of precipitation or some other climatic variables over some time period. This is usually done by comparing the current situation to the historical average, often on a 30-year period of record (Okorie, 2003)

2.5 CLASSIFICATION OF DROUGHT

According to Wilhite and Glantz (1985), drought can be classified on sectoral basis as follows:

i. Meteorological Drought,
ii. Agricultural Drought,
iii. Hydrological Drought and

iv. Socio-economy Drought

2.5.1 Meteorological Drought

Meteorological drought refers to a deficiency of precipitation, as compared to average conditions, over an extended period of time. It basically originates from the deficiency of precipitation and focuses on the physical characteristics of drought (Mokhtari, 2005) rather than impacts associated with shortage of precipitation. Meteorological drought leads to a depletion of soil moisture (Legesse, 2010).

2.5.2 Agricultural Drought

Agricultural drought is defined as a reduction in soil moisture available below the optimal level required by crops during the different growth stages, resulting in impaired growth and reduced yields. It typically occurs after meteorological drought but before hydrological drought (Okorie, 2003).

2.5.3 Hydrological Drought

Hydrological drought results when precipitation deficiencies begin to reduce the availability of natural and artificial surface and subsurface water resources. It occurs when there is a substantial deficit in surface runoff below normal conditions or when there is a depletion of ground water recharge (Okorie, 2003).

2.5.4 Socio-economy Drought

Socio-economy drought occurs when human activities are adversely affected by reduced precipitation and related water availability. This form of drought associates the supply and demand of some economic goods with elements of meteorology, agricultural and hydrological droughts (Okorie, 2003; Legesse, 2010).

2.6 DROUGHT TIME SCALES

The most commonly used time scale in drought analysis is the year, followed by the month (Sen 1980a,b; Bonacci, 1993; Sharma, 1997; Pann and Sharma, 2002). Although, the yearly time scale is rather long, it can be used to abstract information on the regional behaviour of droughts (Panu and Sharma, 2002). The monthly time scale seems to be more appropriate for monitoring drought effects in situations related to agriculture, water supply and groundwater abstractions (Panu and Sharma, 2002). For studying the behaviour of short-time droughts within a year or a season, the daily time scale has also been used (Gupta and Duckstein, 1975; Smart, 1983; Zelenhesic and Salvai, 1987; Sharma, 1996; Tallaksen *et al.,* 1997)

2.7 DROUGHT PARAMETERS

The important parameters quantifying a drought are: (a) duration (b) severity (c) location in absolute time, that is, initiation and termination time points, and (d) areal coverage. At times; the ratio of severity to duration (called magnitude or intensity) is also used (Dracup *et. al*. 1980). The concept of the above parameters is illustrated in Fig. 2.1

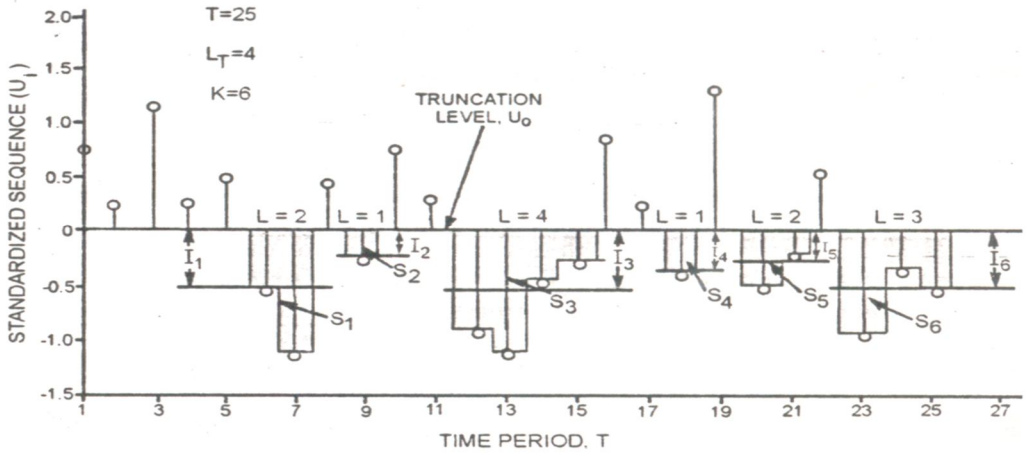


Figure 2.1: Definition Sketch of Drought Parameters
Source: Otun, 2005.

According to Panu and Sharma (2002), the most basic element for deriving the above parameters is the truncation or the threshold level, which may be a constant or a function of time. The truncation level specifies some statistic of the drought variable and serves to divide the time series of the variable in question into "deficit" and "surplus" sections. The parameters of a drought such as duration, severity and intensity are based on the properties of the deficit sections. Dracup *et al.* (1980) defined the truncation level by the expression:

$$x_0 = x_m - e.s = x_m(1 - e.c_v) \quad (2.1)$$

in which x_0 is the truncation level, x_m, s and c_v are the mean, standard deviation and the coefficient of variation of time series of the drought variable x, such as rainfall or streamflow time series, and e is the effective scaling factor. Since the important drought characteristics depend on the truncation level, the selection of a truncation level is of prime importance in drought analysis. In the case of meteorological or hydrological droughts, the threshold can be mean annual precipitation or streamflow, respectively. However, such a simple threshold does not serve the purpose of agricultural drought analysis.

2.8 DROUGHT VARIABLES

According to Panu and Sharma (2002), a drought variable can be defined as a prime variable responsible for assessing drought effect, and is considered a key element in defining drought and deciding on the techniques for its analysis. The determinant variable for the meteorological drought is precipitation, whereas for the hydrological drought it is either river runoff/streamflow or reservoir levels and/or groundwater levels. For agricultural drought, the governing variables are soil moisture and/or consumptive use. Hence, the time series of the above variables provide the framework for evaluating the

drought parameters of interest. However, the earlier work on drought analysis has been confined to meteorological and hydrological point droughts (referring to a fixed point or a very small region) since the historic record of precipitation and streamflow is generally available at a point. In the case of agricultural drought, the measurement of its determinant factor (soil moisture) is difficult and hence, such droughts could be best studied through a complex regional analysis involving a battery of variables (soil moisture, crop yield, leaf area index, vegetative growth, amongst others) rather than a simple point analysis (Panu and Sharma, 2002).

2.9 DROUGHT INDICES AND THEIR APPLICATION IN DROUGHT ASSESSMENT

Drought indices are developed as means of analyzing drought. A drought index assimilates thousands of data on rainfall, temperature, snow pack, streamflow and other water-supply indicators into a comprehensible picture. Hence, drought indices are continuous functions of measurable drought variables. There are several indices that measure how much precipitation for a given period of time has deviated from historically established norms. Rainfall data are widely used to calculate drought indices, because long-term rainfall records are often available (Guttman *et al.,* 1998). Some of the well-known and less-well-known indices used in drought studies, monitoring and management are briefly reviewed below.

2.9.1 Palmer Drought Severity Index

One of the best known indices is the Palmer Drought Severity Index (PDSI) (Palmer, 1965). The index is used to "measure the departure of moisture supply". Since its inception, the PDSI has evolved into numerous modified versions. For example, Karl and Knight

(1985) described a modified version known as the Palmer Hydrological Drought Index (PHDI), which is used for water supply monitoring. PDSI has been used in west-Hungary as soil moisture indicator and has been widely used in the United States of America for drought monitoring (Chopra, 2006). However, Palmer (1965) expressed drought severity (X_i) as:

$$X_i = X_{i-1} + \Delta X_i \quad (2.2)$$

where, X_{i-1} = previous month's drought severity

ΔX_i = monthly contribution to drought severity

Several researchers have observed that PDSI has limitations among which are calibration and spatial comparability (Guttman *et. al.* 1998; Chopra, 2006). PDSI is applied within the United States of America and has less acceptance elsewhere (Kogan, 1990). In order to solve this problem, McKee *et al.,* (1993), developed the Standardized Precipitation Index (SPI) which can be calculated at different time scales to monitor droughts and hence applicable to diverse areas of interests. Moreover, the SPI is comparable in time and space (Hayes and Svoboda, 1999). Palmer classification is illustrated in Table 2.1.

2.9.2 Standardized Precipitation Index

The other index parallel to the PDSI is the Standardized Precipitation Index (SPI) (Guttman, 1998). It has been shown that the values of the PHDI are highly sensitive to errors in precipitation values, where as the SPI has the potential to be a superior yet simpler index of drought severity over the PDSI (Guttman, 1998; Panu and Sharma, 2002).

SPI, developed by McKee *et. al*. (1993) is the most widely used index for understanding the magnitude and duration of drought events. According to Legesse (2010), SPI can be used to

examine the severity and spatial patterns of drought in a given region. Besides, it offers a quick, handy and simple approach with minimal data requirements (Komuscu, 1999). It is designed to quantify the impacts of precipitation deficit on groundwater, reservoir storage, soil moisture, and streamflow for multiple time scales. However, SPI is generally computed using an SPI Program. According to Murad and Saliful (2011), SPI is calculated based on the following equation:

Table 2.1: Classes for wet and dry periods

Drought Severity (X)	**Class**
≥ 4.00	Extremely wet
3.00 to 3.99	Very wet
2.00 to 2.99	Moderately wet
1.00 to 1.99	Slightly wet
0.50 to 0.99	Incipient wet spell
0.49 to -0.49	Near Normal
0.50 to -0.99	Incipient dry spell
-1.00 to -1.99	Mild drought
-2.00 to -2.99	Moderate drought
-3.00 to -3.99	Severe drought
≤ -4.00	Extreme drought

Source: Palmer (1965)

$$SPI = \frac{(X_i - X_m)}{\sigma} \qquad (2.3)$$

where, X_i is monthly rainfall record of the station; X_m is rainfall mean; and σ is the standard deviation.

Guttman (1998) has made comparison of PDSI and SPI, and recommended SPI as a drought index, which is easy to determine and has greater spatial consistence. Moreover, it can be used in risk assessment analysis and making decisions with special ability for adjustments to time periods for which the users are interested, for example, short time

periods in life cycle of crops or longer periods regarding water resources (Legesse, 2010). According to McKee *et. al.* (1993), conditions of soil moisture react to precipitation anomalies in relatively short time period and appearance of drought is happening every time when SPI is negative and its intensity comes to -1.0 or lower, while drought stops when SPI is positive. This is shown in Table 2.2

Table 2.2: Standardized Precipitation Index

SPI Values	**Class**
2.0 and more	Extremely wet
1.5 to 1.99	Very wet
1.0 to 1.49	Moderately wet
-0.99 to 0.99	Near Normal
-1.0 to -1.49	Moderately dry
-1.5 to -1.99	Severely dry
-2 and less	Extremely dry

Source: McKee *et al.* (1993)

2.9.3 Crop Moisture Index

Crop Moisture Index (CMI) was introduced by Palmer (1968). It was specifically designed as an agricultural drought index. CMI is designed to monitor short term moisture conditions affecting a developing crop; therefore, CMI is not a good long-term drought –monitoring tool (Chopra, 2006). Hadish (2010) stated that CMI indicates more favourable moisture conditions over a particularly wet or dry month even in the middle of a serious long-term wet or dry period.

2.9.4 Surface Water Supply Index

According to Hadish (2010), Shafer and Dezman (1982) designed the Surface Water Supply Index (SWSI) to be an indicator of surface water conditions and described the index as “mountain water dependent”, in which mountain snowpack is a major component. The

objective of the SWSI was to incorporate both hydrological and climatological features into a single index value resembling the Palmer Index for each major river basin in the state of Colorado (Shafer and Dezman, 1982). These values would be standardized to allow comparisons between basins. Four inputs are required within the SWSI: snowpack, streamflow, precipitation, and reservoir storage. The SWSI is computed with only the snowpack, precipitation, and reservoir storage in the winter, while during the summer months, stream flow replaces snowpack as a component within the SWSI equation as illustrated by Shafer and Dezman (1982:

$$SWSI = \frac{aP_{snow}+bP_{prec}+cP_{strm}+dP_{resv}-50}{12} \quad 2.4$$

where a, b, c and d = weights for snow, rain, streamflow and reservoir storage, respectively, (a+b+c+d = 1) and P_i is the probability (%) of exceedence for each of these four water-balance components. Calculations are performed based on a monthly time step.

2.9.5 Effective Drought Index

Effective Drought Index (EDI) in its original form is calculated with a daily time step (Byun and Wilhite, 1999). It is a function of precipitation needed for a return to normal condition since the beginning of a drought. The range of EDI variation is from -2 to 2. Like PDSI and SPI, it has thresholds indicating the range of wetness, from extremely dry to extremely wet condition.

The major problem associated with EDI in its original form is that it is based on daily precipitation data (Smakhtin and Hughens, 2004). Hence, its performance cannot be compared with other drought indices that require monthly precipitation data as input.

2.9.6 Deciles

Deciles approach was suggested by Gibbs and Maher (1967) and widely used in Australia (Coughlan, 1987; Smith et. al. 1993). In this method, monthly precipitation totals from a long-term record are first ranked from highest to lowest to construct a cumulative frequency distribution. The distribution is then split into ten parts, that is, tenths of distribution or deciles. According to Smakhtin and Hughens (2004), the first decile is the precipitation value not exceeded by the lowest 10% of all precipitation values in a record, the second is between the lowest 10 and 20%, and so on. Any precipitation value such as monthly, can be compared with, and interpreted in terms of these deciles.

2.9.7 Percent Normal

Percent of normal indices are simple, by definition, easy to calculate and are easily understood by a general audience. "Normal" may be, and usually is, set to a long-term mean or median precipitation value. It may be calculated for a day, a month, a season or a year. The same percent of normal may have different specific impacts at different locations and, therefore, it is a bit of simplistic measure of precipitation deficit and what is normal may be perceived differently in different regions (Smakhtin and Hughens, 2004).

2.10 SATELLITE BASED DROUGHT INDICES FOR DROUGHT ANALYSIS

Satellites images are information available in near real-time for drought monitoring in the arid and semi-arid regions of Africa where timely and reliable ground information is sometimes difficult to obtain (FAO, 1999). Available satellite images suitable for early warning are Cold Cloud Duration (CCD) images and vegetation indices images such as Normalized Difference Vegetation Index (NDVI). For drought monitoring purposes, these

images can be used to compare the current growing season with a historical archive of NDVI images and CCD images.

Sensors carried aboard satellites measure red and near-infrared light waves reflected by land surfaces. These light waves are transformed into vegetation indices using algorithms. A vegetation index is an indicator that describes the greenness – the relative density and health of vegetation – for each picture element, or pixel, in a satellite image. As stated before, a widely used vegetation index is the NDVI which has range of values from +1.0 to -1.0 (USGS, 2011). For instance, non vegetated surfaces such as barren rocks or sands show very low NDVI values while dense vegetations reflect high NDVI values.

According to USGS (2011), NDVI values can be averaged over time to establish "normal" growing conditions in a region for a given time, further analysis can then characterize the health of vegetation in that place relative to the norm. When analyzed through time, NDVI can reflect where and/or when vegetation is thriving and where and/or when it is under stress, as well as changes in vegetation due to anthropogenic activities, and or natural disturbances.

2.10.1 NDVI from Various Sensors

Common sensors used to generate NDVI image products are Advanced Very High Resolution Radiometer (AVHRR), Enhanced Thematic Mapper Plus (ETM+) and Moderate Resolution Imaging Spectroradiometer (MODIS). The AVHRR Sensor is carried aboard National Oceanic and Atmospheric Administration (NOAA) polar-orbiting weather satellites and the sensor has a daily repeat cycle and a 1-km resolution. Enhanced Thematic Mapper is carried aboard Landsat 7 satellite. With a resolution of 30m ETM+ data can be

transformed into NDVI images that have greater spatial details than those derived from AVHRR, but cover a smaller area (USGS, 2011). Furthermore, Landsat's orbit repeats every 16 days, compared to AVHRR's daily coverage, which makes creating cloud free NDVI products from ETM+ data more challenging (USGS, 2011).

The third sensor, MODIS, is another modern and well calibrated daily, moderate-resolution satellite sensor with a proper instrument for studying vegetation greenness. MODIS is carried aboard National Aeronautics and Space Administration (NASA) Terra and Aqua Satellites with 1-2 days orbit frequency. Global MODIS data are readily available for no charge, and are high-quality input for vegetation time-series analysis. According to USGS (2011), MODIS data generate NDVI and enhanced vegetation index (EVI) image products with 250-m, 500-m, and 1-km spatial resolution.

Lastly, another sensor, known as vegetation, is carried aboard SPOT satellite with 1-2 days orbit frequency to generate NDVI image with around 1 to 1.15 km spatial resolution (Argrawal *et. al.* 2003). The SPOT Vegetation programme is the fruit of space collaboration between various European partners consisting of Belgium, France, Italy and Sweden. According to Murad and Saliful (2011) the anomaly of NDVI has been calculated for a specific year using the mean, maximum value of the total durations based on the following equation:

$$\epsilon = (NDVI_{maxi} - mean\ NDVI_{max})/(mean\ NDVI_{max})x\ 100 \qquad (2.5)$$

where ϵ is NDVI anomaly in *i*th year, NDVI max is maximum NDVI and mean NDVI max is the average of maximum NDVI during the period of study.

The threshold values used in this study to classify drought risk using NDVI anomalies was presented in Table 2.3.

Table 2.3: Drought Risk Classification Using NDVI Anomalies

Percent NDVI Anomalies	Drought Class
Above 0%	No Drought
0% to -10%	Slight Drought
-11% to -20%	Moderate Drought
-21% to -30%	Severe drought
-30% and less	Very Severe Drought

Source: Murad and Saliful (2011)

2.11 DROUGHT FORECASTING USING MODELS

According to Cordery and McCall (2000), forecasting of when a drought is likely to begin or to come to an end is extremely difficult. A better understanding of droughts is essential to develop tools for prediction or forecasting of drought initiation (and ending) for timely and appropriate implementation of measures to cope with a drought.

Forecasting can be short-term or long-term, with relevant advantages or disadvantages. For instance, climate change might impose uncertainty on long-term forecasts. However, some school of thoughts are of the opinion that the adverse influence of climate change can be reduced or eliminated by correlating time series data (of PDSI, SPI, temperature and stream flow) with ENSO-related variables, such as the Southern Oscillation Index (SOI) or sea-surface temperature (SST) (Panu and Sharma, 2002; Piechota and Dracup, 1996; Cordery and McCall, 2000). On a short time scale, such as a month or a season, it may be possible to indicate probable timings of inception and termination of drought (Beran and Rodier, 1985; Panu and Sharma, 2002). Besides, the influence of climate change might be easily incorporated, when it occurs, in subsequent short-term forecasting.

According to Panu and Sharma (2002), short-term forecasts essentially employ one or more combinations of the following procedures:

- Linear regression models involving weather variables, such as air pressure, air and sea-surface temperatures, wind velocities and directions.

- Time-series forecasting algorithms employing the notions of ARIMA models, non homogeneous Poisson processes coupled with conditional probabilities have been used for short-term forecasting (Lohani and Lognathan, 1997).

- Recession rates of stream flow hydrographs, stage graphs of other water bodies, and indices based on the status of soil moisture and vegetation in the region under consideration have been used for short-term forecasting (Zelenhasic and Salvai, 1987).

Panu and Sharma (2002) concluded that there is a potential for forecasting droughts based on the behavioural patterns monitored during past droughts. However, several indices based on hydro-climatic, vegetation, ecological and environmental factors need to be monitored for reliable and robust forecasts of droughts.

2.12 RELATIONSHIP BETWEEN CLIMATE CHANGE AND DROUGHT

As stated before, drought is weather –related natural disaster and is often aggravated by human activities. Also, climate change has influence on both the intensity and spatio-temporal distribution of drought throughout the earth. This is buttressed further in the following section.

2.12.1 Changing Climate: The Ocean Connection

The oceans have most significant influence on earth's weather and climate. This should not surprise us as seventy percent of the global surface is covered by water. This great reservoir continuously exchanges heat and moisture, with the atmosphere, driving our weather patterns and controlling the slow, subtle changes in our future climate. Changes in the atmosphere are driven by heat transfer and since oceans store more heat in their uppermost 3 metres than the entire atmosphere, the key to understanding global climate change is inextricably linked to the oceans (NASA, 2010).

The past century alone has witnessed global temperature increase by 0.6 degree Celsius and the average global sea level over the past decade has risen steadily (NASA, 2010; IPCC, 2007). This has been attributed partly to the natural cycle and human activities such as burning of fossil fuels. The global warming, if it continues will probably not be uniform: the real threat is the redistribution of heat over the Earth's surface. This implies that some spots will be warm, while others will cool; these changes and the accompanying shifts in rainfall patterns, could relocate agricultural regions and/or influence drought occurrence, duration and intensity across the planets

2.13 DOWNSCALING OF GENERAL CIRCULATION MODELS TO LOCAL SCENERIOS

General Circulation Models (GCM) are primary tools for simulating past climate and projecting the future climate using different climate forcing scenarios. According to Abiodun *et. al.,* (2011), there are complex computer models that represent interactions between the different components of climate such as the land surface, the atmosphere and the oceans. Investigations in the literature have shown that the climate models are capable

of providing reliable climate projections for the future (Abiodun *et. al.,* 2011; IPCC, 2007). The process of making projections of climate change involves using several GCMs and scenarios of future emission of greenhouse gasses to predict the future climate.

2.13.1 Types of Scenarios

In the context of climate change, scenarios describe potential futures which can be based on changes in the climate systems, socio-economic circumstances or other potential future changes. The IPCC (2000), in its Special Report on Emission Scenarios (SRES), identified, described and published a range of possible scenarios based on four "storylines", taking into consideration two dimensions of development: greater weight given to Economic (A) or Environmental (B) factors; and greater weight given to either Global (1) or Regional (B) factors. Hence, the report reflects the scenarios A1, A2, B1 and B2 representing various combinations of Economic/Global, Economic/Regional, Environmental/Global and Environmental/Regional scenarios respectively, with each having an associated emission pathway.

Abiodun *et al.,* (2011) applied scenarios A2 and B1 to investigate the future climate of Nigeria and observed that both scenarios project a warmer climate change in the future, but the future climate is warmer according to the A2 scenario compared with the B1 scenario. The study further revealed that the projections of the models show a wider spread in A2 than in B1 scenario over all zones. This means that there are larger uncertainties in the A2 projections than in the B1 projections, with a consistent increase of $+0.20^0$C per decade (Abiodun *et al.,* 2011). Consequently, it is adequate to incorporate B1 scenario projection in temperature forecasting models to achieve accurate results in drought forecasting in times of climate change. The application of A2 and B1 model scenarios to historic rainfall

records in Nigeria reflects that there is no specific trend in future rainfall anomalies (Abiodun *et al.,* 2011).

2.14 DROUGHT EARLY WARNING SYSTEMS

A Drought Early Warning System (DEWS) can be defined as a system of data collection to monitor droughts, in order to provide timely notice when a drought crisis threatens and thus to elicit an appropriate response. According to Svoboda (2009), A DEWS has the advantages of early drought detection and improved response to droughts. Besides, he noted that a DEWS forms the foundation of drought plans. Svoboda (2009) and United Nations International Strategy for Disaster Reduction (ISDR) (2006) identified the components of a DEWS among which the fundamental ones are drought risk knowledge, monitoring, forecasting and information dissemination.

CHAPTER THREE

MATERIALS AND METHODS

3.1 MATERIALS

3.1.1 Study Area

The study area is the Sudano-Sahelian Zone (SSZ) of Nigeria. It lies roughly between Latitudes 11^0 and 13^0N and Longitudes 4^0 and 15^0E (Maduakor, 1991) and, constitutes most of Borno, Kano, Sokoto, Adamawa, Bauchi, Gombe, Jigawa, Katsina, Kebbi, Yobe and Zamfara States in Nigeria as shown in Figure 3.1. It has been estimated that 50% to 75% of the eleven frontline states in the Northern Nigeria are being affected by drought (Medugu, 2007). These states with a population of about 50 million people account for about 38% (35,125km^2) of the country's total land area (Medugu, 2007).

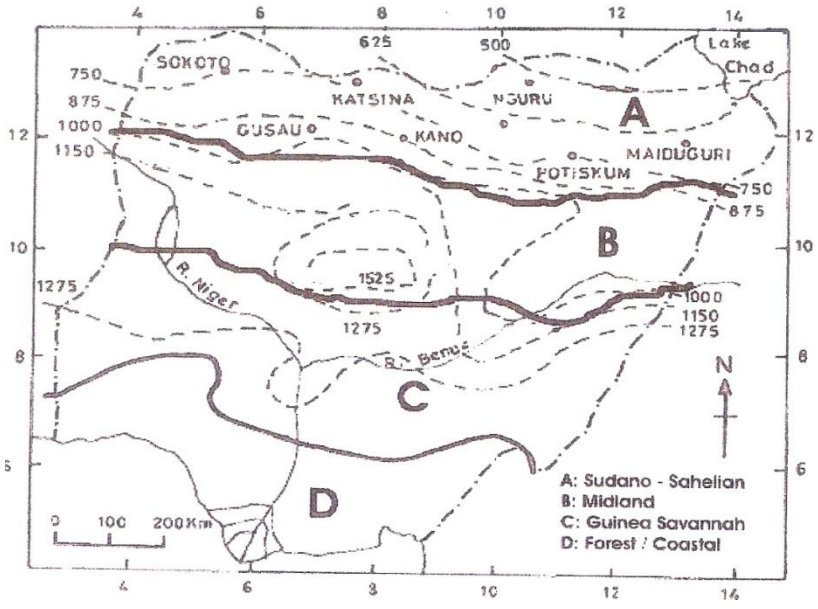


Figure 3.1: Map of Nigeria Showing the Sudano-Sahelian Region and the Synoptic Stations Used in the Study
Source: Otun (2005)

3.1.2 Satellite Imagery

This study applied two sets of data - remotely sensed imageries and ground based meteorological data to investigate drought phenomena in the Nigerian Sudano-Sahelian Region (NSSR). The imageries utilized in this research are the Normalized Difference Vegetation Index (NDVI) images covering the region of study. The NDVI images were used to determine the areal extent of healthy vegetation. The ground based data used for analysis were rainfall and temperature for the seven synoptic meteorological stations namely, Sokoto, Katsina, Nguru, Potiskum, Maiduguri, Kano and Gusau in the study area. NDVI imageries of Africa were downloaded from National Aeronautics and Space Administration (NASA) and Vegetation Programme of Vision on Technology (VITO) websites at high resolution to obtain a record of 31 years from 1981 to 2011.

3.1.3 Preparation of Map of the Study Area

The study area, Nigerian Sudano-Sahelian Region (NSSR), constituting most parts of Borno, Kano, Sokoto, Adamawa, Bauchi, Gombe, Jigawa, Katsina, Kebbi, Yobe and Zamfara States in Nigeria, was digitized from two existing grid maps of Nigeria, geographic map of Nigeria, as shown in Figures 3.1 and administrative map of Nigeria, shown in Figure 3.2. The two maps served as background maps for the digitization of NSSR. The administrative map of Nigeria was uploaded into an ArcGIS 9.2 environment, a Geographic Information System (GIS) application software, and then georeferenced using four identified points (signified as +; each at each corner of the map) as shown in Figure 3.2, with respect to their latitude and longitude. Point and polygon shapefiles prepared in the Arc Catalog component of the software were also uploaded into the ArcGIS environment and used together with the map to digitize the study area. The prepared map of

the study area was processed further by applying labelling. The digitized map was then overlaid on the downloaded imageries of Africa, one after the other, to extract the imageries of the study area, NSSR, using a software known as WinDisp 5.1. The digitized map of the study area is presented Fig. 4.1, Chapter 4.

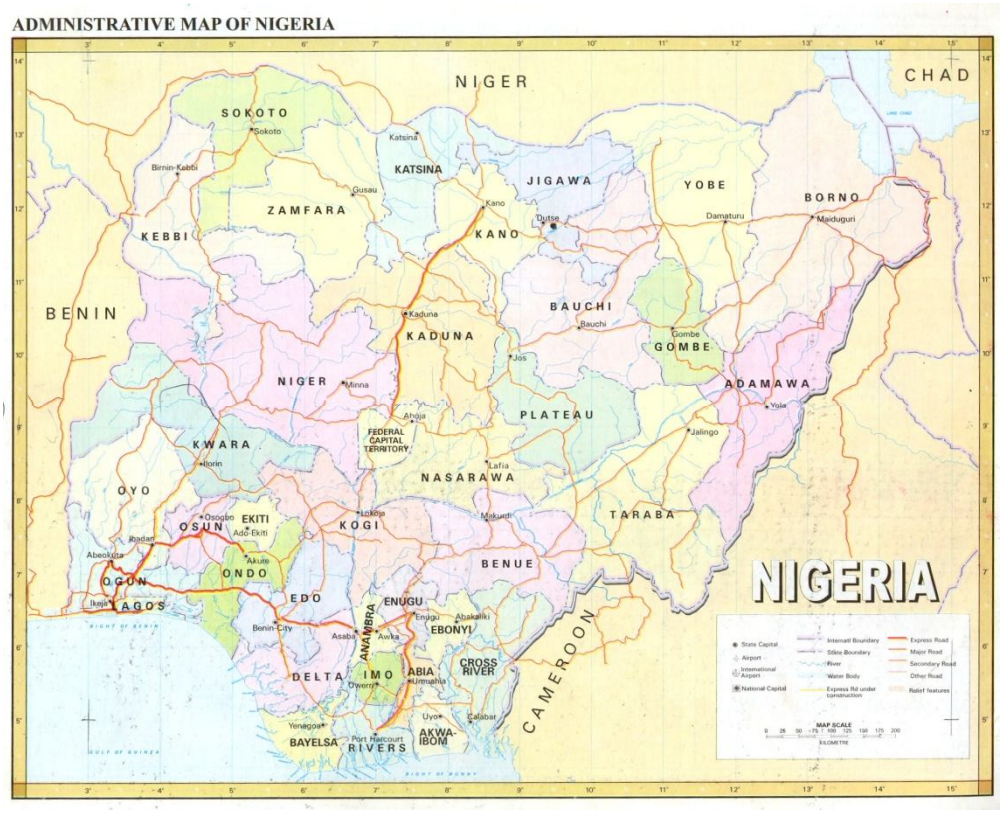


Figure 3.2 Administrative Map of Nigeria

3.1.4 Data Acquisition

The data necessary for this investigation was acquired from different sources such as the Nigerian Meteorological Organisaion (NIMET), Oshodi, Lagos, the National Aeronautics and Space Administration (NASA), located in Washington, DC, the SPOT – Vegetation Programme of Vision on Technology (VITO), formed by various European partners and based in Belgium and the literature. Hence the data used for analysis were two types:

i. The ground based meteorological data was collected from the NIMET and the data consist of 30 years record of rainfall and temperature from 1979 to 2008 covering the seven synoptic meteorological stations in the region.

ii. The imageries covering the study area were downloaded from the websites of NASA and VITO at earlywarning.usgs.gov and www.free.vgt.vito.be respectively. The image data, that is, Normalized Difference Vegetation Index (NDVI), provided by NASA consists of imageries from 1981 to 2008 while the imageries available from VITO covers the period 1989-2012. This implies that the two sets of data consist of 27 and 10 years of records respectively. However, in other to have a robust hydrologic analysis, a record of 30 years, minimum, is required (WMO, 1988). As a result, imageries covering the study area and spanning 31 years were extracted from the two sets to form a continuous record from 1981 to 2011. However, conformity analyses for similarity and continuity of the image data from the two sets were ensured before proceeding with further processing of the imageries.

3.1.5 Data Extraction and Processing

The remotely sensed data was extracted and processed using the following methods:

Extraction and processing of imageries: The imageries were processed with an Imagery Display and Analysis (IDA) GIS application software, known as Windisp 5.1, developed by FAO (1999). The NASA imageries can be displayed, processed and analyzed with this software but the VITO imageries have to be processed to IDA formats readable by Windisp 5.1. Hence, an application software called VGT Extract was used to extract the

imageries from VITO imagery files and imported into Windisp 5.1 for further processing and analysis.

The NASA image data comprised of NDVI dimensionless datasets stored as pixels. But the VITO image data was stored as eight bits per pixel (or Bytes) values between 0 and 255 that have to be converted to Physical Values (PV) using the Eq. 3.1 developed by Jacob et.al. (2010) below:

$$PV = (DN\ x\ \text{scale}) + \text{offset} \quad (3.1)$$

in which PV = Physical Value, DN = Digital Number, scale = 0.004 and offset = - 0.1.

Hence the real dimensionless NDVI values were derived from the equation. This conversion was done for all the VITO data set after extraction. The data sets were temporarily smoothed by NASA and VITO, to remove noise as a result of aerosols and cloud. The SPOT Vegetation data were gathered by Landsat 7's Enhanced Thematic Mapper Plus (ETM+) Sensors. The other set were obtained from Moderate Resolution Imaging Spectroradiometer (MODIS) carried aboard NASA Terra and Aqua Satellite.

The WinDisp 5.1 software was used to open each of the imageries of Africa (containing dekadel data) while the digitized map of NSSR was super imposed on, in order to extract the NDVI for the region alone. The extracted NDVI data in form of pixels, and ASCII format, were then imported into Excel Spreadsheet for further analysis such as computation of NDVI anomalies using Equation 3.2, in section 3.2, which was executed by applying command functions in Excel Spreadsheet. The data extracted for analysis were yearly dekadel NDVI and 31 year dekadel NDVI average. The extraction was done for the 7

synoptic stations in the study area and the average was computed for NSSR. Hence, the data were analyzed for each of the synoptic stations and at regional level.

Imagery similarity test: The two sets of imageries, that is NASA and VITO imageries were tested for similarity by using QQ Plot, that is, Quantile Quantile Plot in statistics. The plot should approximate a straight line such that the median of the two data sets are equal. The plot was obtained by plotting the cumulative values of average NDVI of NASA imageries against the corresponding cumulative values of VITO imageries for their overlapping years of records.

Validation of imageries: Image validation was achieved by using phonological metric approach devised by USGS (2011). The approach involves plotting an annual NDVI and observing if the rising part and point of inflexion for falling part of the curve correspond with the beginning of raining season/growing season and end of raining season, respectively. This is in accordance with the expectation that the NDVI, a measure of vegetative surface reflectance, values increase during the beginning of the rainy season and also, reduce during the end of the rainy season.

3.1.6 Processing of Meteorological Data

Homogeneity test: In order to ensure reliability of the meteorological data collected, they were analyzed for homogeneity. This is necessary because the manual method of collection could cause errors such as parallax that renders data unreliable, unlike the satellite based data that are collected by improved systems. Besides, the reliability of the data ought to be ensured before processing it for modelling and forecasting. Hence, in the study reported herein the relative homogeneity of the data was examined by the double

mass curve test, a commonly used data analysis approach for this purpose. Double mass curve was obtained by plotting the cumulative rainfall of each station (on y axis) against the cumulative average rainfall of the remaining 6 stations as a group (on x-axis), starting the current or recent year from the origin. It is expected that the data would plot as a straight line and the slope of this line will represent the constant of proportionality between the two quantities. A break in slope indicates a change in the constant of proportionality and hence, represents an inconsistency of the data over time.

Distribution test: In order to compare the distributions of the data series for all stations, the empirical cumulative distribution function plots of the data were plotted. The distribution test was applied to both the rainfall and temperature data of the seven stations under study. This was to check for correlation of the data sets and be sure of the data quality before modelling and using it for forecasting. The empirical cumulative distribution functions were computed using functions in Excel 2007 Spreadsheet. The computed values were then plotted to obtain empirical cumulative distribution function plots for each station.

3.2 METHODS

3.2.1 Analysis of Drought in the NSSR using NDVI Anomalies

The NDVI were analyzed at different time scales of 1 month (SPI_1), 3 months (SPI_3), 6 months (SPI_6), 12 months (SPI_12) and 24 months (SPI_24) using the percent NDVI anomaly. The percent NDVI anomaly for a particular dekad, *i,* deduced from Murad and Saliful (2011) is expressed as:

$$\epsilon = \frac{NDVI_i - NDVI_{mean}}{NDVI_{mean}} x100\% \qquad (3.2)$$

where, ϵ = percent NDVI anomaly, $NDVI_{mean}$ = average of dekadel (*i)* NDVI during the period of study.

The percent NDVI anomaly was processed for each of the dekad i.e., ten days, in the annual data extracted and plotted with respect to dekad ranging from the first dekad to the last dekad of the study period (totally an average of 3 dekads in a month x 12 months in a year x 31 years of study period = 1116 dekads). The graph obtained was analyzed with respect to drought occurrence in the region. The drought events in the region were classified by using Table 2.3; hence, negative percent NDVI anomalies implied drought events of different severity depending on the negative values.

Apart from the dekadel time scale, other time scales considered are monthly, wet season, dry season and annual time scales. The monthly percent NDVI anomaly was obtained by adding the three dekads in a month and dividing by 3. The seasonal values for wet and dry seasons were computed by averaging the total monthly records for the wet season and dry season percent NDVI anomalies, respectively. In the same way, the annual percent NDVI anomalies were obtained for all stations by adding and averaging the total monthly percent NDVI anomalies. Table 3.1 was used to classify drought in the region using NDVI anomalies. The NDVI anomalies at different time scales were compared to choose the one that reliably represents the NSSR drought situation and then compared with the ground-based index method.

3.2.2 Analysis of drought in the NSSR using Standard Precipitation Index

An application software, spi_sl_6.exe, was used to compute the SPI at different time scales (SPI_1, SPI_3, SPI_6, SPI_12, and SPI_24), using the precipitation data from the synoptic

stations using the approach devised by NDMC (2010). The input file was prepared with all the data for one station in the following column format:

Header

yyyy mm pppp

in which, Header = a string which described the name of the station, yyyy = year, mm = month (in digit format 1,2,3 etc), pppp = precipitation multiplied by 100. The yyyy mm and pppp were separated by space. This file was named stdin (with no extension) and saved in the same directory as the SPI program. The directory was accessed at the DOS prompt by typing SPI and then uploading the file (stdin). The SPI time scales were specified before running the program. The output was automatically written to a file, stdout (in the same directory). The output of the program was in the following format:

Header

yyyy mm spi1 spi3 spi6 spi12 spi24

in which, yyyy and mm are as before, spi1 = SPI for a 1 month rainfall total, spi3 = SPI for a 3 month rainfall total, spi6 = SPI for a 6 month rainfall total, spi12 = SPI for a 12 month rainfall total, spi24 = SPI for a 24 month rainfall total.

The time series of the output SPI at different time scales were then plotted for comparison and further analysis of drought in the study area. Droughts were identified as negative SPIs for the different time scales and then classified using Table 2.2. The SPI at different time scales were compared to select a time scale that could be compared with the NDVI chosen anomaly method.

3.2.3 Temperature and Rainfall Analysis

Annual records of monthly mean temperature from 1979 to 2008 for all stations were averaged to get representative annual monthly mean records (1979-2008), from which annual monthly mean records (1979-2008) were computed for the region of study. The annual mean values were plotted against the corresponding years to observe the trend over years. The rainfall record was analyzed by adding total rainfall in each year and then the annual time series was plotted so as to establish rainfall trend during the period of study and relate it to drought occurrences.

3.2.4 Comparison of SPI and NDVI Anomalies

Having selected suitable NDVI and SPI time scales in section 3.2.1 and 3.2.2, respectively, the two indices were compared with respect to yearly accumulated negative values of SPI and NDVI anomalies which were drought indicators and, drought severity identified by each index using their respective classification in Tables 2.2 and 2.3. The computation of the yearly accumulated negative SPI was done by adding up all the negative SPI in each year. The same approach was applied to obtain the yearly accumulated NDVI anomalies. In the case of drought severity, three cases considered were very severe, severe and moderately severe droughts with respect to severity thresholds defined in Tables 2.2 and 2.3 for SPI and NDVI anomalies, respectively.

3.2.5 Degree of Spatial Drought Occurrence Analysis

The spatial drought occurrence was determined using statistical methods. The long term NDVI pixels were analyzed for each of the stations and the entire study area. The statistical parameters considered were, namely: range, mean and standard deviation of the stations'

NDVI. The statistical parameter values were compared from one station to another using the regional statistical parameters as the reference standard.

The spatial-temporal drought distribution was represented in maps produced by overlaying the digitized map of NSSR on average monthly dekadel NDVI anomalies of Africa. The region of interest, that is, NSSR was clipped from the imagery after which labelling was applied. This process was done for imagery collected during drought and vegetative periods for comparison. The maps of drought spatial distribution were compared with the statistical analyses to classify the region into drought risk zones.

3.2.6 Seasonal Drought Pattern Analysis

The long term average of 31 year NDVI record for each of the station was plotted on the same graph with the 31 year average record of the region for comparison.

3.2.7 Development of Predictive Models for Drought Management in NSSR

The main focus of this research is to proffer effective management of the incessant drought in the NSSR. In order to achieve this, a system should be put in place that can be used to forecast drought some months (at least) ahead. Towards this end, Auto Regressive Integrated Moving Average (ARIMA) stochastic models were developed for forecasting purpose; in this case, multiplicative Seasonal ARIMA models were considered to take care of the seasonal periodicity. The identified index from SPI and NDVI time scale series, which was suitable for drought early warning system and real-time drought forecasting was used to develop drought forecasting models for the NSSR by applying the following steps:

Model identification: This involves identifying suitable models from the families of ARIMA/SARIMA models and selecting the orders of non-seasonality and seasonal

parameters, (p,q and P, Q respectively) of the selected models. The parameters of the models were identified from the ACF and PACF plots using XLSTAT program.

ACF and PACF generation: After opening the program, the "Time" appearing on the toolbar was selected to choose "Descriptive Analysis" from a drop down menu. By clicking the "Descriptive Analysis", a page (or window) was displayed for entering a station's SPI_1 time series prepared in excel spreadsheet. After clicking OK, ACF and PACF graphs of the data set were generated. The graphs were then analyzed for trend, seasonality and necessary differencing, and model parameters for the ARIMA/SARIMA modeling. Numbers of significant spikes in the ACF and PACF structures were used to identify the orders of Moving Average (MA) and Auto Regressive (AR) parameters respectively, in the ARIMA/SARIMA models. The values of the parameters were regarded as the maximum limits; this allows for trials of a number of suitable models with parameters less than and equal to this limits by the program and the program would generate suitable models out of a number of trials. The same process was repeated for temperature time series.

Nevertheless, Abiodun et. al., (2011) studied the future climate of Nigeria downscaled from Global Circulation Models (GCM) and observed a future trend of 0.02^0C/annum increase in temperature. However, their study reflected no specific trend in future rainfall anomalies. The positive trend in temperature in the region, as a result of climate change, was removed by logging, i.e., by finding the natural logarithmic of the series after which the logarithmic transformed time series was processed similarly as described for SPI_1 above.

Modelling within parameters limits: After opening XLSTAT program, the "Time" appearing on the toolbar was selected to choose "ARIMA" from a drop down menu. By clicking "ARIMA" a page was displayed for entering a station's SPI_1 time series in excel format and supplying maximum values of the model parameters identified from ACF and

PACF above. After clicking OK, the computer program simulates different possible models; the models and respective graphs, and goodness of fit measures were generated. The program could also estimate the values of the parameters for inclusion in the mathematical models in place of the graphs. The same process was repeated for the transformed temperature time series.

Model parameters estimation: Parameters of all identified models above were estimated and generated using the same package, XLSTAT.

Model diagnostics: Different models identified can be of various combinations of AR and MA individually and/or collectively. The best model was selected based on (Khadr, 2011):

i. Akaike Information Criteria (AIC) and
ii. Schwarz-Bayesian Information Criteria (SBC)
iii. Sum of Squared Errors (SSE) of Prediction

Models with the lowest AIC, SBC and SSE were selected as suitable models. In addition to using model goodness of fit measures (AIC and SBC), other measures, such as least square based measures (e.g., SSE) was used to evaluate model qualities and ascertain goodness of fit.

Plot of residuals' ACF and PACF: After fitting the appropriate model, the goodness of fit of the model was examined by plotting the ACF and PACF of the residuals. If the fitted models are adequate, the residuals should be approximately white noise, that is, the residuals should have zero mean and uncorrelated. The ACF and the PACF of the residuals were plotted using Minitab 16 statistical software.

Residual normality tests: Histogram and normal probability plots were used for judging the normality of a distribution of residuals. The histogram plot was obtained by distributing the data in regularly-spaced cells and plotting each cell frequency versus the center of the cell. The normal probability plot should produce an approximately straight line if the points come from a normal distribution. Both the histograms and normal probability plots were produced with Minitab 16 statistical application software.

The same process of model identification was applied to temperature data to obtain suitable models for temperature forecasting in the region

3.2.8 Model Validation and Forecasting

Suitable models were used to predict corresponding time series data from the observed/computed index and temperature. The predicted time-series data were then used to forecast index and temperature monthly values into the future for a period of 1 year, that is, short time forecasting. A future trend of 0.02^0C/annum increase in temperature was incorporated into the temperature forecasts in accordance with Abiodun et. al., (2011) study which projects a consistent increase of $+0.20^0$C per decade in the future climate of Nigeria downscaled from Global Circulation Models (GCM). Short time forecasting was proposed for managing the NSSR drought because it is usually applied to time series which do not change dramatically very quickly (Khadr, 2011). The suitable models were validated using available data. This was to determine the reliability of the selected models for drought forecasting. The process involved comparing available actual data series with the forecast data series to see how the models actually simulate the actual observation.

3.2.9 Performance Criteria

Root Mean Square Error (RMSE) and Sum of Square for Errors (SSE) were applied as performance criteria for model validation. RMSE and SSE were computed for the forecast residuals to ascertain the goodness of fit between the observed data and forecasts.

3.2.10 Developing a Drought Management Plan for NSSR

The drought management plan proposed in this study has three phases:

Drought monitoring: Drought monitoring phase involves the use of the selected models for monthly drought forecasting. The forecast data series were then assessed and compared with the drought classification parameters of the identified suitable drought index to determine the likely occurrence of drought for the forecast period. Measures to be taken to reduce the adverse effect were suggested

Drought warning: Thresholds were defined for the selected drought predictive models such that the monthly forecast data series could be compared with. A drought warning would be declared if the negative value of the threshold was lower than the negative forecast monthly index. Measures to be taken to reduce the adverse effect were suggested

Drought emergency: Drought emergency were declared when conditions under drought warning were observed to progress for two or more consecutive months as forecasted by the models using the thresholds. Also, measures to be taken to reduce the impact of drought were suggested.

CHAPTER FOUR

RESULTS AND DISCUSSION

4.1 DIGITIZATION OF NIGERIAN SUDANO-SAHELIAN REGION

The map produced from the digitization of the study area is shown in Figure 4.1. As shown, the NSSR consists of most parts of northern states in Nigeria. The map was overlaid on the imageries of Africa to extract NDVI pixels of the study area for analyses as discussed in subsequent sections

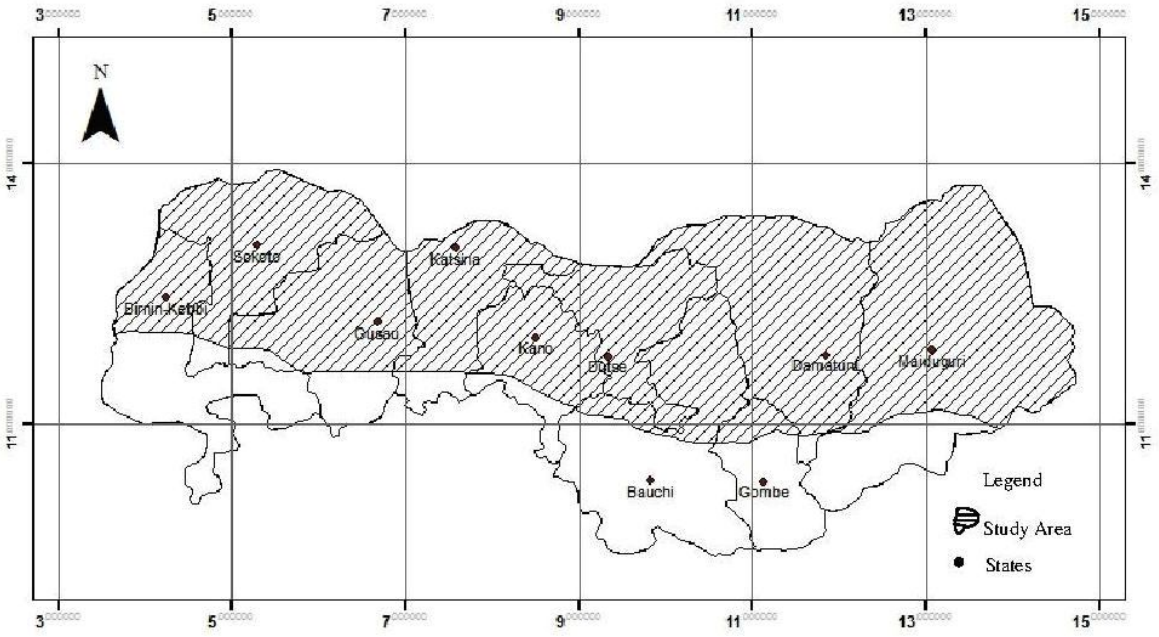


Figure: 4.1 Digitized Study Area: Nigeria Sudano Sahelian Region

4.2 DATA EXTRACTION AND PROCESSING

The imageries were extracted using the application softwares discussed in section 3.2, Chapter 3 and, the results obtained from the processing of the imageries are discussed as follows:

4.2.1 Imageries Similarity Test

Figure 4.2 represents the results of NASA and VITO imageries similarity test and the figure shows that the trend of VITO imageries is directly proportional to that of NASA.

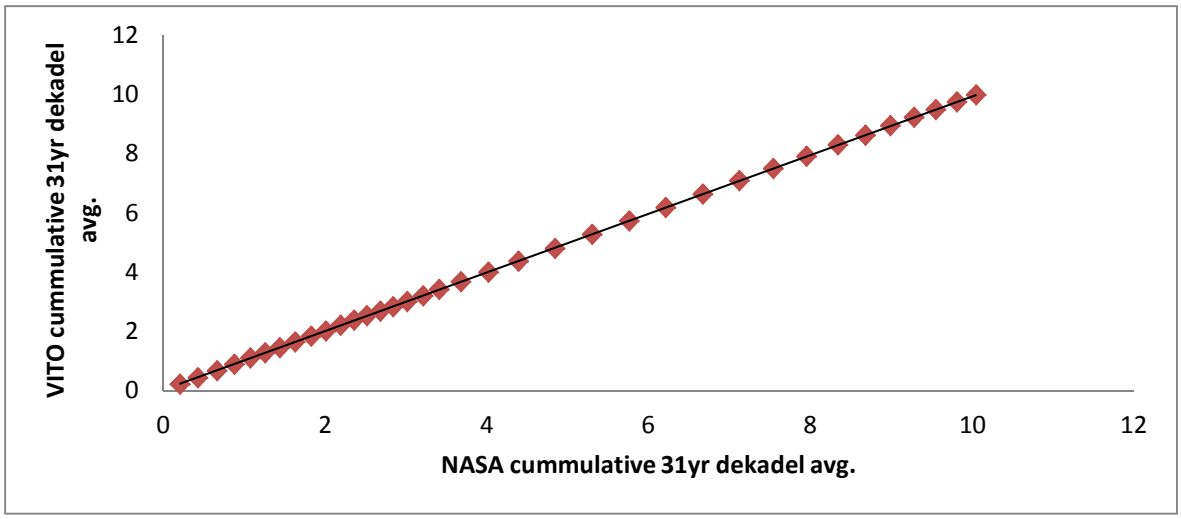


Figure 4.2: Similarity Test for NASA and VITO Imageries

The figure shows that the two data sets are similar, since the plot approximately plots as a straight line. This implies that the median of NASA imageries approximately equal to the median of the VITO imageries. Also, quantiles from the former approximately equal to the corresponding quantiles of the latter.

4.2.2 Validation of Imageries

Figure 4.3 presents the result of imageries validation using phonological metric and reflects that the trends of VITO and NASA dekadel NDVI are similar. Figure 4.3 indicates that the rise in NDVI average graph corresponds to the beginning of the rainy season, which is May, and the fall in NDVI average occurs during the end of the rainy season, September in the region.

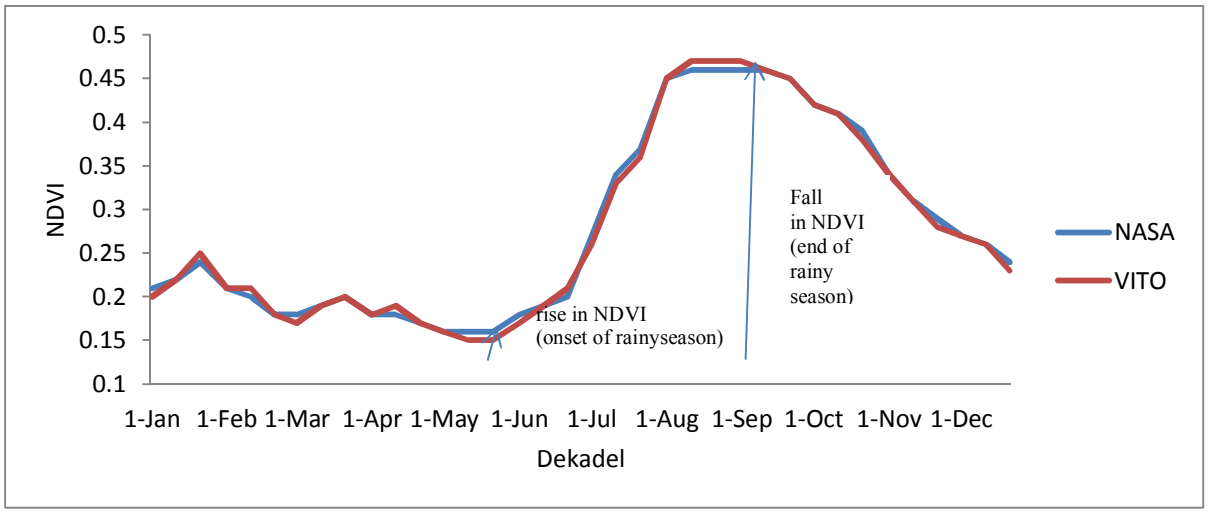


Figure 4.3: Validation of imageries using phonological metric

4.3 PROCESSING OF METEOROLOGICAL DATA

4.3.1 Homogeneity Test

Figures 4.4a and 4.4b show the results of homogeneity tests of rainfall for Sokoto and Katsina Stations, respectively. Homogeneity test results for Temperature at Sokoto and Katsina Stations were represented in Figs. 4.4c and 4.4d, respectively. The homogeneity tests of rainfall and temperature for the other stations were reflected in Appendices A and B respectively. As shown in Figs. 4.4a and 4.4b rainfall records of Sokoto and Katsina Stations were very consistent and homogeneous as the data sets approximately plotted as straight lines. From Figs. 4.4c and 4.4d, one can conclude that the temperature records were consistent for all the stations in the region under study. The graphs of homogeneity tests for the other stations as presented in Appendices A and B for rainfall and temperature respectively, were consistent and homogeneous for all the stations.

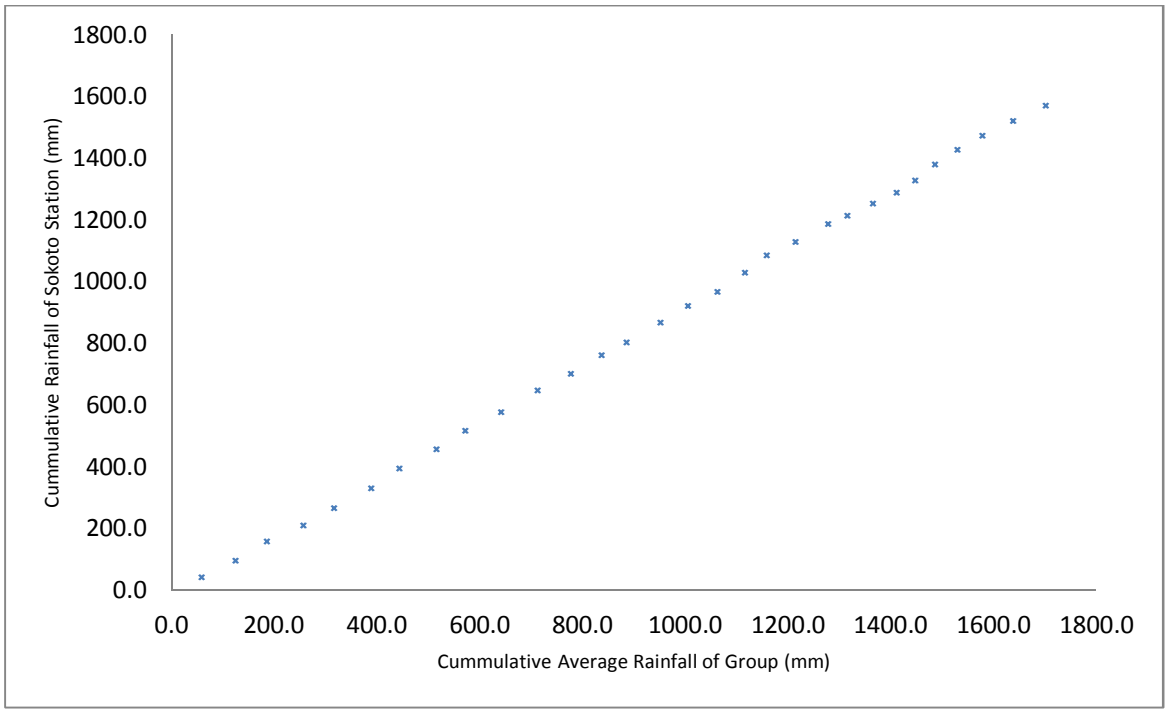


Figure 4.4a**:** Cumulative precipitation for Sokoto Station vs other stations (1979-2008)

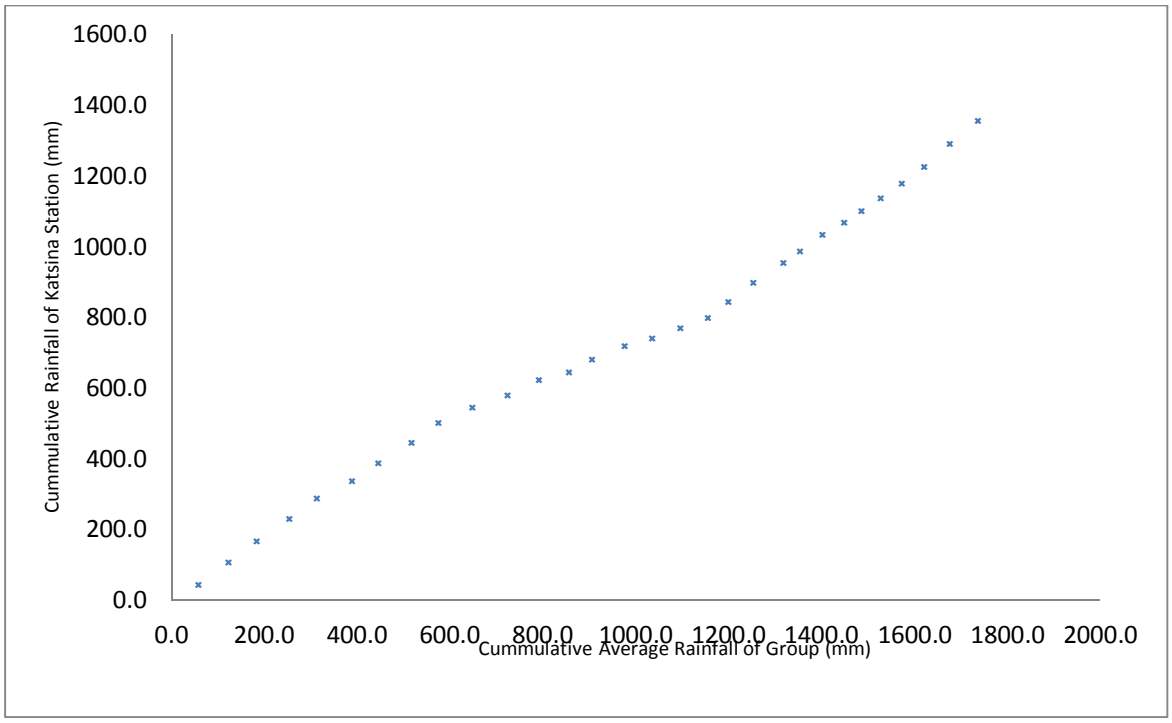


Figure 4.4b**:** Cumulative precipitation for Katsina Station vs other stations (1979-2008)

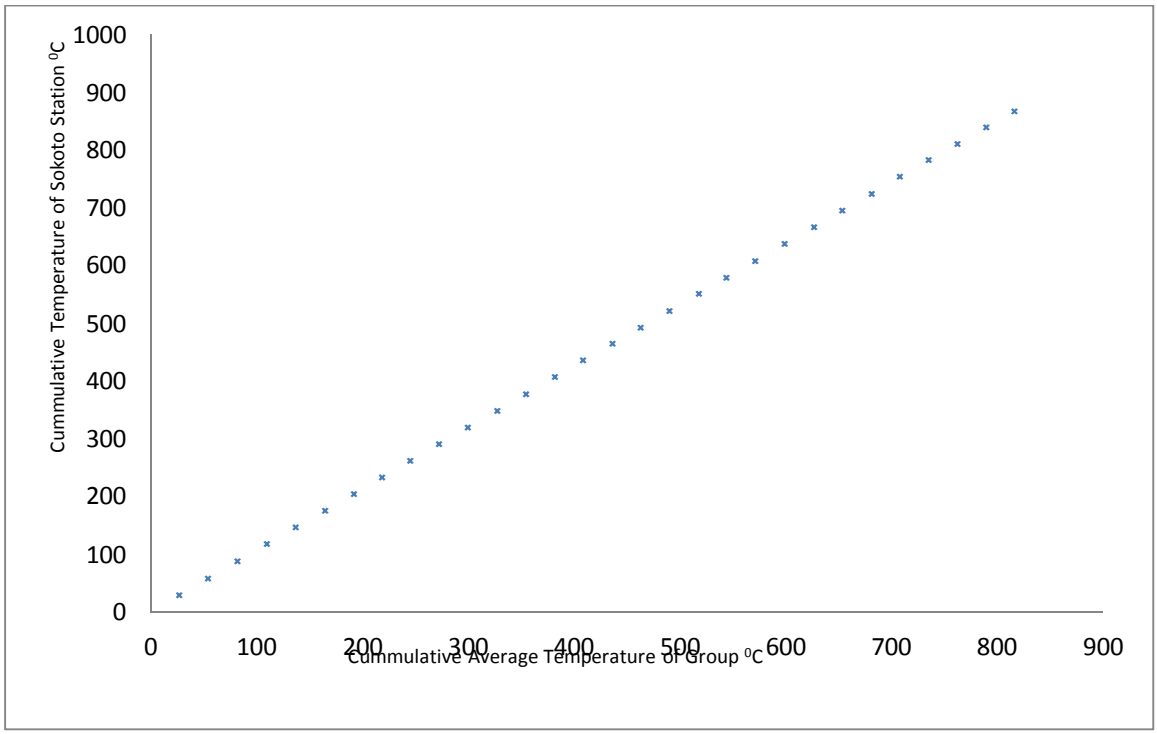


Figure 4.4c**:** Cumulative temperature for Sokoto Station vs other stations (1979-2008)

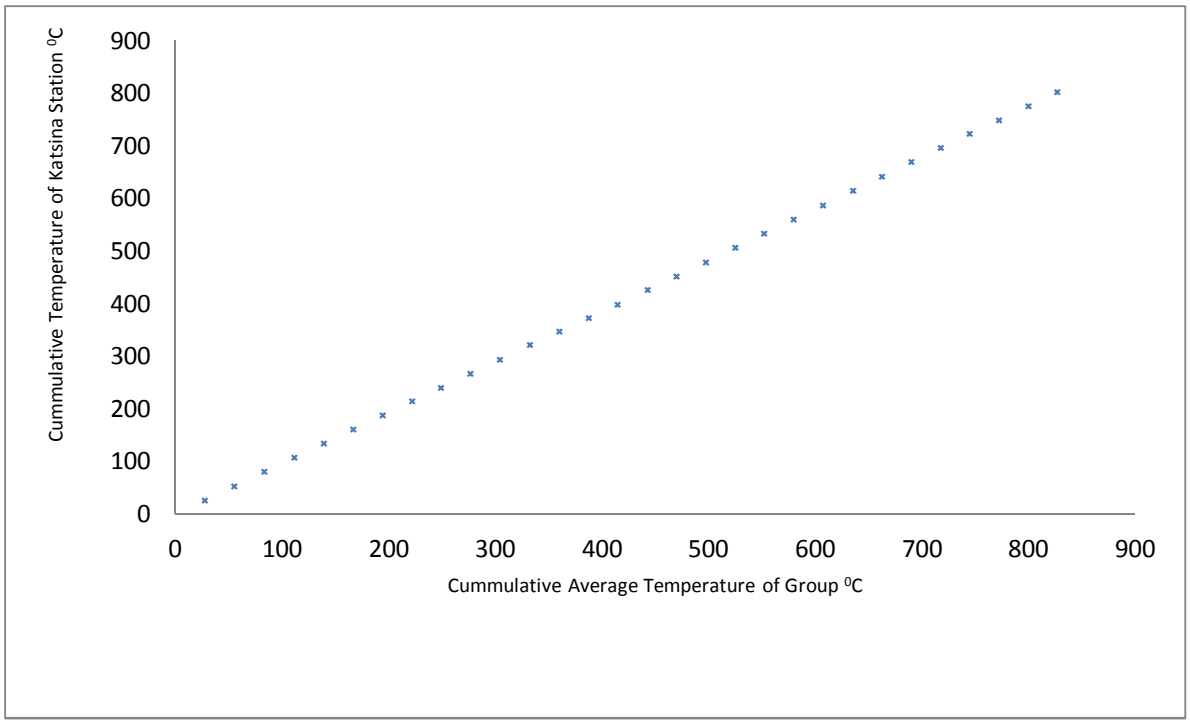


Figure 4.4d**:** Cumulative temperature for Katsina Station vs other stations (1979-2008)

4.3.2 Distribution Test

Figures 4.5a and 4.5b reflect rainfall data distribution test results while Fig. 4.5c and 4.5d present temperature distribution test results for Sokoto and Katsina Stations, respectively. Rainfall and temperature distribution test results for other stations were presented in Appendices C and D, respectively. The rainfall records at Sokoto and Katsina stations reflect the same distribution as presented in Figs. 4.5a and 4.5b. The same distribution trend was noticed in temperature data at the two stations as shown in Figs. 4.5c and 4.5d. The distribution test results of rainfall and temperature for other stations reflected the same trend as presented in Appendices C and D, respectively.

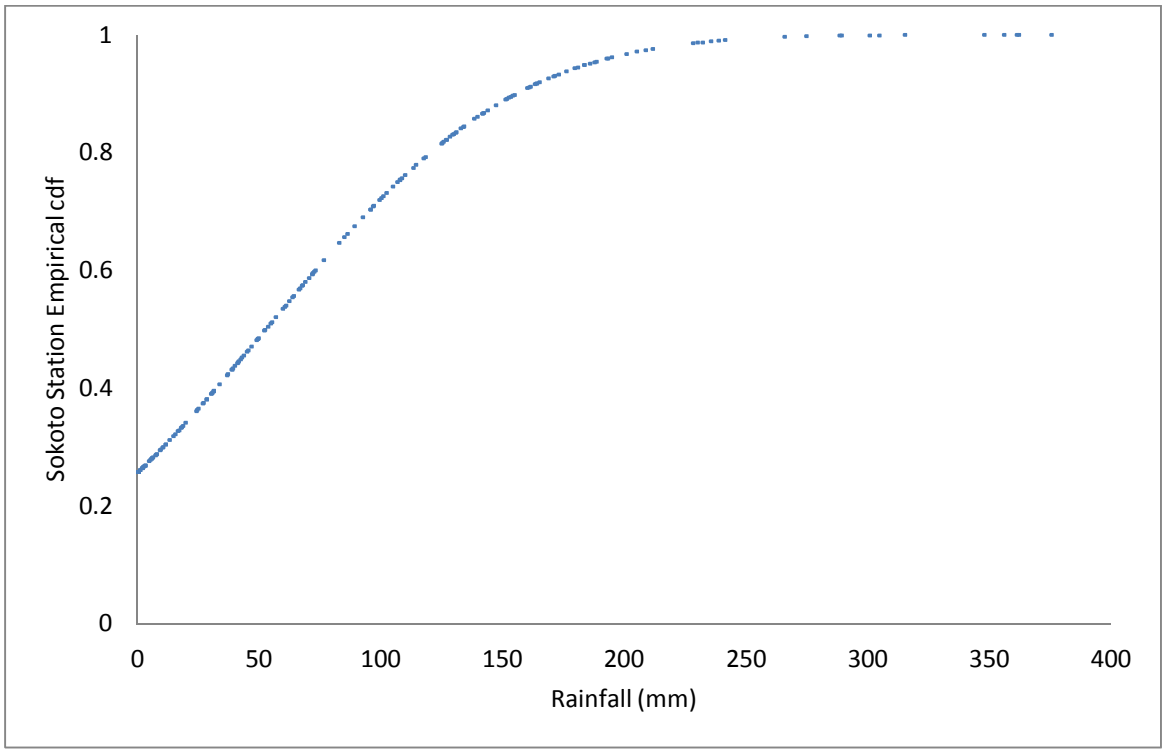


Figure 4.5a**:** Empirical cumulative distribution function (cdf) for Sokoto Station precipitation data Series (1979 2008)

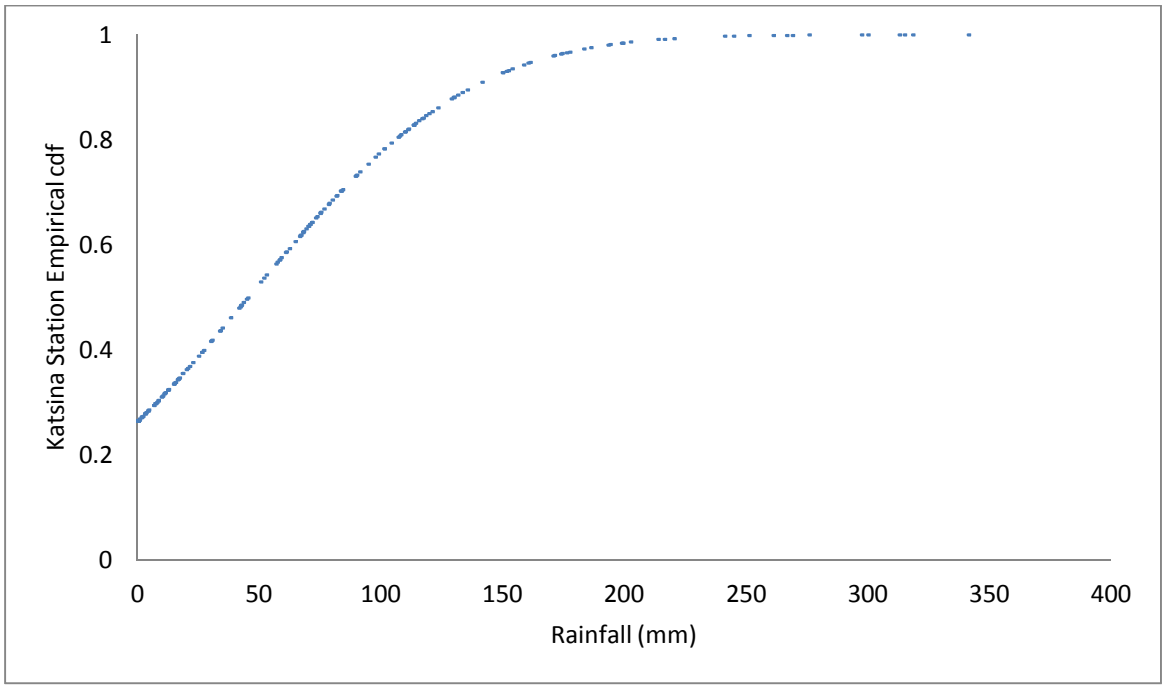


Figure 4.5b**:** Empirical cumulative distribution function (cdf) for Katsina Station precipitation data Series (1979-2008)

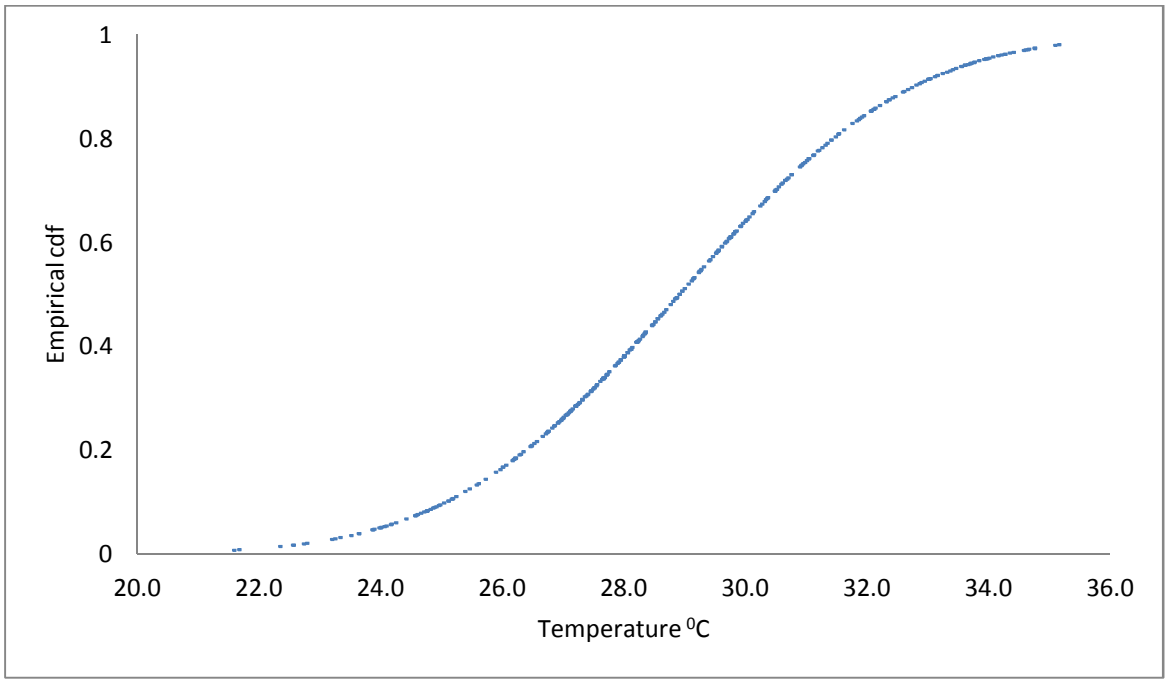


Figure 4.5c: Empirical cumulative distribution function (cdf) for Sokoto Station temperature data Series (1979-2008)

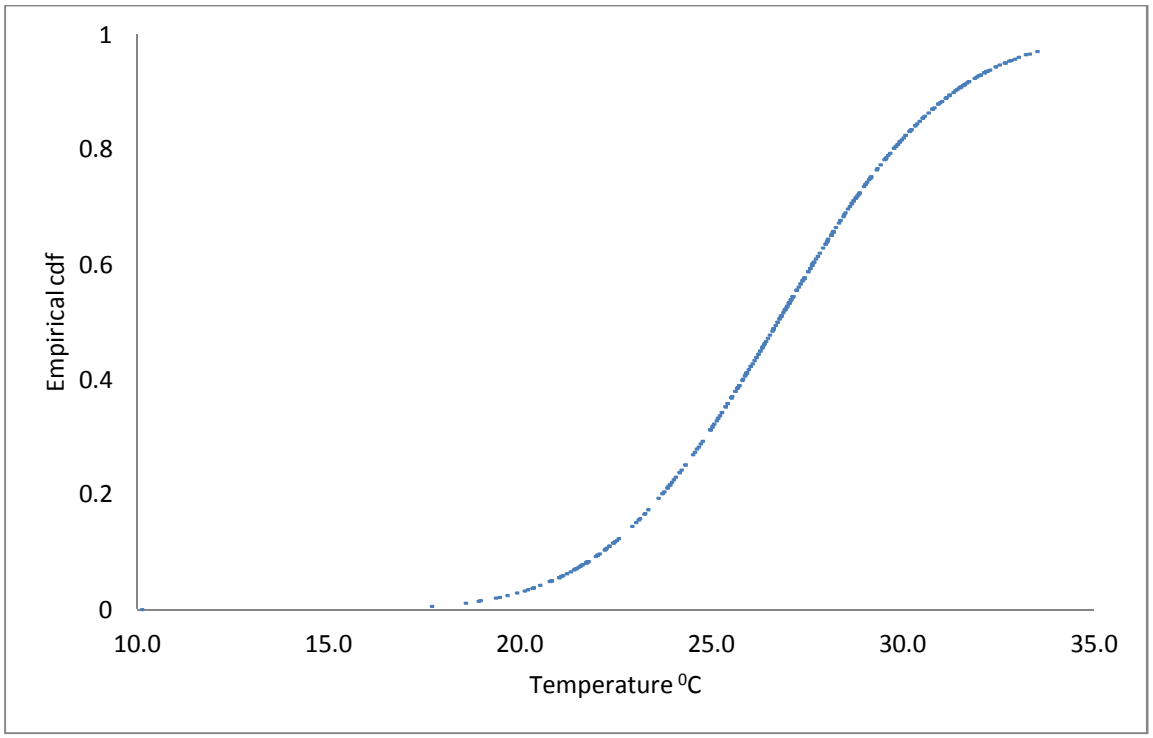


Figure 4.5d: Empirical cumulative distribution function (cdf) for Katsina Station temperature data Series (1979-2008)

4.4 DROUGHT ANALYSIS IN NSSR REGION BASED ON PERCENT NDVI ANOMALIES

Figures 4.6a to 4.6e show NSSR percent NDVI anomalies at different time scales.

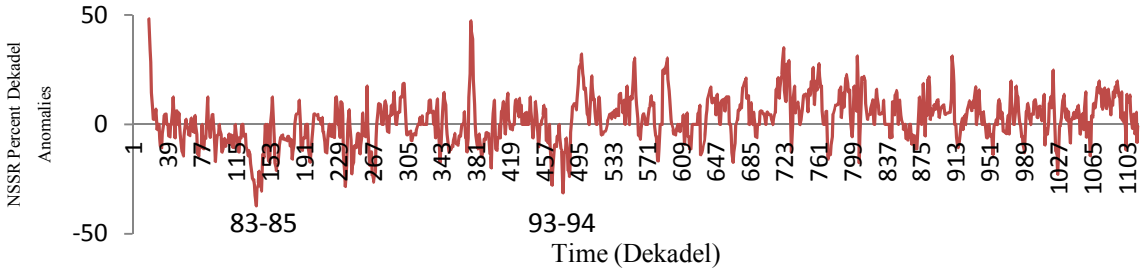


Figure 4.6a: NSSR Percent Dekadel Anomaly Trend

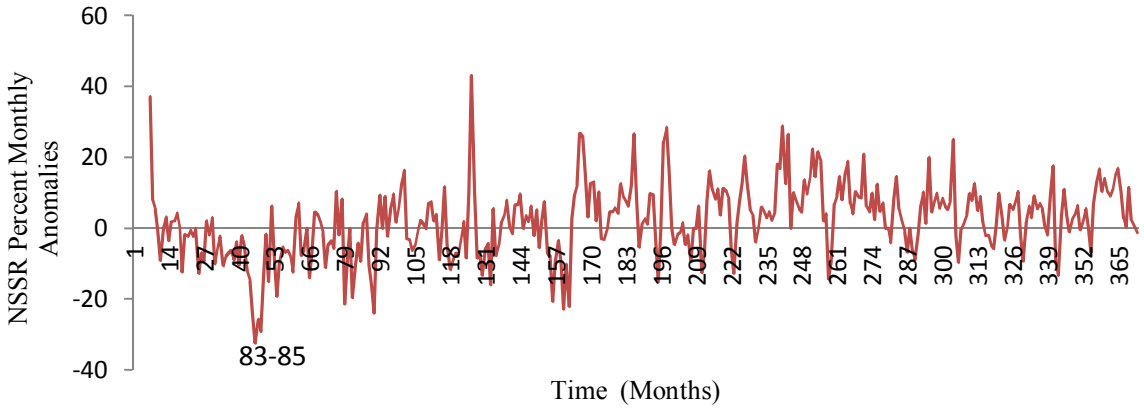


Figure 4.6b: NSSR Percent Monthly Anomaly Trend

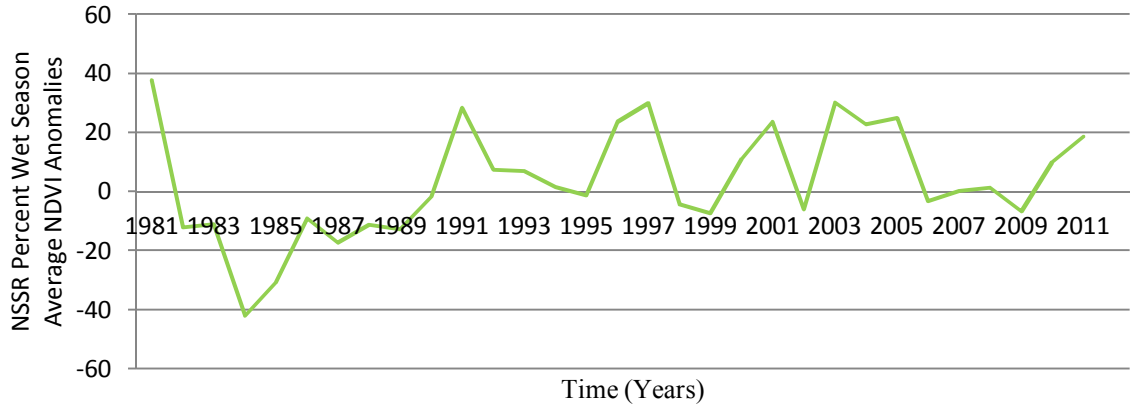


Figure 4.6c: NSSR Percent Wet Season Average NDVI Anomaly Trend

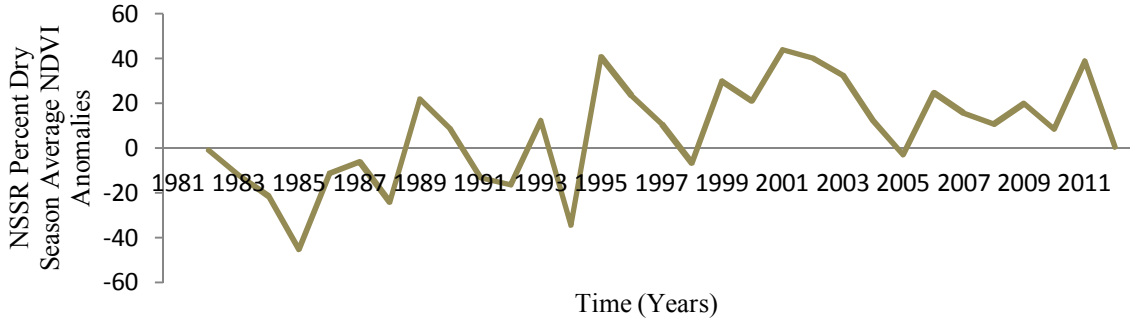


Figure 4.6d: NSSR Percent Dry Season Average NDVI Anomaly Trend

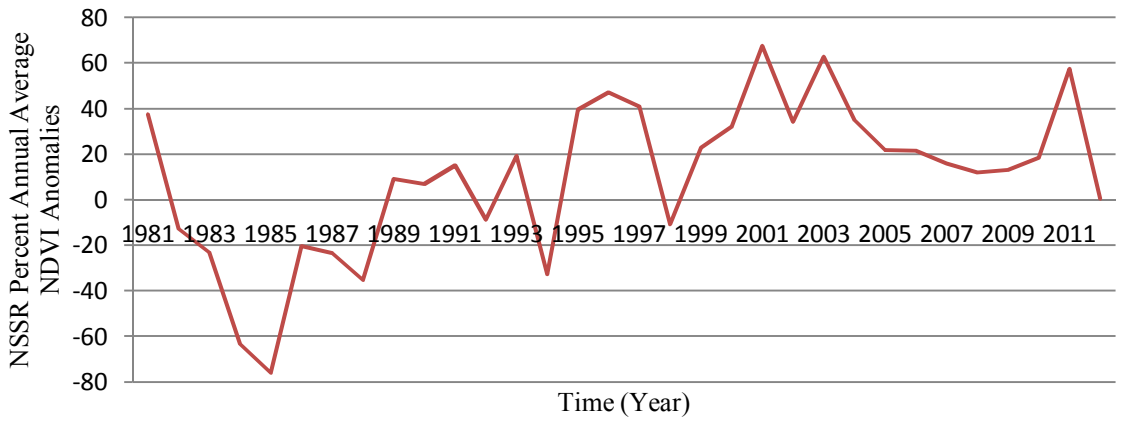


Figure 4.6e: NSSR Percent Annual Average NDVI Anomaly

The percent NDVI anomalies were obtained for the period under study by using Eq. 3.2, chapter 3. The graph of the anomalies with respect to the dekadels gives a picture of drought trend in the region. Fig. 4.6a reflects that the Nigerian Sudano-Sahelian Region had experienced a lot of drought events of different magnitudes and intensities from 1981 to 2011. The various drought classes are slight drought (0 to -10% percent anomalies), moderate drought (-10 to -20% percent NDVI anomalies), severe drought (-20 to -30% percent NDVI anomalies) and very severe drought (percent NDVI anomalies $\leq$ - 30%). Fig. 4.6a shows that the period of worst drought in the region is from first dekad of July, 1983 to last dekad of March 1985 with the peak of -37% in the last dekad of October 1984. This observation confirms drought episode of 1984 to 1985 as stated by Medugu (2007). This is another lengthy drought observed in NSSR after those of 1911-1914 and 1951-1954. Nevertheless, the very severe drought of 1983-1985 was preceded and succeeded by slight to moderate drought at different time and duration as shown in Fig. 4.6a.

The second observed 'very severe' drought, although of smaller magnitude, shorter duration and low intensity, was in October, 1993 - July, 1994 with its peak in April 1994. It

is worth mentioning that the drought of 1983-1984 was mainly during the dry season probably due to insufficient annual rainfall in the preceding wet season(s). Also, severe drought events noticed in the region during the period of study were those of 1984, 1985, 1987, 1988, 1993, 1994 and 2009. However, the severe drought event of shortest duration was that of 2009 occurring between the first dekad of June to the first dekad of August, 2009 probably as a result of delay in the year seasonal rainfall. Moreover, there are slight to moderate drought episodes in between the stated drought events as shown in Fig. 4.6a. In order to have an in depth understanding of the representation of the historic drought patterns and events in the region at different time scale, for effective drought management, the percentage decade anomalies were presented graphically using different time scale. Hence, the other time scales apart from the dekadel analysis were the monthly, wet season, dry season and annual percentage average NDVI anomalies as presented in Figs. 4.6b, 4.6c, 4.6d and 4.6e respectively.

The monthly average percent dekadel graph, shown in Figs. 4.6b, reflects the 'very severe' drought of 1983-1985, but masked the 'very severe' drought event of 1993-1994 and severe drought of 2009, although of short duration, magnitude and low intensity. The same trend is observed in Figs. 4.6c, 4.6d and 4.6e. Figure 4.6c shows the drought of 1983-1985 and undermines the remaining drought events mostly as slight drought episodes (0 to -10%) while Fig. 4.6d reflects both the 'very severe' drought episodes. The drought of 1993-1994 occurred during the dry season, this justifies its observed absence and presence in Figs. 4.6c and 4.6d, respectively. In similar manner, Fig. 4.6e presents a false impression as if the region had not been experiencing slight and moderate drought events from 1999 to 2011, unlike Fig. 4.6a that shows drought events on dekadel time scale and reflects drought of

whatever low intensity or magnitude. This implies that dekadel time scale is a suitable scale for developing predictive models for drought early warning systems and real time drought management.

4.5 DROUGHT ANALYSIS IN NSSR STATIONS BASED ON PERCENT NDVI ANOMALIES

Figures 4.7a to 4.7g, 4.8a to 4.8g and 4.9a to 4.9g show the percent dekadel NDVI, percent monthly NDVI and percent annual NDVI for the stations.

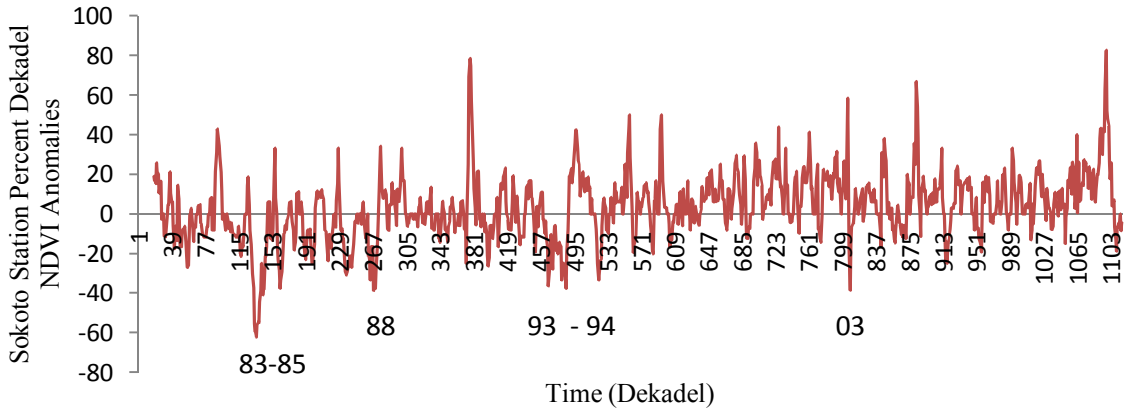


Figure 4.7a: Sokoto Station Percent Dekadel NDVI Anomaly Trend

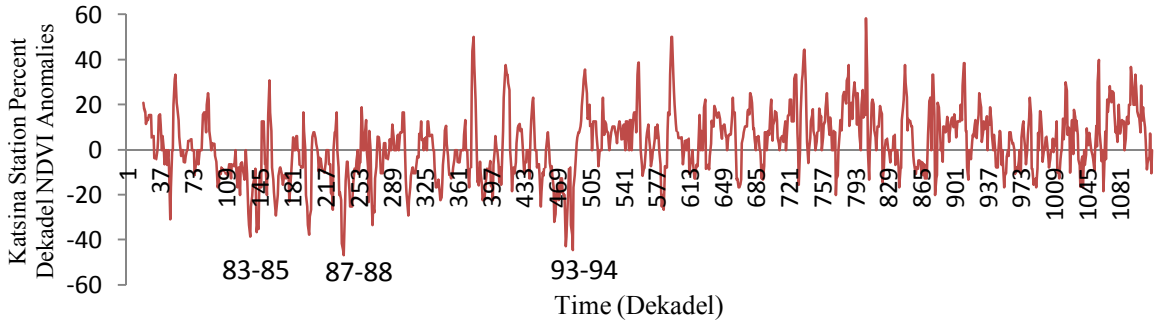


Figure 4.7b: Katsina Station Percent Dekadel NDVI Anomaly Trend

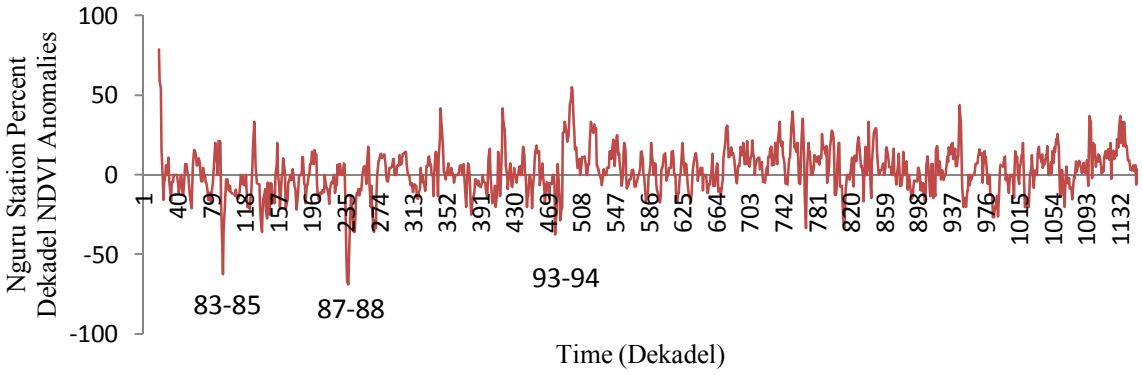


Figure 4.7c: Nguru Station Percent Dekadel NDVI Anomaly Trend

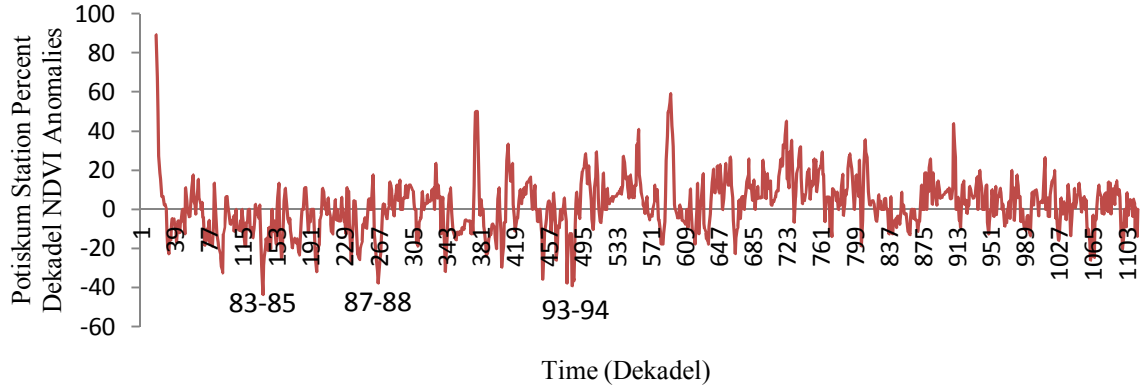


Figure 4.7d: Potiskum Station Percent Dekadel NDVI Anomaly Trend

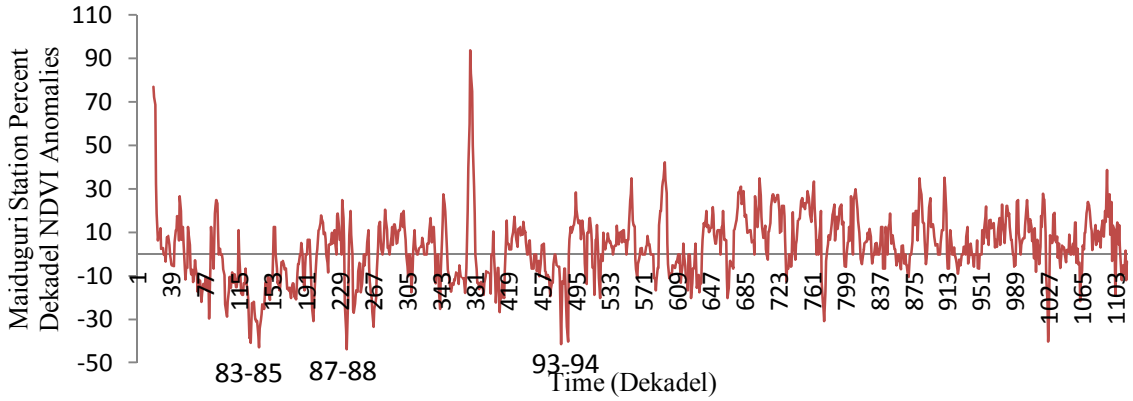


Figure 4.7e: Maiduguri Station Percent Dekadel NDVI Anomaly Trend

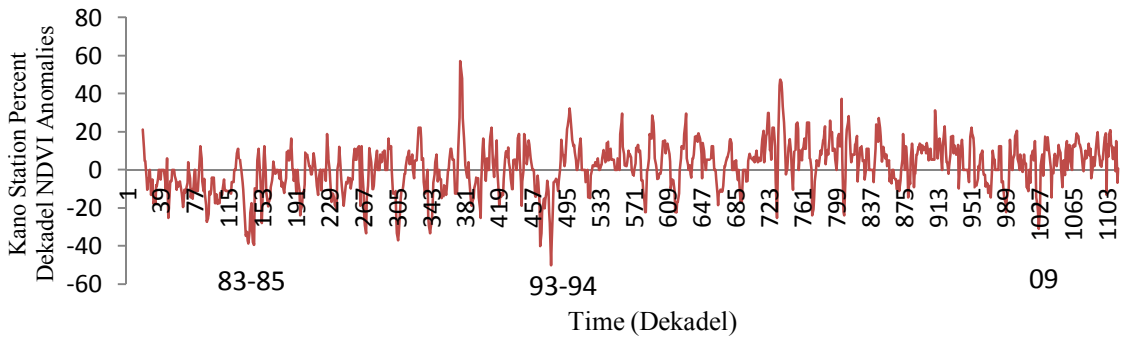


Figure 4.7f: Kano Station Percent Dekadel NDVI Anomaly Trend

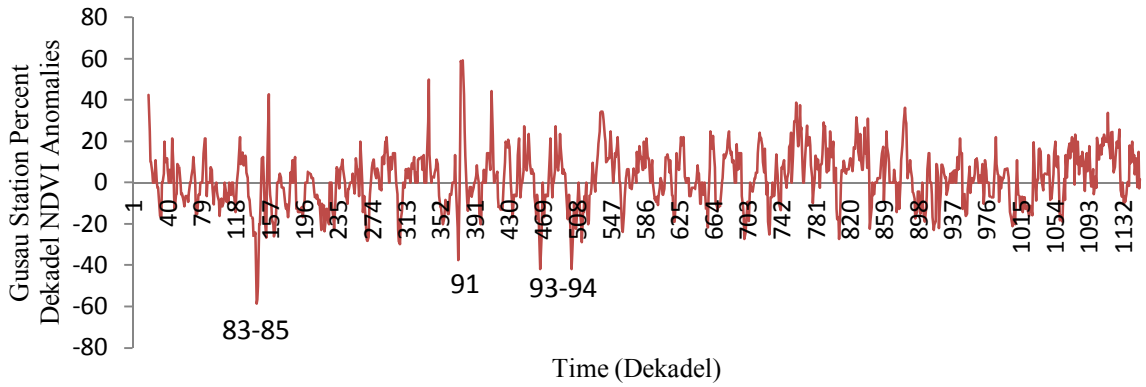


Figure 4.7g: Gusau Station Percent Dekadel NDVI Anomaly Trend

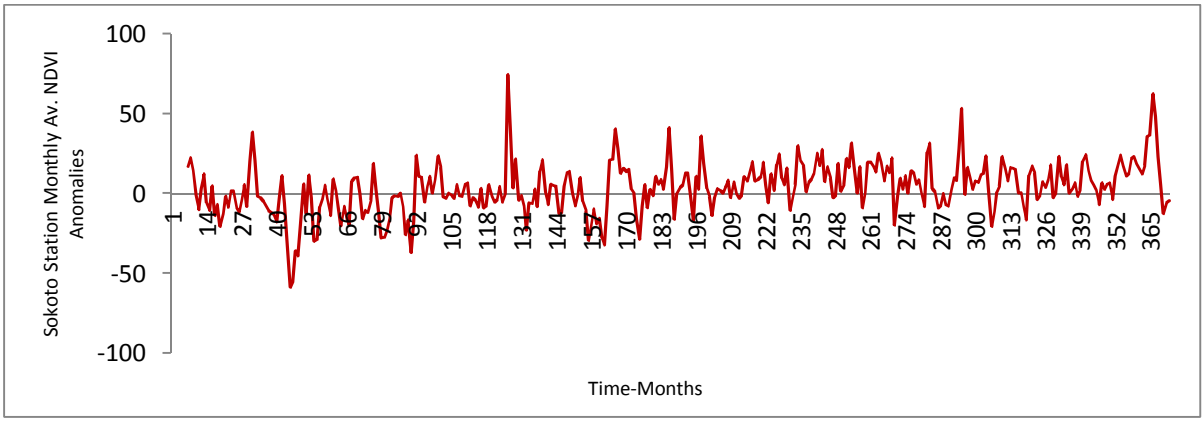


Figure 4.8a: Sokoto Station Percent Monthly NDVI anomalies

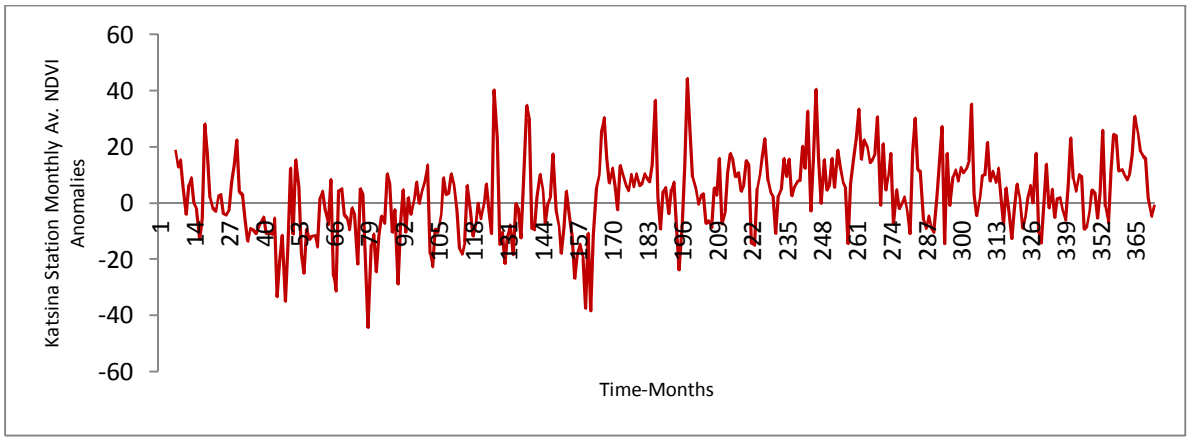


Figure 4.8b: Katsina Station Percent Monthly NDVI anomalies

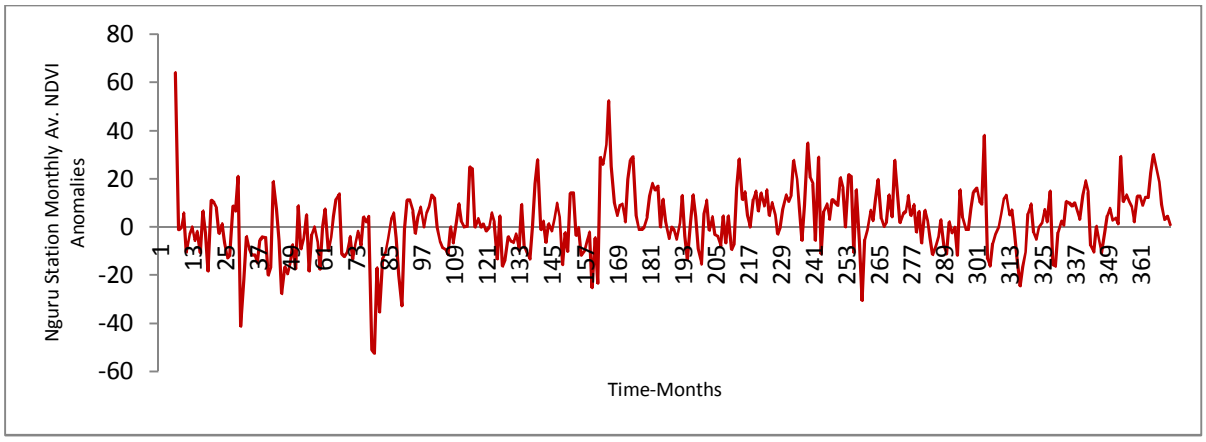


Figure 4.8c: Nguru Station Percent Monthly NDVI anomalies

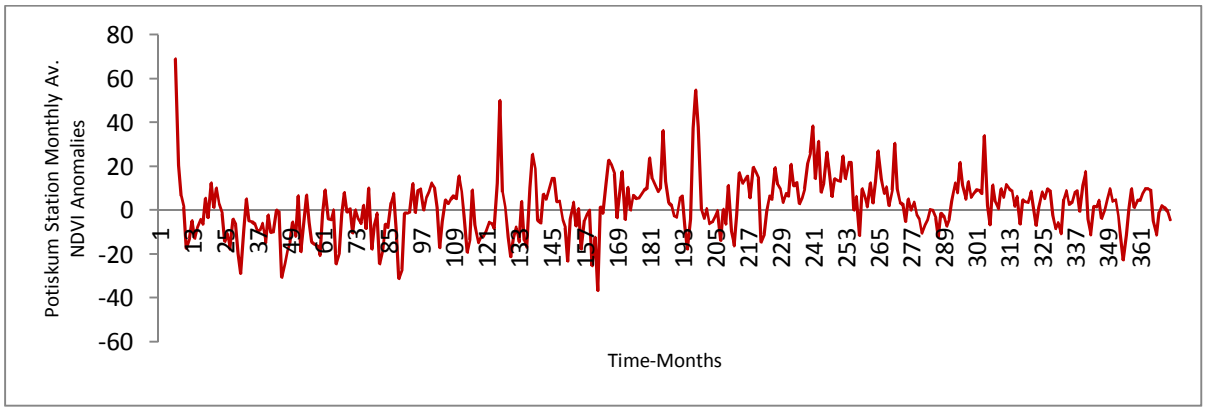


Figure 4.8d: Potiskum Station Percent Monthly NDVI anomalies

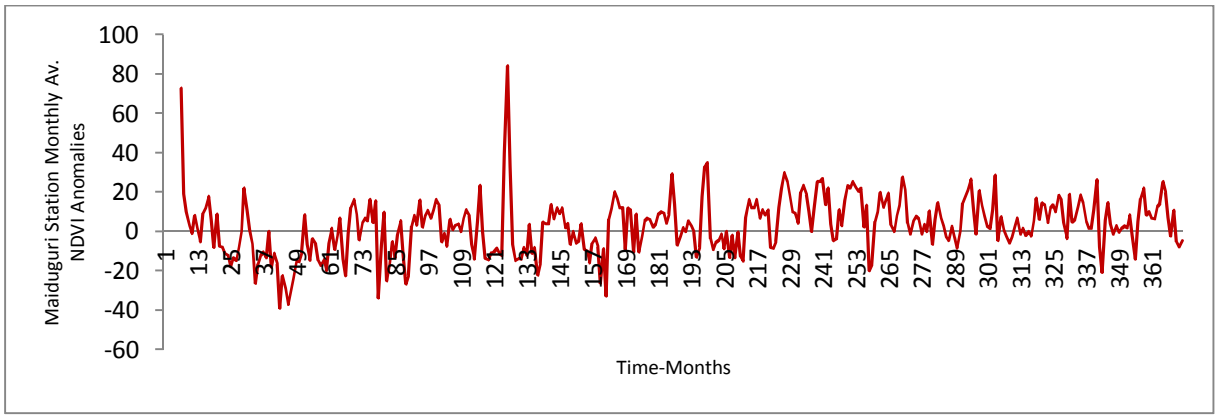


Figure 4.8e: Maiduguri Station Percent Monthly NDVI anomalies

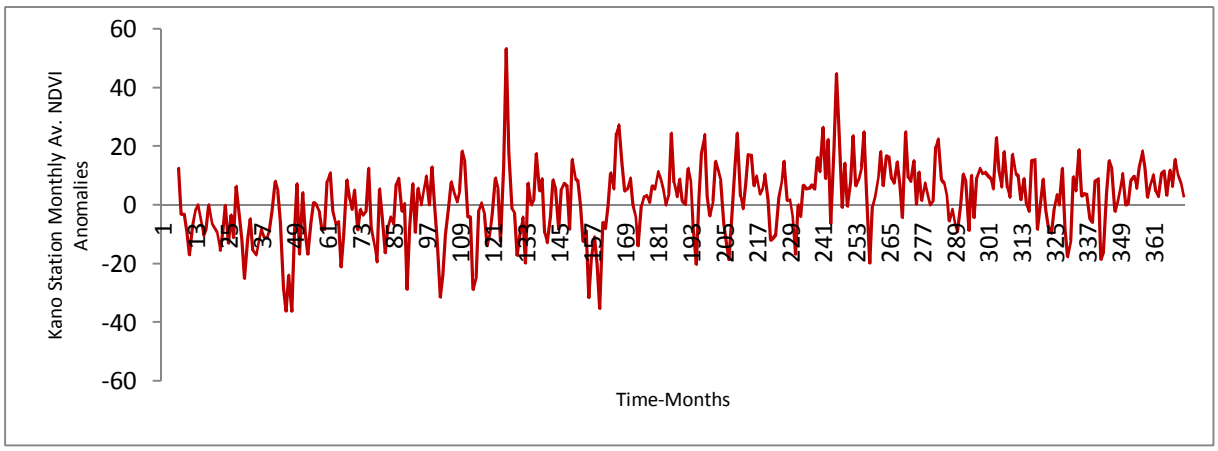


Figure 4.8f: Kano Station Percent Monthly NDVI anomalies

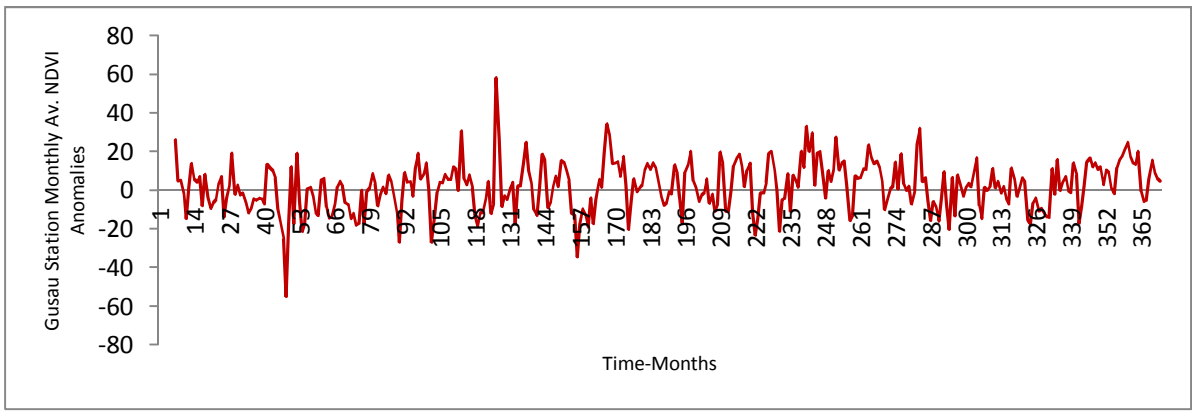


Figure 4.8g: Gusau Station Percent Monthly NDVI anomalies

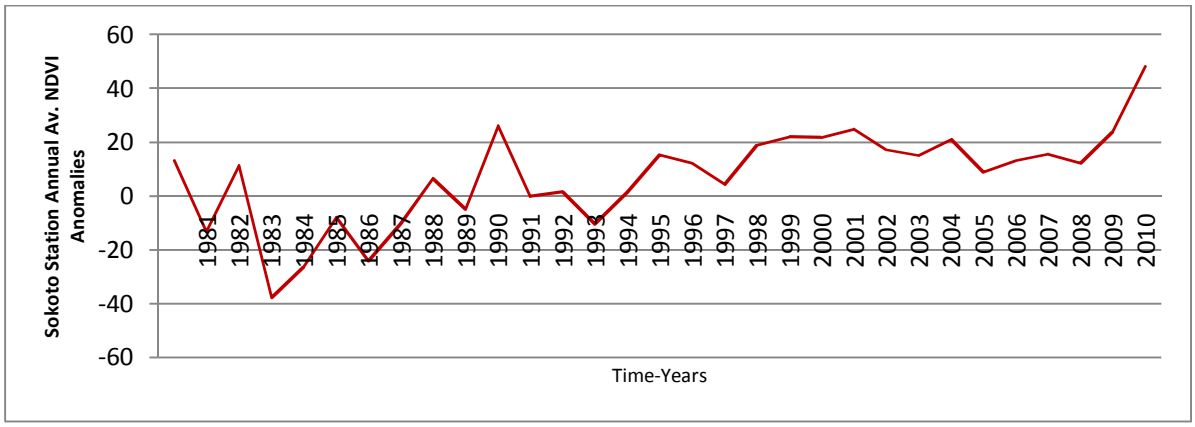


Figure 4.9a: Sokoto Station percent annual NDVI anomalies

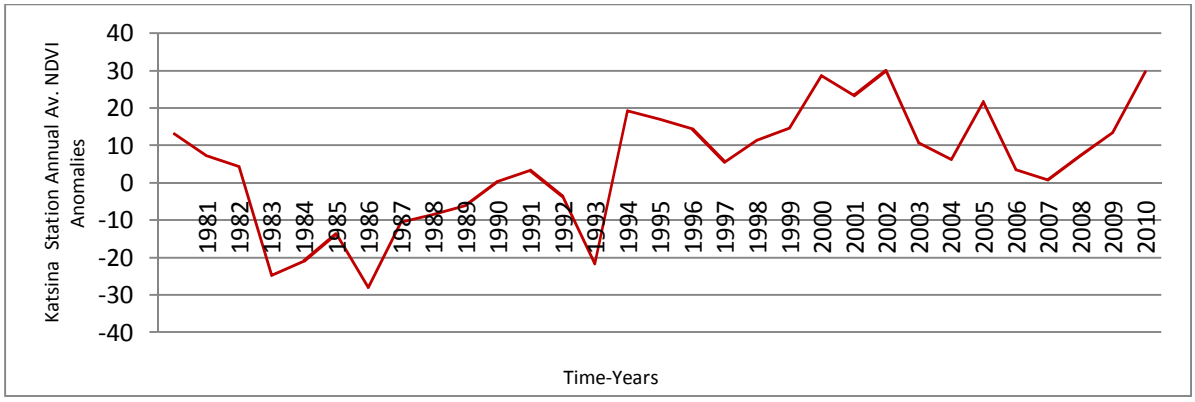


Figure 4.9b: Katsina Station percent annual NDVI anomalies

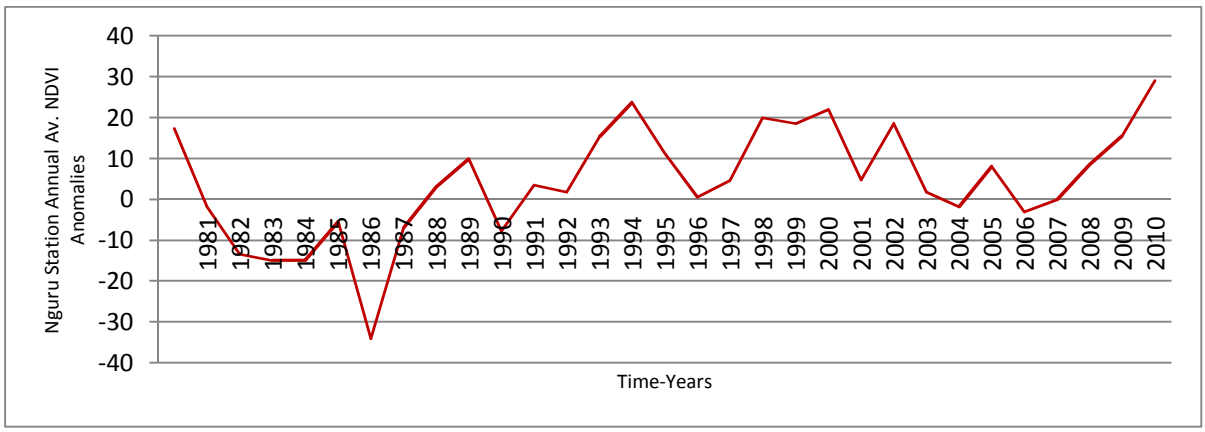


Figure 4.9c: Nguru Station percent annual NDVI anomalies

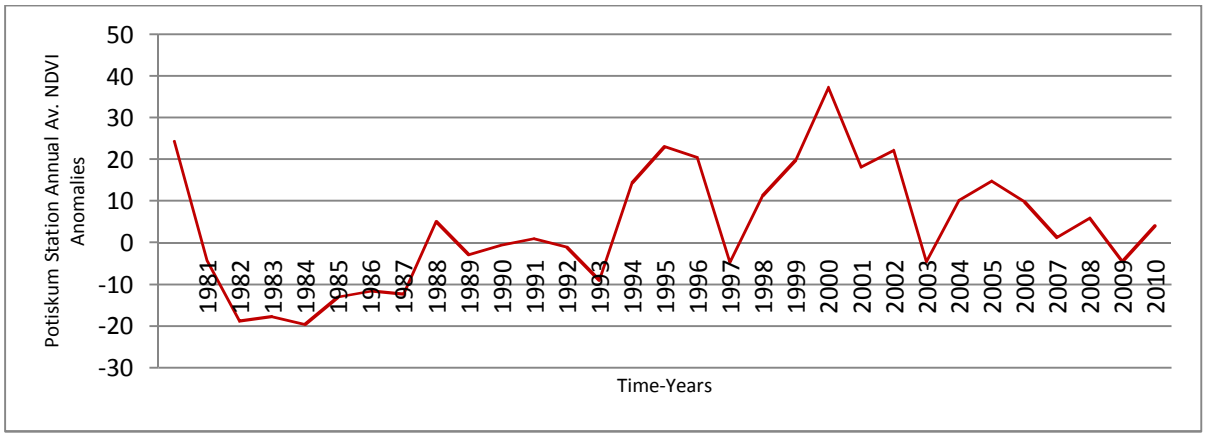


Figure 4.9d: Potiskum Station percent annual NDVI anomalies

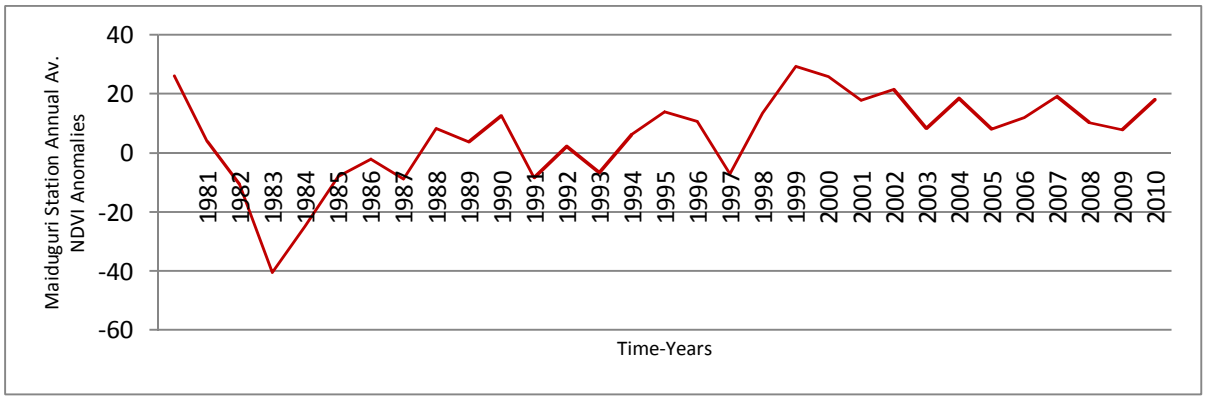


Figure 4.9e: Maiduguri Station percent annual NDVI anomalies

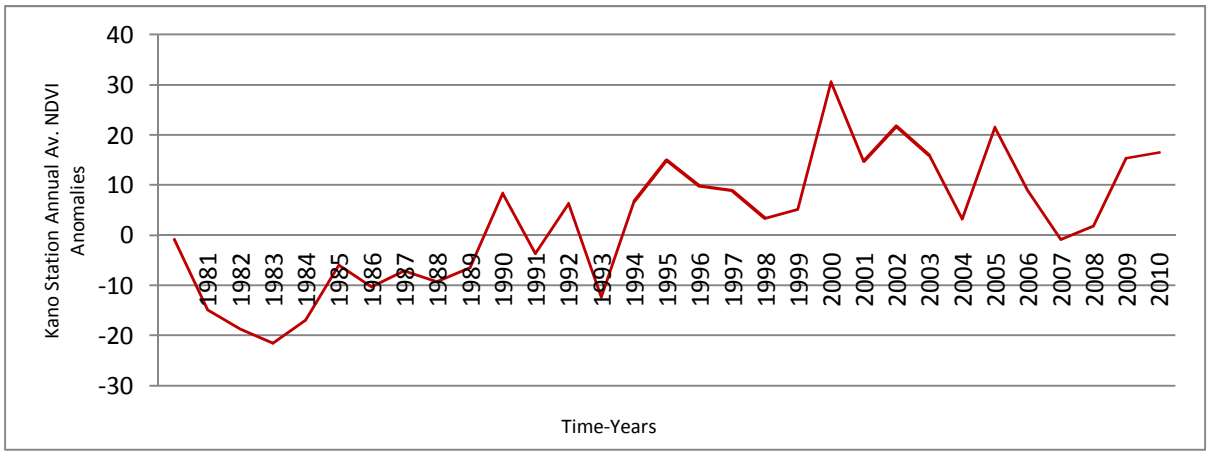


Figure 4.9f: Kano Station percent annual NDVI anomalies

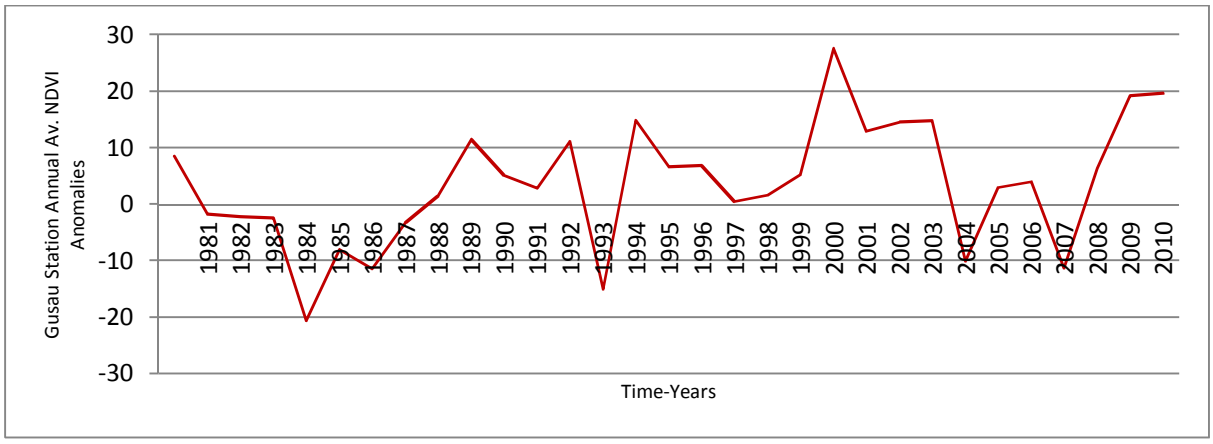


Figure 4.9g: Gusau Station percent annual NDVI anomalies

Drought variations are observed in the seven stations in the NSSR. The observed regional drought events of 1983-1985 and 1993-1994 reflect in all the stations as very severe drought as well, that is, with percent NDVI anomalies □ 30% as presented in Figs. 4.7a to 4.7g. However, drought event of 1987-88 observed as being severe at regional level in Figs. 4.6a was more pronounced locally as very severe drought events in some of the stations namely: Katsina, Nguru, Potiskum and Maiduguri (Figs. 4.7b, 4.7c, 4.7d and 4.7e). Moreover, Maiduguri and Kano synoptic stations results indicated very severe drought of small magnitude in 2009 (Figs. 4.7e and 4.7f) whereas the same drought was presented in Fig. 4.6a as being severe regionally. This implies that the impact would be more in Kano and Maiduguri in that year. Also, a drought event observed in 1991 appears to be very severe in Gusau Synoptic Station localty (Fig. 4.7g) but it appears slight or moderate in other locations. The results indicate that though, the NSSR is generally being threatened by drought but, its severity, magnitude and intensity vary from one location to another.

By comparing the graphs of percent dekadel NDVI anomalies with the percent monthly NDVI anomalies for each station, the drought trend observed in the former is similar to that

observed in the latter for each station as reflected in Figs. 4.7a to 4.7g and Figs. 4.8a to 4.8g, respectively. However, there is slight mask of drought episode using the monthly time scale compared to the dekadel scale. This observation is more pronounced in the percent annual NDVI anomaly time scale as presented in Figs. 4.9a to 4.9g for the seven stations. This observation reflects that for real-time drought forecasting, percent dekadel and percent monthly NDVI anomalies are adequate.

4.6 DROUGHT ANALYSIS IN NSSR BASED ON SPI

Figures 4.10a – 4.10e present the results of SPI at different time-scales (SPI_1, SPI_3, SPI_6, SPI_12, SPI_24) for the NSSR while Appendix E show the different SPI time scales for the seven stations.

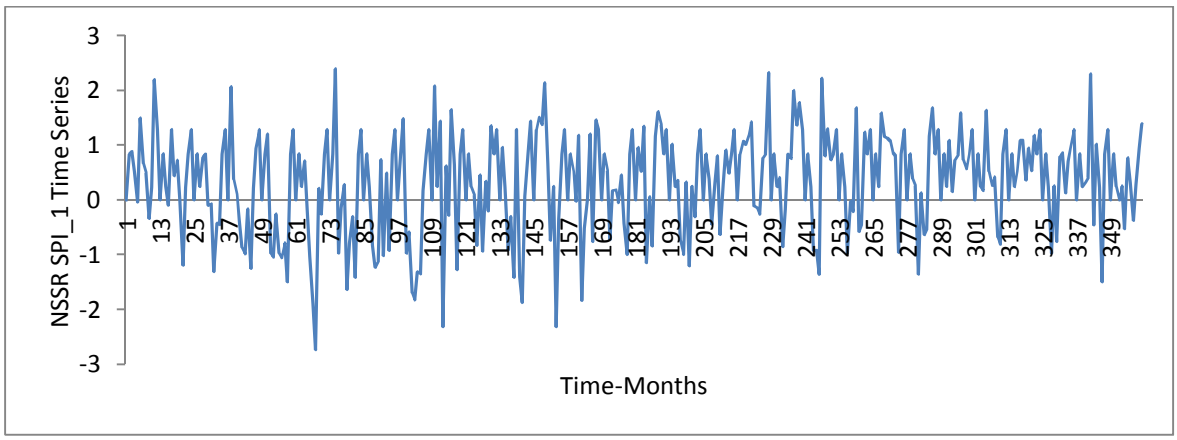


Figure 4.10a: NSSR SPI_1 Time Series

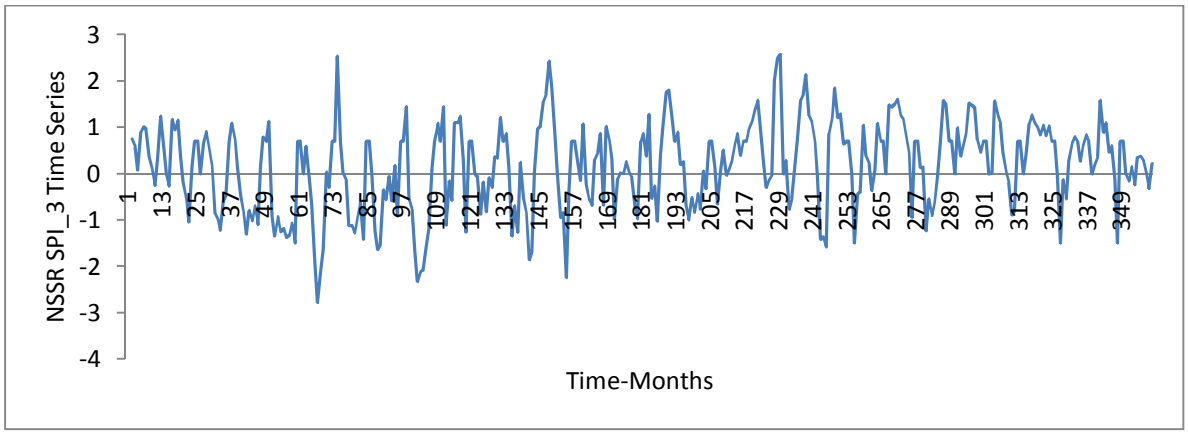


Figure 4.10b: NSSR SPI_3 Time Series

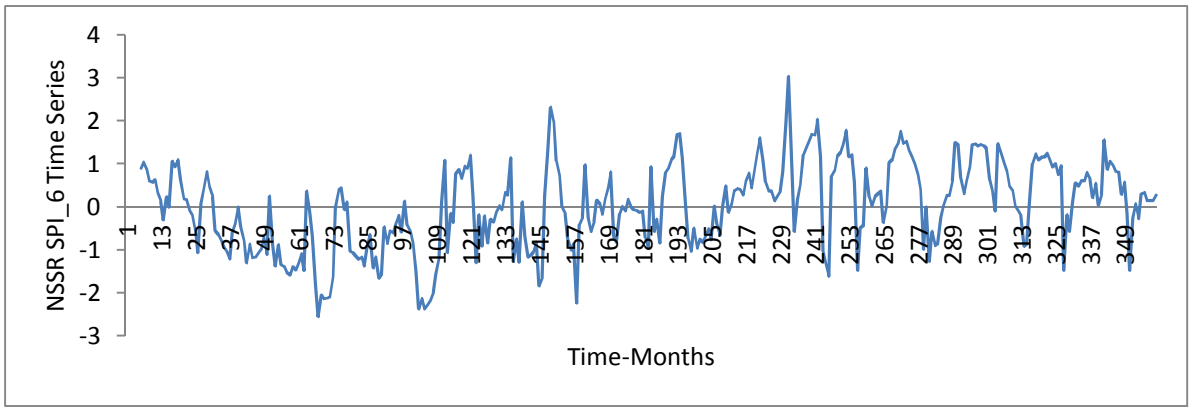


Figure 4.10c: NSSR SPI_6 Time Series

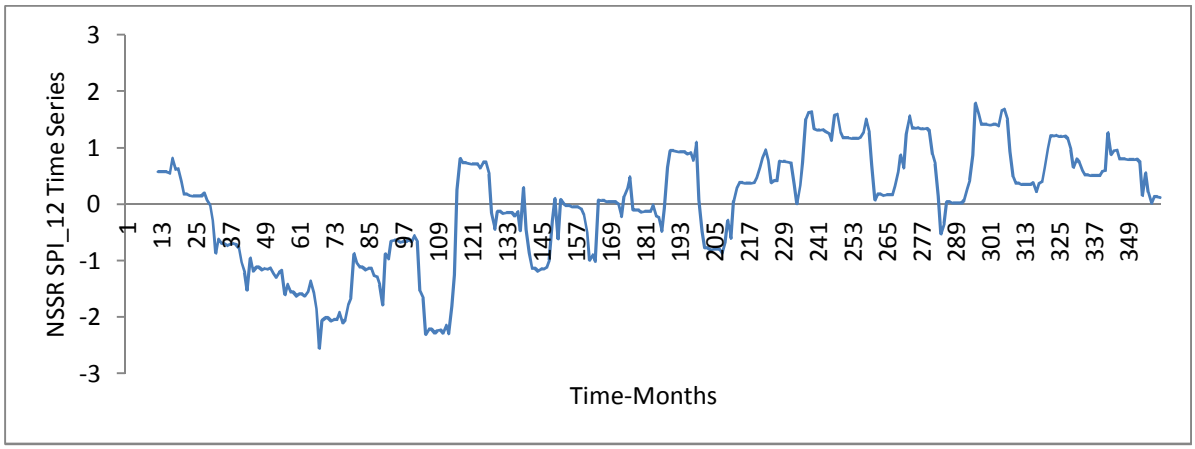


Figure 4.10d: NSSR SPI_12 Time Series

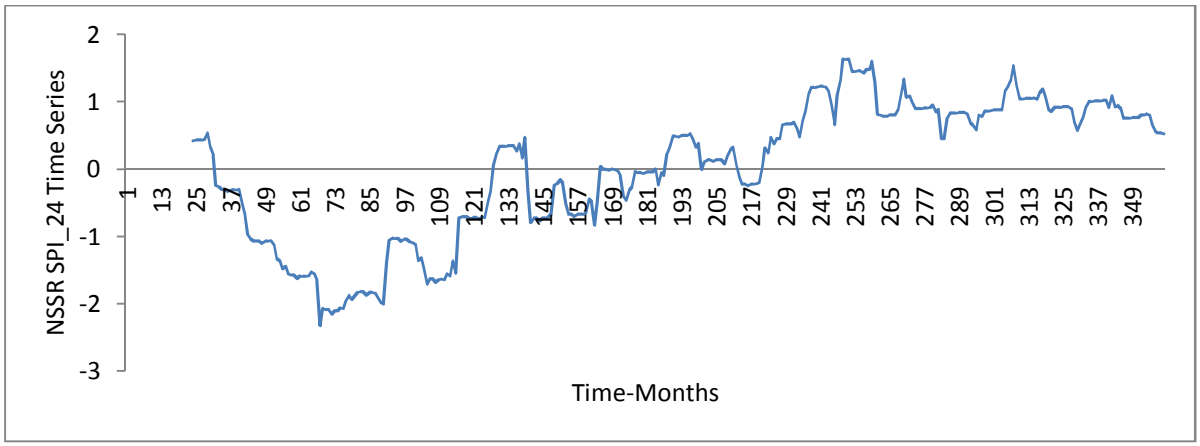


Figure 4.10e: NSSR SPI_24 Time Series

Just like the NDVI anomalies, the SPI time scales reflect drought intensity and magnitude for the various stations. Also, the longer SPI time scales, for example, SPI_24, mask some of the drought identified by the shorter SPI time scales. For example, out of the 360 months (of 30 years study period), Figs. 4.10a, 4.10b and 4.10c for SPI_1, SPI_3 and SPI_6 reflect the occurrence of drought though, in smaller magnitude and severity, up to 353rd month (2008), whereas, Figs. 4.10d and 4.10e, showing SPI_12 and SPI_24, indicate drought occurrence of very small magnitude and severity in the 287th (2002) and 217th months (1997), respectively. The same observation holds for the figures in each of the seven stations as reflected in Appendix E.

This is to say that the longer time scale obviously underestimate drought especially, during the later part of the study period. Hence, SPI_1 is considered for developing real-time forecasting model for managing drought in the NSSR. Also, it can be compared with the percent monthly NDVI anomalies.

4.7 TEMPERATURE AND RAINFALL ANALYSIS

Figures 4.11 and 4.12 present the plot of the NSSR annual monthly mean temperature and rainfall, respectively. Figure 4.12 reflects an increase in temperature trend. From the temperature record, the annual mean for the time series from 1979 to 2008 is computed as 27.5^0C. Figure 4.12 shows that some years have extreme mean temperatures in excess of 27.5^0C. Notable years are 1984, 1987, 1990, 1993 1997, 1998, 2006 and 2007. It is possible that the high temperature contributes to drought occurrence during these stated years as discussed below. Also, Fig. 4.12 reflects that the region had increased rainfall trend.

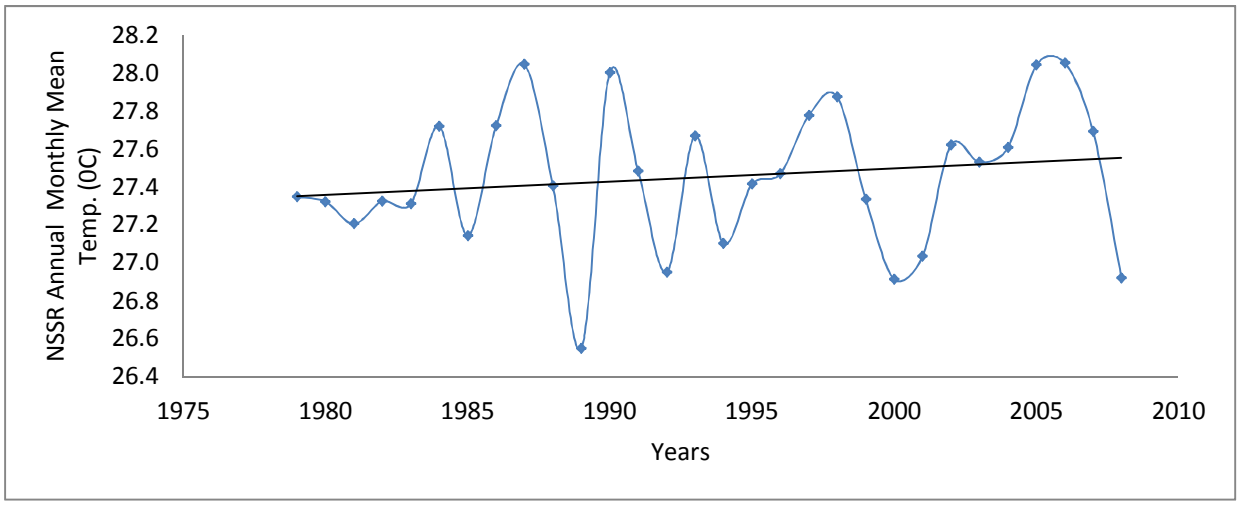


Figure 4.11: Annual monthly mean temperature (1979-2008)

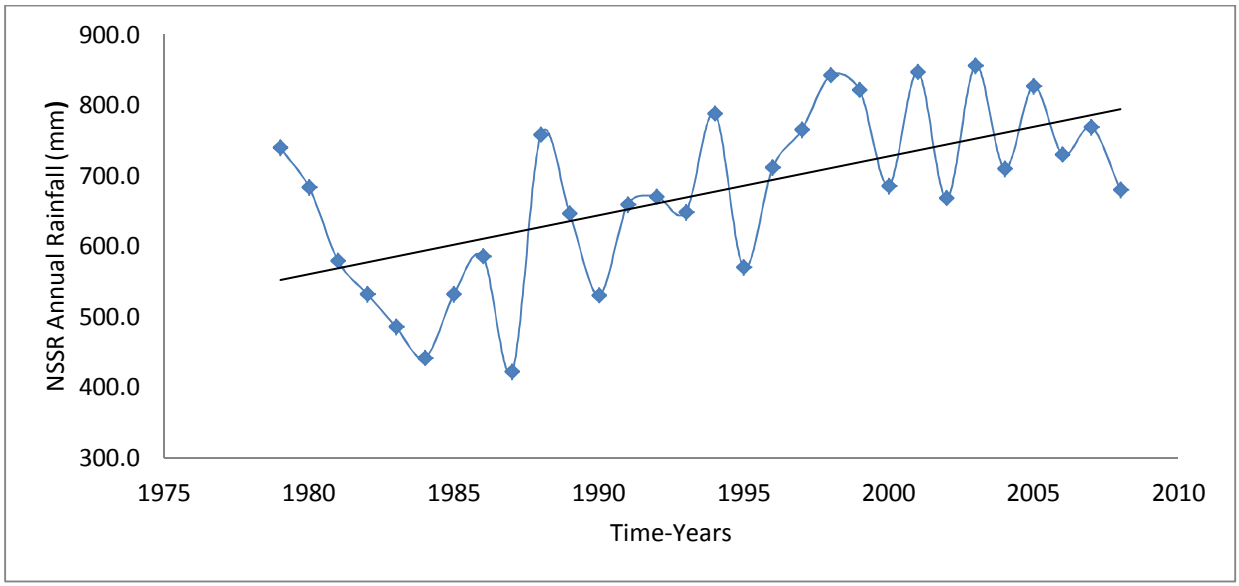


Figure 4.12: Annual rainfall (1979-2008)

The years of lowest rainfall are 1984 and 1987 and correspond to the period of very severe droughts in the region as discussed in the next section. The increase in rainfall is more pronounced from 1996 to 2008, with the exception of the year 2002 in which a lower annual mean record of 668mm was observed within this period of higher rainfall. The remaining years had annual rainfall higher than the long-term mean of 673mm, from 1996 to 2008. The increased rainfall amount might be the reason for the transition of the once severe/very severe drought nature to the moderate type observed during this period unlike the initial part of the study period.

4.8 COMPARISON OF ANNUAL ACCUMULATED NEGATIVE SPI_1 AND ANNUAL ACCUMULATED NEGATIVE PERCENT MONTHLY NDVI ANOMALIES

Figure 4.13 show the plot of annual accumulated negative values of SPI_1 while Fig. 4.14 presents the plot of annual accumulated negative percent monthly NDVI anomalies.

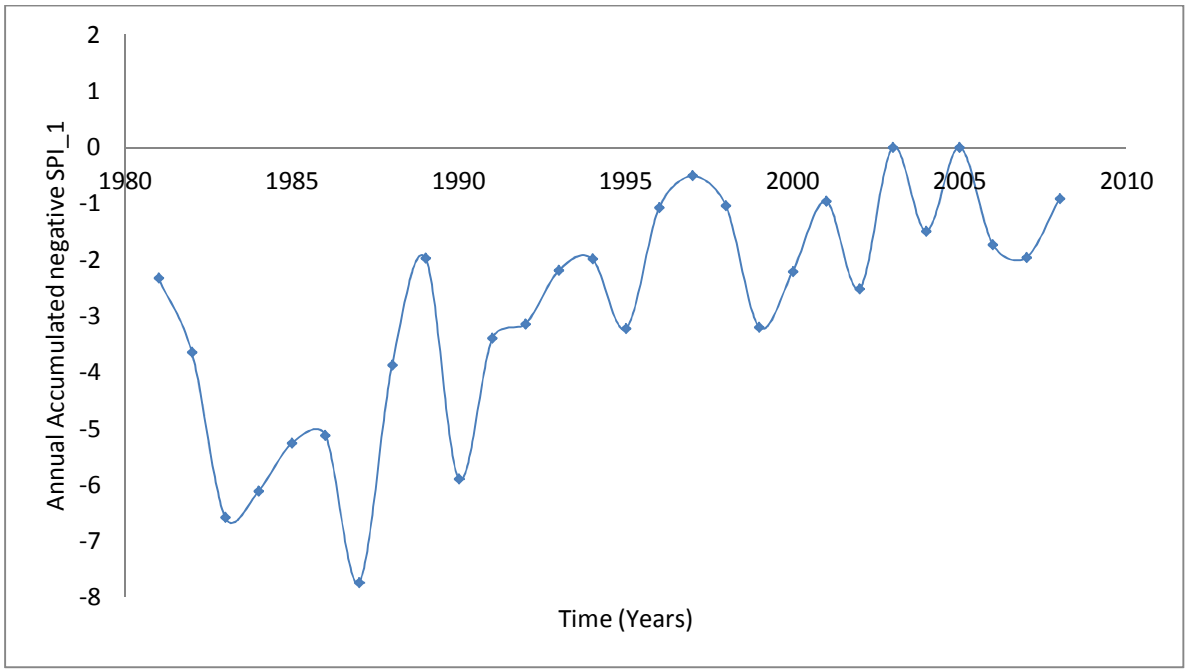


Figure 4.13: Annual accumulated negative SPI_1 (1979-2008)

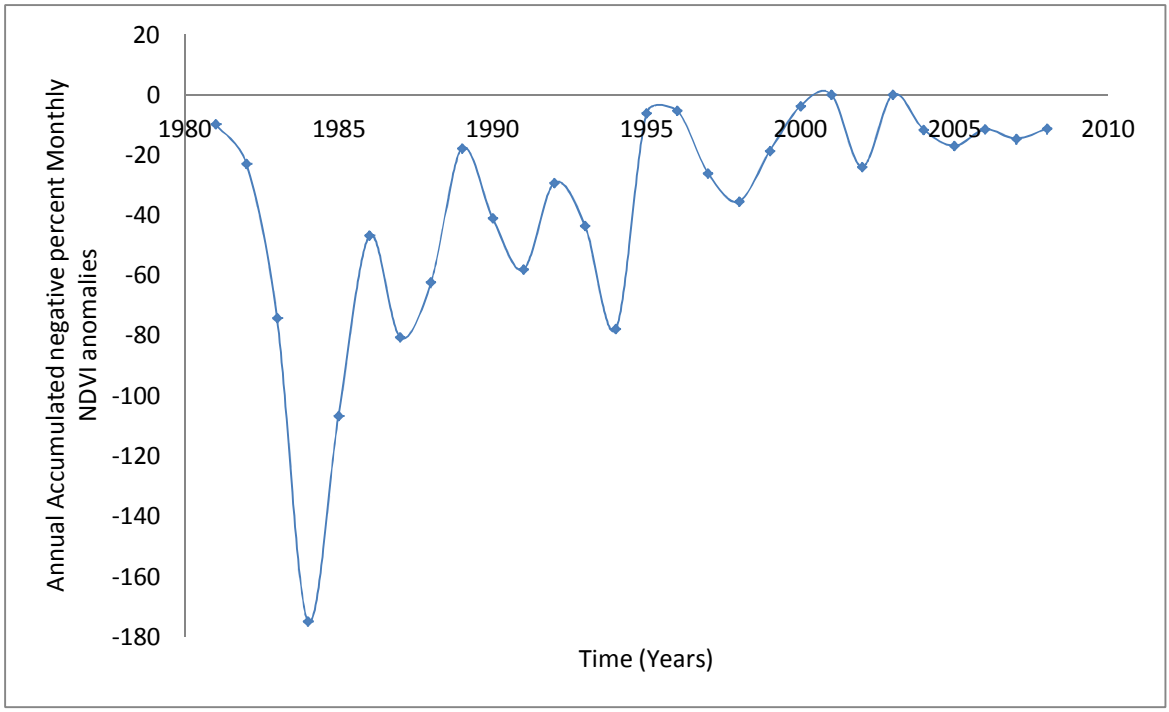


Figure 4.14: Annual accumulated negative percent monthly NDVI anomalies

The two graphs show the same trend and it is obvious that years of intense drought are between 1980 and 1995. This is to say that very severe or extreme drought events are observed in between this period. However, 1996 to 2008 years are observed as years with relatively less intense drought events and therefore, most of the moderate droughts occurred in this period probably as a result of climate change which is a function of increased rainfall amount observed in the same period, 1996-2008, as shown in Fig. 4.12. The temperature influences drought occurrence in the region because the peaks in Fig. 4.11 occurred and corresponded to the years the region experienced drought based on SPI_1 and percent monthly NDVI anomalies as shown in Figs. 4.13 and 4.14, respectively. However, the reduction in the drought intensity and magnitude observed between 1996 and 2008 is as a result of increased amount of rainfall. Hence, it is evident that temperature and rainfall especially, influence drought occurrence in the region.

4.9 COMPARISON OF SPI_1 AND NDVI DROUGHT EVENTS

The comparison between SSPI_1 and percent monthly NDVI anomalies was done with respect to severity of drought – very severe, severe and moderately severe.

4.9.1 Comparison of Very Severe Drought Events

Table 4.1 shows the result of comparison of very severe drought events between the two stated methods. From the Table, it is evident that three very severe drought episodes were discovered with SPI_1, specifically in 1984, 1988 and 1991. These years are in between 1981 and 1995 when very severe droughts were observed as stated in section 4.8. Also, percent monthly NDVI anomaly graph reflects only one drought episode of October, 1984,

Table 4.1: Comparison of very severe drought events based on SPI_1 and percent monthly NDVI anomalies

SPI_1 (-2 and less)			Temperature (^{o}C)		NDVI Anomalies (less than -30%)			
Year	**Month**	**Value**	**Monthly Mean Temp.**	**Long Term Mean Monthly Temp.**	**Year**	**Month**	**Value (%)**	**Comments/Remarks**
1984	August	-2.74	28.3	26.6	1984	October	-32	Drought occurrence lag by 3 month
1988	June	-2.31	30.1	30.0	-	-	-	Observed as a severe drought (Table 4.2)
1991	September	-2.32	28.7	27.7	1991	October	-13	1991 and 1992 NDVI are unstable due to the occurrence of Pinatubo. However, the corresponding NDVI Anomaly is -13% in October, 1991

NB: Percentage of very severe drought events based on SPI_1 is 3.06 %
Percentage of very severe drought events based on NDVI Anomalies is 0.75%

and this observation was lagged by 3 months after August observation based on SPI_1. This is in agreement with the past investigation on impact of rainfall on vegetation growth by Legesse (2010) who discovered that NDVI, since it is a measure of reflectance by vegetative surfaces, is lagged by 1 to 3 months after the preceding rainfall events. Moreover, the drought event observed in 1988 as very severe based on SPI is shown as severe drought based on NDVI anomalies, as presented in Table 4.2, which reflects comparison of severe drought events. Also, the drought episode of 1991 observed in September as very severe using SPI_1 was observed in October, after 1 month lag, as moderate drought of -13% magnitude, based on the second method although, 1991 and 1992 NDVI were declared unusable due to the occurrence of Pinatubo, because the volcanic eruption generated dust into the surrounding atmosphere and interfered with the sensing of the environment. Hence, this might be the reason for the drought variation

observed in the two approaches in 1991. The Table reflects that the percentage of very severe droughts with respect to SPI_1 and percent monthly NDVI anomalies were 3.06% and 0.75%, respectively.

4.9.2 Comparison of Severe Drought Events

Table 4.2 presents the results of severe drought events comparison using SPI_1 and percent monthly NDVI anomalies. Just like the previous observations, drought occurrence based on percent monthly NDVI anomalies are usually lagged by a number of months compared to the corresponding drought episodes using SPI_1. Some drought events are underestimated by percent monthly NDVI anomalies. Notable ones are 1983, 1985, 1990 and 2007 droughts. From the Table, the percentage of severe droughts based on SPI_1 is 8.16% while that of percent monthly NDVI anomalies is 6.77% of the total droughts in the region.

4.9.3 Comparison of Moderate Drought Events

Table 4.3 shows comparison of moderate droughts based on SPI_1 and percent monthly NDVI anomalies. The table reflected that moderate droughts were common features of the NSSR as they occurred repeatedly and at short intervals such that they occurred twice within a year as presented in the table. Besides, the percentages of moderate drought are 19.4% and 23.3% for SPI_1 and percent monthly NDVI anomalies, respectively. The latter method indicates higher percentage because the dry season months such as November, December, January and April are included in the observed drought period. During this period, the NDVI values are very low and hence, signify drought occurrence moderately and slightly though, unlike SPI_1 with no record of rainfall for its computation, as monthly

Table 4.2: Comparison of severe drought events based on SPI_1 and percent monthly NDVI anomalies

SPI_1 (-1.5 to -1.99)			Temperature (°C)		NDVI Anomalies (-20% to -30%)			
Year	Month	Value	Monthly Mean Temp.	Long Term Mean Monthly Temp.	Year	Month	Value	Comments/Remarks
1983	October	-1.5	28.2	28.4	1984	September	-24	SPI_1 drought of 1983 was observed as moderate drought (of magnitude -11 % in Oct.) based on NDVI Anomaly (Table 4.3)
1984	July	-1.9	27.8	27.5	1984	November	-26	Lag of 3 months; Drought years:
1985	July	-1.6	26.9	27.5	1984	December	-29	Severe drought of 1985 based on SPI_1 was computed as slight drought (-7%) using NDVI
1987	June	-1.7	30.5	30.0	1987	June	-21	Lag of 0 month
1987	July	-1.8	29.4	27.5	1987	October	-20	Lag of 3 months
1990	September	-1.8	28.5	27.7	1988	June	-24	1988 drought computed as severe drought based on NDVI was estimated as very severe based on SPI_1 (Table 4.1)
1992	June	-1.8	30.1	30.0	1993	December	-21	Lag of 6 months
2007	October	-.15	28.2	28.4	1994	April	-23	Severe drought of 2007 based on SPI_1 was computed as slight drought (-3%) using NDVI
-	-	-			1994	June	-22	Severe drought of 1994 based on NDVI was computed as moderately dry (-1.15) in May using SPI_1, (Table 4.3). Lag of 1 month; Drought years:

NB: Percentage of severe drought events based on SPI_1 is 8.16 %
Percentage of severe drought events based on NDVI Anomalies is 6.77%

Table 4.3: Comparison of moderate drought events based on SPI_1 and percent monthly NDVI anomalies

SPI_1 (-1.0 to -1.49)			Temperature (°C)		NDVI Anomalies (-10 to 20%)			
Year	Month	Value	Monthly Mean Temp.	Long Term Mean Monthly Temp.	Year	Month	Value	Comments/Drought Years
1980	September	-1.19	28.2	27.7	1982	July	-12	1980 and 1982
1981	August	-1.31	27.0	26.6	1983	January	-13	1981 and 1983
1982	September	-1.25	28.1	27.7	1983	July	-10	See above
1983	May	-1.04	33.5	32.2	1983	October	-11	See above
1983	August	-1.05	26.8	26.6	1984	April	-10	1984
1984	June	-1.03	30.6	30.0	1984	July	-12	See above
1985	October	-1.42	28.6	28.4	1984	August	-15	1985
1986	May	-1.23	32.7	32.2	1985	January	-14	1986
1986	June	-1.11	30.8	30.0	1985	March	-15	See above
1986	August	-1.02	26.8	26.6	1985	June	-19	See above
1987	August	-1.31	27.4	26.6	1985	July	-10	1987
1987	September	-1.35	29.0	27.7	1985	December	-12	See above
1988	October	-1.28	27.4	28.4	1986	June	-14	1988
1990	June	-1.41	31.3	30.0	1986	December	-11	1990
1990	August	-1.40	27.2	26.6	1987	August	-10	See above
1994	May	-1.15	32.1	32.2	1987	November	-10	1994
1995	August	-1.20	26.5	26.6	1988	April	-10	See above
1999	June	-1.36	31.3	30.0	1988	May	-16	1999
2002	May	-1.36	32.2	32.2	1990	October	-12	2002
					1991	October	-13	1991
					1992	January	-16	1992
					1994	January	-10	See above
					1994	May	-10	See above
					1997	March	-15	1997
					1998	July	-13	1998
					1999	July	-13	1999
					2002	June	-14	See above
					2002	July	-10	See above
					2006	June	-10	2006
					2009	June	-10	2009
					2009	July	-13	See above

NB: Percentage of moderate drought events based on SPI_1 is 19.39 %
Percentage of moderate drought events based on NDVI Anomalies is 23.31%

rainfall records are usually zero as reflected in the raw rainfall data collected, during this period. Hence, SPI_1 reflects drought occurrence mostly within the rainy season only.

Drought observations estimated with percent monthly NDVI are lagged behind values of SPI_1 hence, observed temperature records corresponding to the SPI_1 drought occurrences were used for analysis of temperature influence on drought by comparing the values with the long term monthly mean temperature. The months of drought occurrence usually have higher temperatures than the long term monthly mean. From Tables 4.1 to 4.3, twenty out of twenty six monthly drought observations have higher temperatures than the corresponding long term monthly mean, reflecting percentage of occurrence of about 76.9%. This means that long-term monthly mean temperature could be used as a monthly temperature threshold against which forecasted monthly temperature could be compared to ascertain the possibility of drought occurrence in forecasting.

4.10 ANALYSIS OF DEGREE OF SPATIAL DROUGHT OCCURRENCE

Table 4.4 reflects the summary of statistical analysis of 31 year average dekadel NDVI data extracted for the 7 synoptic stations and NSSR region.

Table 4.4: Statistical Analysis of NSSR and Synoptic Stations NDVI

Stastistical Parameters	**Sokoto**	**Gusau**	**Katsina**	**Kano**	**Nguru**	**Potiskum**	**Maiduguri**	**NSSR**
Max	0.38	0.46	0.39	0.50	0.38	0.47	0.46	0.45
Min	0.12	0.14	0.12	0.16	0.14	0.15	0.15	0.16
Range	0.26	0.32	0.27	0.34	0.20	0.32	0.31	0.29
Mean	0.221	0.274	0.229	0.287	0.226	0.273	0.264	0.267
Sta. Dev.	0.085	0.115	0.092	0.120	0.072	0.109	0.099	0.100
Sum	7.95	9.86	8.25	10.32	8.13	9.83	9.52	9.62

Table 4.4 shows that Sokoto and Nguru had the minimum average $NDVI_{max}$, lower mean and standard deviation compared to others. Sokoto station had a mean of 0.221 and standard deviation of 0.085 while Nguru station had a mean of 0.226 and standard deviation of 0.072. Since standard deviation shows how much variation or disparity exists from the average or mean, the low standard deviation indicates that most of the dekadel NDVI values at the two locations tend to be very close to the low mean values. Hence, the results indicate that Sokoto and Nguru in Yobe State, experience more frequent drought than other stations. The sum of the average NDVI values further indicated that Sokoto is the most exposed location to drought while Kano, with the highest $NDVI_{max}$ (0.5), mean (0.287), and standard deviation (0.120), is the least exposed. Next to kano is Potiskum, followed by Maiduguri, Guzau and then Katsina.

Spatial-temporal distributions of NDVI anomalies for September, 1984, September, 1994 and September, 2004 are presented in Figs. 4.15a to 4.15c. Figure 4.15 represents drought

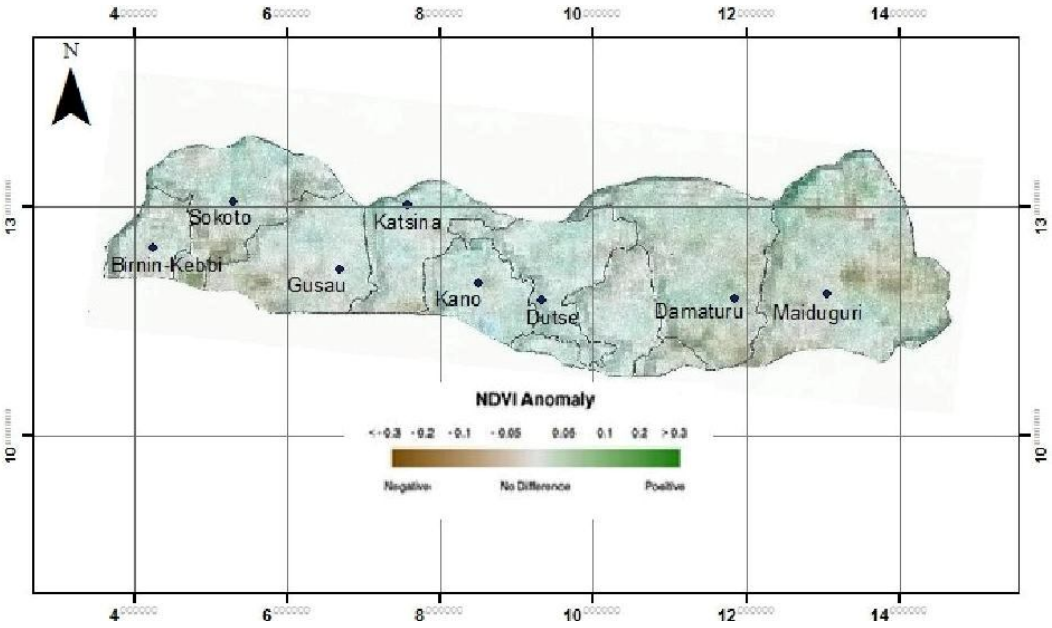


Figure 4.15a: Spatial distribution of average dekadel NDVI anomaly (September, 1984)

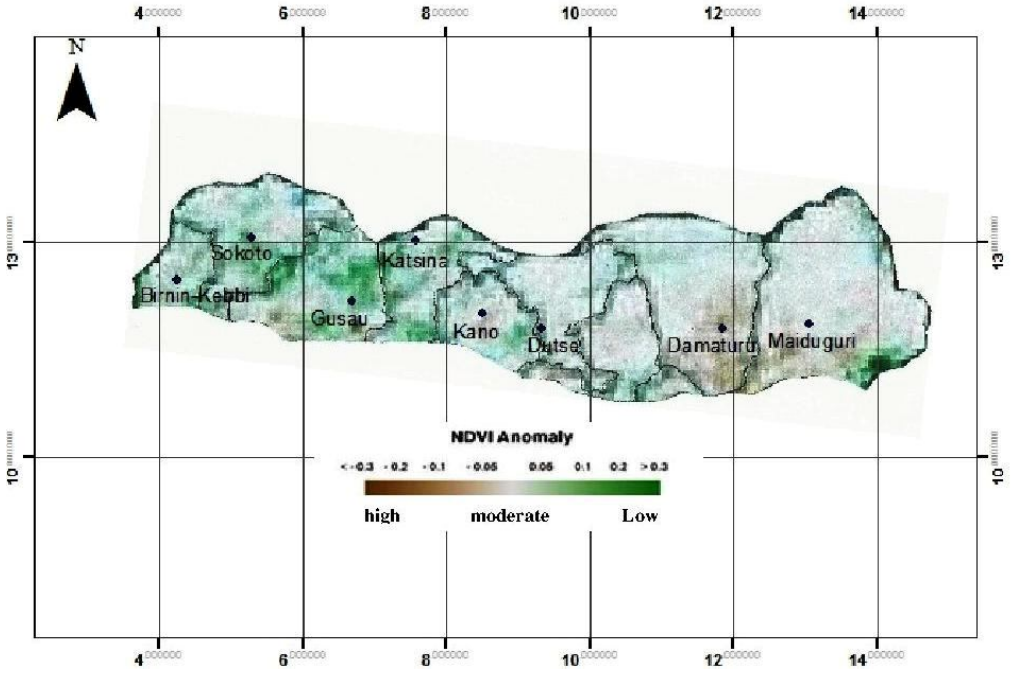


Figure 4.15b: Spatial distribution of average dekadel NDVI anomaly (September, 1994)

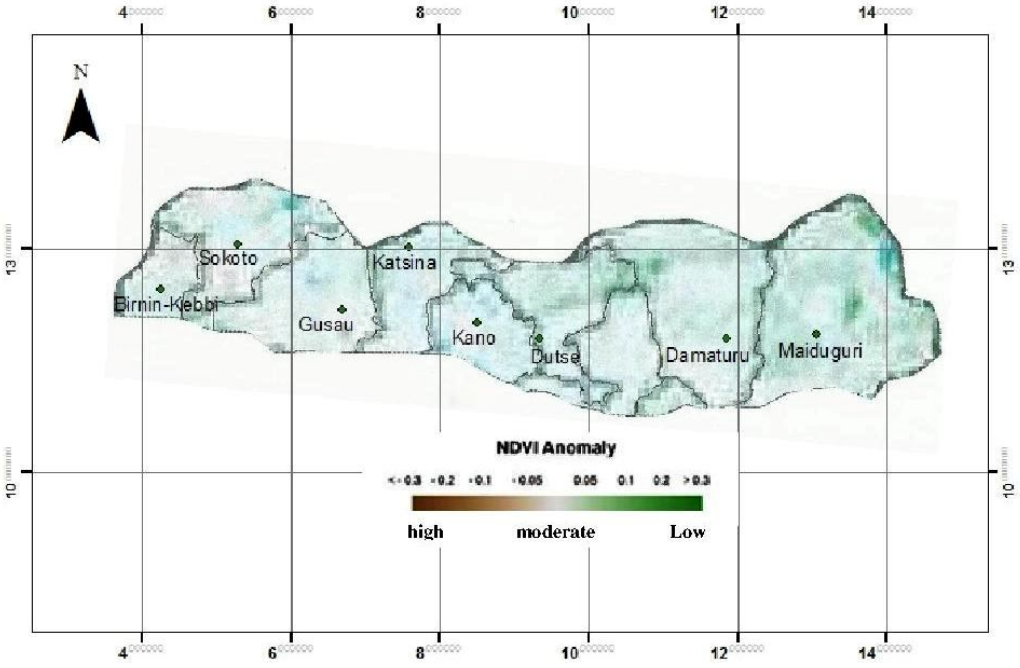


Figure 4.15c: Spatial distribution of average dekadel NDVI anomaly (September, 2004)

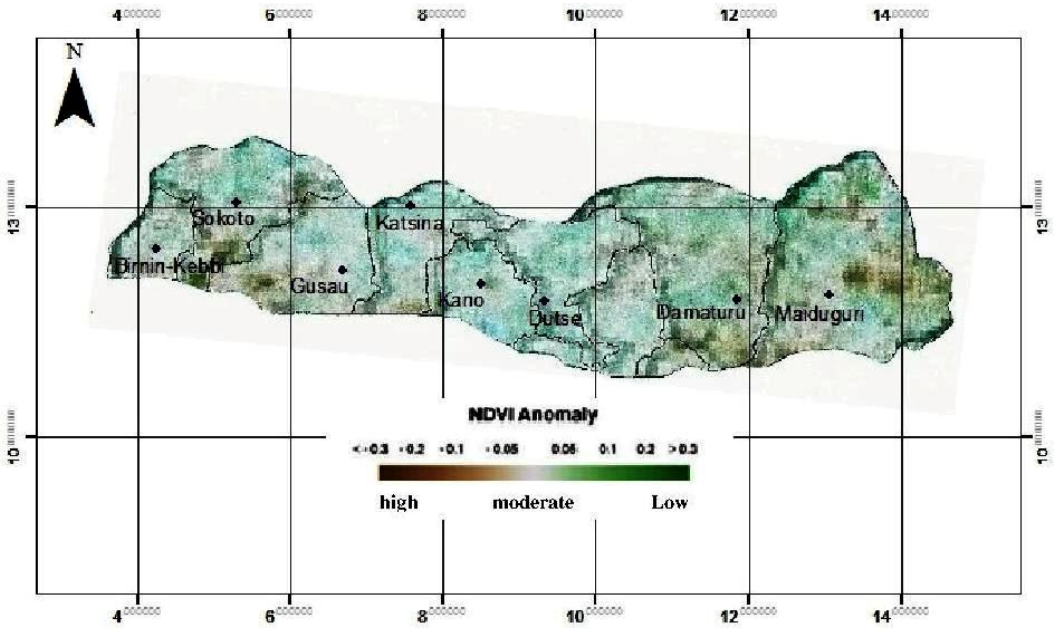


Figure 4.15d: Drought risk map based on NDVI anomalies

risk map based on overlaid NDVI anomaly maps. The three periods have an interval of decades in between them and were selected such that the drought severities of 1983-1985, 1993 - 1994 and 2004 could be reflected by September 1984, September, 1994 and September, 2004 NDVI anomalies, respectively. Figures 4.15a to 4.15c showed that the intensity of drought decreased progressively from 1984 to 2004. Fig. 4.15a reflected very severe drought events at parts of Sokoto, Gusau, Katsina, Damaturu, in the same Yobe State with Nguru, and Maiduguri while other parts of NSSR reflected moderate drought events. Fig. 4.15b showed drought events of very severe intensity at parts of Damaturu and Maiduguri while Gusau show low risk and other parts indicated drought of moderate to slight intensities. Figure 4.15c reflected drought of slight to moderate intensities throughout NSSR. From Fig. 4.15d, Sokoto, Katsina, Damaturu and Nguru Station in Yobe State, and Maiduguri were regarded as drought high risk zones. This is justified by the values of NDVI for Sokoto, Katsina and Nguru Stations in Table 4.4. Moderate risk zone constitutes

Guzau Kano and Dutse; this is in agreement with the statistical analyses above. Identified low risk zones are parts of Bauchi and Gombe.

4.11 ANALYSIS OF SEASONAL DROUGHT TREND IN NSSR

The seasonal trend of the recurrent drought in the NSSR is analyzed by plotting the average of the NDVI records of the region and each station and, the results are shown in Figures 4.16a to 4.16g.

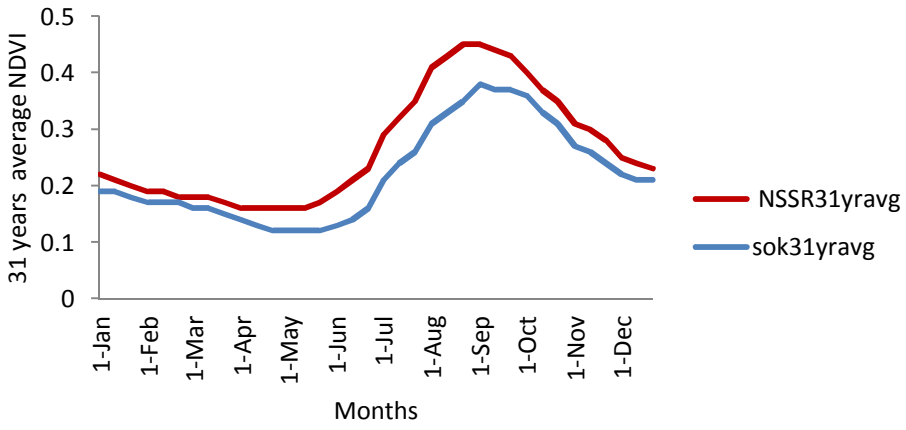


Figure 4.16a: Sokoto Station Seasonal Drought Pattern

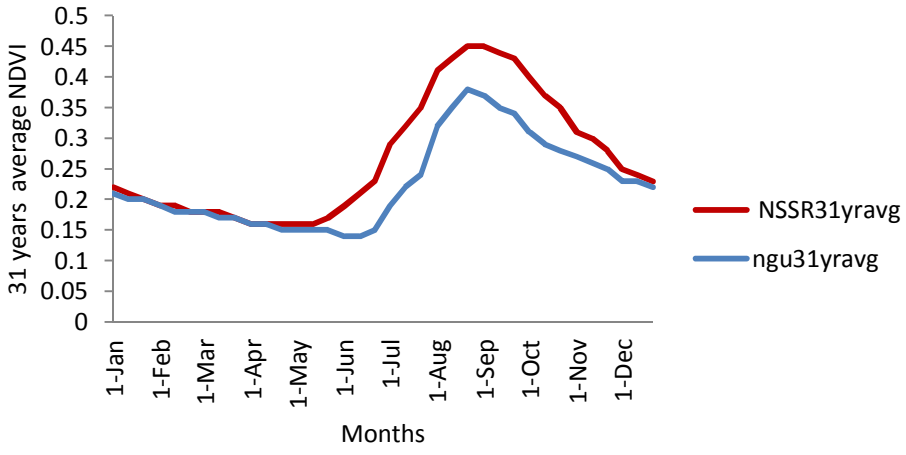


Figure 4.16b: Nguru Station Seasonal Drought Pattern

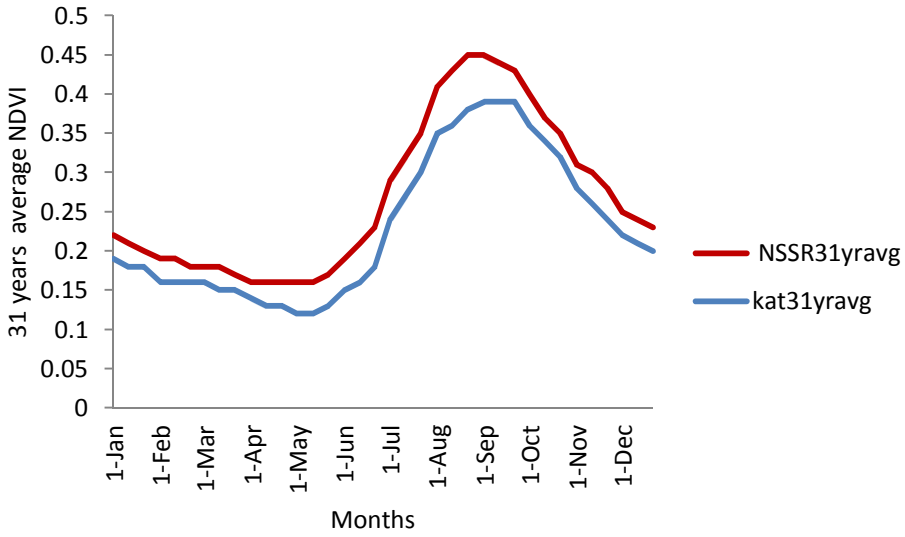


Figure 4.16c: Katsina Station Seasonal Drought Pattern

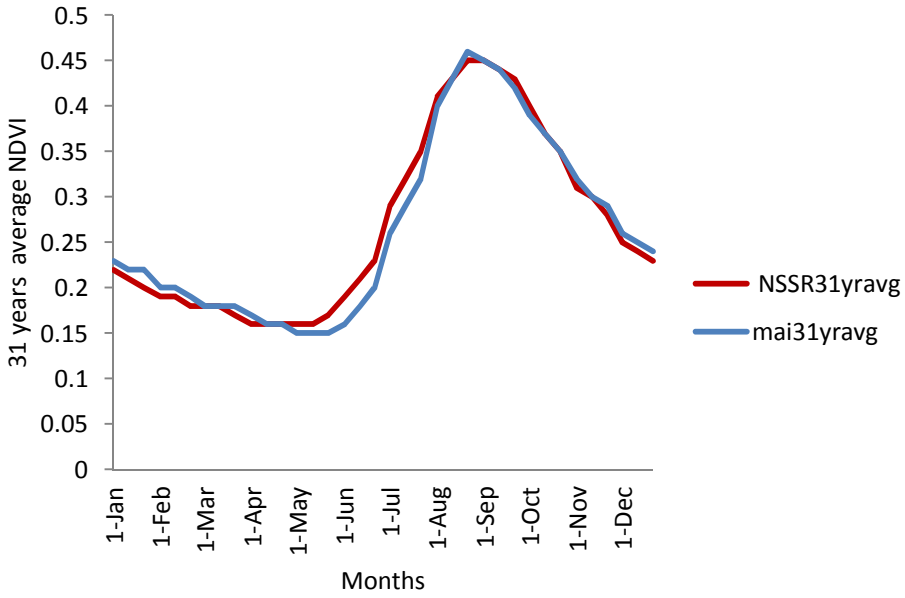


Figure 4.16d: Maiduguri Station Seasonal Drought Pattern

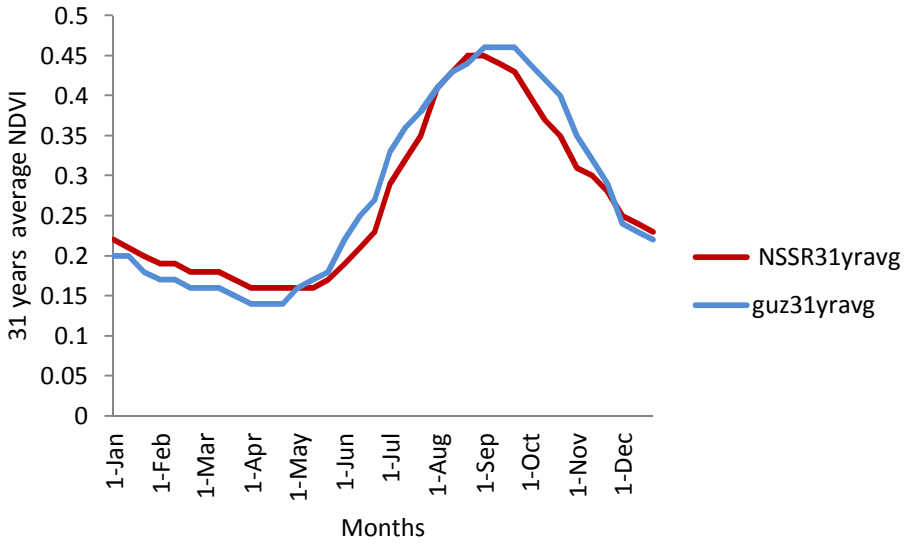


Figure 4.16e: Guzau Station Seasonal Drought Pattern

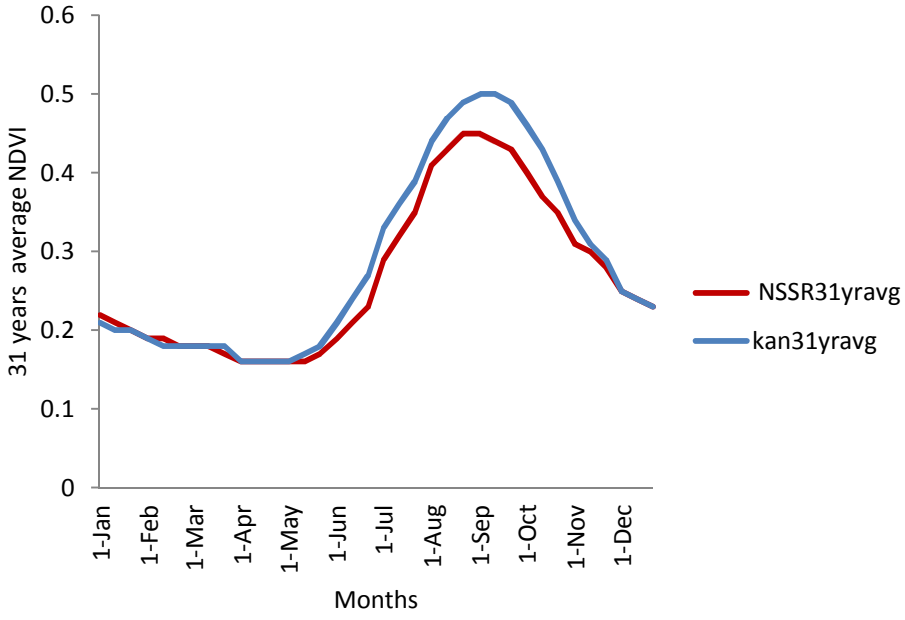


Figure 4.16f: Kano Station Drought Pattern

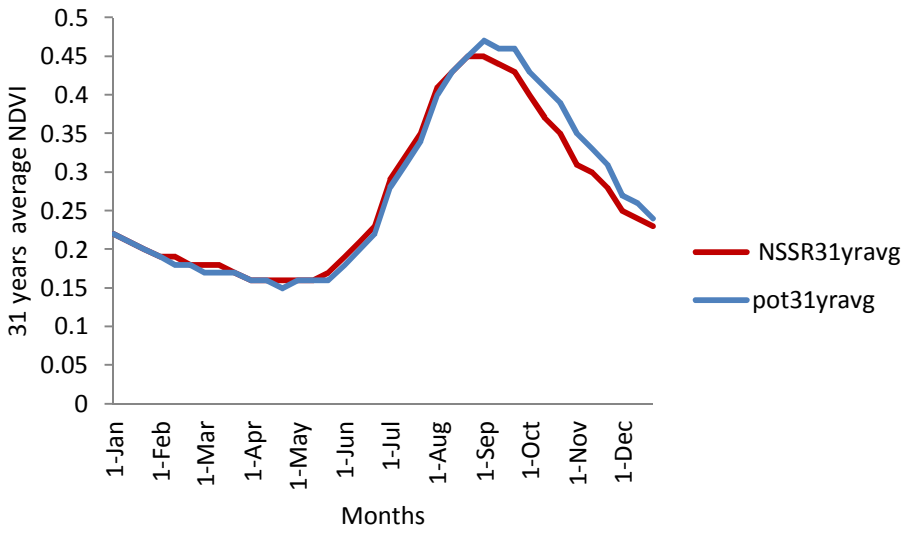


Figure 4.16g: Potiskum Station Drought Pattern

Figure 4.16a shows that Sokoto station is mostly under drought most of the year as indicated by the graphs since curve of average record of Sokoto is observed to be under the average curve for the region. Also, similar trends were observed for Nguru and Katsina stations as shown in Figure 4.16b and 4.16c, respectively.

Figure 4.16d reflects that Maiduguri used to experience drought from May to July most of the year while Figure 4.16e indicates that Guzau recurrent drought is common from September to November most of the year. Figure 4.16f shows that Kano station scarcely have drought during the rainy season (June to September), likewise Potiskum as shown in Figure 4.16g, but there is high possibility of drought occurrence during the dry seasons. By knowing the recurrent periods using the figures, agencies responsible for disaster management can have a clue with respect to drought preparedness before its incidence in each of the locations.

4.12 ANALYSIS OF STOCHASTIC MODELS FOR DROUGHT MANAGEMENT IN NSSR

As stated in section 3.2.7, time series model development consists of three stages of identification, estimation and diagnostic checking (Box and Jenkins, 1970). The identification stage involves transforming the data (if necessary) to improve the normality and the stationarity of the time series and determining the general forms, that is, the orders of the models to be developed using ACF and PACF. The model parameters are calculated during the estimation stage. Lastly, diagnostic checking of the models were performed to reveal possible model inadequacies and to assist in selecting the best model. It was observed that droughts as a result of NDVI anomalies are lagged behind those due to SPI_1 hence, the latter series were considered for modelling in this section for near real time drought forecasting. Secondly, the temperature series were also considered for modelling because of the observed higher values than the long term monthly mean temperature during drought periods as explained before.

4.12.1 SPI_1 Model Identification

Figures 4.17a and 4.17b present the Autocorrelation Function and (ACF) and Partial Autocorrelation Function (PACF) for the NSSR SPI_1 while Appendix F shows the ACF and PACF for the SPI_1 of the seven stations. Table 4.5 presents the results of various possible combinations of SARIMA Models after analyzing the ACF and PACF while Figs. 4.18a to 4.18h present the selected SPI_1 models from the table. The details of the analyses of the considered models in Table 4.5, together with their estimated parameters are as presented in Appendix G

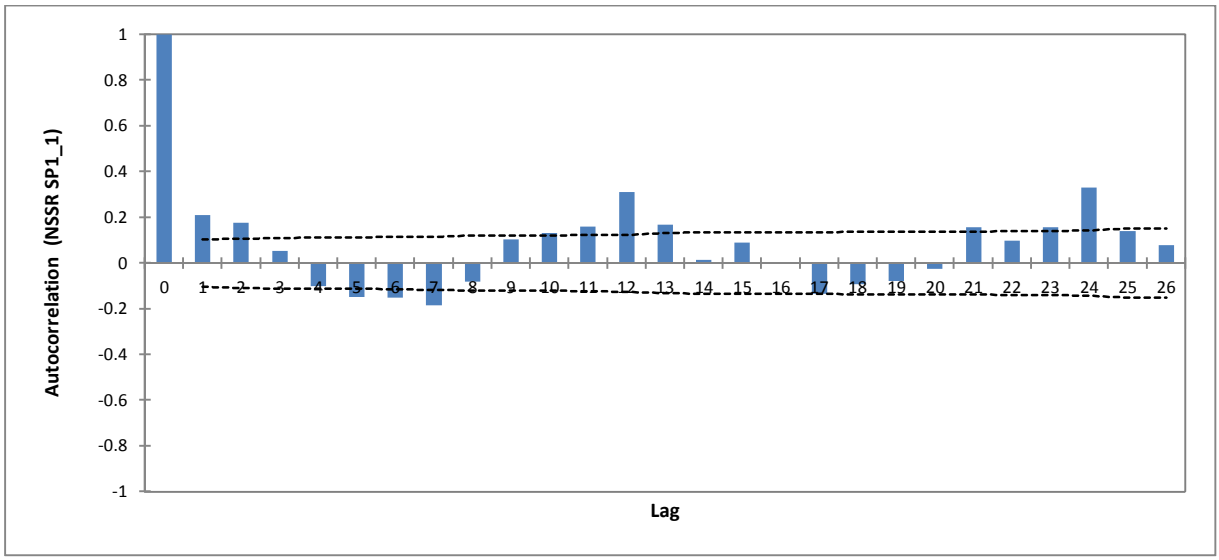


Figure 4.17a: ACF plot for selecting relevant models for NSSR SPI_1 series

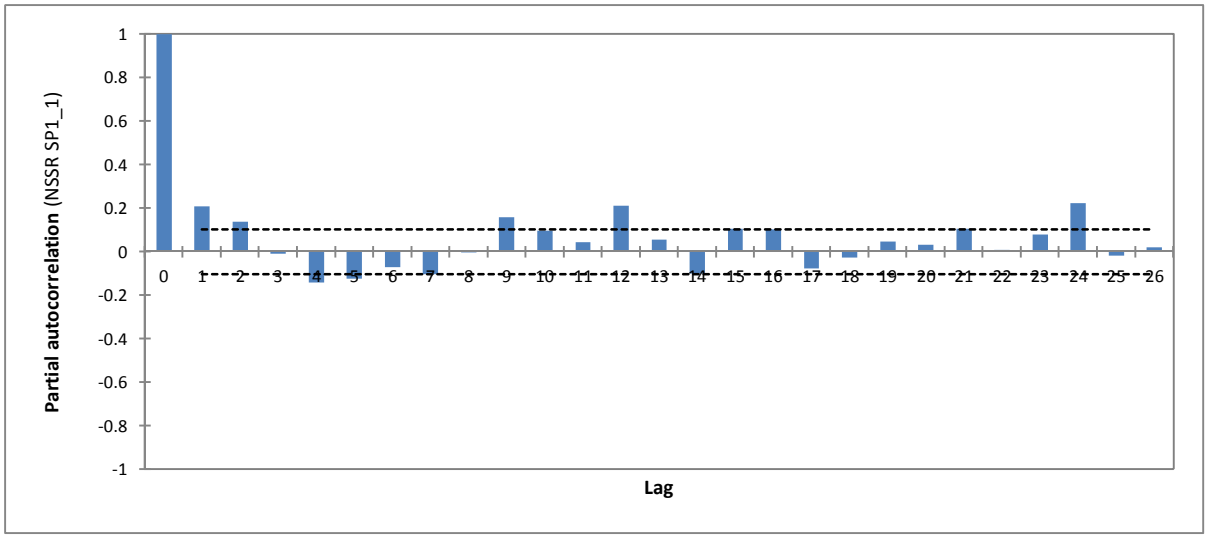


Figure 4.17b: PACF plot for selecting relevant models for NSSR SPI_1 series

The NSSR ACF and PACF reflects that the first two spikes are significant which indicate that the process can be modelled as a combination of both AR and MA processes, with $p \leq 2$, $q \leq 2$ and $P \leq 2$, $Q \leq 2$. Also, the PACF shows that the differencing is ≤ 2. The ACF and PACF for all the stations, especially, Katsina, Kano and Gusau show spikes at the first lag

and then cut off to zero. This implies that the time series can be modelled with a combination of Auto Regressive (AR) and Moving Average (MA) process and the order of p=1, q=1 and P=1, and Q=1. The non-seasonal differencing, d, or seasonal differencing, D, is usually 0, 1 or 2 in practice (Berthouex and Brown, 2002). The seasonal difference (s) observed at lags 12, 24, and so on, in the ACF and PACF structures was removed by a 12-month lag difference. Hence one of the possible SARIMA Model of $(p,d,q)x(P,D,Q)_s$ is $(1,1,1)x(1,1,1)_{12}$.

The results of the various combination of SARIMA $(p,d,q)x(P,D,Q)_{12}$ models are as shown in Table 4.5. From the Table 4.5, the model found suitable for the NSSR SPI_1 prediction is SARIMA $(202)x(212)_{12}$ as highlighted. The model is selected because it has the lowest AIC, SBC and Sum of Squares for Error (SSE). Besides, it has mean of 0.309 which is close to the SPI_1 data time series mean of 0.325. SARIMA model $(011)x(011)_{12}$ was found suitable for SPI_1 forecasting in Sokoto, Nguru, Potiskum, Kano and Gusau Stations because it had lowest values for at least two out of the three criteria (AIC, SBC and SSE) for selecting suitable models in each case. By applying the same rationale, SARIMA model $(111)x(111)_{12}$ was found suitable for SPI_1 forecasting in Katsina and Maiduguri Stations. The selected SPI_1 time series models for the NSSR and the seven stations are as shown in Figs. 4.18a to 4.18h; they show fairly good agreement with the computed SPI_1 while the model estimated parameters are as presented in Appendix G.

Table 4.5: Comparison of Goodness of Fit Statistics and Statistical Parameters of SPI_1 Models

Item No	Station	Series/ SARIMA Model	Mean	Standard Deviation	AIC	SBC	SSE
1	NSSR	SP1_1	0.325	0.896	-	-	-
		$(212)x(212)_{12}$	0.274	0.678	823.698	858.025	202.244
		$(202)x(212)_{12}$	**0.309**	**0.630**	**811.253**	**845.607**	**195.428**
		$(222)X(222)_{12}$	0.335	0.917	983.899	1017.837	300.923
2	Sokoto	SP1_1	0.478	0.978	-	-	-
		$(111)x(111)_{12}$	0.464	0.784	766.703	785.774	171.000
		$(110)x(110)_{12}$	0.486	1.073	982.230	993.672	358.304
		$(011)x(011)_{12}$	**0.465**	**0.778**	**774.314**	**762.872**	**142.581**
3	Katsina	SP1_1	0.168	0.768	-	-	-
		$(111)x(111)_{12}$	**0.125**	**0.481**	**750.794**	**769.865**	**153.599**
		$(110)x(110)_{12}$	0.178	0.864	949.033	960.475	324.352
		$(011)x(011)_{12}$	0.132	0.495	752.012	763.455	171.282
4	Nguru	SP1_1	0.332	0.873	-	-	-
		$(111)x(111)_{12}$	0.295	0.670	753.789	772.860	171.894
		$(110)x(110)_{12}$	0.333	0.907	912.474	923.916	288.396
		$(011)x(011)_{12}$	**0.289**	**0.631**	**760.154**	**771.596**	**130.835**
5	Potiskum	SP1_1	0.276	0.885	-	-	-
		$(111)x(111)_{12}$	0.252	0.576	798.742	817.813	177.748
		$(110)x(110)_{12}$	0.274	0.943	1029.408	1040.851	412.452
		$(011)x(011)_{12}$	**0.251**	**0.575**	**795.257**	**806.699**	**177.945**
6	Maiduguri	SP1_1	0.275	0.895	-	-	-
		$(111)x(111)_{12}$	**0.212**	**0.695**	**767.899**	**786.970**	**172.777**
		$(110)x(110)_{12}$	0.279	0.968	945.855	957.297	321.493
		$(011)x(011)_{12}$	0.239	0.693	771.312	782.454	180.994
7	Kano	SP1_1	0.512	0.958	-	-	-
		$(111)x(111)_{12}$	0.501	0.816	726.041	745.112	150.620
		$(110)x(110)_{12}$	0.510	0.987	857.550	868.992	246.408
		$(011)x(011)_{12}$	**0.505**	**0.807**	**727.253**	**738.695**	**98.408**
8	Gusau	SP1_1	0.516	1.024	-	-	-
		$(111)x(111)_{12}$	0.467	0.770	823.398	842.469	195.099
		$(110)x(110)_{12}$	0.503	1.070	987.165	998.607	362.589
		$(011)x(011)_{12}$	**0.468**	**0.769**	**820.589**	**832.041**	**176.131**

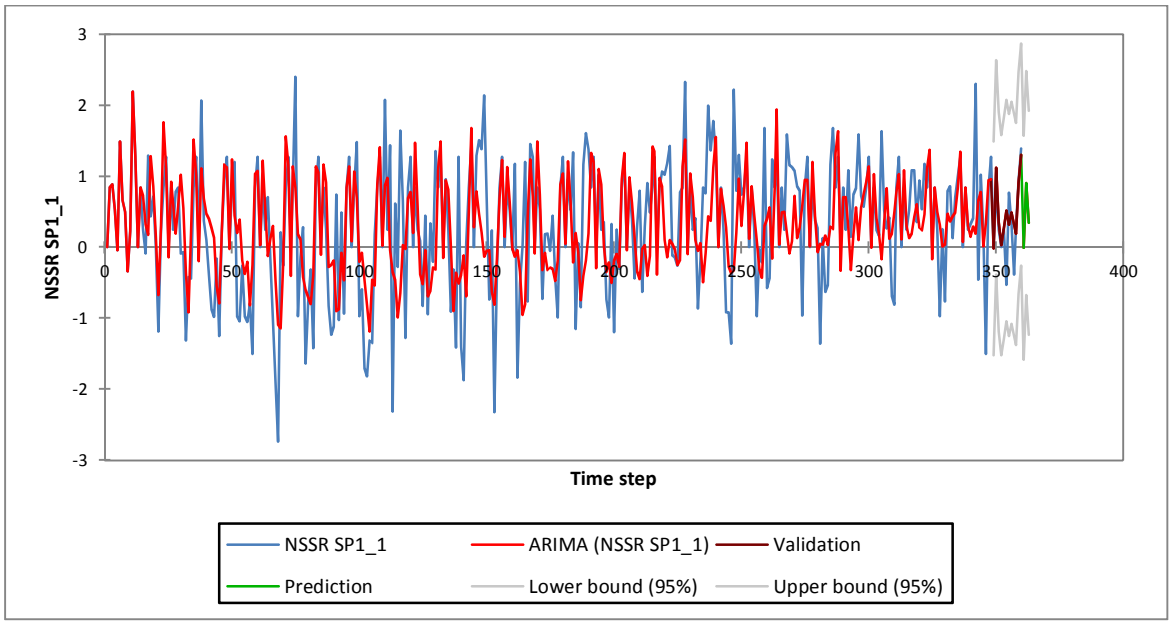


Figure 4.18a: Comparison of computed NSSR SPI_1 with forecasted SPI_1 using SARIMA $(2,0,2)x(2,1,2)_{12}$

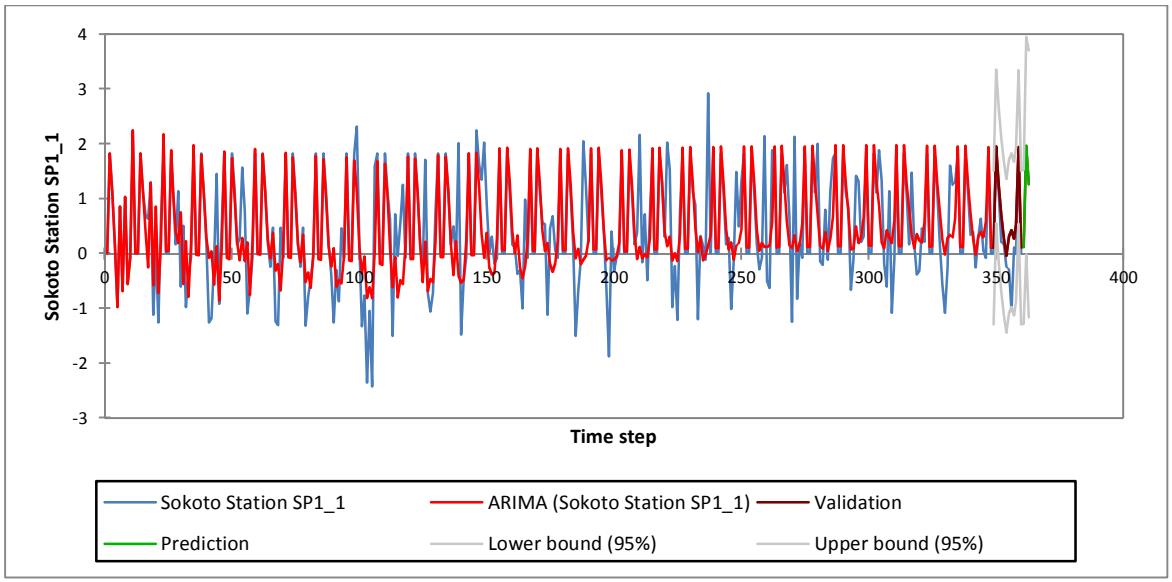


Figure 4.18b: Comparison of computed Sokoto Station SPI_1 with forecasted SPI_1 using SARIMA $(0,1,1)x(0,1,1)_{12}$

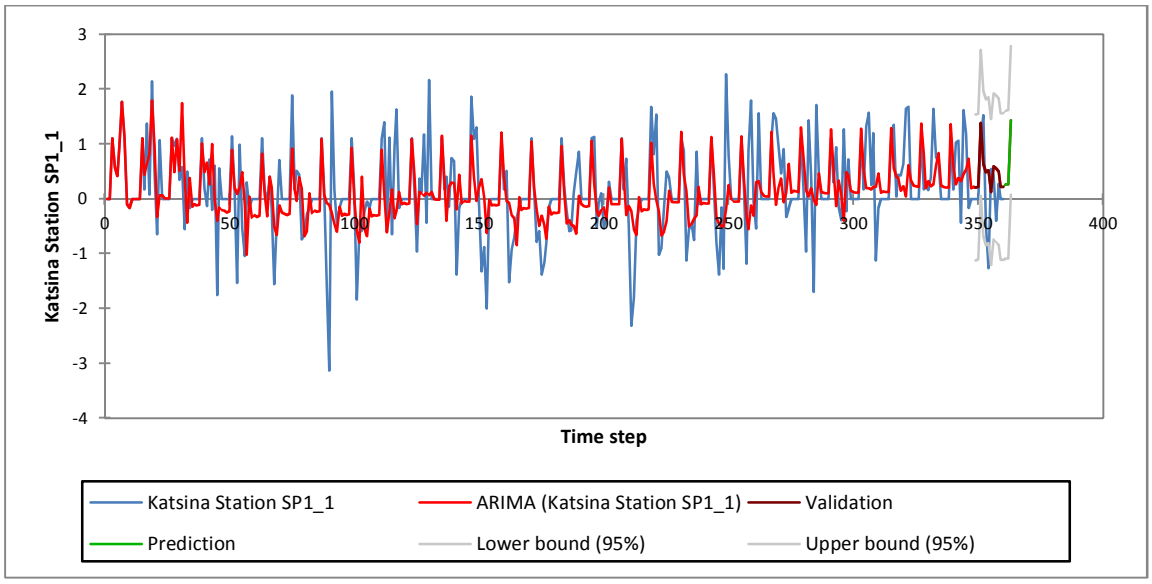


Figure 4.18c: Comparison of computed Katsina Station SPI_1 with forecasted SPI_1 using SARIMA $(1,1,1)x(1,1,1)_{12}$

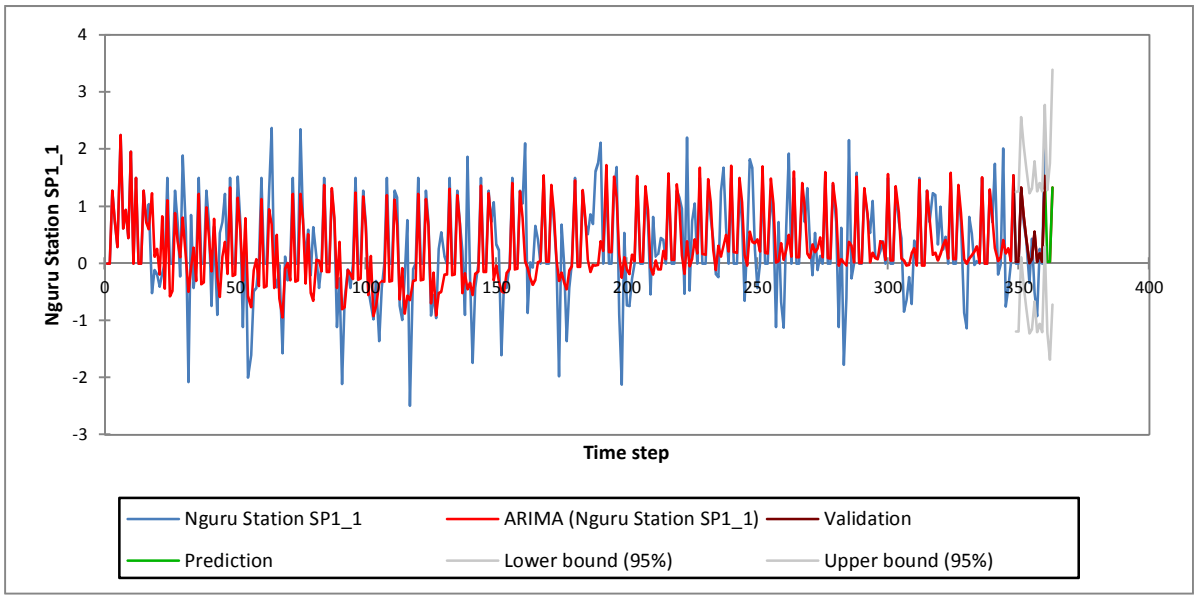


Figure 4.18d: Comparison of computed Nguru Station SPI_1 with forecasted SPI_1 using SARIMA $(0,1,1)x(0,1,1)_{12}$

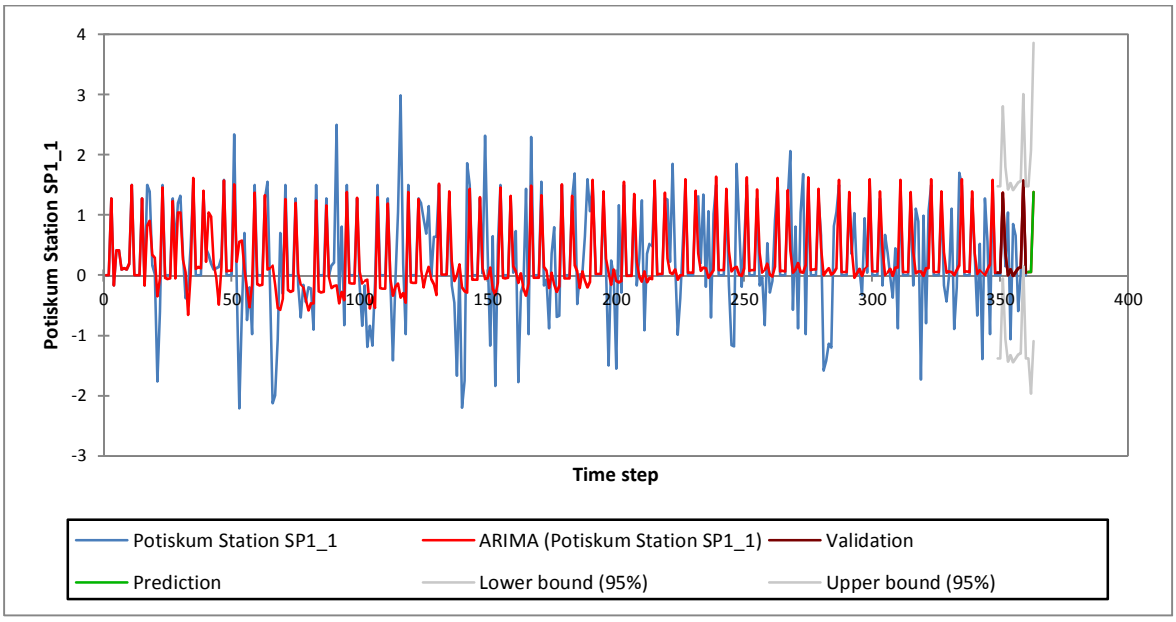


Figure 4.18e. Comparison of computed Potiskum Station SPI_1 with forecasted SPI_1 using SARIMA $(0,1,1)x(0,1,1)_{12}$

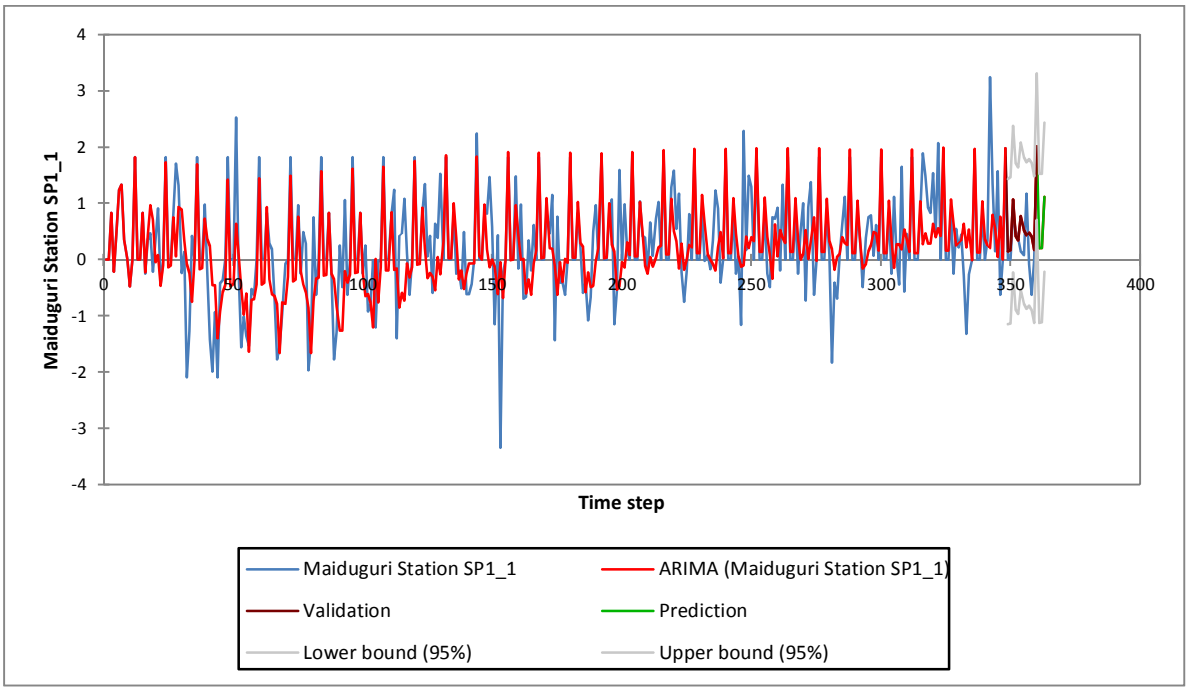


Figure 4.18f. Comparison of computed Maiduguri Station SPI_1 with forecasted SPI_1 using SARIMA $(1,1,1)x(1,1,1)_{12}$

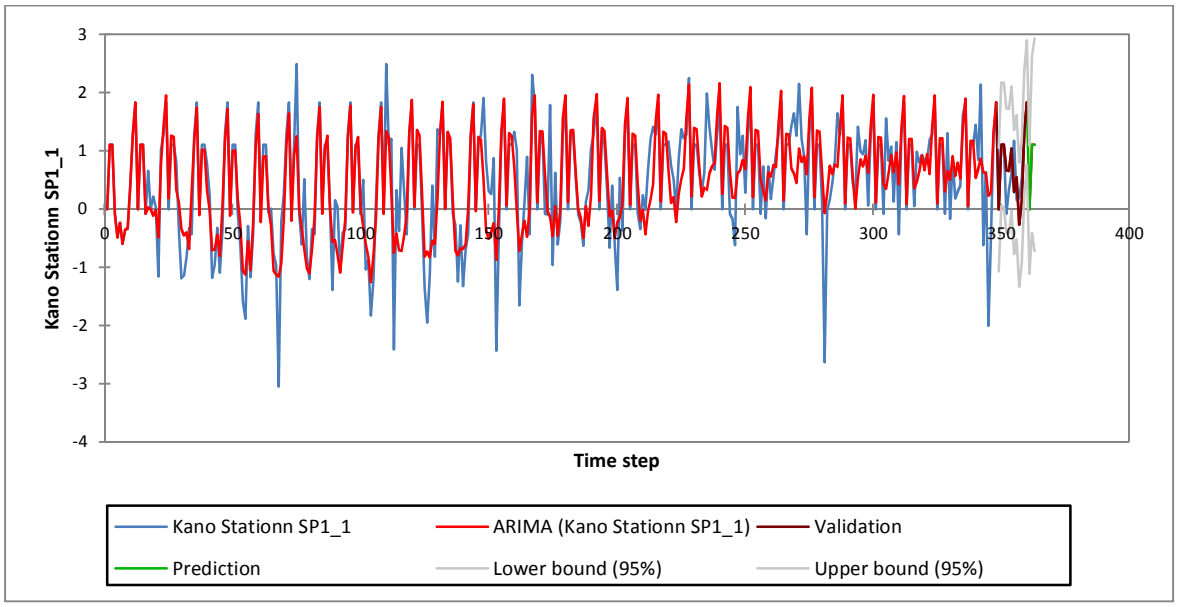


Figure 4.18g. Comparison of computed Kano Station SPI_1 with forecasted SPI_1 using SARIMA $(0,1,1)x(0,1,1)_{12}$

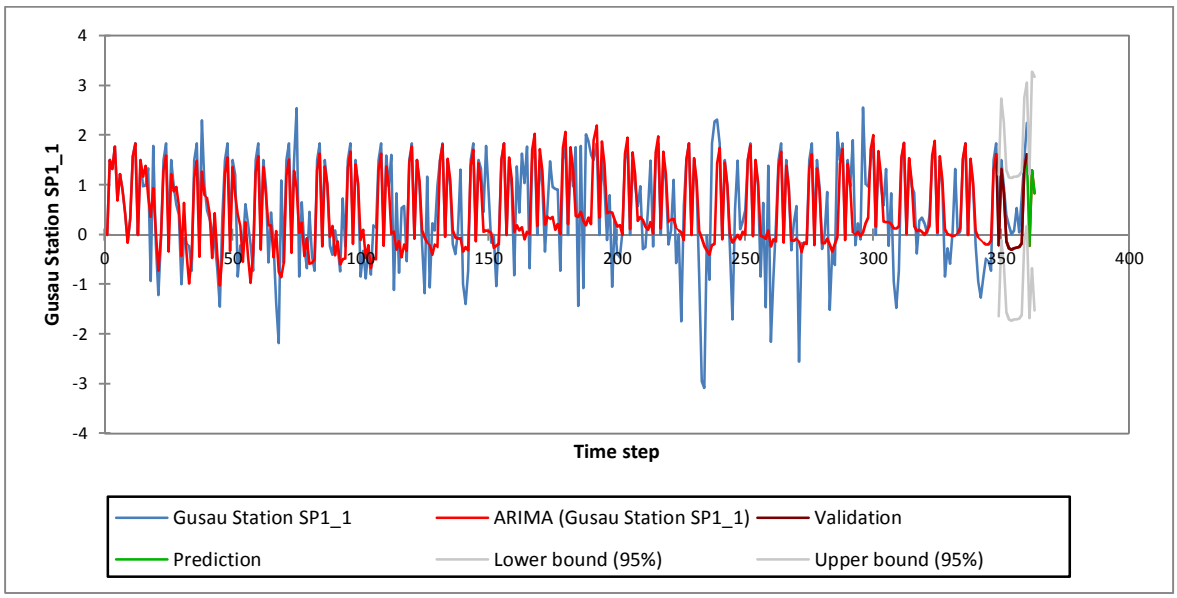


Figure 4.18h. Comparison of computed Gusau Station SPI_1 with forecasted SPI_1 using SARIMA $(0,1,1)x(0,1,1)_{12}$

4.12.2 Parameter Estimation and Diagnostic Checking

The estimated parameters for selected model $(0,1,1)x(0,1,1)_{12}$ for SPI_1 prediction at Sokoto Station is presented in Table 4.6 while the results for the other stations are as shown in Appendix G.

Table 4.6: SPI_1 Model Parameters

Parameter	Value	Hessian standard error	Lower bound (95%)	Upper bound (95%)	Asympt. standard error	Lower bound (95%)	Upper bound (95%)
Constant	0.000	0.000	0.000	0.000	0.000	0.000	0.000

Parameter	Value	Hessian standard error	Lower bound (95%)	Upper bound (95%)	Asympt. standard error	Lower bound (95%)	Upper bound (95%)
MA(1)	-1.000	0.023	-1.046	-0.954	0.055	-1.107	-0.893
SMA(1)	-1.096	0.044	-1.182	-1.010	0.055	-1.203	-0.989

Table 4.6 shows that the Moving Average (MA) (1) and Seasonal Moving Average (SMA) (1) have values -1.000 and -1.096 which are significantly different from 0 as the 95% confidence interval excluded 0. The Table reflected that the Hessian and Asymptotical standard errors from the XLSTAT optimization process were negligible and ranged from 0.023 to 0.044 and 0.055, respectively. The model $(0,1,1)x(0,1,1)_{12}$ parameter function, $Y_{(t+1)}$, is expressed thus:

$$Y_{(t+1)} = 0.000 + Z_{(t-1)} - 1.000*Z_{(t-1)} - 1.096*Z_{(t-12)} + Z_{(t-13)} \quad (4.1)$$

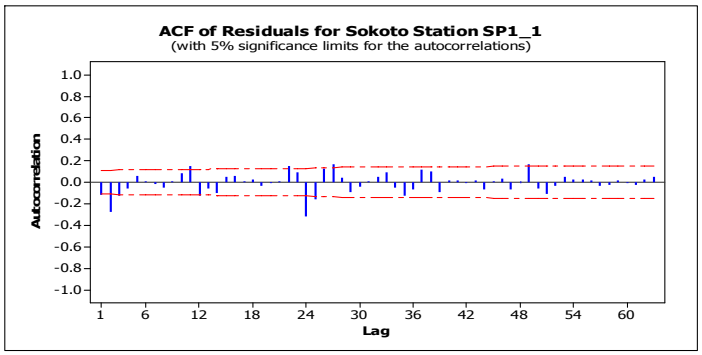
where $Z_{(t)}$ is a white noise, N(0, 000), that is, with zero mean and zero Hessian standard error. Eq. 4.1 can be re-written as follows to introduce the backshift operator (B) and the time series $X_{(t)}$:

$$Y_{(t)} = (1-B)(1-B^{12})*X_{(t)} \quad (4.2)$$

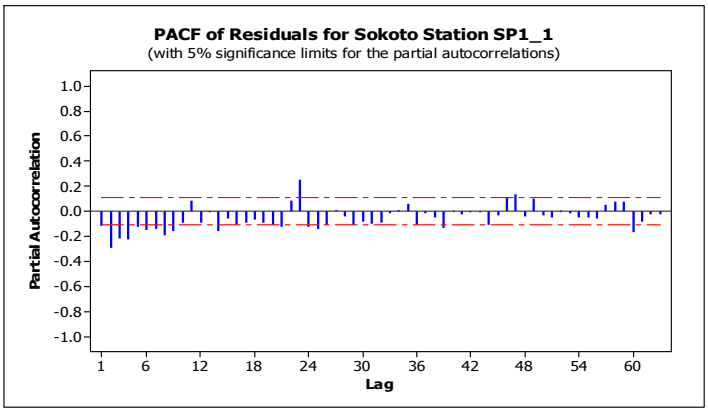
in which $X_{(t)}$ represents SPI_1 time series at Sokoto Station. The forecasting equation for the $X_{(t)}$ series is given by:

$$X_{(t+1)} = Y_{(t+1)} + X_{(t-1)} + X_{(t-12)} - X_{(t-13)} \quad (4.3)$$

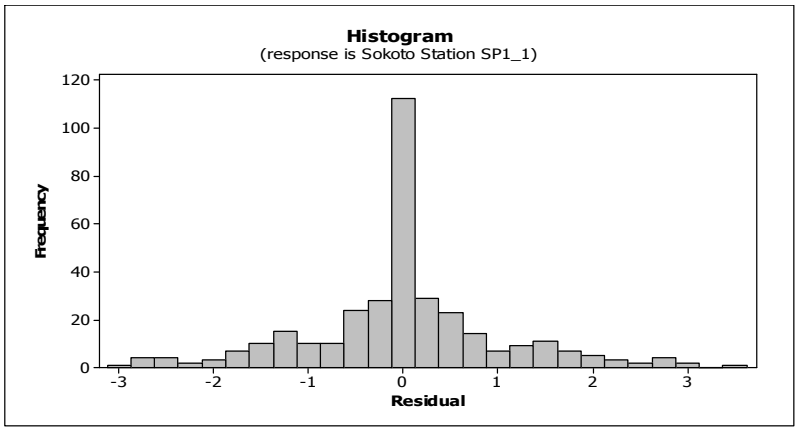
The results of ACF, PACF, histograms of residuals and normality probability plots for the diagnostic check analysis for model $(0,1,1)(0,1,1)_{12}$ for Sokoto Station are presented in Figs. 4.19a, 4.19b, 4.19c and 4.19d, respectively. The results of diagnostic check for the other stations are as shown in Appendix H.



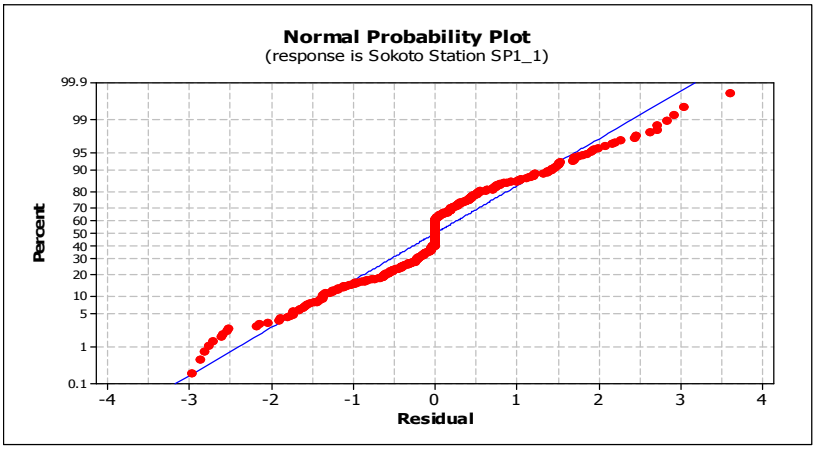
Figures 4.19a: Partial Autocorrelation function (PACF) of SPI_1 model for Sokoto Station



Figures 4.19b: Partial Autocorrelation function (PACF) of SPI_1 model for Sokoto Station



Figures 4.19c: Normal Probability Plot of SPI_1 model for Sokoto Station



Figures 4.19d: Normal Probability Plot of SPI_1 model for Sokoto Station

The diagnostic check was carried out on the residuals of the selected model. For a good forecasting model, the residuals left over after fitting the model should be white noise. This was done by examining the ACF and PACF of the residuals in Figs. 4.19a and 4.19b which were close to zero. This means that they were approximately white noise. The histogram in Fig. 4.19c showed that the residuals were normally distributed. The normal probability plot of the residuals as shown in Fig. 4.19 was fairly linear. This implies that the normality assumptions of the residuals hold (Durbin, 1960; Khadr, 2011).

4.12.3 Temperature Model Identification

Figures 4.20a and 4.20b show the ACF and PACF of the logarithmic transformed NSSR temperature data (1979-2008). Using the same approach of logarithmic transformation, data for the seven stations were analysed and the results obtained were as presented in Appendix I. Table 4.7 shows the various combinations of models out of which the selected models are presented in Figs. 4.21a to 4.21h which were extracted from the results of considered and analyzed models shown in Appendix J

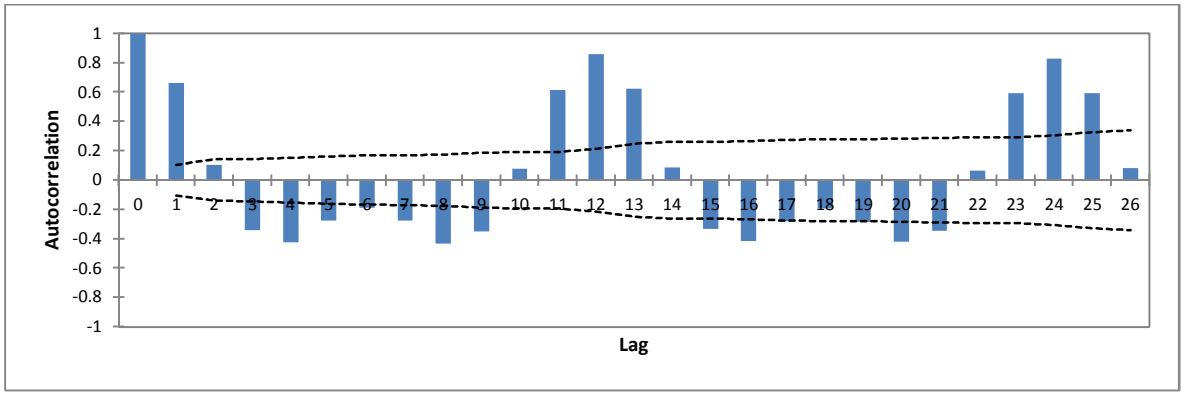


Figure 4.20a: ACF plot for selecting relevant models for transformed NSSR temperature series

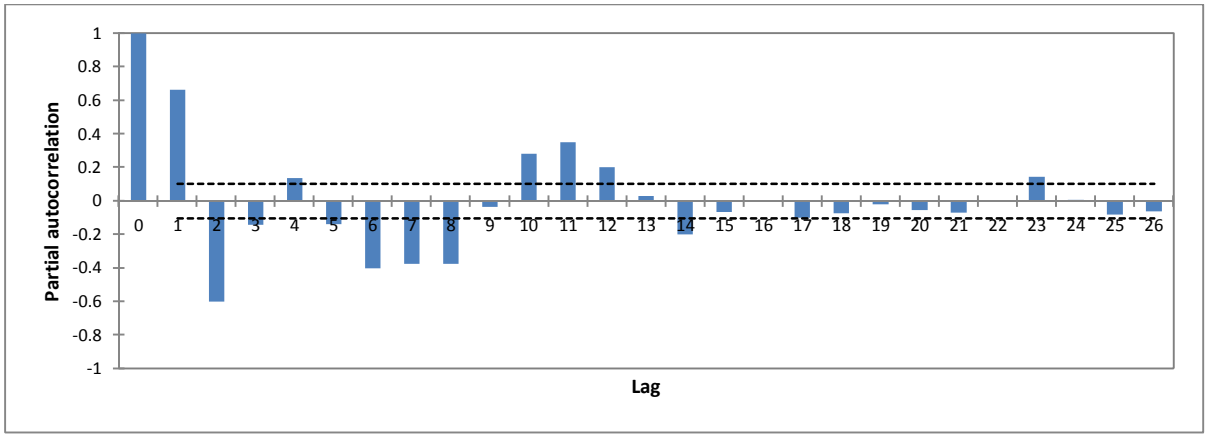


Figure 4.20b: PACF plot for selecting relevant models for transformed NSSR temperature series

The ACF of all the stations is damping out in Sine-wave manner with significant spikes at the first two lags before dying out. This implies that the "Moving Average" (MA) term or q is equal to or less than 2 (i.e., $q \leq 2$). Also, the PACF has 2 to 3 significant spikes before dying out for most of the stations. This shows that the "Auto Regressive" (AR) term or p parameter is equal to or less than 2 or 3 (i.e., $p \leq 2$ or ≤ 3). Though, four significant spikes were identified for Kano Station transformed data series PACF. This implies that the AR order is ≤ 4 for Kano Station transformed series Besides, the graph show seasonality with significant spikes at lag 12 and 24. Hence the temperature series processes at all the stations are seasonal and the patterns were removed by a 12-month lag differencing.

The summary of the various combinations of models are as presented in Table 4.7 and the selected models are as highlighted. For instance, SARIMA $(2,1,1)x(2,1,1)_{12}$ perfectly describe the time series of the NSSR with the same mean (3.305) and approximately the same standard deviation and also, the model has the lowest AIC, SBC and SSE. The same explanation holds for other stations as well. Hence, SARIMA $(2,1,1)x(2,1,1)_{12}$ is found suitable for forecasting temperature in Sokoto, Nguru, Potiskum, Kano and Gusau, while SARIMA $(3,1,1)x(3,1,1)_{12}$ was selected for temperature forecasting in Katsina and Maiduguri. The selected temperature models for the NSSR and the seven stations are as shown in Figs. 4.21a to 4.21h. The figures showed that the stochastic models are in good agreement with the observed data at each station.

Table 4.7: Comparison of Goodness of Fit Statistics and Statistical Parameters of Monthly Mean Temperature Models

Item No	Station	Series/ SARIMA Model	Mean	Standard Deviation	AIC	SBC	SSE
1	NSSR	Monthly Mean Temp. Series	3.305	0.121	-	-	-
		(211)x(211)	**3.305**	**0.116**	**-1188.334**	**-1161.635**	**0.465**
		(221)x (221)	3.307	0.124	-956.734	-930.312	0.731
2	Sokoto	Monthly Mean Temp. Series	3.359	0.105	-	-	-
		(211)x(211)	**3.360**	**0.101**	**-1229.247**	**-1202.548**	**0.348**
		(221)x(221)	3.359	0.107	-1004.704	-978.282	0.632
3	Katsina	Monthly Mean Temp. Series	3.276	0.144	-	-	-
		(311)x(311)	**3.279**	**0.130**	**-1065.411**	**-1031.084**	**0.703**
		(321)x(321)	3.281	0.137	-857.382	-823.411	0.972
4	Nguru	Monthly Mean Temp. Series	3.330	0.132	-	-	-
		(211)x(211)	**3.330**	**0.128**	**-1228.400**	**-1201.475**	**0.000**
		(221)x(221)	3.332	0.135	-948.804	-922.382	0.752
5	Potiskum	Monthly Mean Temp. Series	3.287	0.153	-	-	-
		(211)x(211)	**3.283**	**0.130**	**-633.111**	**-606.412**	**2.449**
		(221)x(221)	3.288	0.162	-402.956	-376.534	4.111
6	Maiduguri	Monthly Mean Temp. Series	3.315	0.138	-	-	-
		(311)x(311)	**3.313**	**0.125**	**-851.467**	**-817.140**	**1.268**
		(321)x(321)	3.315	0.144	-639.006	-605.035	1.896
7	Kano	Monthly Mean Temp. Series	3.281	0.128	-	-	-
		(211)x(211)	**3.280**	**0.122**	**-1128.158**	**-1090.017**	**0.000**
		(311)x(311)	3.279	0.123	-1128.139	-1093.812	0.000
		(311)x(411)	3.275	0.127	-1128.158	-1090.017	0.000
		(411)x(311)	3.278	0.124	-1126.157	-1088.016	0.000
		(411)x(411)	3.280	0.132	-1126.162	-1084.207	0.000
8	Gusau	Monthly Mean Temp. Series	3.280	0.105	-	-	-
		(211)x(211)	**3.283**	**0.096**	**-1116.642**	**-1089.943**	**0.587**
		(221)x(221)	3.288	0.157	-900.257	-873.835	0.000

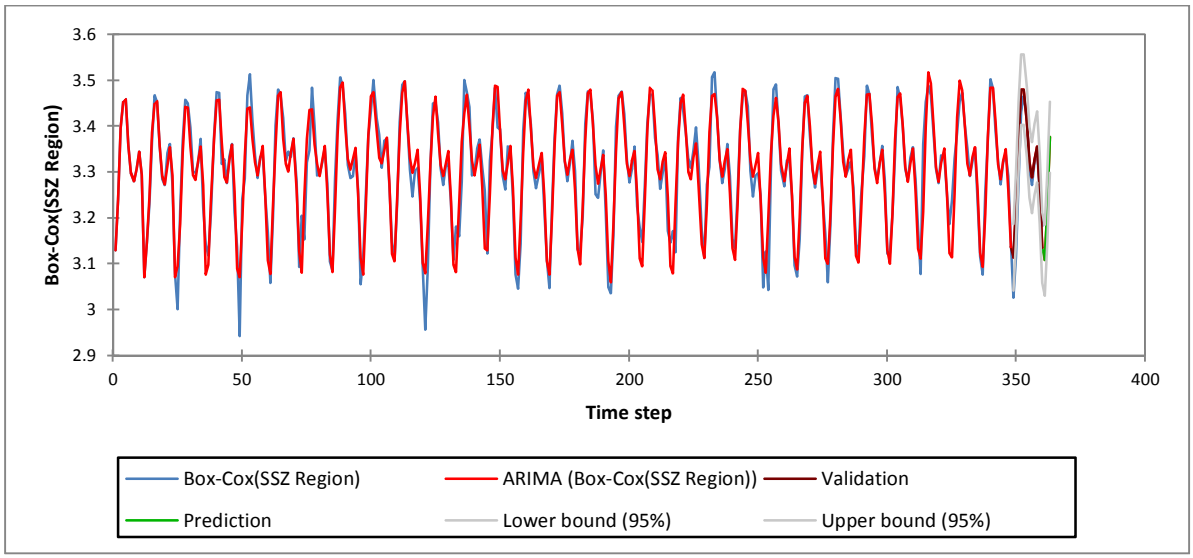


Figure 4.21a: Comparison of NSSR Observed and predicted Transformed Temperature using SARIMA $(2,1,1)x(2,1,1)_{12}$

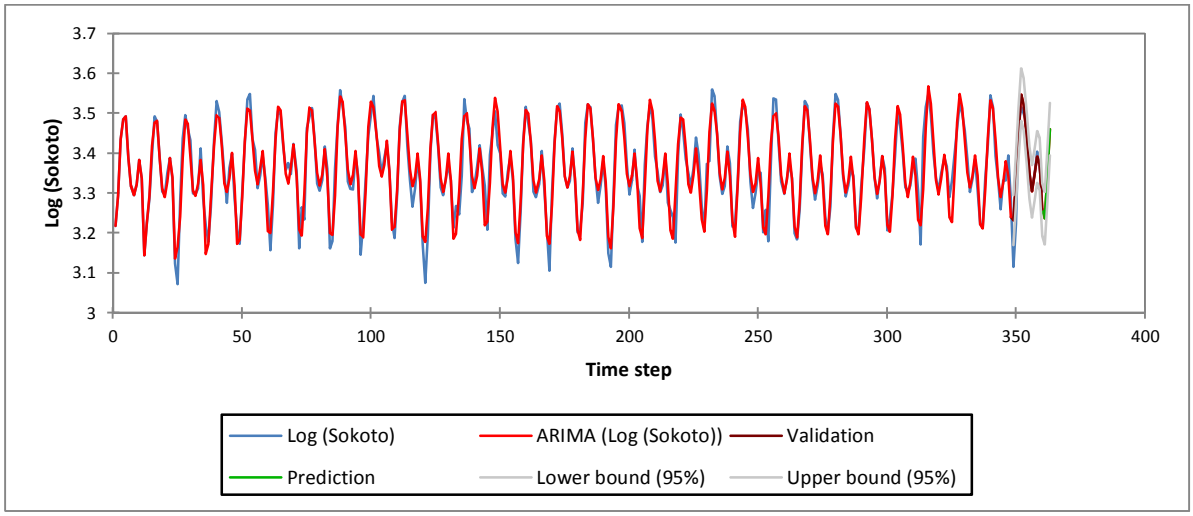


Figure 4.21b: Comparison of Sokoto Station Observed and predicted Transformed Temperature using SARIMA $(2,1,1)x(2,1,1)_{12}$

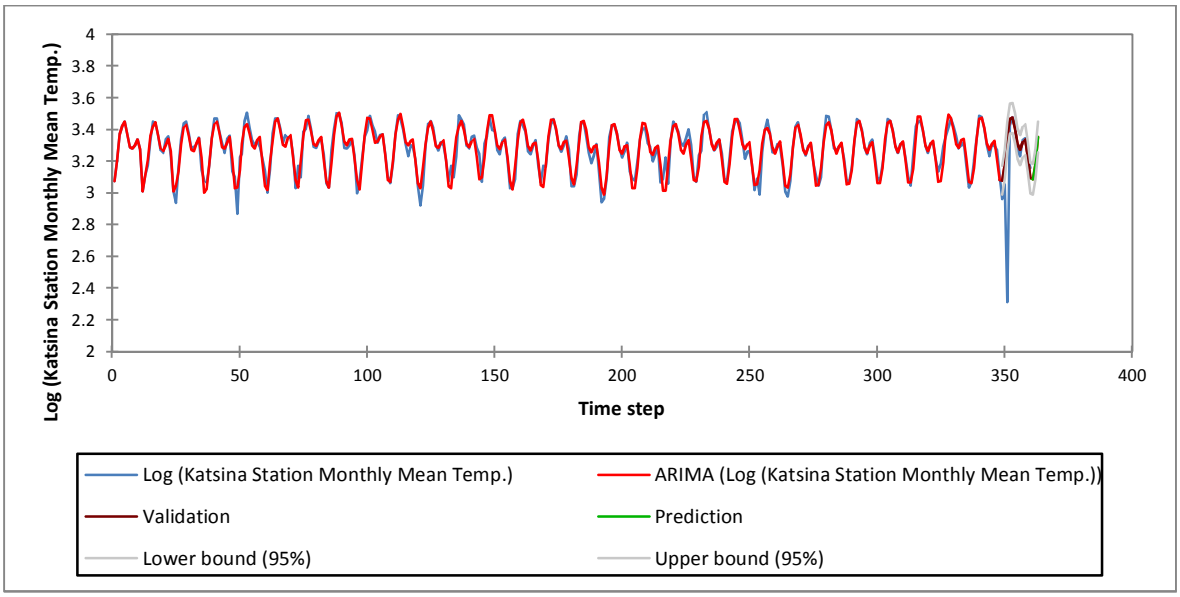


Figure 4.21c: Comparison of Katsina Station Observed and predicted Transformed Temperature using SARIMA $(3,1,1)x(3,1,1)_{12}$

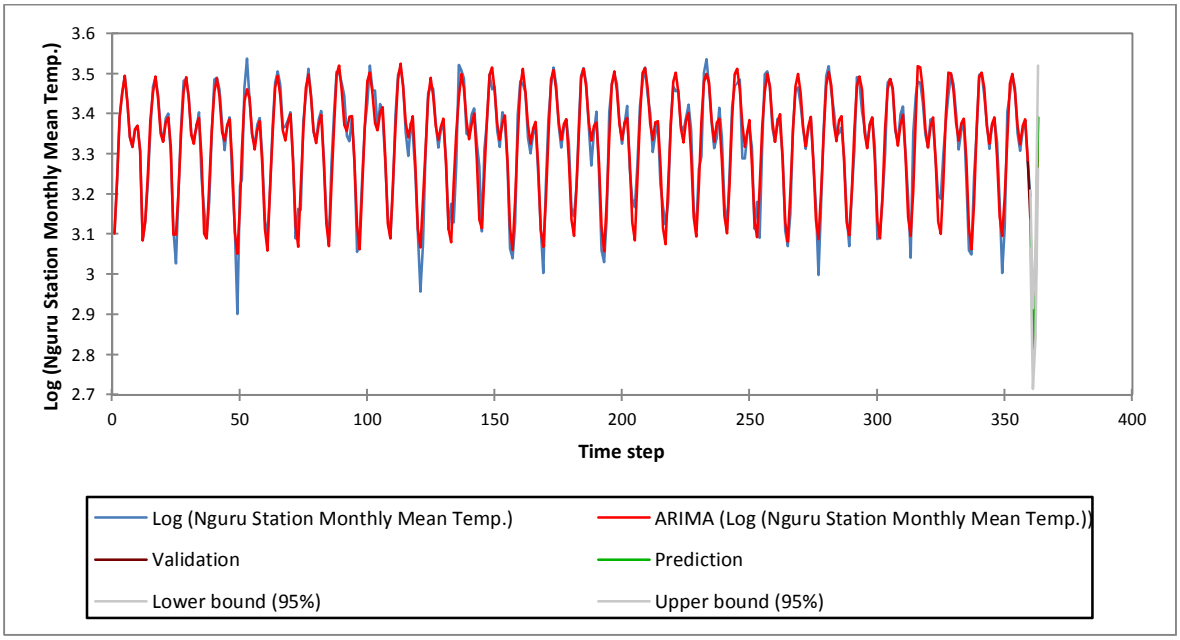


Figure 4.21d: Comparison of Nguru Station Observed and predicted Transformed Temperature using SARIMA $(2,1,1)x(2,1,1)_{12}$

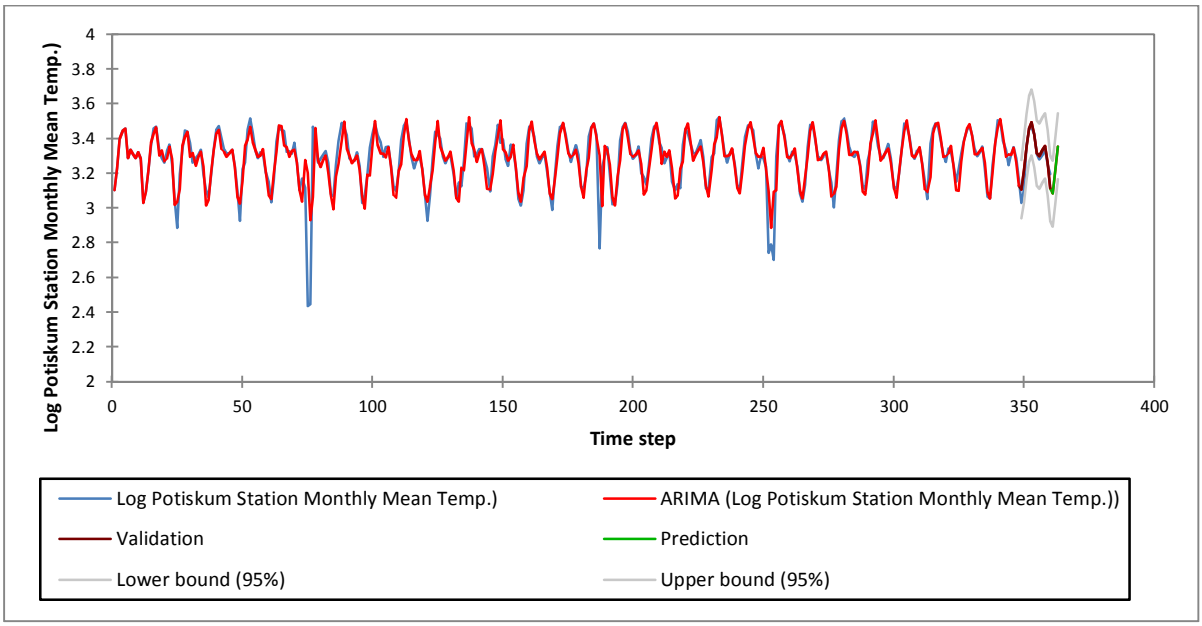


Figure 4.21e: Comparison of Potiskum Station Observed and predicted Transformed Temperature using SARIMA $(2,1,1)x(2,1,1)_{12}$

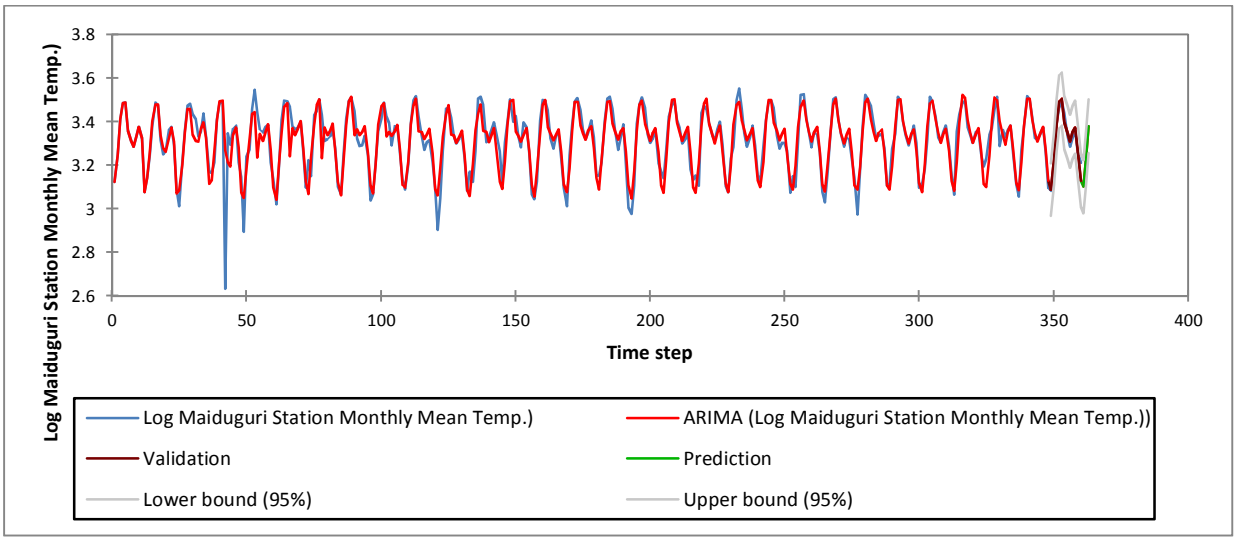


Figure 4.21f: Comparison of Maiduguri Observed and predicted Transformed Temperature using SARIMA $(3,1,1)x(3,1,1)_{12}$

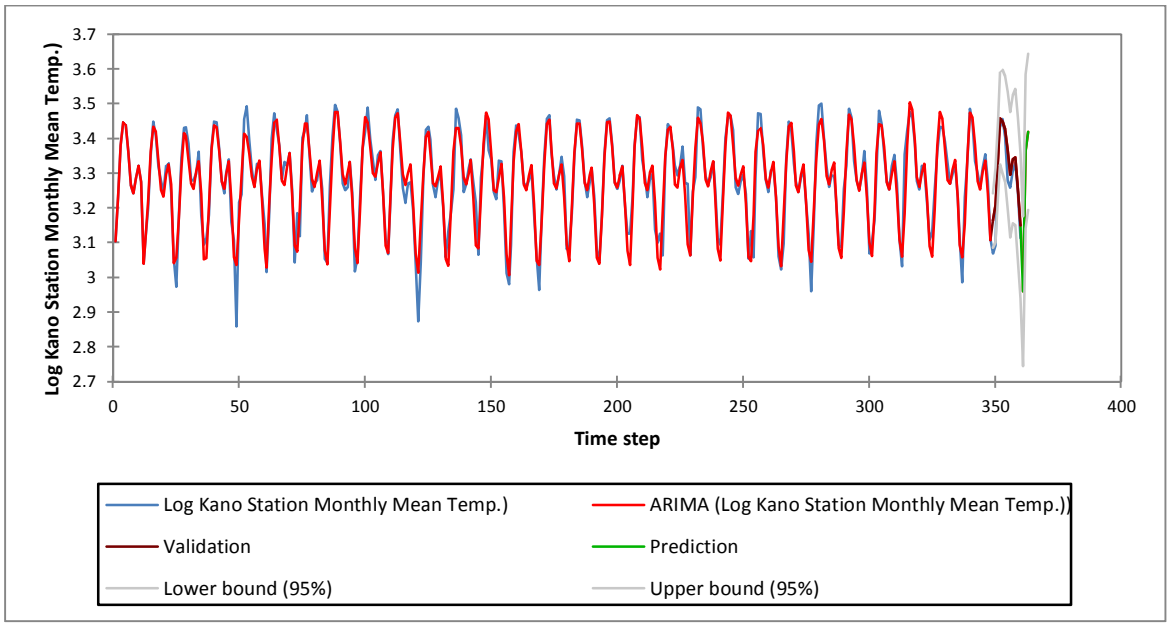


Figure 4.21g: Comparison of Kano Station Observed and predicted Transformed Temperature using SARIMA $(2,1,1)x(2,1,1)_{12}$

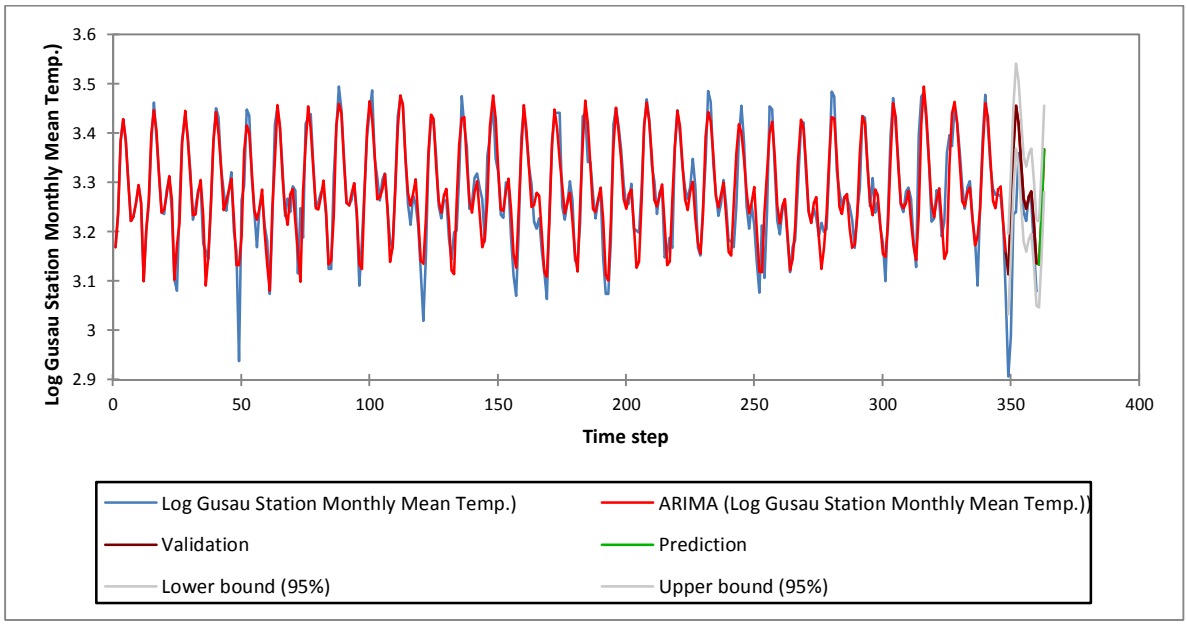


Figure 4.21h: Comparison of Gusau Station Observed and predicted Transformed Temperature using SARIMA $(2,1,1)x(2,1,1)_{12}$

4.12.4 Parameters Estimation and Diagnostic Checking

The estimated parameters for model $(2,1,1)x(2,1,1)_{12}$ for temperature prediction at Sokoto Station is presented in Table 4.8 while the remaining parameters for the other stations are as shown in Appendix J.

Table 4.8: Temperature Model Parameters

Parameter	Value	Hessian standard error	Lower bound (95%)	Upper bound (95%)	Asympt. standard error	Lower bound (95%)	Upper bound (95%)
Constant	0.000	0.000	0.000	0.000	0.000	0.000	0.000

Parameter	Value	Hessian standard error	Lower bound (95%)	Upper bound (95%)	Asympt. standard error	Lower bound (95%)	Upper bound (95%)
AR(1)	0.207	0.062	0.085	0.329			
AR(2)	0.154	0.053	0.051	0.258			
SAR(1)	-0.015	0.075	-0.161	0.131			
SAR(2)	-0.076	0.070	-0.213	0.061			
MA(1)	-1.000	0.024	-1.046	-0.954			
SMA(1)	-1.133	0.058	-1.247	-1.019			

Table 4.8 indicated that the seasonal and non-seasonal Auto Regressive (AR) and Moving Average (MA) parameters were significantly different from 0 as the 95% confidence intervals excluded 0. The Hessian standard errors from the optimization were minimal and ranged from 0.024 to 0.075. The expression describing the parameter function (Y_t) for Seasonal ARIMA is expressed as (Khadr, 2011; Suhartono, 2011):

$$\varphi_p(B)\emptyset_P(B^s)(1-\mathrm{B})^d(1-B^s)^D\, Y_t = \Theta_Q(B^s)\theta_q(B)\varepsilon_t \quad (4.4)$$

in which, for non-seasonal and seasonal SARIMA of order p, q and P, Q, respectively,

$$\varphi_p(B) = 1 - \varphi_1 B - \cdots - \varphi_p B^p \quad (4.5)$$

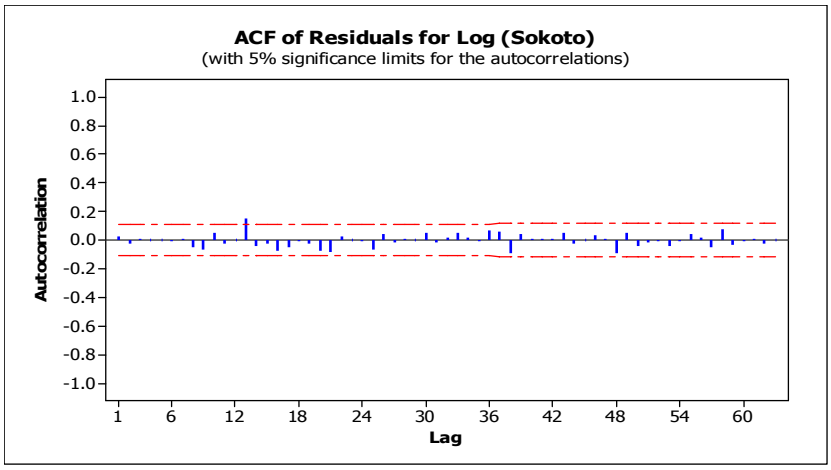
$$\theta_q(B) = 1 - \theta_1 B - \cdots - \theta_q B^q \quad (4.6)$$

$$\emptyset_P(B^s) = 1 - \emptyset_1 B^s - \cdots - \emptyset_p B^{sP} \quad (4.7)$$

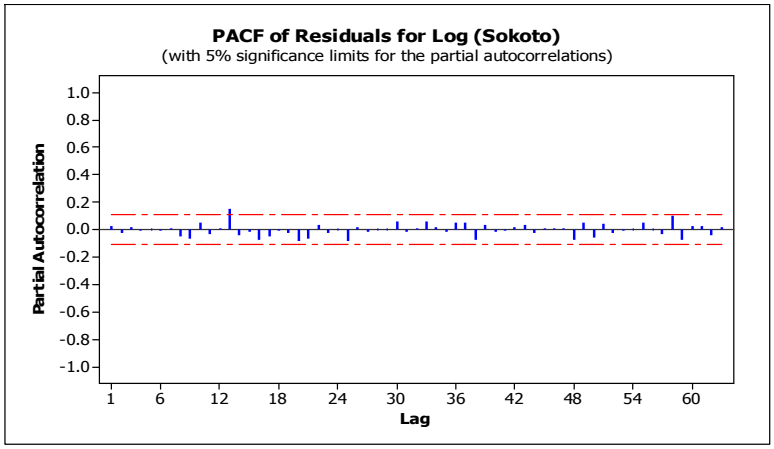
$$\Theta_Q(B^s) = 1 - \Theta_1 B^s - \cdots - \Theta_Q B^{sQ} \quad (4.8)$$

where B is the backshift operator (i.e. B $y_t = y_{t-1}$, $B^2 y_t = y_{t-2}$ and so on),'s' is the seasonal lag and 'εt' is the sequence of independent normal error variables with mean 0 and variance σ^2 (0.000 from Table 4.8. Ø and φ are the seasonal and non-seasonal auto regressive parameters of the order 1 and 2 as shown in Table 4.8, respectively . Θ and θ are seasonal and non-seasonal moving average parameters of the order 1 each as shown in the Table, respectively. P and Q are the seasonal auto regression and moving average parameters whereas p and q are orders of non-seasonal auto regression and moving average parameters, respectively. D and d denote seasonal and non-seasonal differences, respectively. The values of p, d, q, P, D, Q and s were figured out from the forecasting model $(2,1,1)x(2,1,1)_{12}$ by correlating the model with the general SARIMA form (pdq)x(PDQ)s. Substitution of the values of parameters into Eqs. 4.4 to 4.8 aided the determination of the parameter function, Y_t, in Eq. 4.4, which was substituted into Eq. 4.2 to obtain temperature time series ($X_{(t)}$) at Sokoto Station. The forecasting equation for the series was expressed by Eq. 4.3.

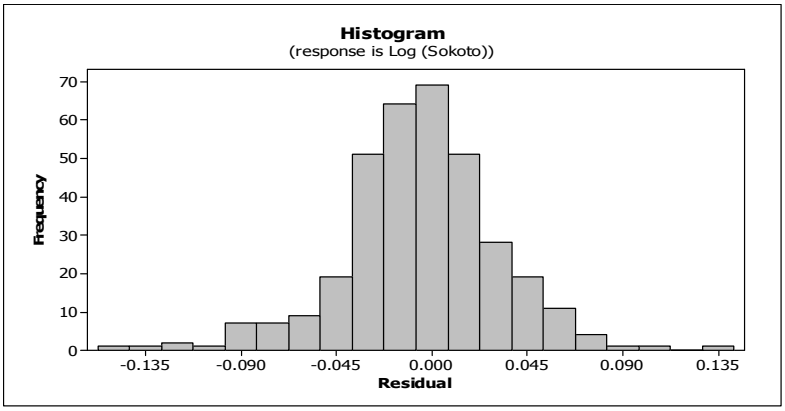
Figures 4.22a to 4.22d shows the ACF, PACF, histograms for the residuals and the normal probability plot of the selected model, $(2,1,1)x(2,1,1)_{12}$, for temperature prediction at Sokoto Station while the results for the other stations were presented in Appendix K. The ACF and PACF of the residuals in Figs. 4.22a and 4.22b were close to zero. This means that they were approximately white noise. The histogram in Fig. 4.22c showed that the residuals were normally distributed and the normal probability plot of the residuals as shown in Fig. 4.22d was fairly linear.



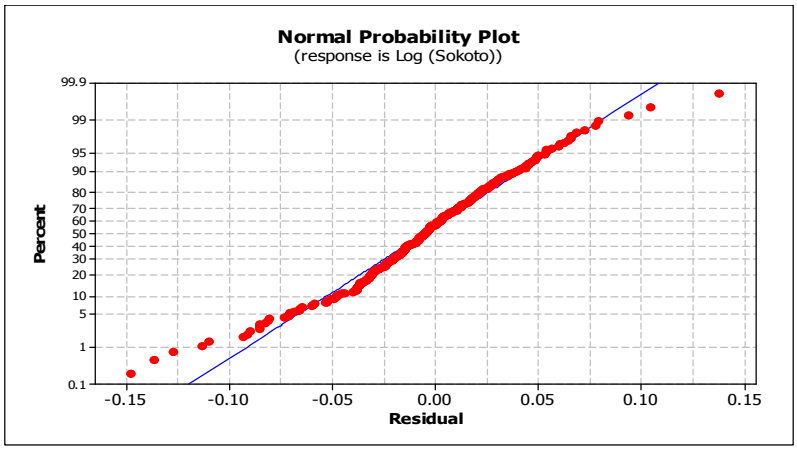
Figures 4.22a: Autocorrelation Function (ACF) of temperature model for Sokoto Station



Figures 4.22b: Partial Autocorrelation Function (PACF) of temperature model for Sokoto Station



Figures 4.22 c: Residuals Histograms of temperature model for Sokoto Station



Figures 4.22 d: Normal Probability Plot of temperature model for Sokoto Station

4.13 Model Validation

Tables 4.9 to 4.14 show the results of model validation for the selected SPI_1 and temperature models. Available data were used to validate relevant models. The predictive models were used to forecast SPI_1 and temperature 3 months into the future. Available actual data for the forecasted months were compared with the forecasts to validate the models. The validations of the forecasted SPI_1 are carried out by comparing the forecasted SPI_1 with the computed SPI_1 (from observed SPI_1). The results show good agreement between observations and forecasts as presented in Tables 4.9 to 4.11. Using similar approach, the results of validation of temperature models show good agreement between observations and forecasts as shown in Tables 4.12 to 4.14. The goodness of fit of the forecasts were ascertain further using Sum of Squared Errors

Table 4.9: Validation of SARIMA Model for Sokoto Station SPI_1

Months	Computed SPI_1	Predicted SPI_1	Computed SPI_1 (for validation)	SPI_1 Forecasts	SSE	RMSE
357	0.110	0.602				
358	-0.010	0.543				
359	1.830	1.830				
360	0.000	0.000				
361			0.000	0.000		
362			1.850	1.830		
363			1.130	1.110	0.001	0.016

Table 4.10: Validation of SARIMA Model for Katsina Station SPI_1

Months	Computed SPI_1	Predicted SPI_1	Computed SPI_1 (for validation)	SPI_1 Forecasts	SSE	RMSE
357	-0.400	0.996				
358	0.280	0.218				
359	0.000	0.000				
360	0.000	0.000				
361			0.000	0.000		
362			0.000	0.000		
363			1.130	1.110	0.001	0.012

Table 4.11: Validation of SARIMA Model for Gusau Station SPI_1

Months	Computed SPI_1	Predicted SPI_1	Computed SPI_1 (for validation)	SPI_1 Forecasts	SSE	RMSE
357	0.040	-0.267				
358	0.760	-0.325				
359	1.500	1.500				
360	2.250	1.830				
361			0.000	0.000		
362			1.520	1.500		
363			0.990	0.970	0.001	0.016

Table 4.12: Validation of SARIMA Model for Sokoto Station transformed temperature

Months	Obs. Transformed Temperature	Pred. Transformed Temperature	Obs. Transformed Temperature (for validation)	Transformed Temperature Forecasts	SSE	RMSE
357	3.348	3.346				
358	3.405	3.391				
359	3.362	3.373				
360	3.305	3.260				
361			3.277	3.238		
362			3.409	3.344		
363			3.486	3.460	0.006	0.046

Table 4.13: Validation of SARIMA Model for Katsina Station transformed temperature

Months	Obs. Transformed Temperature	Pred. Transformed Temperature	Obs. Transformed Temperature (for validation)	Transformed Temperature Forecasts	SSE	RMSE
357	3.332	3.322				
358	3.345	3.339				
359	3.229	3.228				
360	3.161	3.095				
361			3.157	3.087		
362			3.277	3.184		
362			3.363	3.353	0.014	0.068

Table 4.14: Validation of SARIMA Model for Gusau Station transformed temperature

Months	Obs. Transformed Temperature	Pred. Transformed Temperature	Obs. Transformed Temperature (for validation)	Transformed Temperature Forecasts	SSE	RMSE
357	3.273	3.271				
358	3.258	3.283				
359	3.170	3.218				
360	3.080	3.137				
361			3.208	3.134		
362			3.303	3.238		
363			3.351	3.368	0.010	0.058

(SSE) and Root Mean Square Error (RMSE) as discussed in the next section.

4.14 PERFORMANCE CRITERIA

The results of Sum of Squared Errors (SSE) and Root Mean Square Error (RMSE) computed for forecast residuals, to ascertain performance criteria for model validation are as shown in Tables 4.9 to 4.14. The range of SSE and RMSE are from 0.001 to 0.014 and 0.012 to 0.068, respectively. The values were close to zero and this ascertains the goodness of fit between the observed data and forecasts.

4.15 DROUGHT FORECASTING USING MODELS

The selected models for SPI_1 and temperature were used to forecast drought occurrence at each of the stations and the results were presented in Appendices L and M, respectively. Zoom windows of twelve month forecasts, from 361th to 372nd month, were extracted from Appendices H and I and shown in Figs. 4.23a to 4.23h and Figs. 4.24a to 4.24h for SPI_1 and temperature forecasts, respectively.

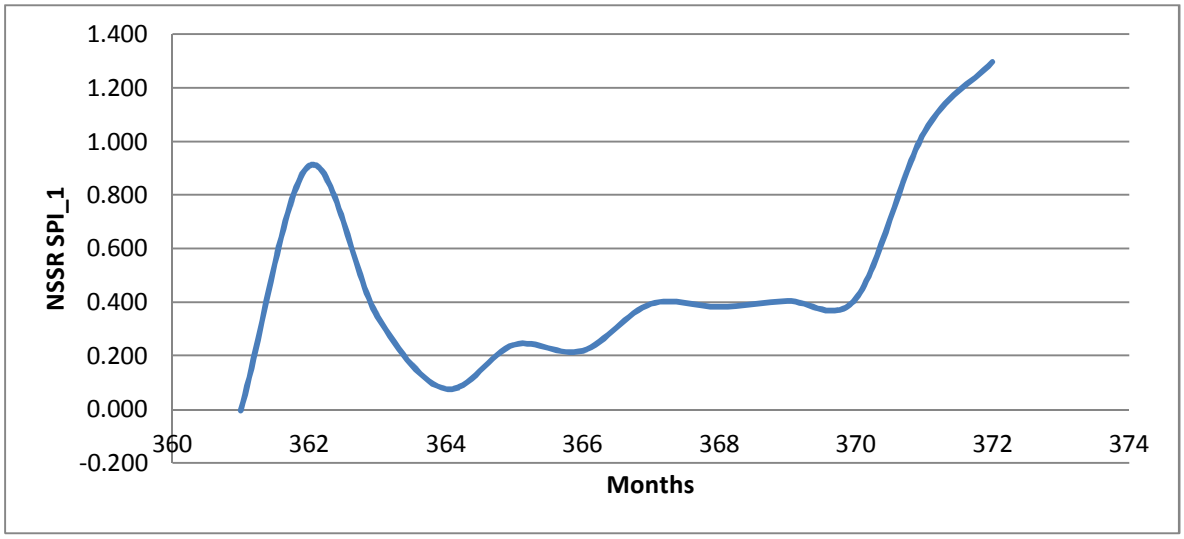


Figure 4.23a: 12 months NSSR SPI_1 forecast

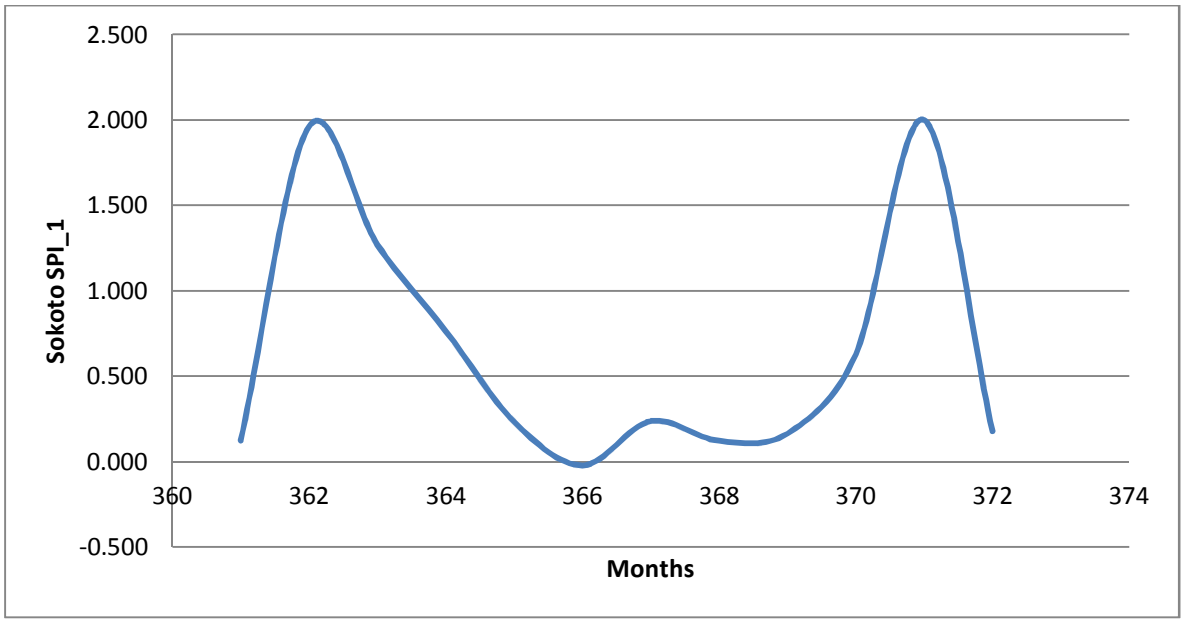


Figure 4.23b: 12 months Sokoto Station SPI_1 forecast

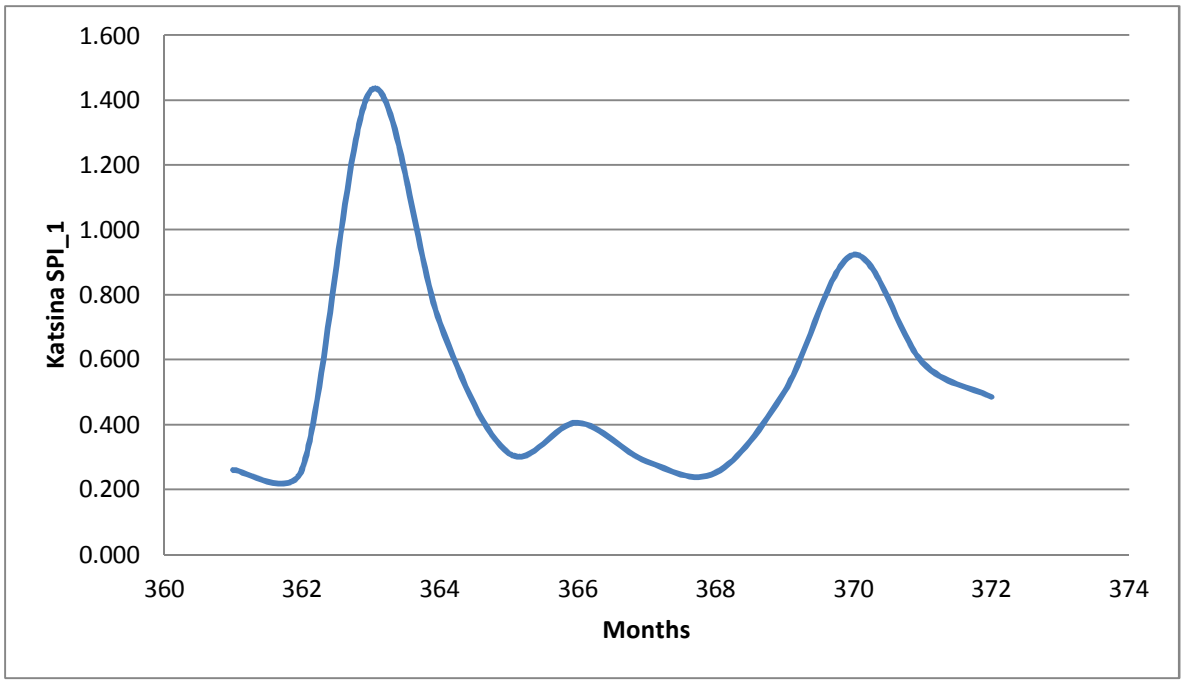


Figure 4.23c: 12 months Katsina Station SPI_1 forecast

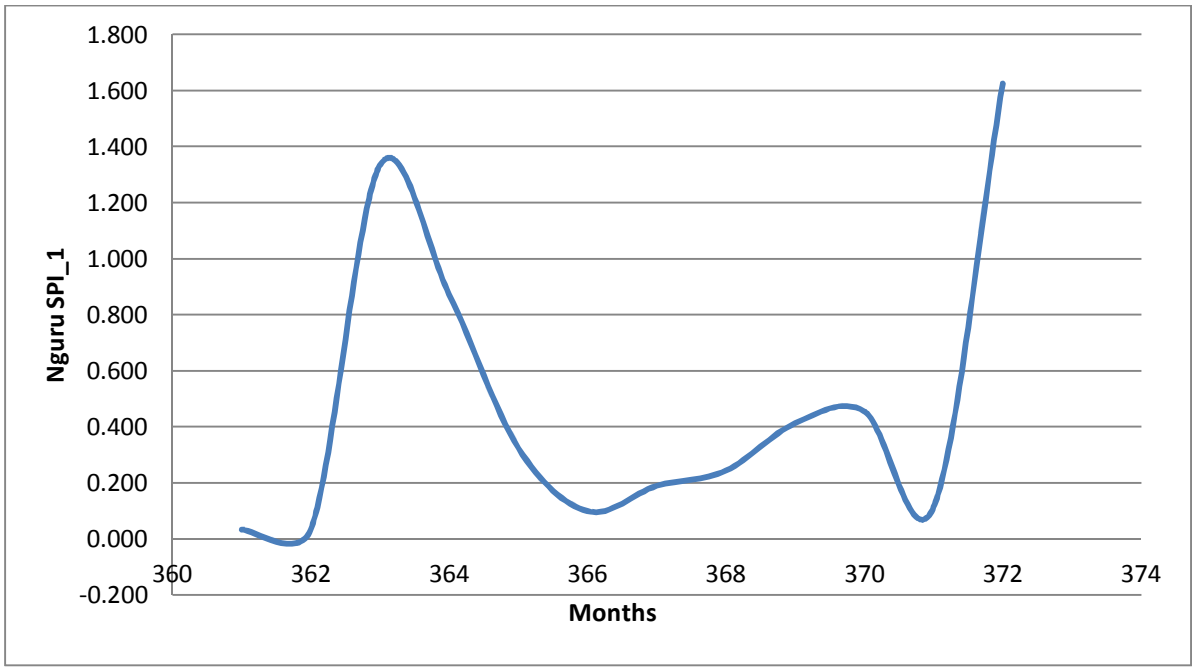


Figure 4.23d: 12 months Nguru Station SPI_1 forecast

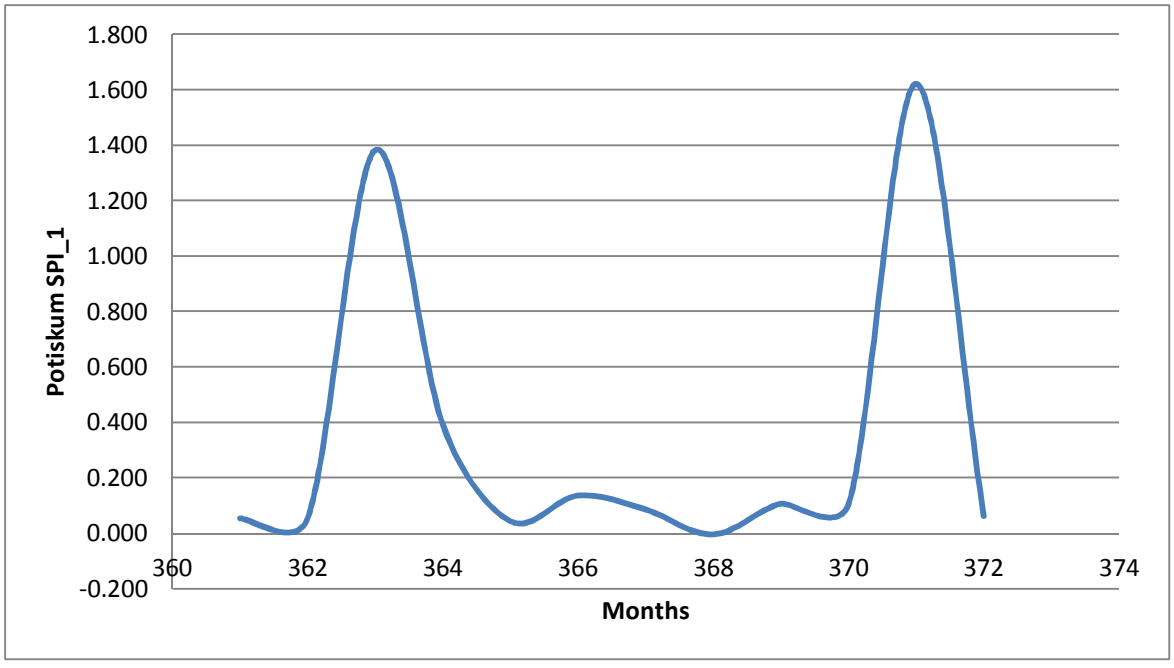


Figure 4.23e: 12 months Potiskum Station SPI_1 forecast

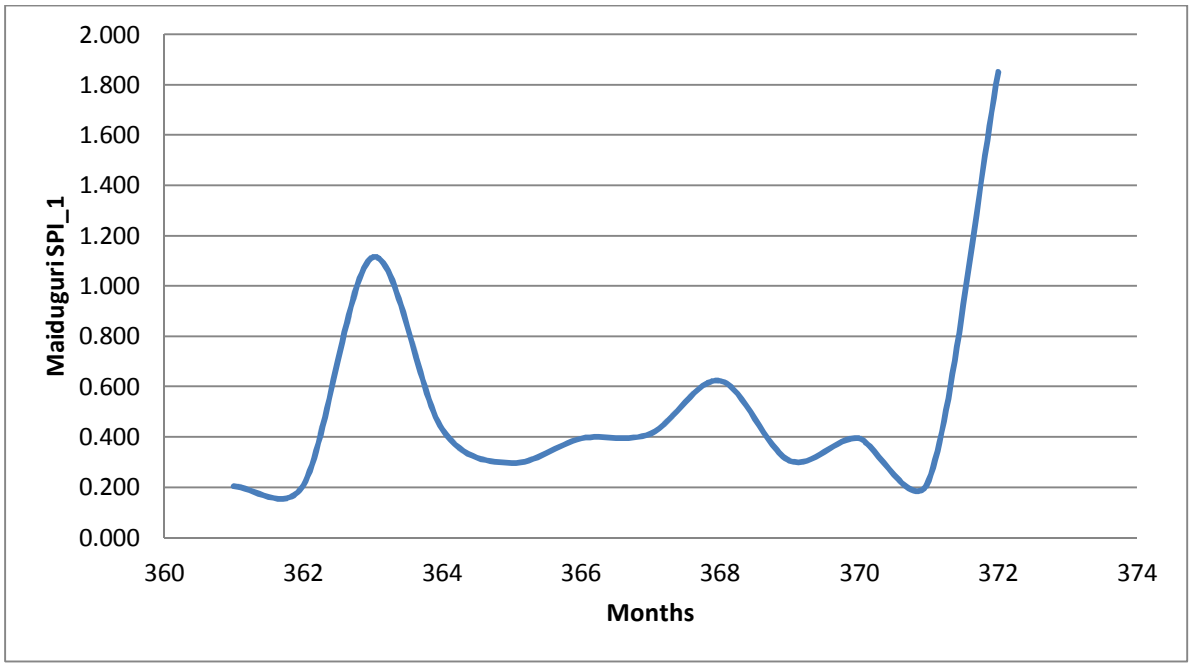


Figure 4.23f: 12 months Maiduguri Station SPI_1 forecast

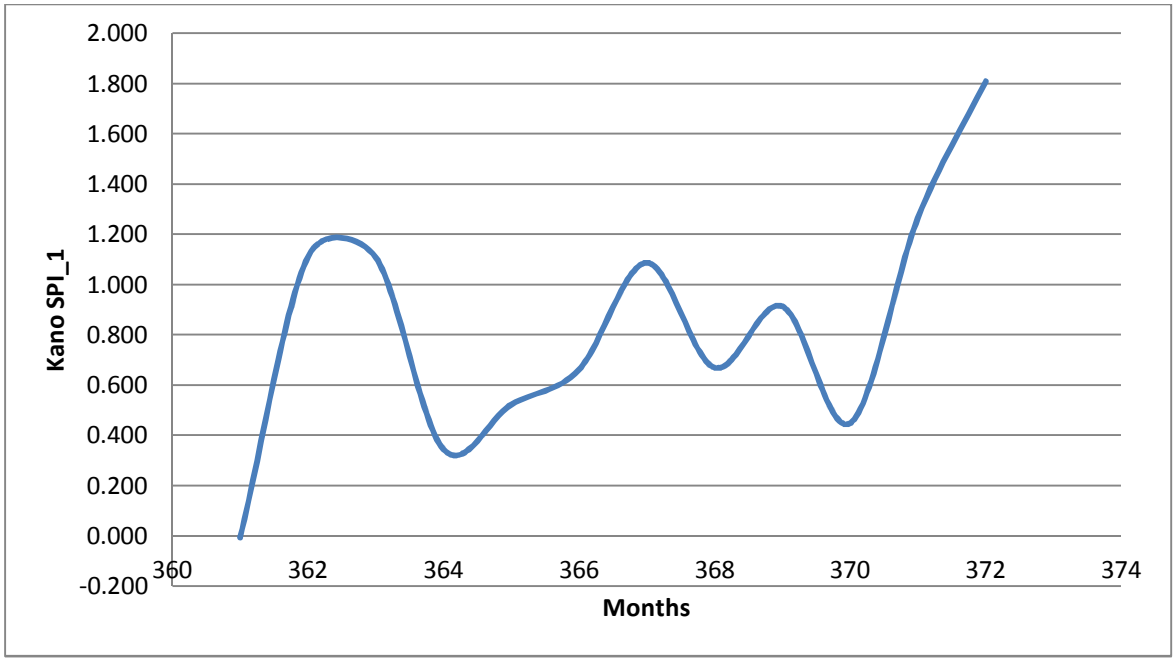


Figure 4.23g: 12 months Kano StationSPI_1 forecast

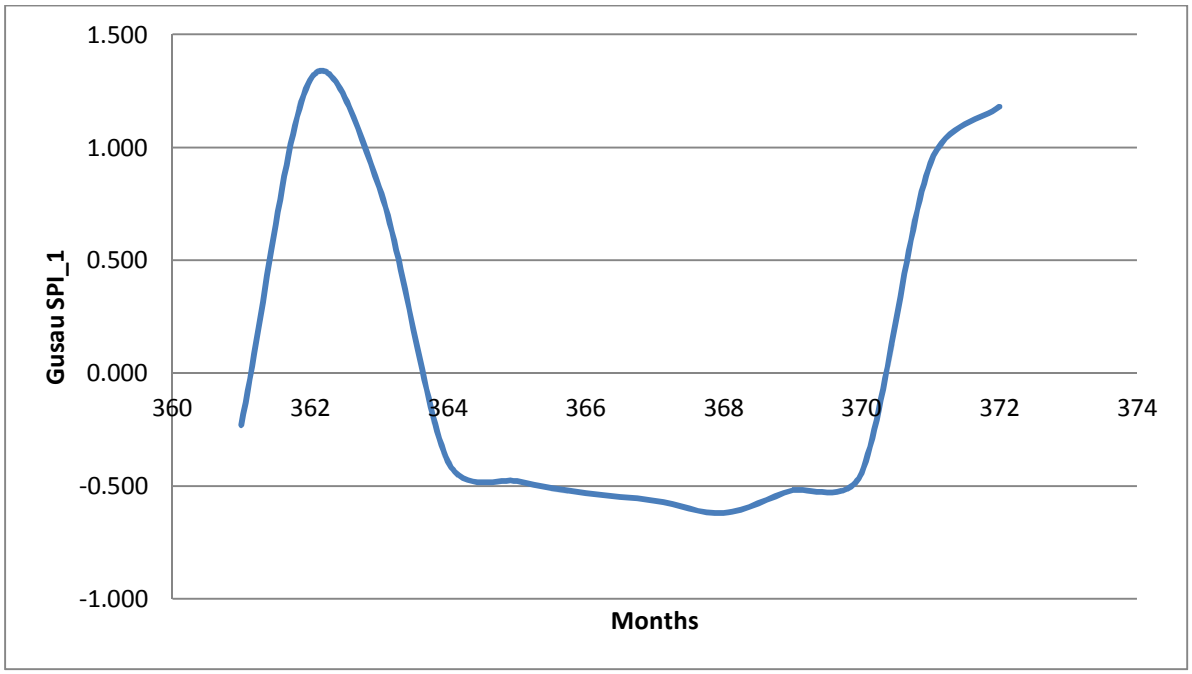


Figure 4.23h: 12 months Gusau Station SPI_1 forecast

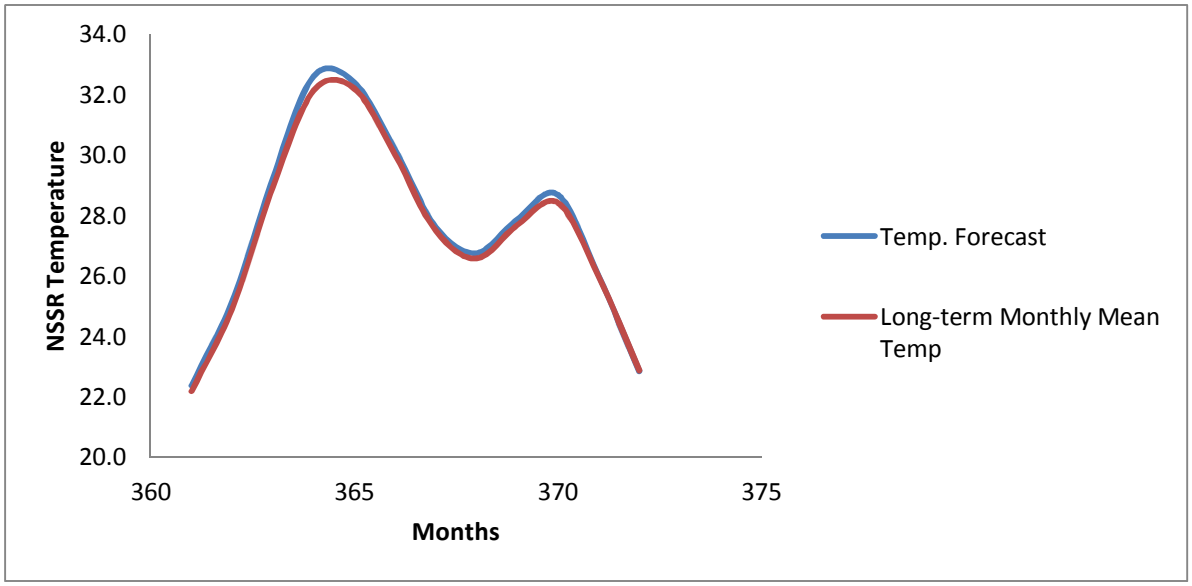


Figure 4.24a: NSSR transformed temperature forecast

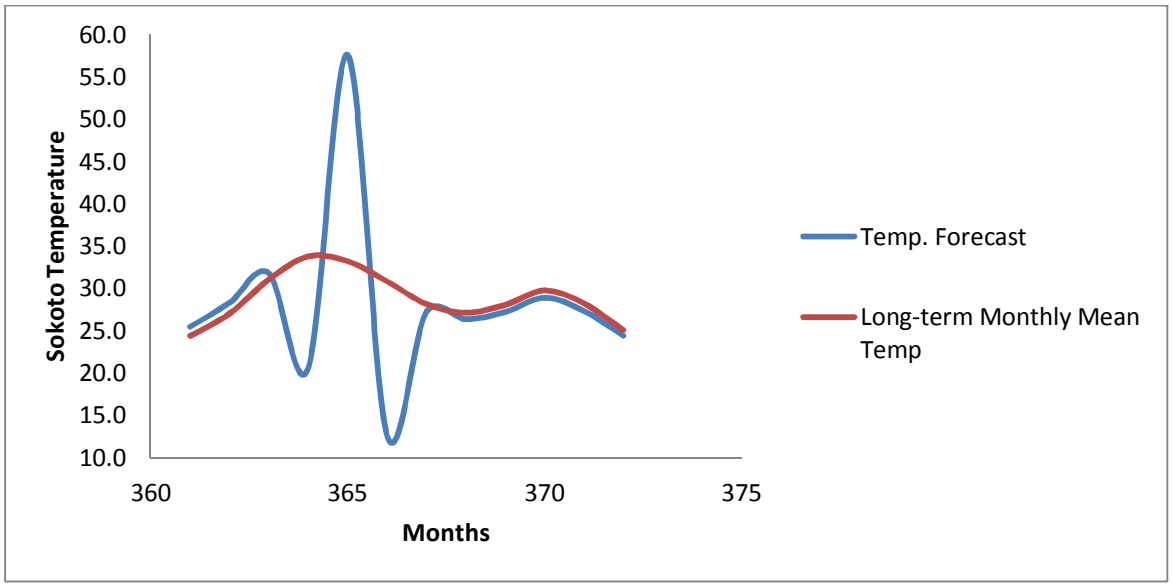


Figure 4.24b: Sokoto Station transformed temperature forecast

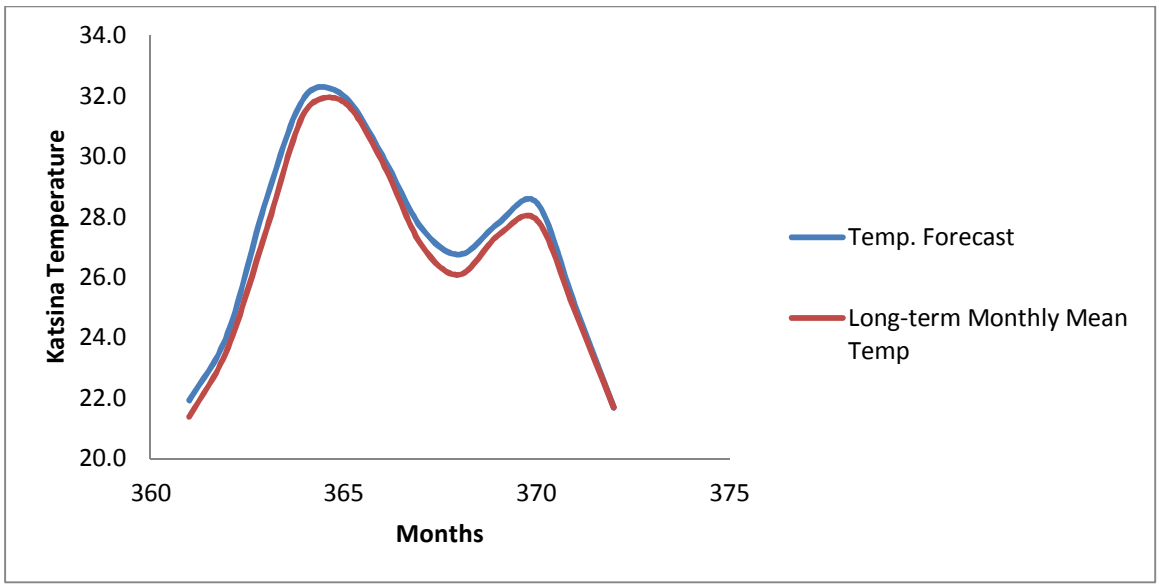


Figure 4.24c: Katsina Station transformed temperature forecast

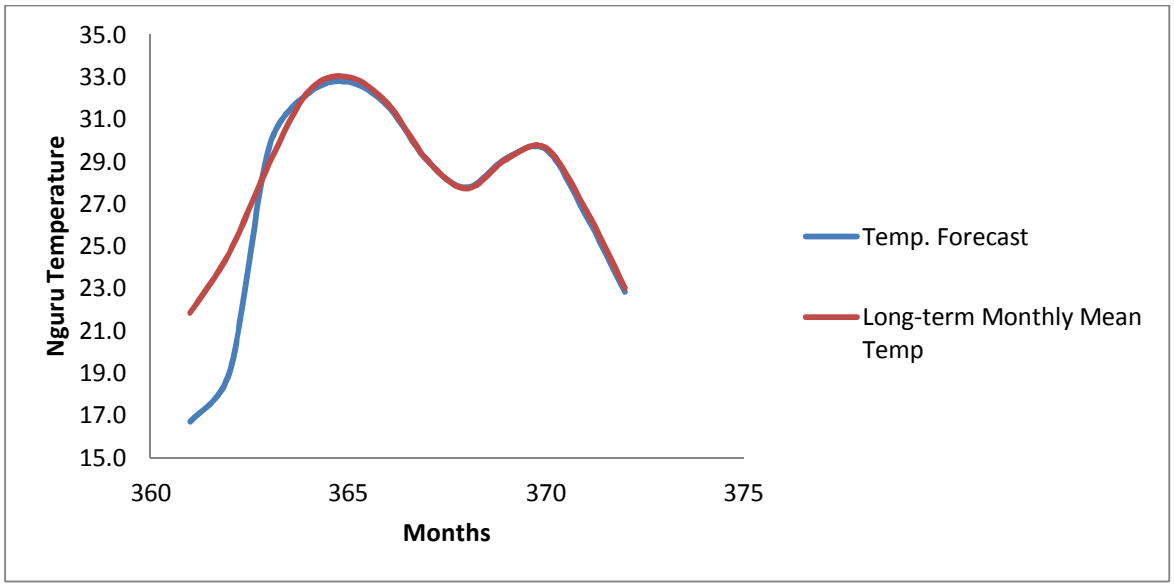


Figure 4.24d: Nguru Station transformed temperature forecast

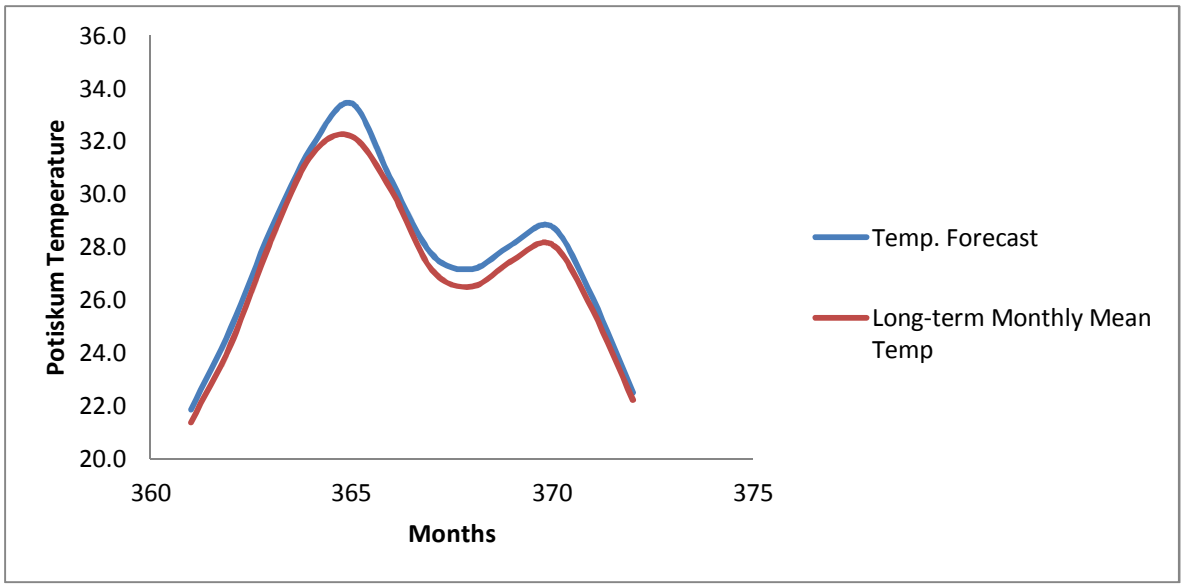


Figure 4.24e: Potiskum transformed temperature forecast

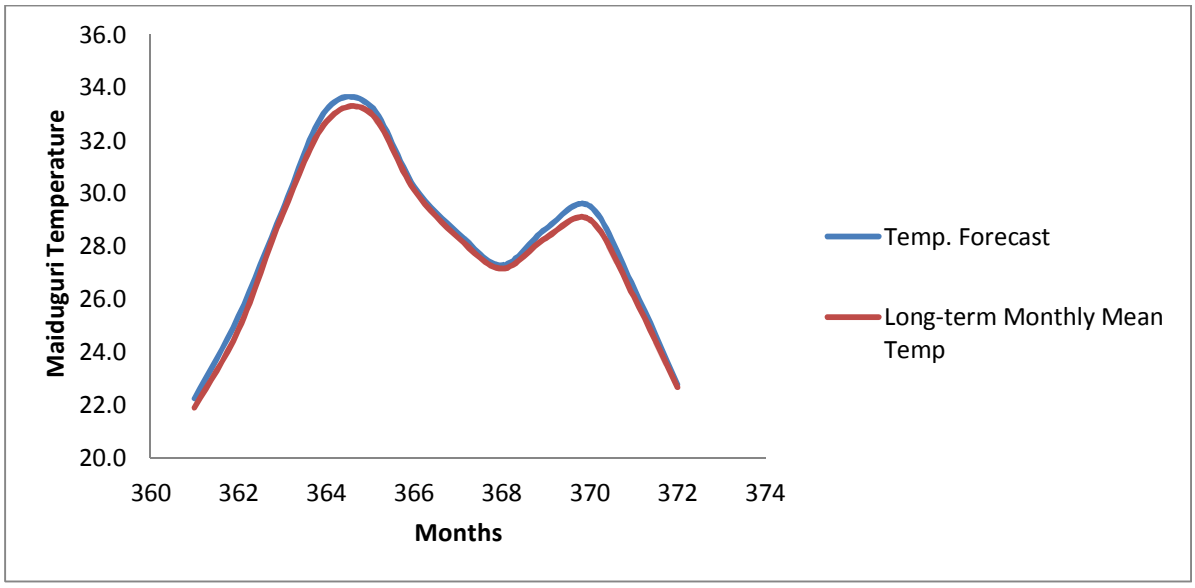


Figure 4.24f: Maiduguri Station transformed temperature forecast

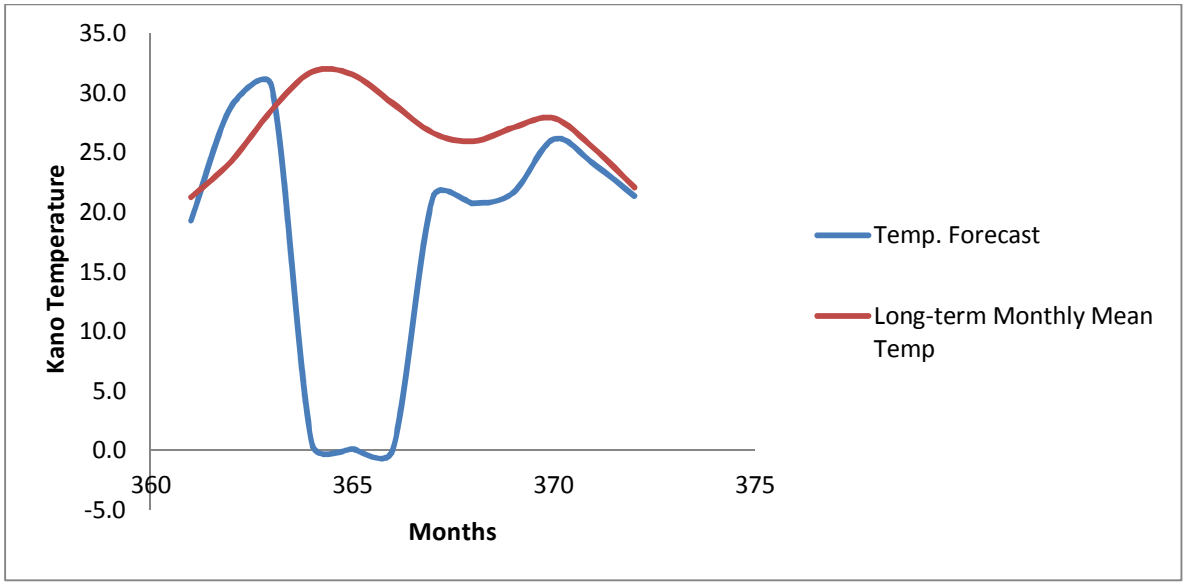


Figure 4.24g: Kano Station transformed temperature forecast

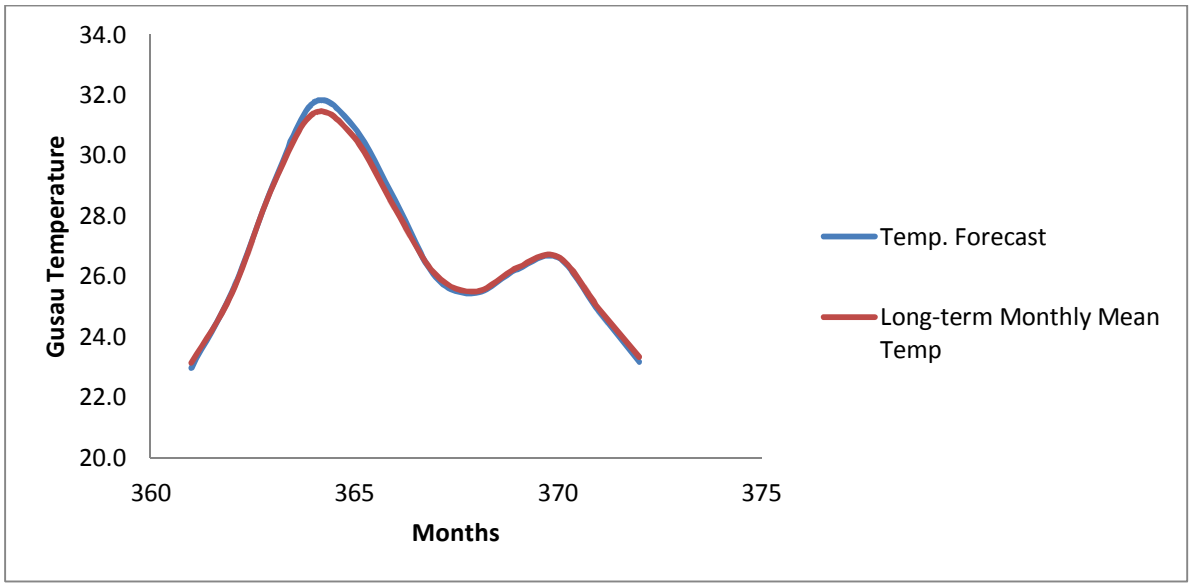


Figure 4.24h: Gusau Station transformed temperature forecast

It is obvious from Figs. 4.23a to 4.23h that drought or dry spell would likely occur at Sokoto (in June), Nguru (in February), Potiskum (August and October) and Gusau Station (from April to October, because of the negative values in the forecasted data series. However, Figs. 4.24a to 4.24h show that the forecasted temperature is higher than the long term temperature in nearly all the stations especially in April and May. The observation is more pronounced in Katsina, Potiskum and Maiduguri. Since drought is caused by some factors including precipitation deficiency and/or high temperature, this implies that Sokoto, Nguru, Guzau ,Katsina, Potiskum and Maiduguri might experience drought during the periods shown in the figures.

4.16 COMPARISON OF MODEL FORECASTS AND NIGERIAN METEOROLOGICAL AGENCY CLIMATE PREDICTIONS

The Nigerian Meteorological Agency (NIMET) predictions for 2009 climate were compared with the trend observed in temperature and rainfall in this study. According to

NIMET (2009), predicted 2009 rainfall values tend to be lower than normal over large portion of the country with the exception of only few states in the east and west which would experience longer rainy season. The onset of rainy season was expected to be delayed by one week in parts of Borno, starting from 1st June (NIMET, 2009). The onsets of rainy season in other stations were as indicated: Sokoto (28th May), Katsina (6th June), Nguru (20th June), Potiskum (16th June), Maiduguri (1st June), Kano (6th June), Gusau (28th May). This is in agreement with the results of Figs. 4.24a to 4.24h which show that the temperature forecasts are higher than the long-term temperature in nearly all the stations especially, in April and May preceding the beginning of the rainy season. Also, NIMET (2013) reported that the daytime temperature was expected to continue to increase in the north with associated heat and discomfort in April. Moreover, dry spells were likely to occur in Katsina, Sokoto, Zamfara, Yobe and Borno States particularly in the month of June 2013 (NIMET, 2013) and similar trends of near normal conditions, characterized by SPI values from -0.99 to 0.99, were observed during most of the months at nearly all the stations as shown in Figures 4.23a to 4.23h. Hence, the results in this study correlate NIMET prediction.

4.17 PROPOSED DROUGHT MANAGEMENT PLAN FOR NSSR

Analysis shows that there is no suitable model for percent monthly NDVI anomaly prediction and also, the index usually lags by some months in response to the preceding rainfall and consequently, SPI_1 observations. Hence, it is not considered in the choice of models for drought management in the region. Results have shown that most of the selected multiplicative SARIMA models, for SPI_1 forecasting in the region are good. The selected multiplicative SARIMA models for temperature forecasting show very good simulation

with the observed records. Hence, using the selected stochastic models developed for SPI_1 and temperature as tools, the drought management plan proposed for the NSSR has the following three phases:

i. Drought Emergence Watch,
ii. Drought Warning and,
iii. Drought Emergency.

Drought Emergence Watch: Drought emergence watch shows the likely occurrence of drought in the near future. It involves monitoring future temperature values on monthly basis using suitable SARIMA models for temperature, developed in this study. The highlighted models in Tables 4.5 and 4.6 are to be used to watch drought occurrence one to three months into the future. The forecasting should be done on monthly basis and, at regional and station level.

Drought emergency watch would be declared if either or both of the following conditions hold for SPI_1 and temperature forecasts respectively:

$$-0.99 \leq SPI_1 \leq 0.99 \tag{4.9}$$

$$T_{fm} \geq T_{lm} \tag{4.10}$$

in which SPI_1 is Standardized Precipitation Index (1 month time scale), T_{fm} is the forecasted monthly mean temperature and T_{lm} is the long term monthly mean temperature.

Equation 4.9 is the expression for near normal condition extracted from the classification table for drought occurrence based on SPI. As discussed in the last paragraph of section 4.7,

drought periods or months usually have monthly mean temperature higher than the long term monthly mean. This is the rationale for Eq (4.10).

At the declaration of drought emergence, the focus of water resources planners should be geared towards public awareness and the conservation of water resources. This can be achieved by:

i. Informing the public and requesting their cooperation in water conservation efforts
ii. Reducing the use of water at home, commercial places and industries, and
iii. Identifying independent alternative water sources for water dependent industries.

Drought Warning: Drought warning should be declared if in addition to the condition of Eq. (4.10) in a particular month, a moderately dry condition is observed based on SPI drought classification. Therefore, for a drought warning, the following must hold:

$$T_{fm} \geq T_{lm} \tag{4.10}$$

$$-1.49 \leq SPI_1 \leq -1.00 \tag{4.11}$$

The moderately dry condition is selected, in the SPI drought classification, as drought warning parameter because it is considered adequate. This is because near normal (-0.99 to 0.99), preceding moderately dry condition, is considered a common weather phenomenon in the NSSR as shown in the drought indices analyzed because it occurs frequently and the drought response detailed out under drought emergence watch could easily curtail it. Hence, moderate droughts or moderately dry conditions require additional drought response that will be triggered by the conditions stated for the declaration of drought warning, stated above.

On the other hand, severely dry condition (-1.5 to -1.99) was not selected as a warning parameter because adverse impacts of a drought might have become noticeable before declaring warning about its incidence. When drought warning is declared, drought response should be directed towards measures that ensure strict compliance to conservation of water resources. Additional actions are to be implemented to prevent and prepare for extreme drought as follows:

i. To forbid the use of water for washing vehicles, filling of swimming pools, public fountains and watering of public parks.
ii. To forbid the use of clean water for watering of lawns and gardens.
iii. To increase public enlightenment and appeal to the public to improve on the water conservation efforts.

Drought Emergency: Drought emergency is declared if the conditions under drought warning assessment continue for two consecutive months and/or the SPI_1become more negative. Drought response is directed towards measures that ensure both strict adherence to water conservation and importation of drinking water. The necessary actions are:

i. Reducing water supply on some hours of the day
ii. Disconnecting high water consuming industries from public supply
iii. Sourcing for other alternative water sources by industries
iv. Importation of drinking water from other regions.

In addition, reforestation should be encouraged in the study area in order to lower rate of warming, preserve soil moisture and enhance rainfall in the region. Plants should be planted

around reservoirs in the region to break wind and reduce evaporation from the water surfaces.

CHAPTER FIVE

SUMMARY, CONCLUSIONS AND RECOMMENDATIONS

5.1 SUMMARY

This research investigated droughts in Nigeria Sudano-Sahelian Region and developed forecasting models for drought monitoring and management in the region. Ground-based data and satellite imageries were collected, analyzed and modelled. The ground-based data consists of temperature and rainfall data, both from 1979 to 2008, collected from Nigeria Meteorological Organisation (NIMET), Oshodi, Lagos. The Imageries consist of Normalized Difference Vegetation Index (NDVI) spanning 1981 to 2011, obtained from National Aeronautics and Space Administration (NASA) and SPOT – Vegetation Programme of Vision on Technology (VITO), websites at earlywarning.usgs.gov and www.free.vgt.vito.be respectively.

Standardized Precipitation Index (SPI) at time scales of one month (SPI_1), three months (SPI_3), six months (SPI_6), twelve months (SPI_12), and twenty four months (SPI_24) were extracted from the rainfall record and compared to determine the most suitable one for real time and early warning tool for drought forecasting and, it was discovered that SPI_ reflected nearly all droughts from near normal condition to very severe dry condition. As a result, SPI_1 was chosen for modeling, but it was compared with monthly NDVI anomaly to select the better one. The results indicated that drought episodes detected by NDVI anomaly were lagged some months behind the corresponding ones identified by SPI_1. Hence SPI_1 was modelled, based on Auto Regressive Moving Average/Seasonal Auto Regressive Moving Average (ARIMA/SARIMA), to simulate drought occurrence at each station. Temperature was modelled in addition.

The ARIMA model development was based on model identification, parameter estimation and diagnostic checking. The models were compared, using goodness of fit measures, to select the best model for drought prediction at each station. Multiplicative SARIMA model was found suitable for SPI_1 forecasting at Sokoto, Nguru, Potiskum, Kano and Gusau Stations was $(011)x(011)_{12}$ while SARIMA model $(1,1,1)x(1,1,1)_{12}$ was found suitable for SPI_1 forecasting in Katsina and Maiduguri Stations. The multiplicative SARIMA temperature models developed for Sokoto, Nguru, Potiskum, Kano and Gusau Stations was SARIMA $(2,1,1)x(2,1,1)_{12}$ while SARIMA $(3,1,1)x(3,1,1)_{12}$ was found suitable for Katsina and Maiduguri Stations. Parameter functions of the models were estimated and diagnostic test was done for each model using Autocorrelation Function (ACF) and Partial Autocorrelation Function (PACF), residual histogram and normal probability plots.

The ACF and PACF structures of the model residuals in which the residual values were close to zero reflecting that they were approximately white noise. Histograms of the model residuals reflected normal distribution while the model residual normal probability plots approximate a straight for each of the selected models. The selected models were validated, using available data. Sum of Squared for Errors (SSE) and Root Mean Square Error (RMSE) were applied as performance criteria for validation. The range of SSE and RMSE, from 0.001 to 0.014 and 0.012 to 0.068, respectively, were close to zero and these ascertained the goodness of fit between the observed data and forecasts. SPI_1 and temperature models were used to forecast SPI_1 and temperature into the future for a period of 12 months, at a step of 3-month time step. The forecast negative SPI_1 were used to predict drought severities occurrences into the future. A drought management plan was proposed for the study area based on the developed forecasting models.

5.1.1 Areas of Contribution to Knowledge

Areas of contribution to knowledge are:

i. The research has updated drought information in NSSR

ii. The region has been classified into drought risk zones

iii. It has been discovered that drought analysis based on NDVI are lagged by few months compared to drought events analyzed using SPI_1 in the region.

iv. Predictive models have been developed for drought monitoring and forecasting in the study area.

v. Drought management plan has been proposed for effective drought management in the study area.

5.2 CONCLUSIONS

The seven stations analyzed for drought in the Nigerian Sudano-Sahelian Region are observed to have been threatened by drought at one time or the other. Many drought episodes ranging from very severe to near normal drought conditions have been observed in the region, and the notable ones that cut across the investigated stations are: 1983-1985, 1987-1988 and 1993-1994 drought events. Consequently, the stations are considered drought risk zones although, the level of risk varies from one location to another. The region has been classified into high drought risk zone consisting of Sokoto, Katsina, Damaturu as well as Nguru (Yobe State) and Maiduguri using a drought risk map based on NDVI anomalies. This is justified with the long term mean Normalized Difference Vegetation Index of 0.221, 0.226 and 0.229 for Sokoto, Katsina and Nguru, respectively. Moderate risk zone include Guzau, Kano and Dutse while parts of Bauchi and Gombe States are identified as low risk zone.

SPI and NDVI are adequate for drought analysis. However, drought episodes detected with monthly NDVI anomalies are lagged by few months behind the ones identified by SPI_1. As a result, SPI_1 time series is suitable for real time and early warning drought forecasting. Hence, SPI_1 and temperature were modelled and used as forecasting tools for monitoring drought. Based on the predictive models, a drought management plan has been developed and proposed for Nigerian Sudao-Sahelian Region. The plan has three phases of drought emergence watch, warning and emergency.

Mitigation measure suggested for the region is reforestation, in order to lower the rate of warming, preserve soil moisture and enhance rainfall in the region. Plants should be planted around reservoirs in the region to break wind and reduce evaporation from the water surfaces.

5.3 RECOMMENDATIONS

The following recommendations are drawn from the study:

i. The predictive model developed should be updated monthly before monthly forecasts to incorporate the influence of climate change on the models.
ii. Similar researches should be carried out on remotely sensed temperatures and SPI based on rainfall estimates for a real term forecasting purpose.
iii. The forecasting is basically short-time and hence should be used for prediction at a 3-month time step, up to one year, into the future to guarantee reliability and accuracy of the models.
iv. The proposed drought management plan should be applied to the region and reviewed occasional to improve on it.

v. Reforestation should be encouraged in the study area. The practice will go a long way to enable the region adapt to climate change and drought in particular.

REFERENCES

Abiodun, B. J., Salami, A. T. & Tadross, M. (2011). Climate Change Scenarios for Nigeria: Understanding Biophysical Impacts. Climate Systems Analysis Group, Cape Town, for Building Nigeria's Response to Climate Change Project. Ibadan, Nigeria: Nigerian Environmental Study/Action Team (NEST).

Akeh, L. E., Nnoli N., Gbuyiro S., Ikehua F., and Ogunbo S., (2001): Meteorological Early Warning Systems (EWS) for Drought Preparedness and Drought Management in Nigeria, *Nigerian Meteorological Services, Lagos, Nigeria.*

Apeldoorn, G.J.V. (1981): Perspective on drought and famine in Nigeria, George Allen and Unwin, London, 184 pp.

Argrawal S., JoshiP.K., Shukla Y, and Roy P.S., (2003). SPOT Vegetation Mullti temporal Data for Classifying Vegetation in South Central Asia. Research Communication. Current Science, Vol. 84, No 11, 10 June 2003.

Beran. M. A. & Rodier. J. A. (1985) Hvdrological aspects of drought. UNBSCO-WMO, Studies and Reports in Hvdrology no. 39, UNESCO, Paris, France.

Berthouex P.M. and Brown L.C, (2002). Statistics for Environmental Engineers. Lewis Publishers, Washinton D.C.

Bonacci, O. (1993) Hydrological identification of drought. Hydrol. Processes 7, 249-262.

Box, G.E.P. and Jenkins, G.M., (1970). Time Series Analysis; Forecasting and Control. Holden- Day series in time series analysis. Holden-Day, San

Byun, H.R. and Wilhite, D.A., (1999). Objective quantification of Drought Severity and Duration. Journal of Climate 12: 2747-2756.

Chopra P., (2006), Drought Risk Assessment Using Remote Sensing and GIS: A case study of Gujarat. MSc Thesis, International Institute for Geo-Information Science and Earth Observation, Enschede, The Netherlands.

Cordery I., & McCall M., 2000. A model for forecasting drought from teleconnections. Water Resour. Res. 36, 763-768

Coughlan, M.J., (1987). Monitoring Drought in Australia. In Planning for Drought. Toward reduction of Societal Vulnerability, ed. D.A. Wilhite and W.E. Easterling, 131-144. West View Press, Boulder, Colorado.

Diwan, P.L. (2002), Water Environment and Drought, proceedings: All Indian Seminar on 'Water and Environment – Issues and Challenges" October 2002, IIT, Roorkee, India, 21-185.

Dracup, J. A., Fee, K. S. & Paulson, E. G., Jr (1980) On definitions of droughts. Wat. Resour. Res. 16(2), 297-302.

Durbin, J., (1960). The fitting of time series models. review of the international institute of Statistics, 28: pp. 233-140.

EC Report (2006). European Commision report: Water Resources Strategy. In: *Support to the Federal Ministry of Water Resources.* Federal Ministry of Water Resources, Abuja, Nigeria.

FAO (1999) Map and Image Display and Analysis Software: WINDISP 4.0 User's Manual. Technical Report ES:GCP/INT/619/EC. Food and Agricultural Organisation (FAO) of thr United Nations, Rome.

Federal Government of Nigeria, FGN, (1998): Sustainable watershed management: An awareness publication of Federal Ministry of Water Resources & Rural Development, Abuja, Nigeria.

Fidelis, C.O. (2003), Studies on Drought in the Sub-Saharan Region of Nigeria Using Satellite Remote Sensing and Precipitation Data, Department of Geography, University of Lagos, Nigeria.

Gibbs, W. J. & Maher, J. V. (1967) Rainfall deciles as drought indicators. Bulletin. no. 45, Bureau of Meteorology, Melbourne, Australia.

Gupta, V. K. & Duekstein, L. (1975) A stochastic analysis of extreme droughts. Wat. Resour. Res. 27(5), 797-807.

Guttman, N. B. (1998) Comparing the Palmer drought severity index and the standardized precipitation index. J. Am. Wat. Resour. Assoc. 34(1), 113—1

Hadish, L., (2010). Drought Risk Assessment UsingRemote Seneing and GIS: A case study in Southern Zones, Tigray Region, Ethiopia. MSc. Thesis, Addis Ababa University, Addis Ababa, Ethiopia.

Hayes, M.J. and Svoboda M.D., (1999). Monitoring the 1996using the Standardized Precipitation Index.BAMS Vol. 80: pp. 429-438.

IPCC (2000). IPCC special report emissions scenarios, In Special report of IPCC working group III. Intergovernmental panel on climate change (pp 20). Cambridge, UK, New York, US: Cambridge University Press.

IPCC (2007). Synthesis Report. In Climate Change 2007: The Physical Science Basis. Contribution of Working Group I to the Fourth Assessment Report of the Intergovernmental Panel on Climate Change. Cambridge, UK, New York, US: Cambridge University Press.

ISDR. (2006). Global Survey of Early Warning Systems. United Nations International Strategy for Disaster Reduction. Retrieved from http: www.unisdr.org/ppew/info-resources/ewc3/Global-Survey-of-Early-Warning-Systems.pdf

Jacobs, T., Claes, P., Smets.B., Van Roey, T., and Erens., H. (2010). VGTExtract, The Free Vegetation Extraction Tool Software User Guide by VITO. Vision on Technonology (VITO), Belgium.

Jayaseelan, D.T. and Chandrasekar, K. (2002), Satellite Based Identification for Updation of Drought Prone Area in India. ISPRS – TC – VII, International Symposium on Resource and Environmental monitoring, Hyderbad.

Karl, T. R., and Knight, R. W., (1985): Atlas of monthly Palmer Hydrological Drought Indices (1931-1983) for the Contiguous United States. Historical Climatology Series 3-7, National Climatic Data Center, Asheville, NC.

Kogan F.N. (1990),. Remote Sensing of WeatherImpactson Vegetationin Non-homogeneous area. International Journal of Remote Sensing Vol. 11: pp. 1405-1421.

Komuscu,A.U. (1999). Using the SPI to Analyze Spatial and Temporal Patterns of Drought in Turkey. Drought Network News, 11: 7-13

Khadr M. (2011). Water Resources Management in the Context of Drought (An Application to the Ruhr River Basin in Germany). Ph.D Dissertation, Civil Engineering Department, University of Wuppertal, Germany.

Legesse G. (2010), Agricultural Drought Assessment Using Remote Sensing and GIS Techniques. MSc. Thesis, Addis Ababa University, Ethiopia.

Lohani, V. K. & Lognathan, G. V. (1997) An early warning system for drought management using the Palmer drought severity index. Nordic Hydrol. 29(1), 21—40.

Maduakor, H.O. (1991), Physical and Hydraulic Properties of Soils of the Sudano-Sahelian Regions of Nigeria. In: Soil Water Balance in the Sudano-Sahelian Zone (Proc. Of the Niamey Workshop, February 1991). IAHS Publ. no199, 1991.

McKee, T. B., Doesken, N. J. and Kleist, N. J. (1993): The relationship of drought frequency and duration to time scales. Proceedings, 8th Conference on Applied Climatology, 17-22 January, Anaheim, CA, pp. 179-184.

Medugu, I.N. (2007), A Comprehensive Approach to Addressing Drought and Desertification in Nigeria. MSc. Thesis, University of Teknologi, Malaysia.

Mokhtari, M. H. (2005), Agricultural Drought impact assessment using Remote Sensing: A Case Study Borkhar District Iran. MSc. Thesis, International Institute for Geo-Information Science and Earth Observation, Enschede.

Murad H. and Saliful Islam K.M. (2011) Drought Assessment Using Remote Sensing and GIS in North-West Region of Bagladesh. 3rd International Conference on Water and Flood Management (ICWFM-2011).

NASA (2010) Global Warning. In Earth Observatory. National Aeronautics and Space Administration (NASA). Retrieved from http: www.earthobservatory.nasa.gov/Features/GlobalWarming/page1.php

NDMC. (2010). Program to calculate Standard Precipitation Index. National Drought Monitoring Center, University of Nebraska, Lincoln. Retrieved from http://drought.unl.edu/MonitoringTools/DownloadableSPIProgram.aspx

NIMET (2009). Seasonal Rainfall Prediction. Nigeria Meteorological Agency (NIMET), Oshodi, Lagos, Nigeria.

NIMET (2013). Seasonal Rainfall Prediction. Nigeria Meteorological Agency (NIMET), Oshodi, Lagos, Nigeria.

Oguntoyinbo, J.S. and Richards, P. (1977): The extent and intensity of the 1969-73 drought in Nigeria: A provisional analysis of drought in Africa 2nd edition International African

Institute, Environment Special Reports 6. [Dably D. Church J.H and Bezzaz., eds.). London, 114-126.

Okorie F.C., (2003): Studies on Drought in the Sub-Saharan Region of Nigeria using satellite remote sensing and precipitation data, report of a research study conducted in University of Hyderabad, India. Retrieved from http: http://www.mathaba.net/gci/docs/reasearch

Oladipo, E. O. (1992): Drought in Northern Nigeria; an Indication of Abrupt Climatic Change? : paper presented at the 1992 Meteorological Society of New Zealand conference on Weather and Climate Risks, Lincoln University, Lincoln, 26-28 August, 1992.

Oladipo, E.O. (2010). Towards Enhancing The Adaptive Capacity of Nigeria: A Review of the Country's State of Preparedness for Climate Change Adaptation. Heinrich Boll Foundation Nigeria, Nigeria.

Otun, J.A., (2005). Analysis and Quantification of Drought using Meteorological Indices in the Sudano-Sahel Region of Nigeria. Ph.D Thesis, Ahmadu Bello University, Zaria, Nigeria

Palmer, W.C. (1965): Meteorological drought, Tech. Research paper no. 45, 1-58, U.S. Weather Bureau, US Dept. of Commerce, Washington, DC USA.

Panu U.S. and Sharma T.C., (2002). Challenges in Drought Research: Some Perspectives and Future Directions. Special Issue: Towards Integrated Water Resources Management for Sustainable Development. Hydrotogical Sciences-Journal—des Sciences Hydrologiques, 47(5) August 2002.

Piechota, T. C. & Dracup, J. A. (1996) Drought and regional hydrologic variation in the United States: association with the El-Nino southern oscillation. Wat. Resour. Res. 32(5), 1359-1373.

Sen, Z. (1980a) Statistical analysis of hydrological critical droughts. J. Hydraul. Div. ASCE 106, 99-115.

Sen, Z. (1980b) Critical drought analysis of periodic stochastic processes. J.Hydrol. 46, 251-263.

Shafer, B.A. and Dezman, L.E. (1982). Development of a Surface Water Supply Index (SWSI) to assess the severity of drought conditions in snowpack runoff areas. In: Proceedings of the Western Snow Conference, Reno, NV, 19-23, April 1982, pp. 164175. Colorado State University, Fort Collins, Colorado.

Sharma, T. C. (1996) Simulation of the Kenyan longest dry and wet spells and the longest rain sums using a Markov model. J. Hydrol. 178, 55-67.

Sharma, T. C. (1997) A drought frequency formula. Hydrol. Sci. J. 42(6), 803-814.

Smart, G. M. (1983) Drought analysis and soil moisture prediction. J. Irrig. Drain. Div. ASCE 109(2), 251-261.

Smarkhtin V.U. and Hughes D.A. (2004). Review, Automated Estimation and Analyses of Drought Indices in South Asia. Working Paper 83: In Drought Series Paper 1. International Water Management Institude, Colombo, Sri Lanka.

Smith, D.I., Hutchinson, M.F. and McArthur, R.J. (1993). Australian Climatic and Agricultural Drought: Payments and Policy. Drought Network News 5(3): 11-12.

Suhartono (2011). Time Series Forecasting by using Seasonal Autoregressive Integrated Moving Average: Subset, Multiplicative or Additive Model. *Journal of Mathematics and Statistics* 7(1): 20-27

Svoboda, M., (2009) Drought Early Warning Systems. Inter-Regional Workshop on Indices and Early Warning Systems for Drought. University of Nebraska-Lincoln, NE. December 8-11, 2009

Tallaksen, L. M., Madsen, II. & Clausen, B. (1997) On the definition and modelling of streamflow deficit duration and deficit volume. Hydrol. Sci. J. 42(1), 15-33.

USGS (2011) Vegetation Indices. In Remote Sensing Phenology. United State Geological Survey (USGS). Retrieved from http: www.phenology.cr.usgs.gov/ndvi_foundation.php

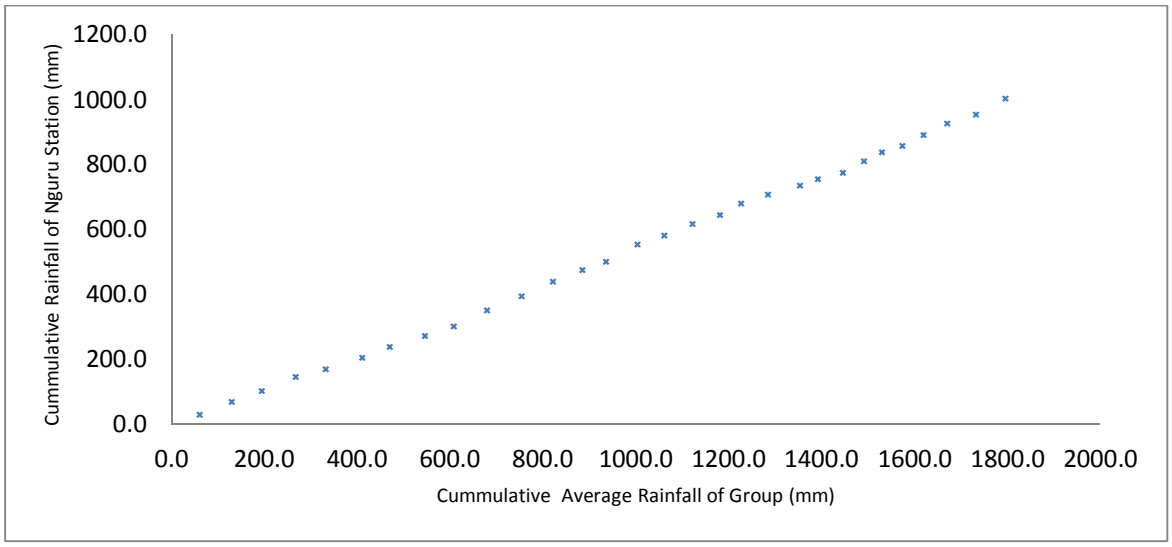
Wilhite, D.A. and Glantz, M.H. (1985), Understanding the drought phenomenon: The role of definitions. Water International, 10: 111-120.

WMO (1988). Analysing Long Time Series of Hydrological Data with Rerspect to Climate Variability. In: World Climate Program Applications. WCAP-3, WMO/TD-No. 224. World Meteorological Organization, Geneva Switzerland,

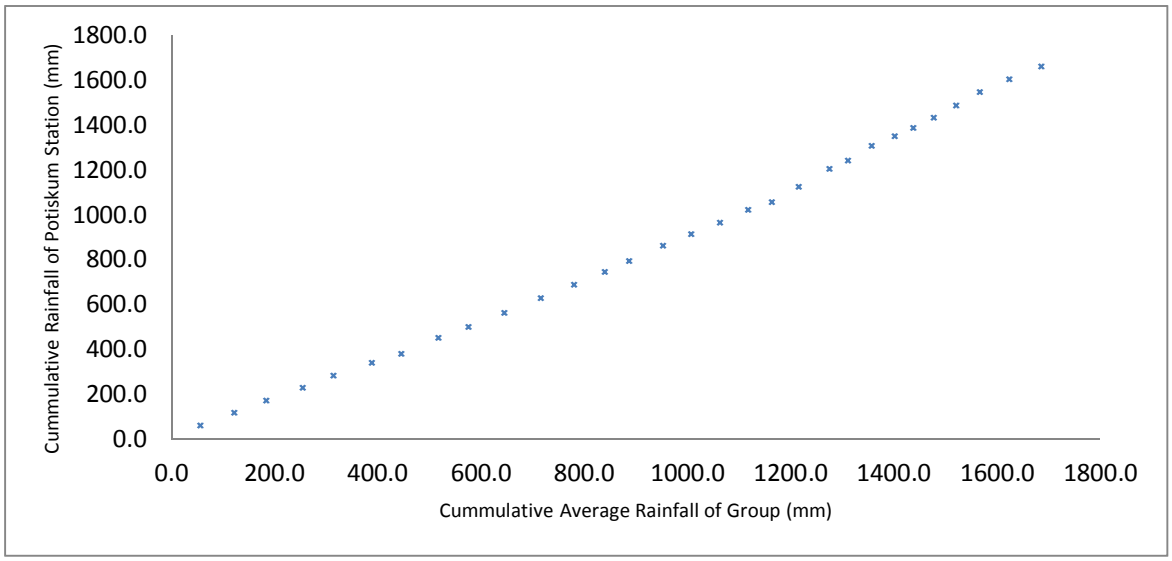
Zelenhasic, E. & Salvai, A. (1987) A method of streamflow' drought analysis. Wat. Resour. Res. 23(1), 156-168.

APPENDICES

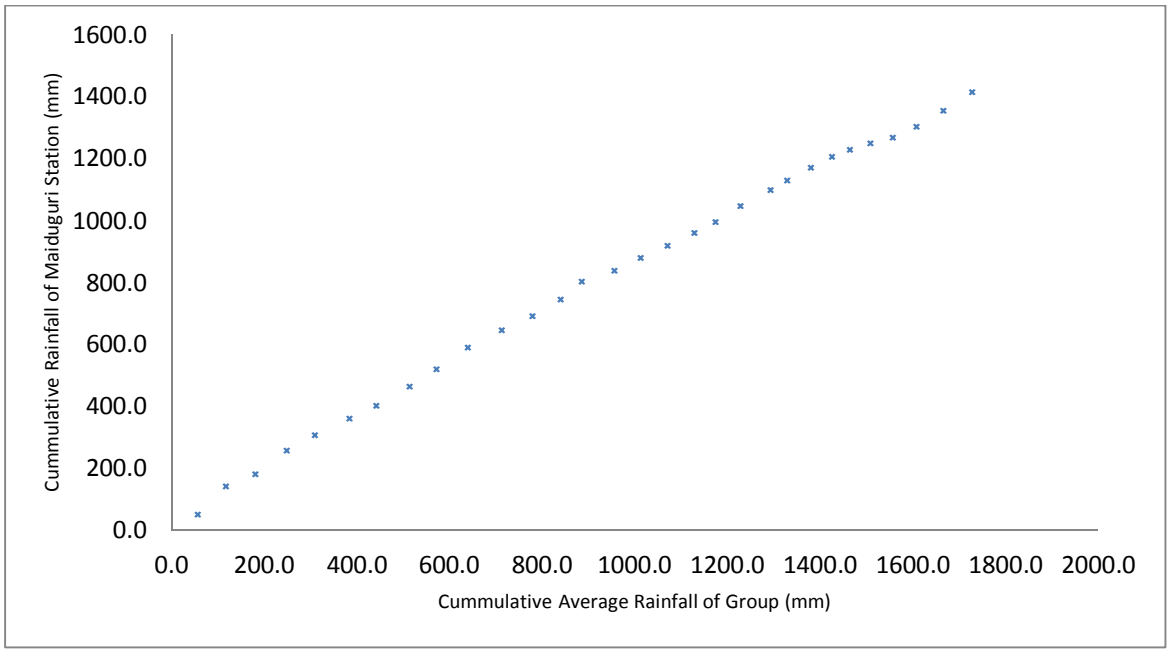
APPENDIX A: Cumulative precipitation for Station vs other stations (1979-2008)



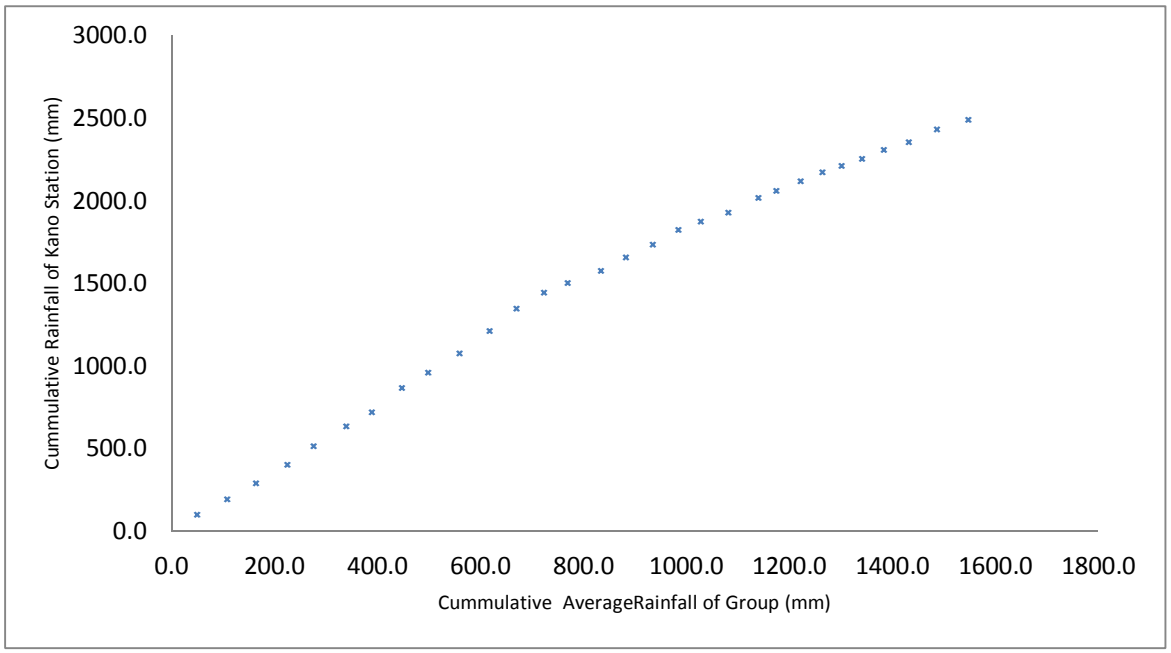
a: Cumulative precipitation for Nguru Station vs other stations (1979-2008)



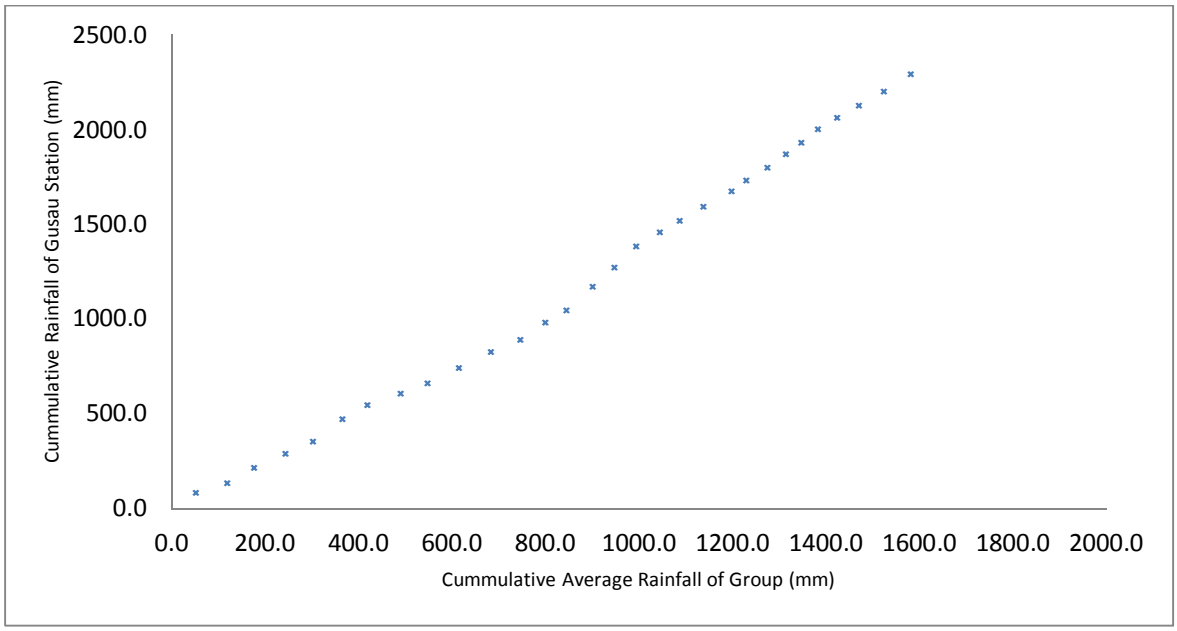
b: Cumulative precipitation for Potiskum Station vs other stations (1979-2008)



c: Cumulative precipitation for Maiduguri Station vs other stations (1979-2008)

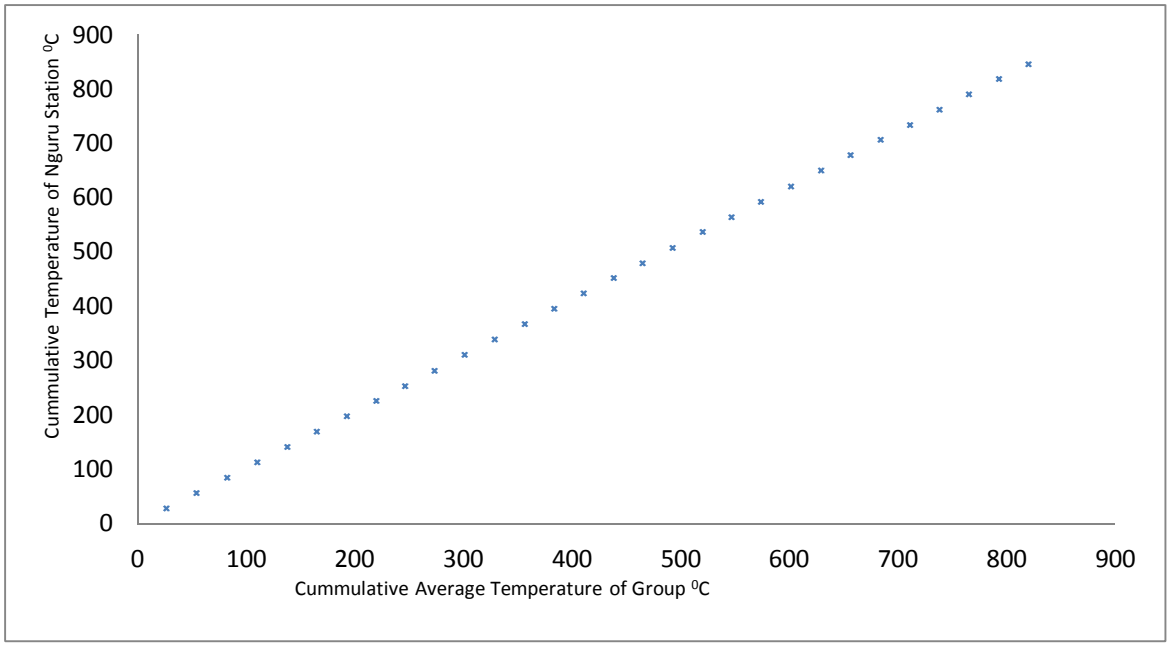


d: Cumulative precipitation for Kano Station vs other stations (1979-2008)

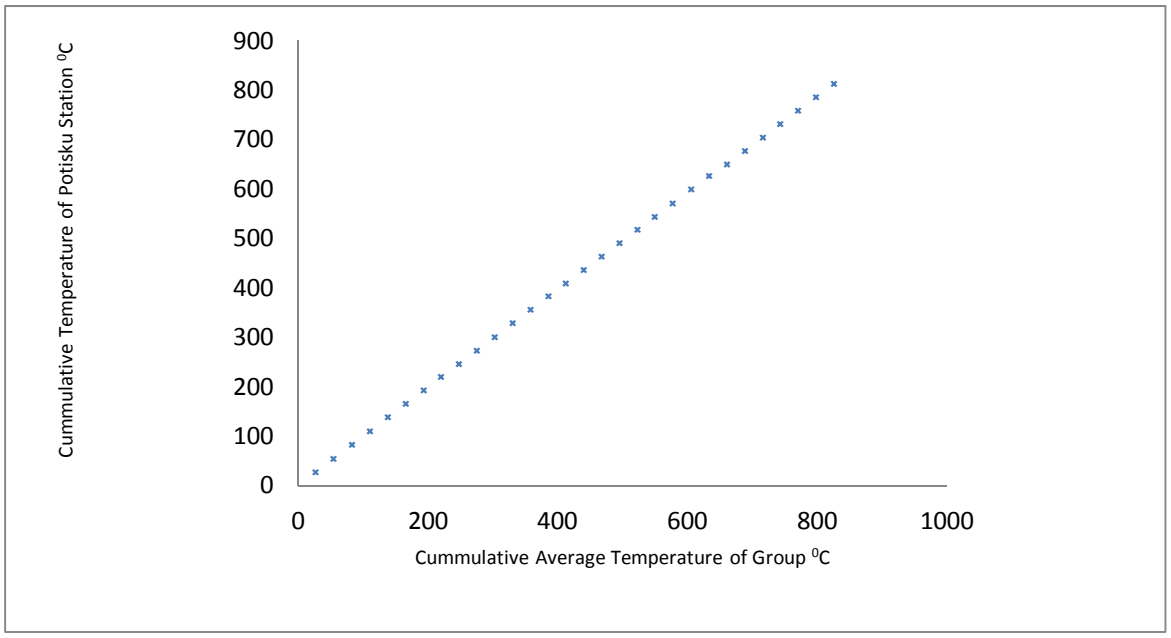


e: Cumulative precipitation for Gusau Station vs other stations (1979-2008)

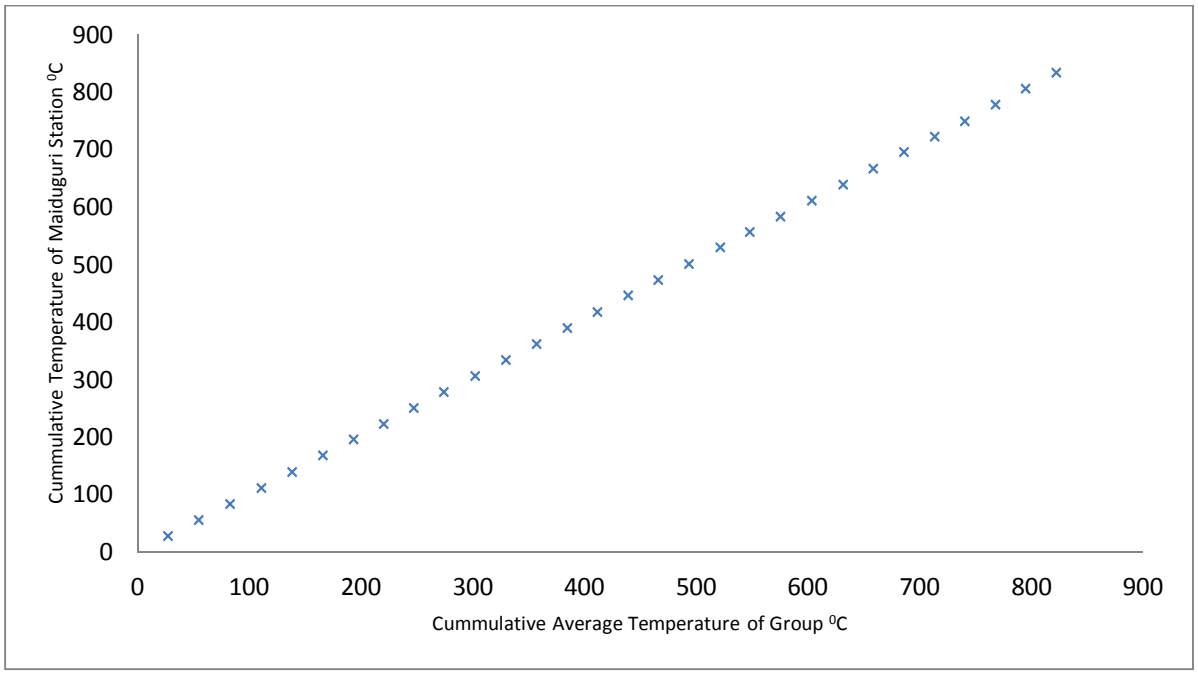
APPENDIX B: Cumulative temperature for Station vs other stations (1979-2008)



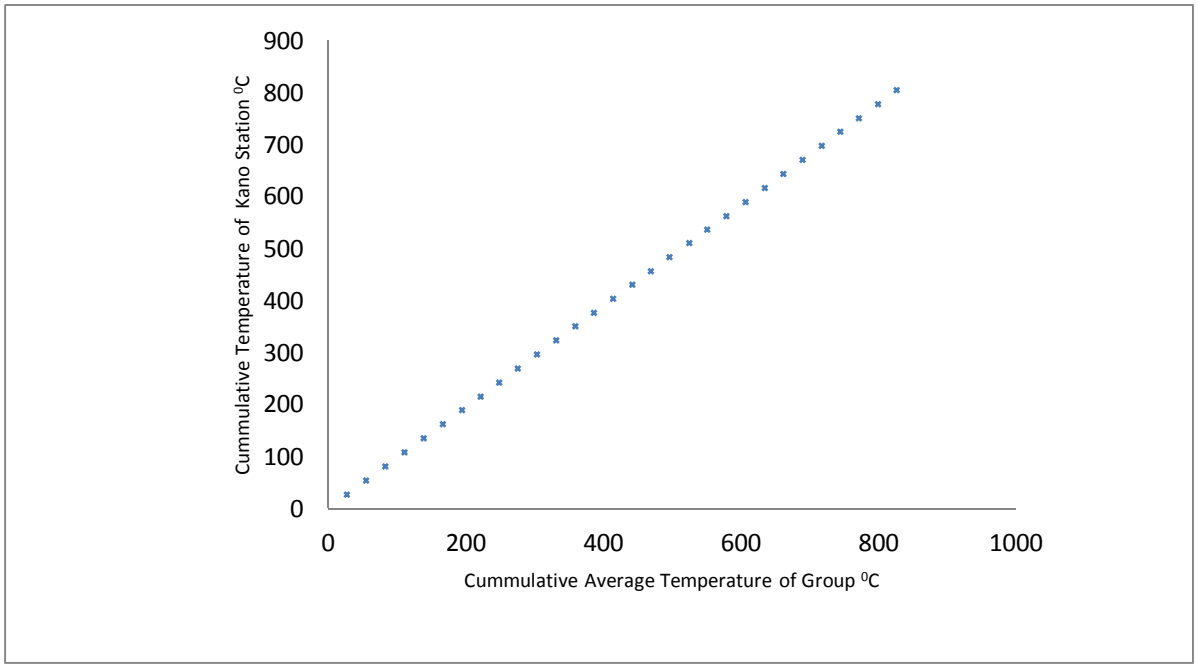
a: Cumulative temperature for Nguru Station vs other stations (1979-2008)



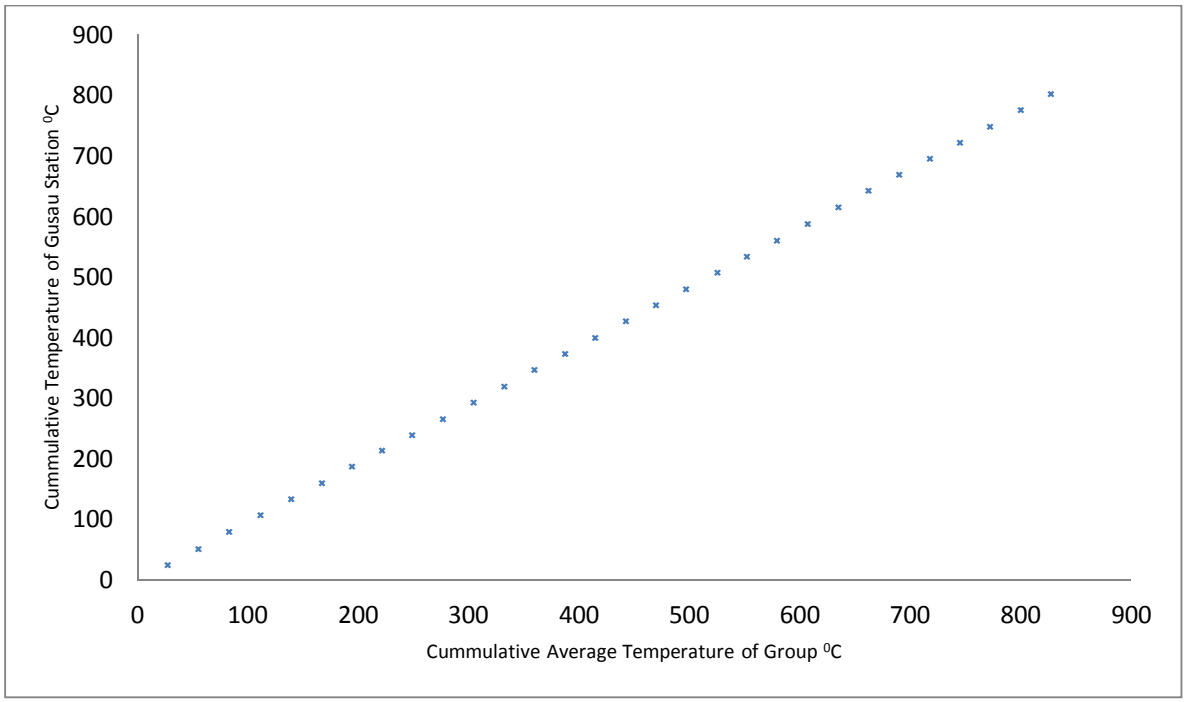
b: Cumulative temperature for Potiskum Station vs other stations (1979-2008)



c: Cumulative temperature for Maiduguri Station vs other stations (1979-2008)

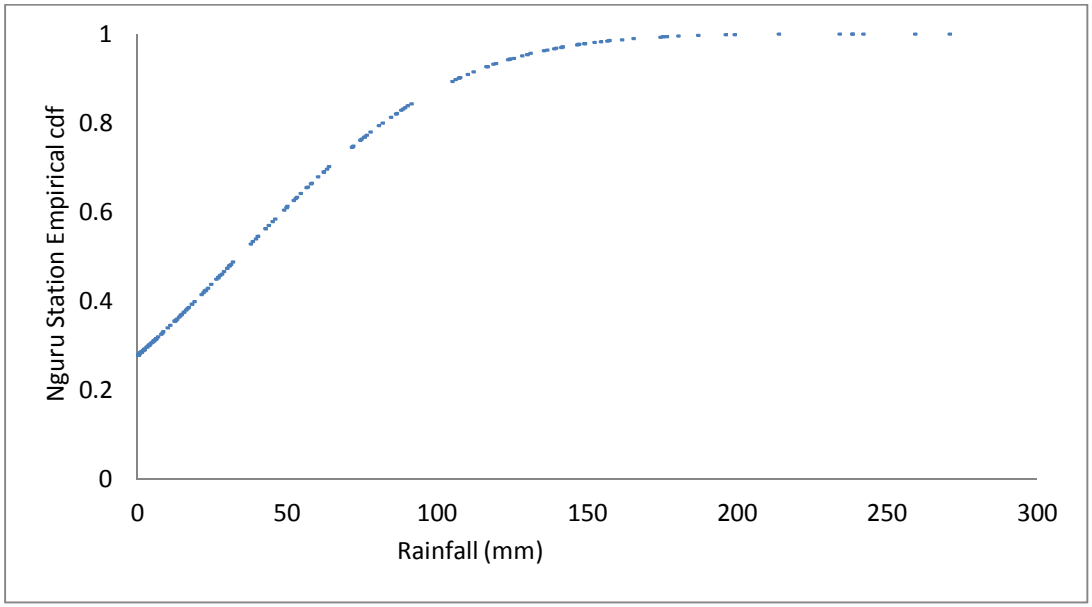


d: Cumulative temperature for Kano Station vs other stations (1979-2008)

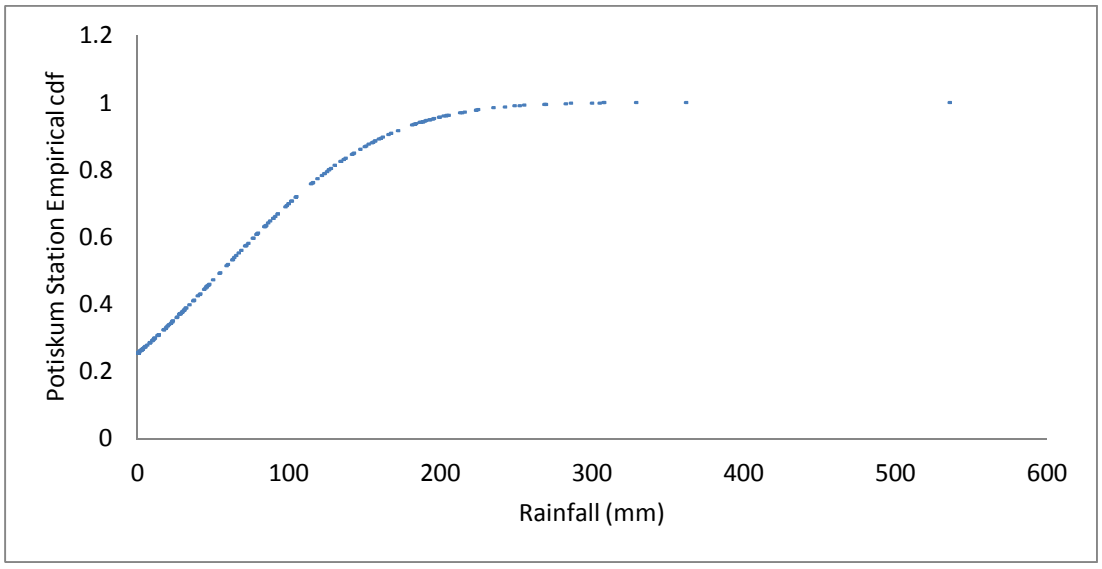


e: Cumulative temperature for Gusau Station vs other stations (1979-2008)

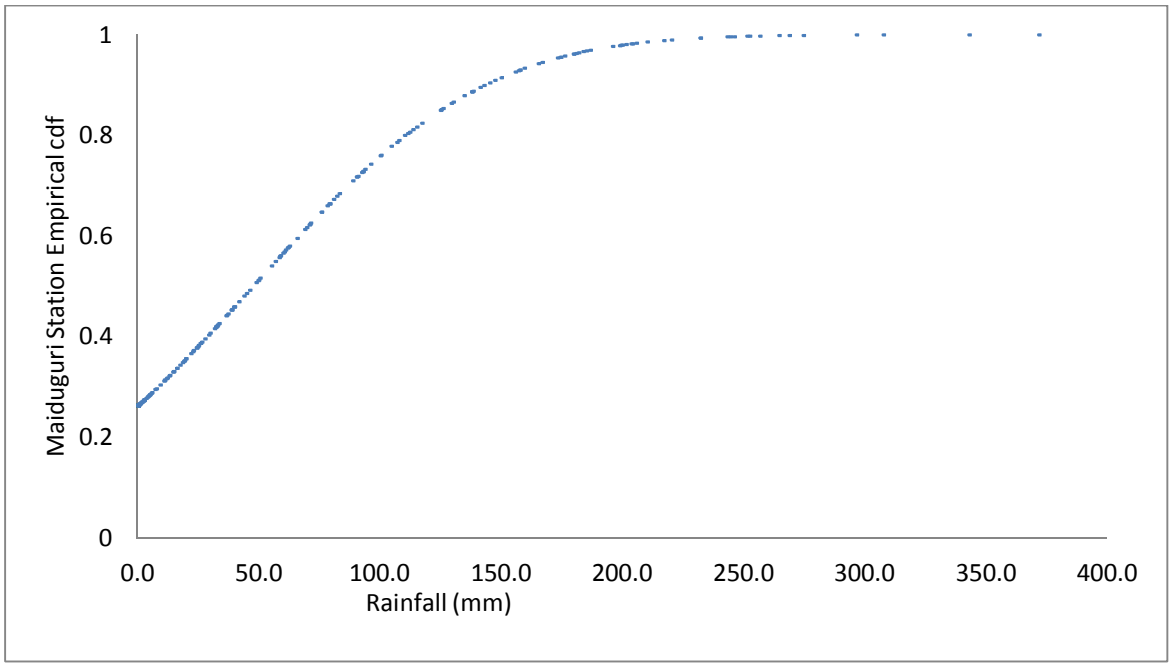
APPENDIX C: Empirical cumulative distribution function (cdf) for precipitation data Series (1979-2008)



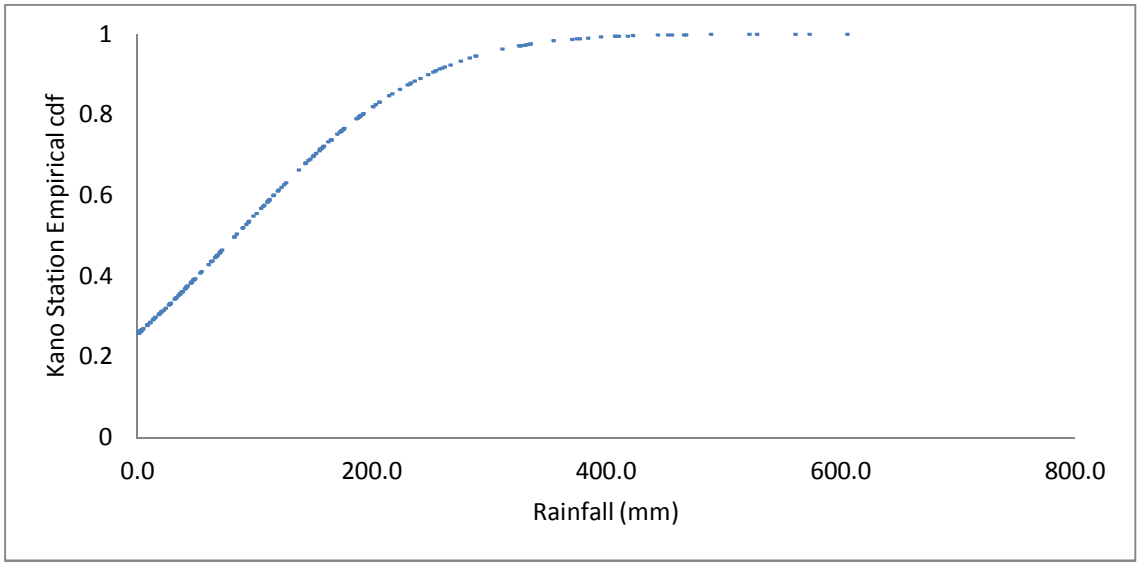
a: Empirical cumulative distribution function (cdf) for Nguru Station precipitation data Series (1979-2008)



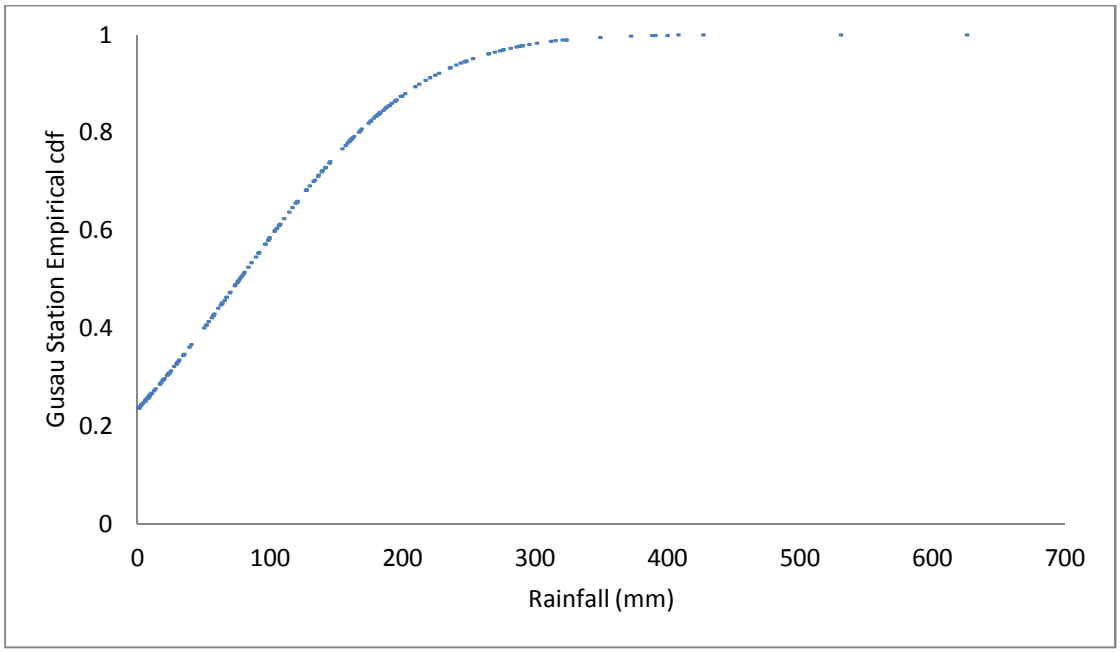
b: Empirical cumulative distribution function (cdf) for Potiskum Station precipitation data Series (1979-2008)



c: Empirical cumulative distribution function (cdf) for Maiduguri Station precipitation data Series (1979-2008)



d: Empirical cumulative distribution function (cdf) for Kano Station precipitation data Series (1979-2008)



e: Empirical cumulative distribution function (cdf)for Gusau Station precipitation data Series (1979-2008)

APPENDIX D: Empirical cumulative distribution function (cdf) for temperature data Series (1979-2008)

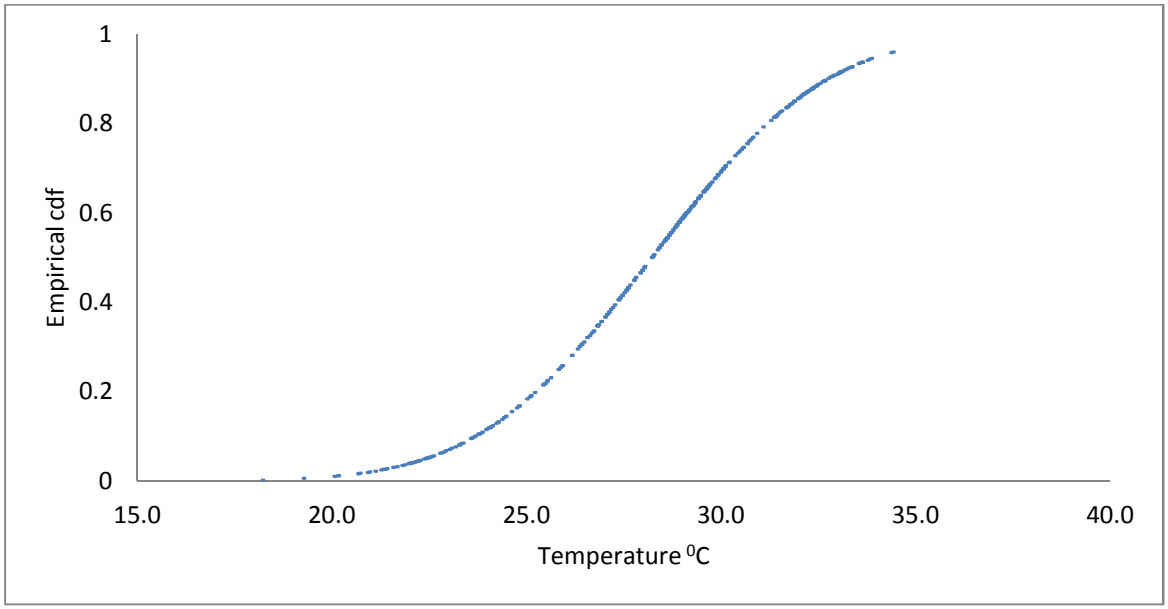


Figure 4.6c: Empirical cumulative distribution function (cdf) for Nguru Station temperature data Series (1979-2008)

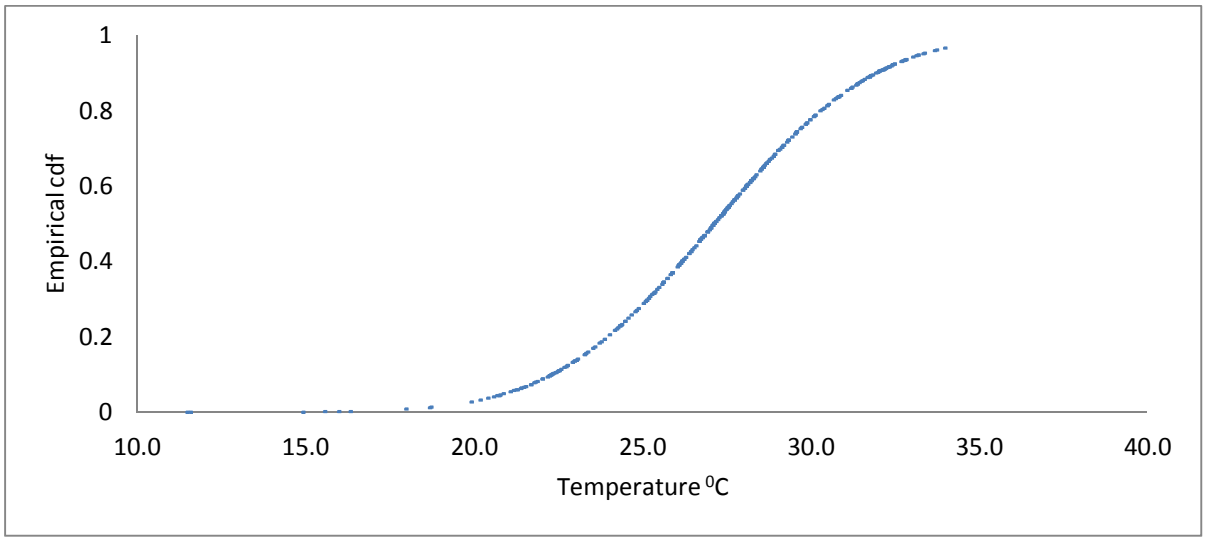


Figure 4.6d: Empirical cumulative distribution function (cdf) for Potiskum Station temperature data Series (1979-2008)

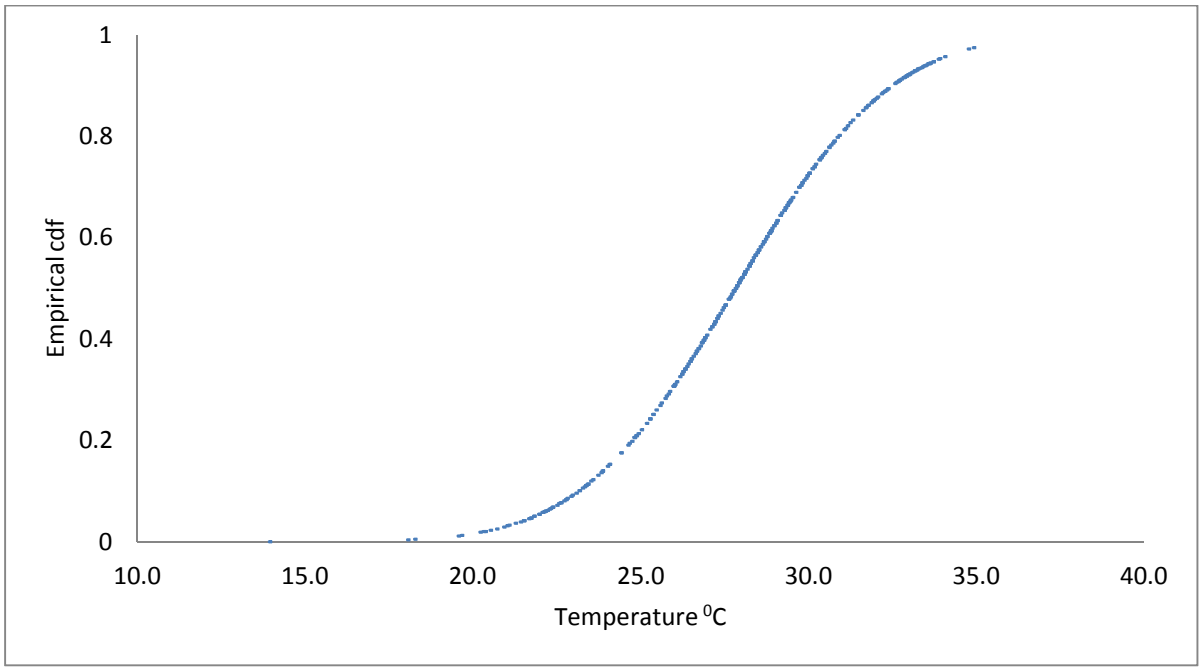


Figure 4.6e: Empirical cumulative distribution function (cdf) for Maiduguri Station temperature data Series (1979-2008)

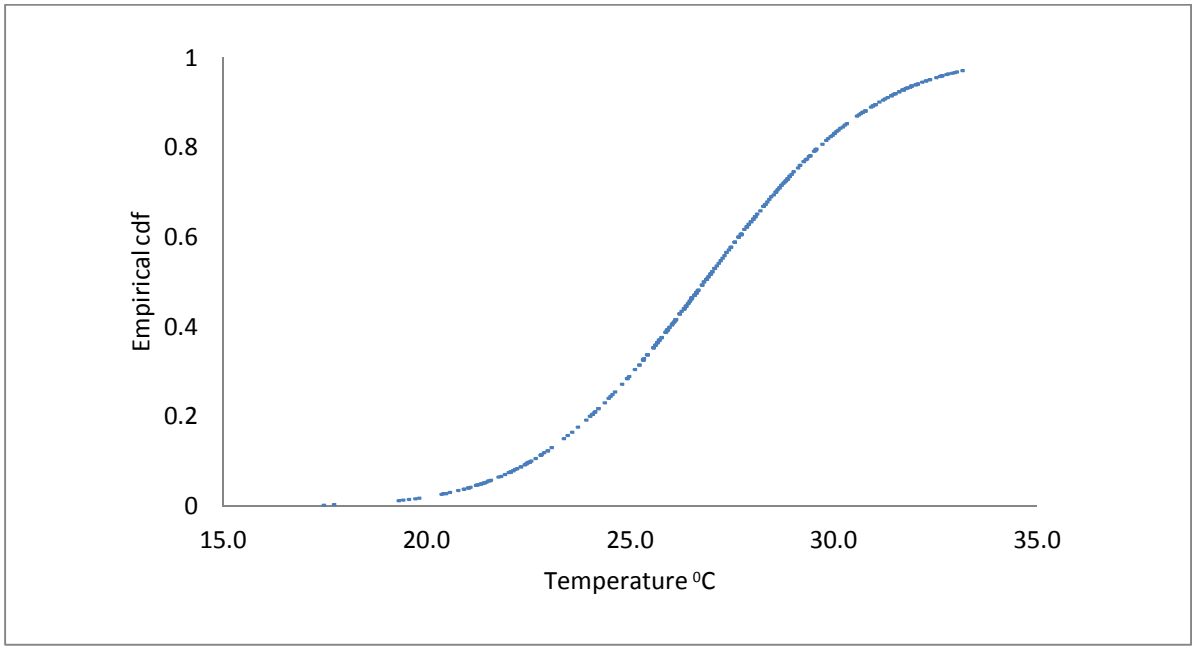


Figure 4.6f: Empirical cumulative distribution function (cdf) for Kano temperature data Series (1979-2008)

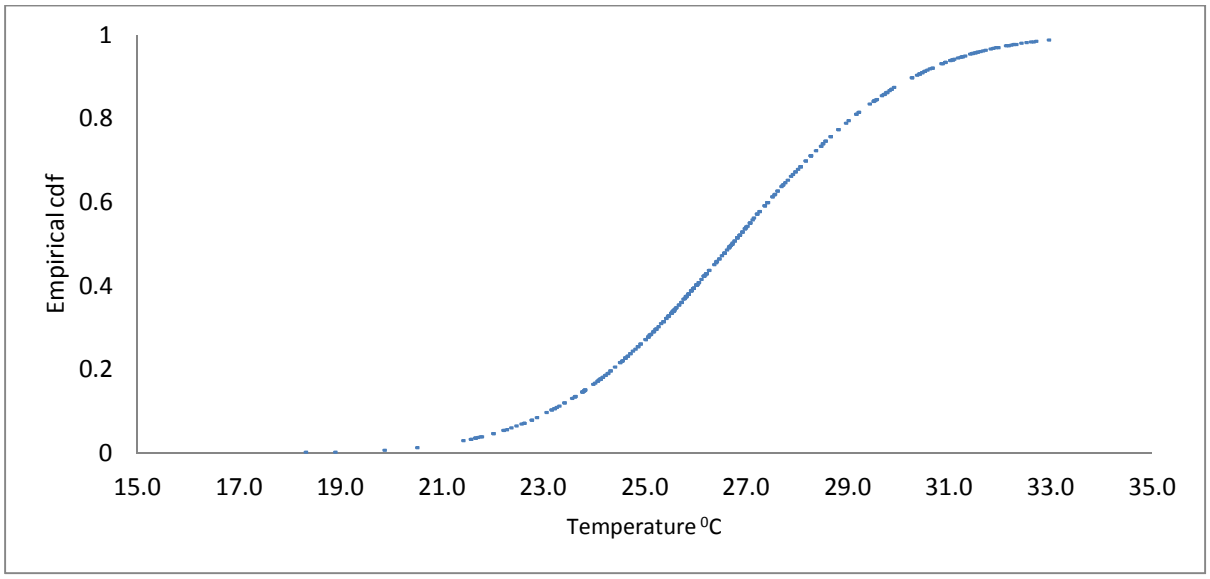
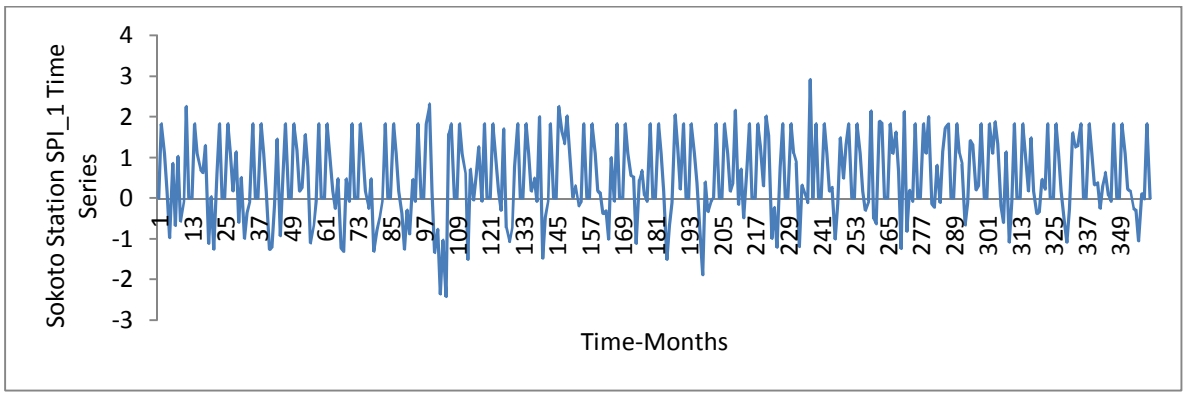


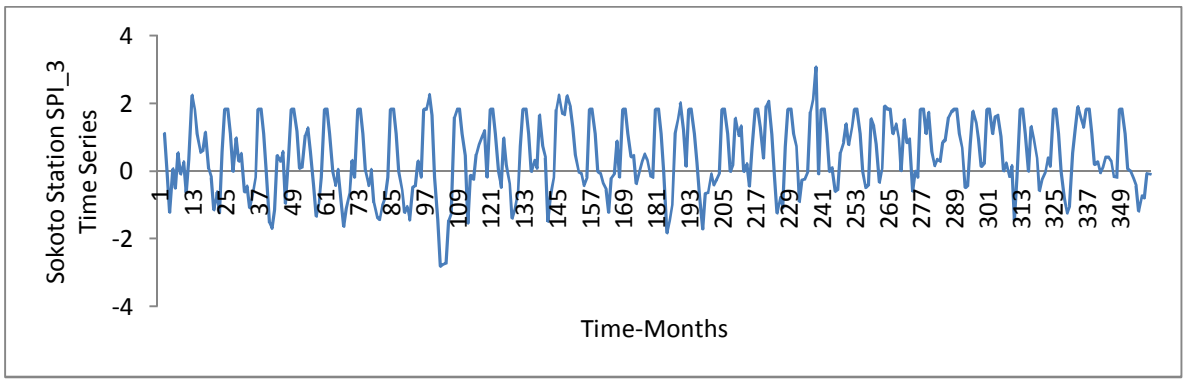
Figure 4.6g: Empirical cumulative distribution function (cdf) for Gusau Station temperature data Series (1979-2008)

APPENDIX E: SPI_1 to SPI_24 Time Series

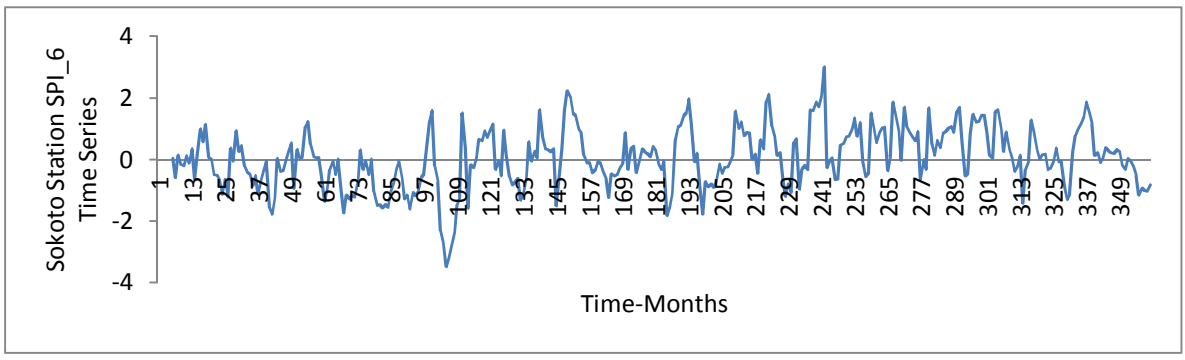
APPENDIX E1: Sokoto Station SPI_1to SPI_24 Time Series



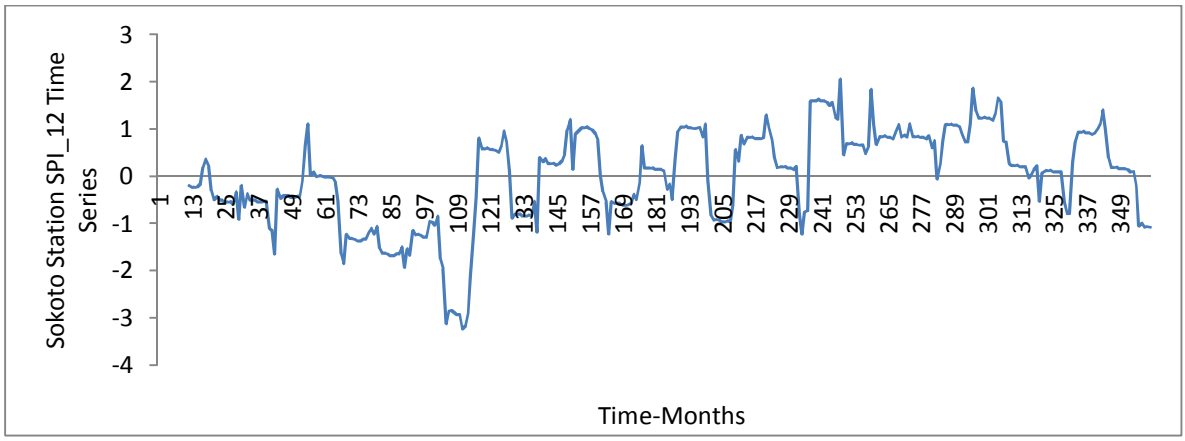
a. Sokoto Station SPI_1Time Series



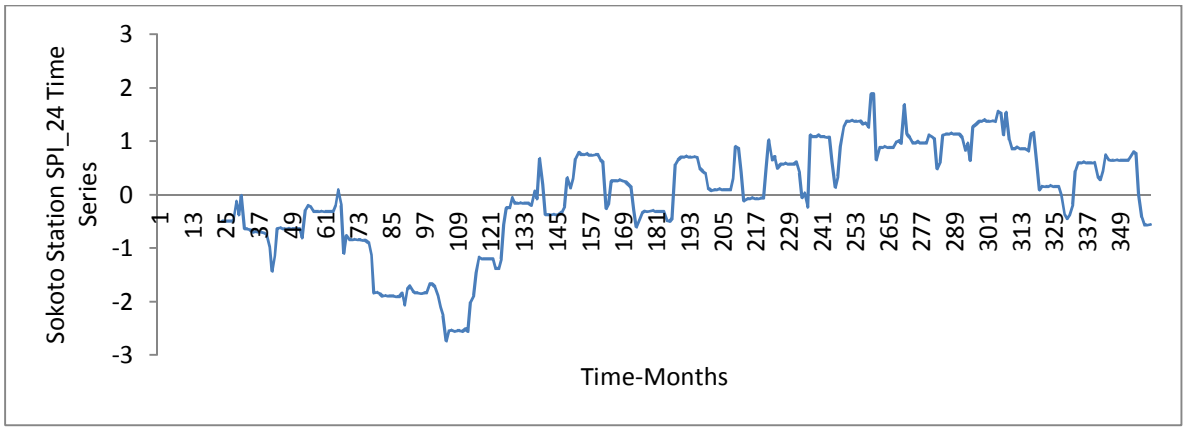
b. Sokoto Station SPI_3 Time Series



c. Sokoto Station SPI_6 Time Series

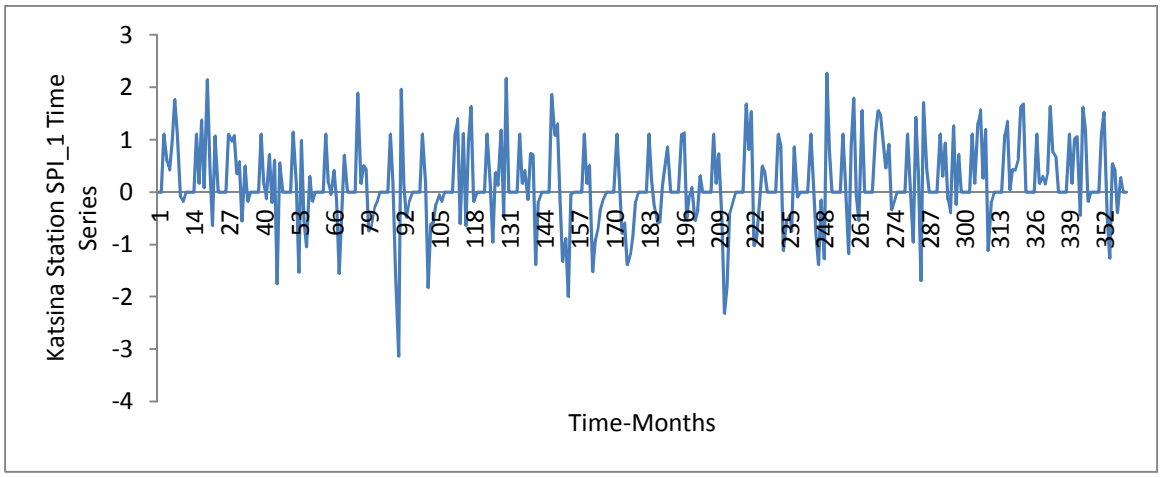


d. Sokoto Station SPI_12Time Series

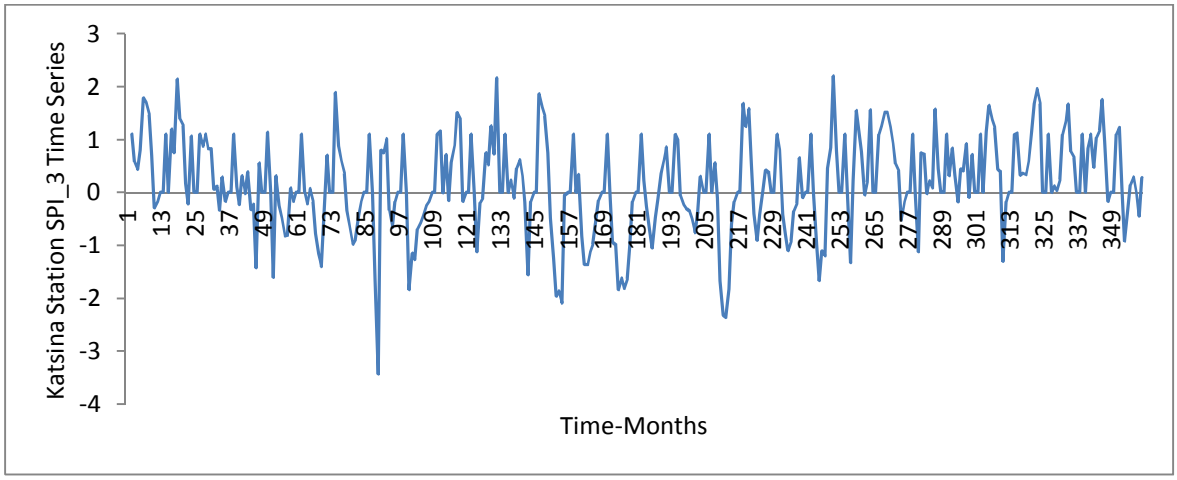


e. Sokoto Station SPI_24 Time Series

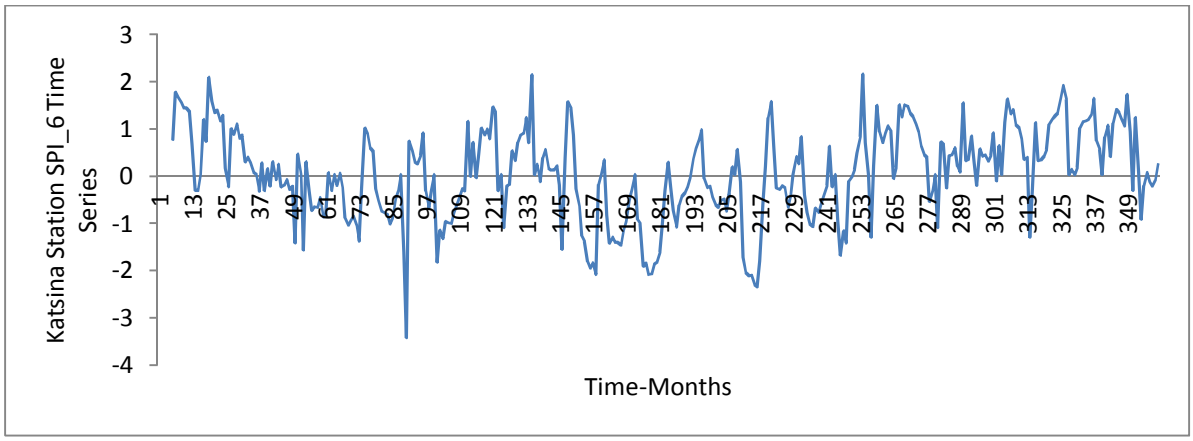
APPENDIX E2: Katsina Station SPI_1to SPI_24 Time Series



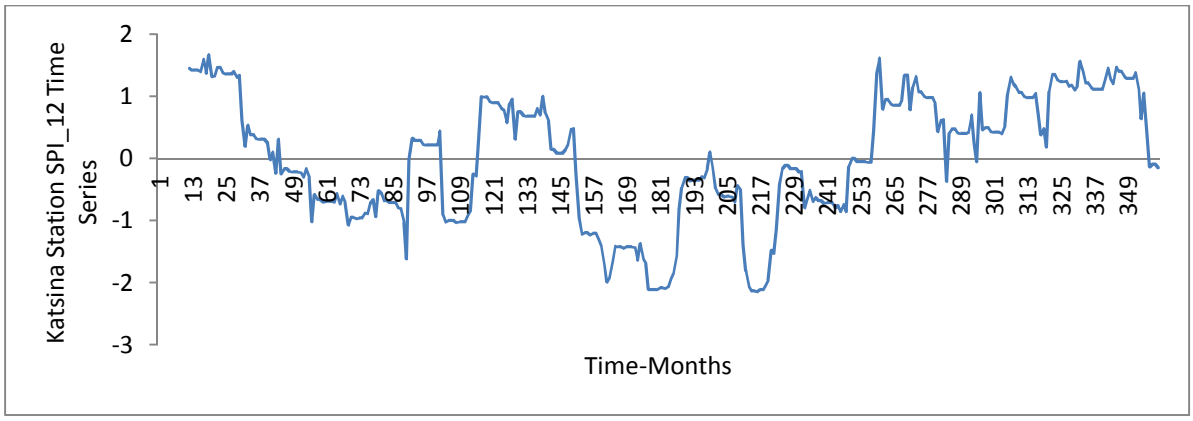
a. Katsina Station SPI_1 Time Series



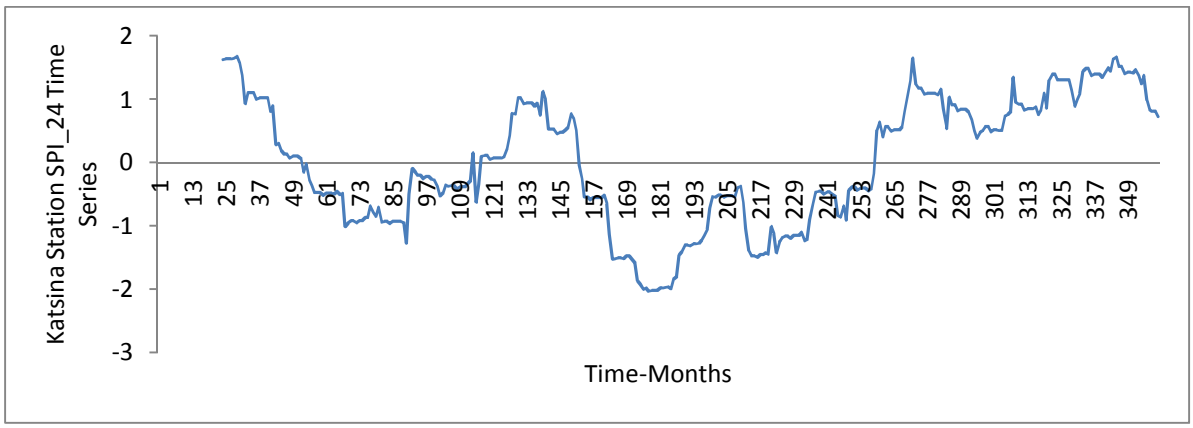
b. Katsina Station SPI_3 Time Series



c. Katsina Station SPI_6 Time Series

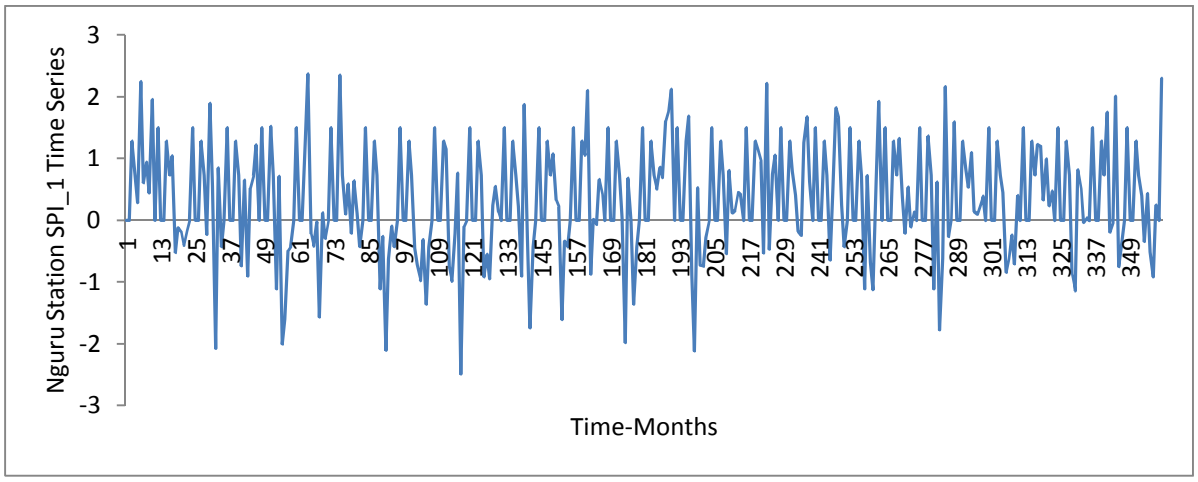


d. Katsina Station SPI_12 Time Series

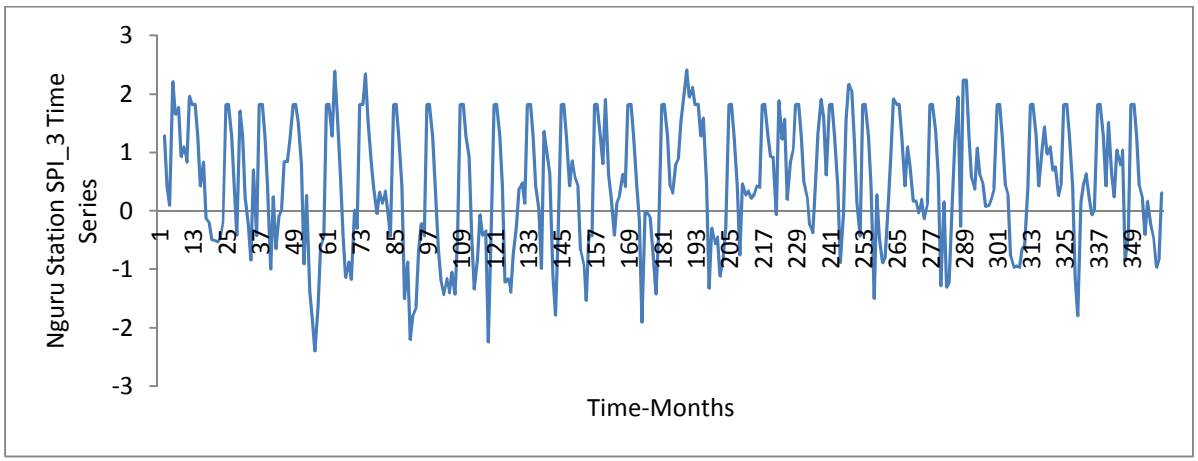


e. Katsina Station SPI_24 Time Series

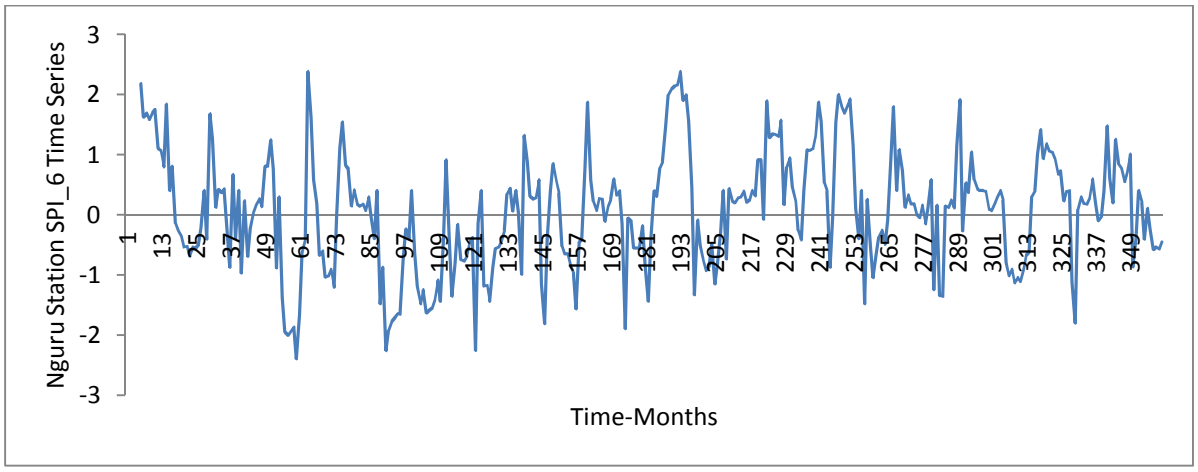
APPENDIX E3: Nguru Station SPI_1to SPI_24 Time Series



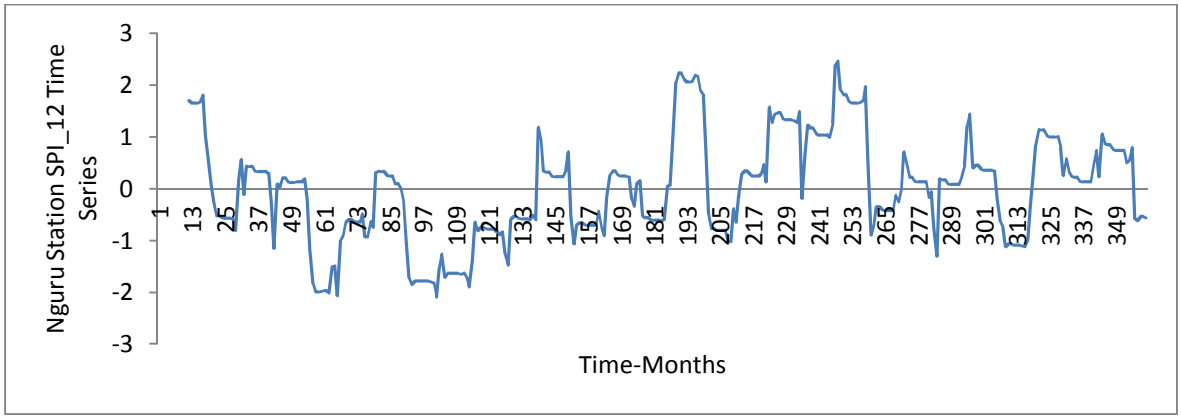
a. Nguru Station SPI_1Time Series



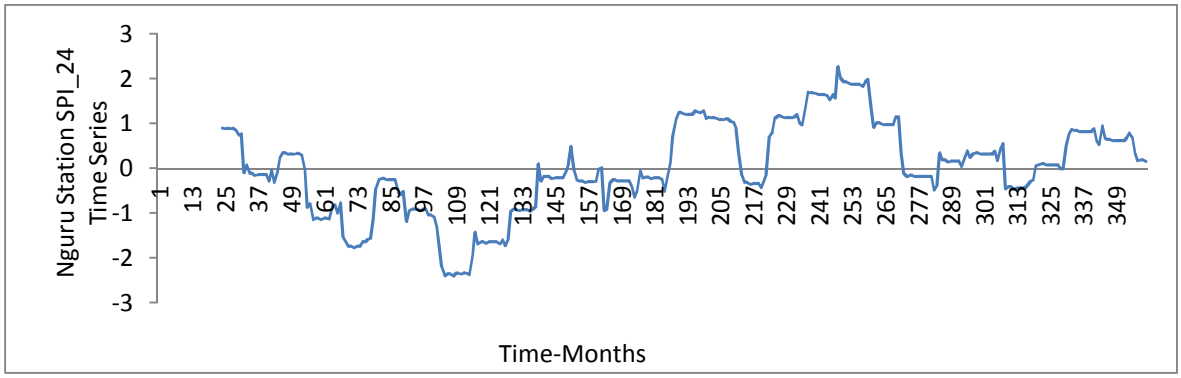
b. Nguru Station SPI_3 Time Series



c. Nguru Station SPI_6 Time Series

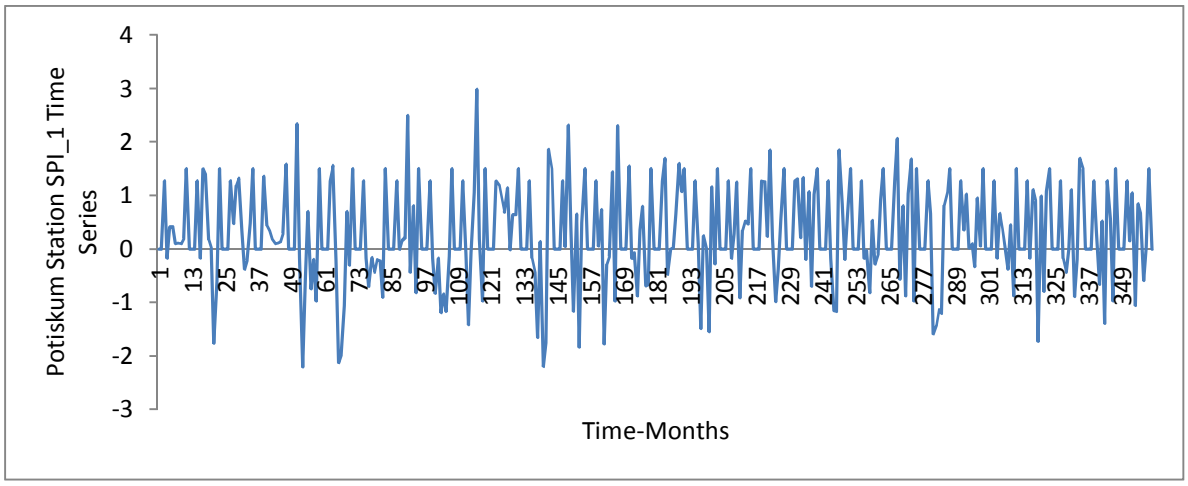


d. Nguru Station SPI_12 Time Series

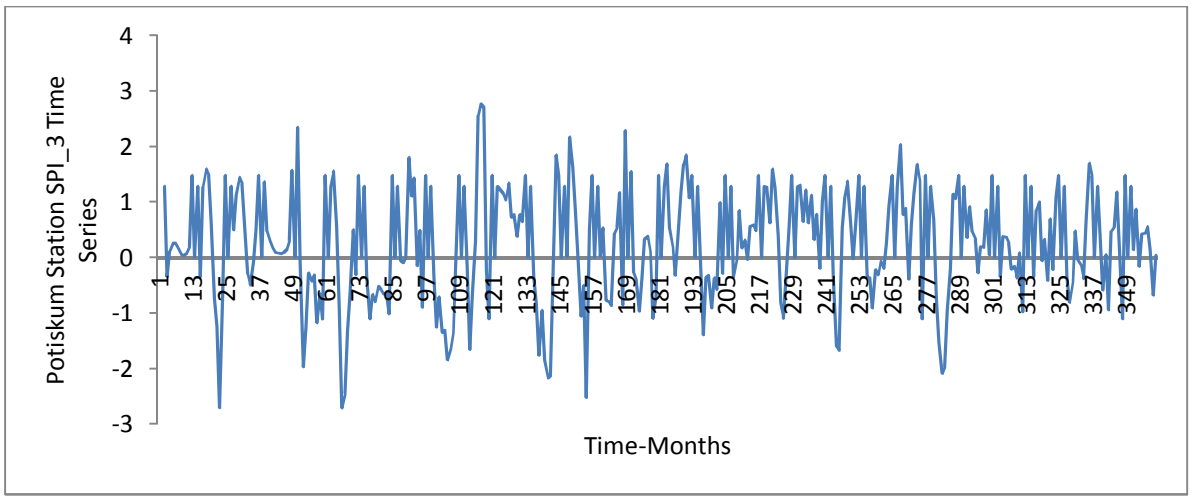


e. Nguru Station SPI_24 Time Series

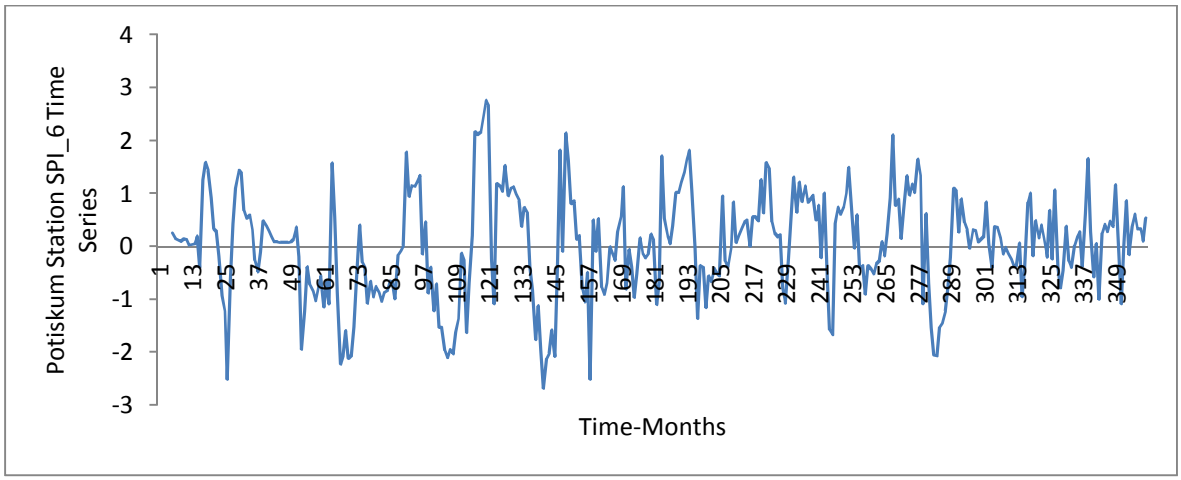
APPENDIX E4: Potiskum Station SPI_1to SPI_24 Time Series



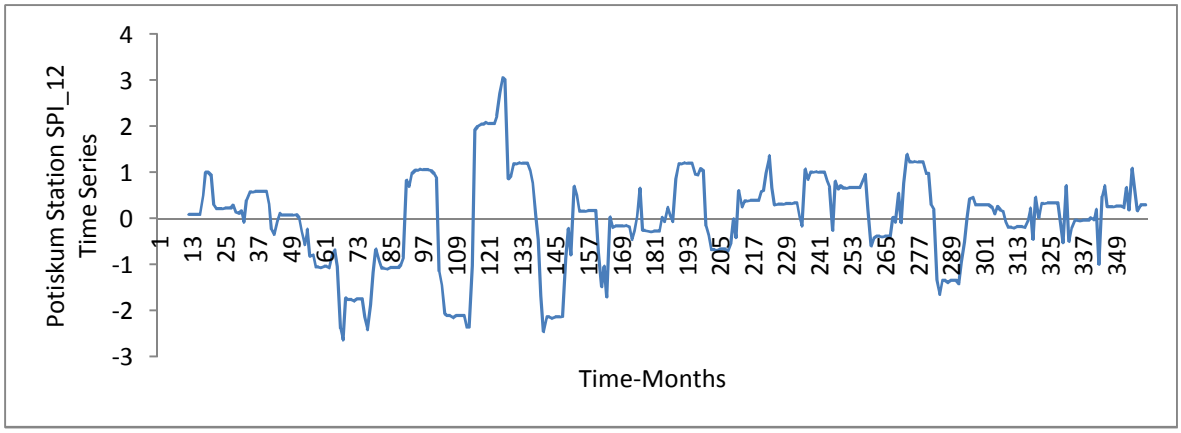
a. Potiskum Station SPI_1 Time Series



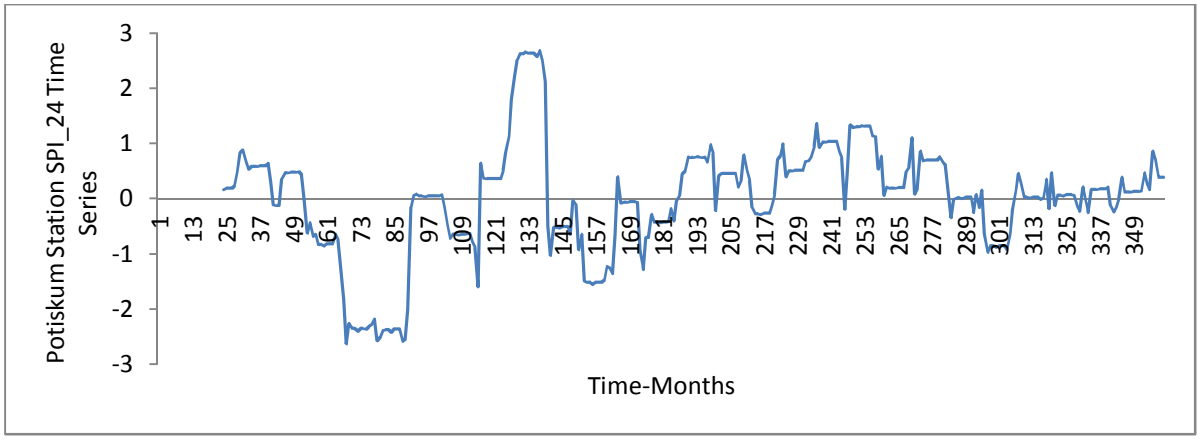
b. Potiskum Station SPI_3 Time Series



c. Potiskum Station SPI_6 Time Series

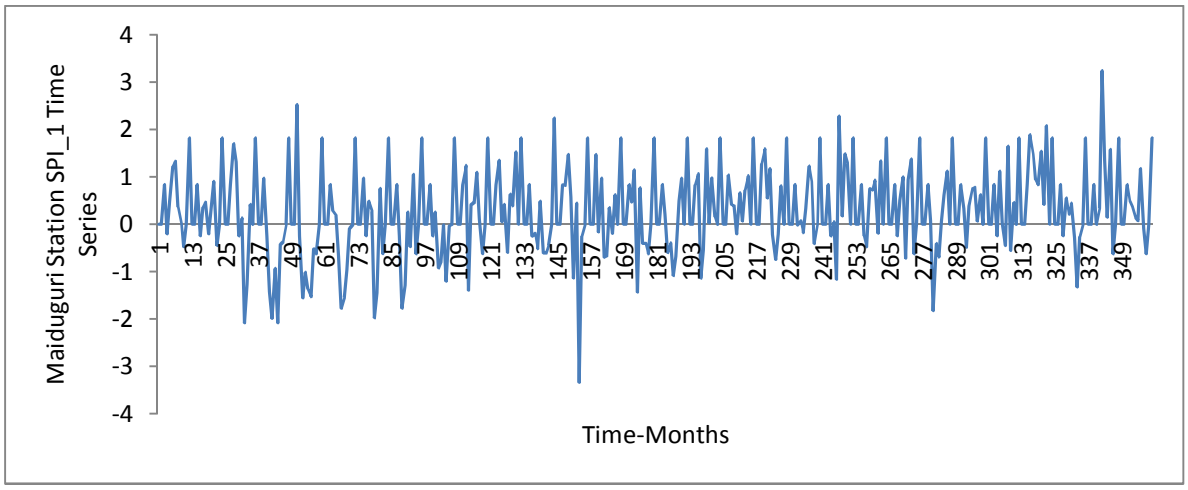


d. Potiskum Station SPI_12 Time Series

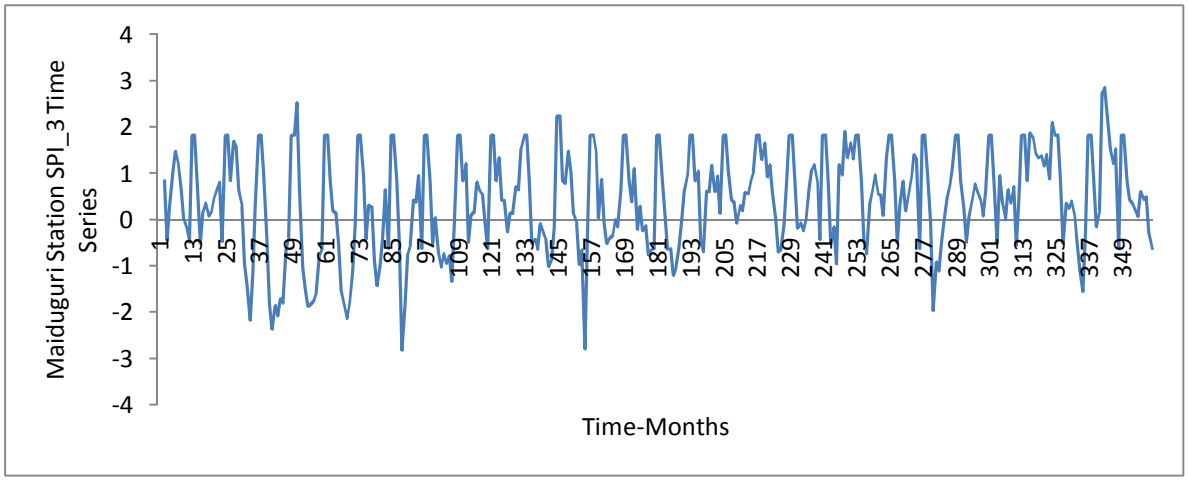


e. Potiskum Station SPI_24 Time Series

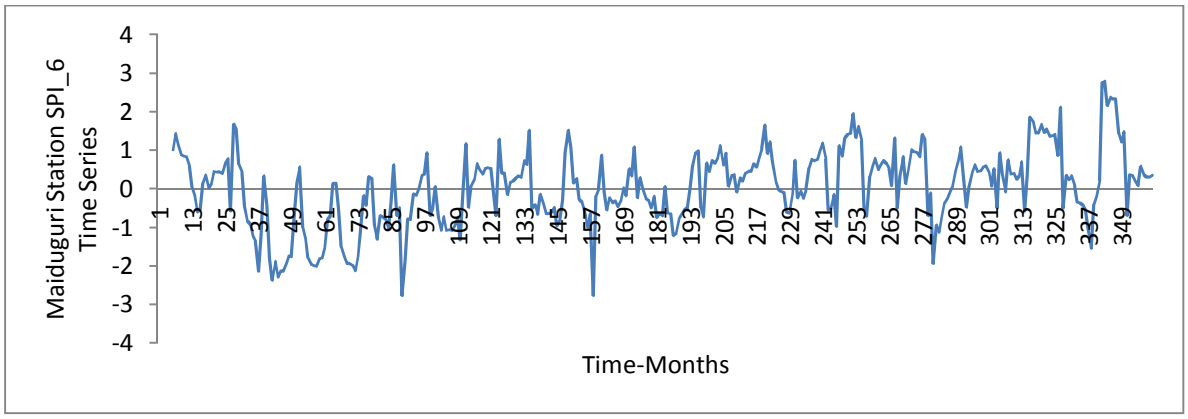
APPENDIX E5: Maiduguri Station SPI_1to SPI_24 Time Series



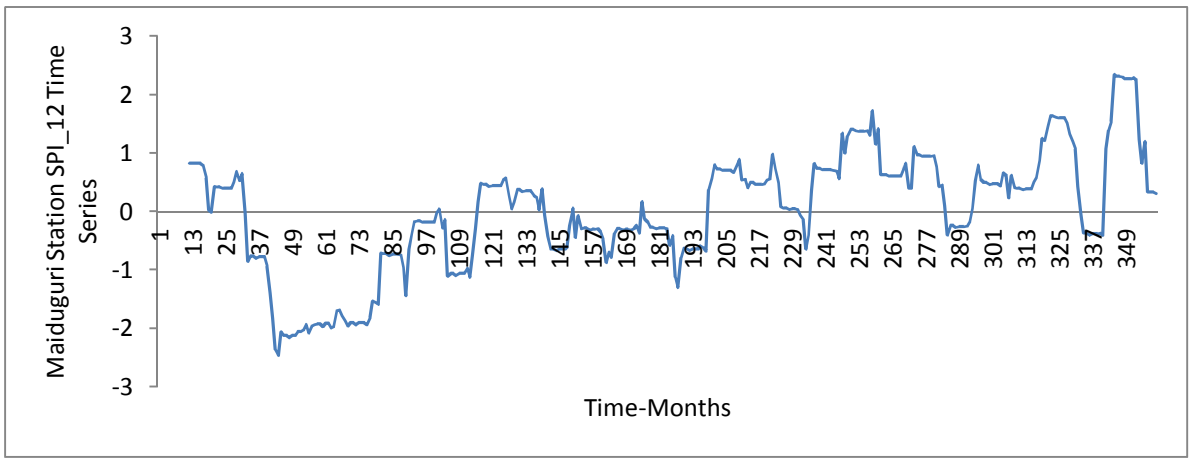
a. Maiduguri Station SPI_1 Time Series



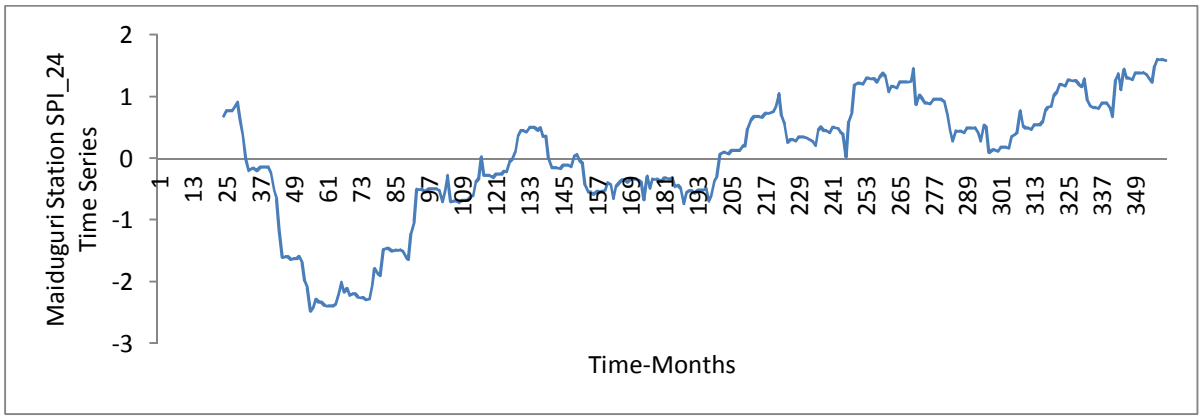
b. Maiduguri Station SPI_3 Time Series



c. Maiduguri Station SPI_6 Time Series

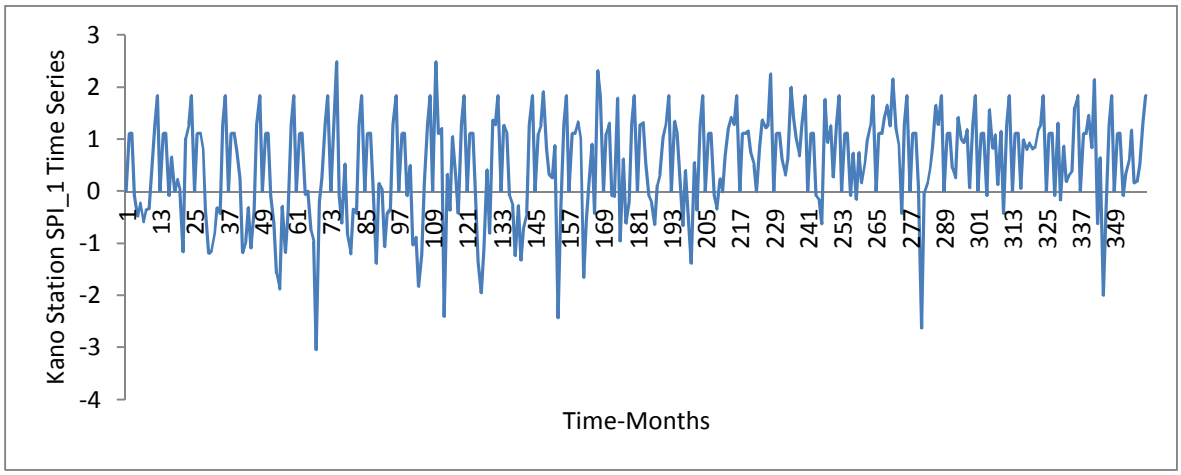


d. Maiduguri Station SPI_12 Time Series

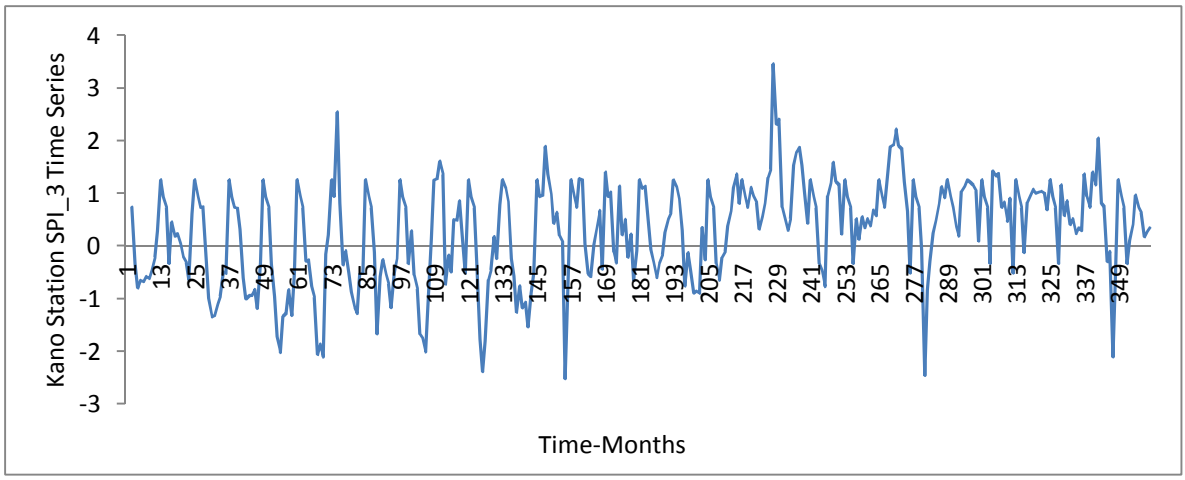


e. Maiduguri Station SPI_24 Time Series

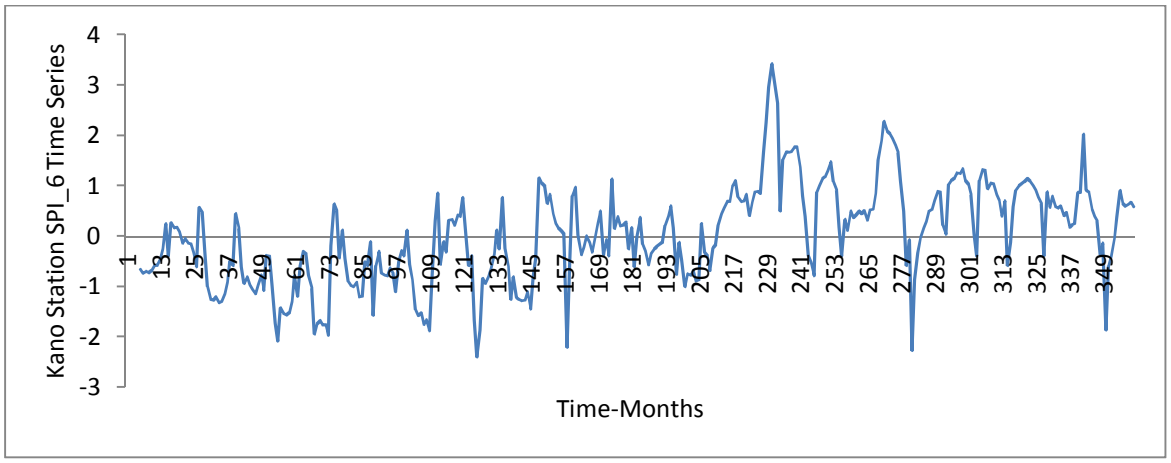
APPENDIX E6: Kano Station SPI_1 to SPI_24 Time Series



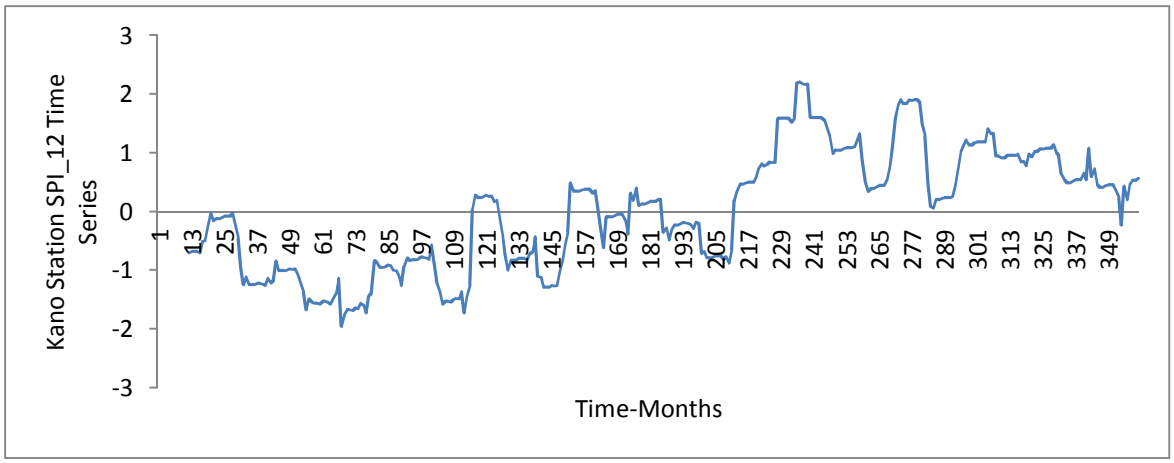
a. Kano Station SPI_1 Time Series



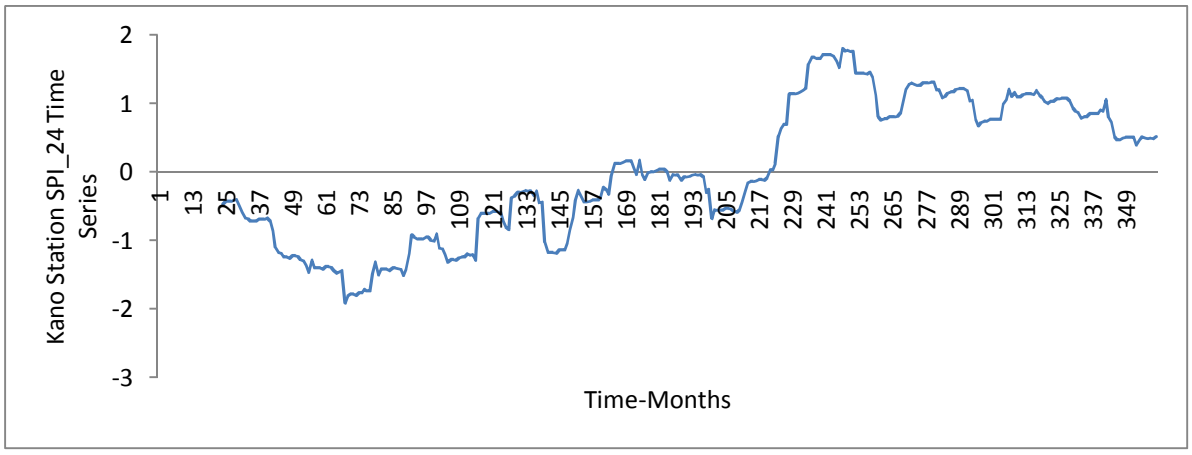
b. Kano Station SPI_3 Time Series



c. Kano Station SPI_6 Time Series

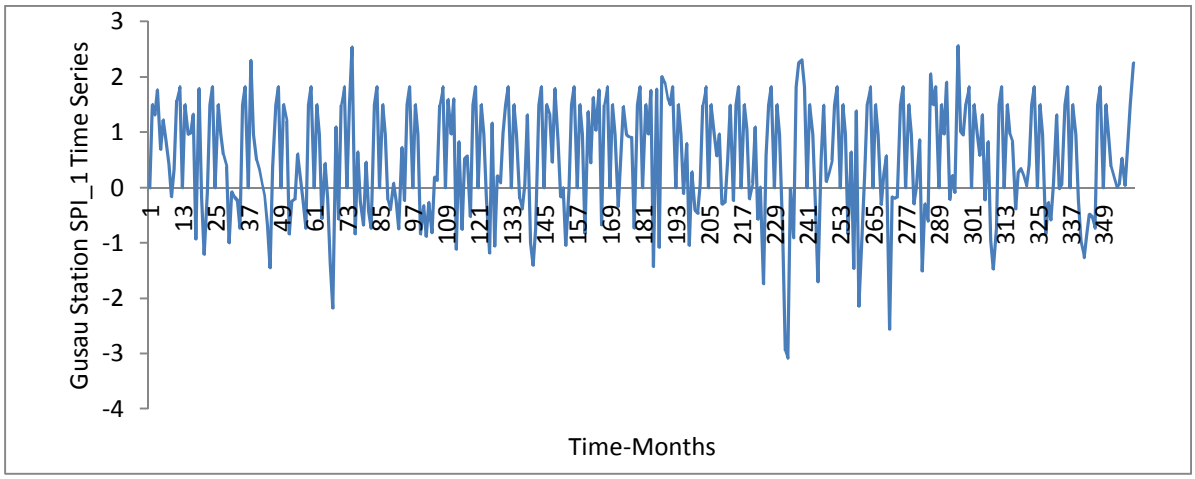


d. Kano Station SPI_12 Time Series

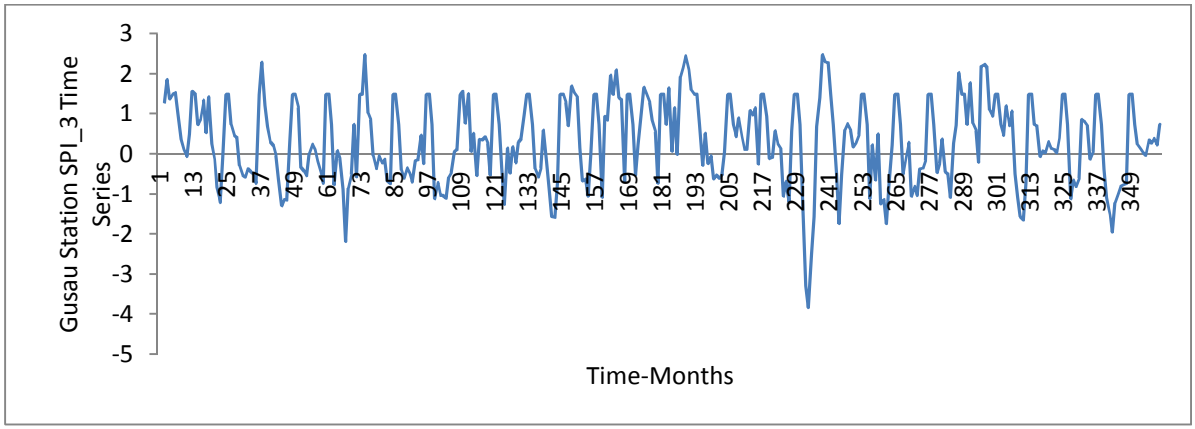


e. Kano Station SPI_24 Time Series

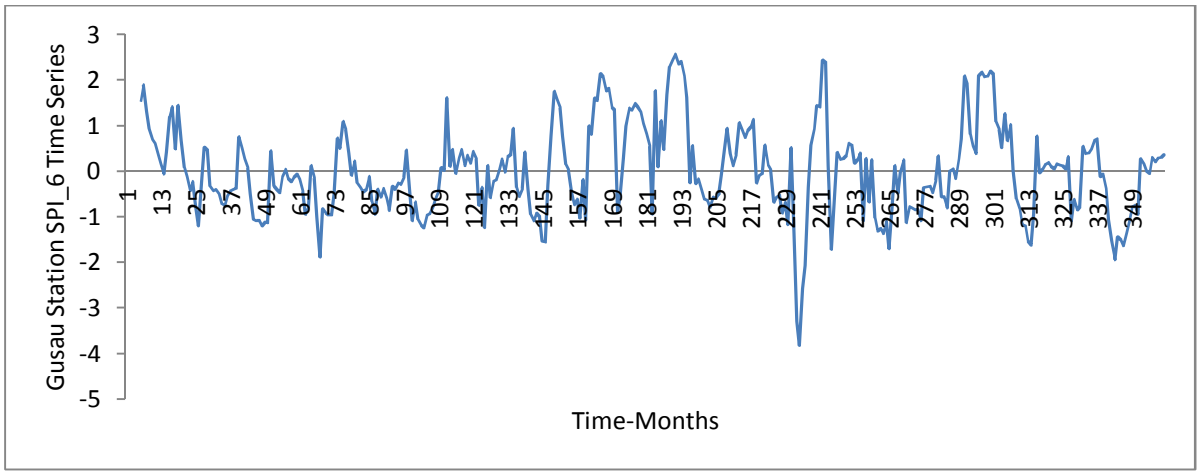
APPENDIX E7: Gusau Station SPI_1 to SPI_24 Time Series



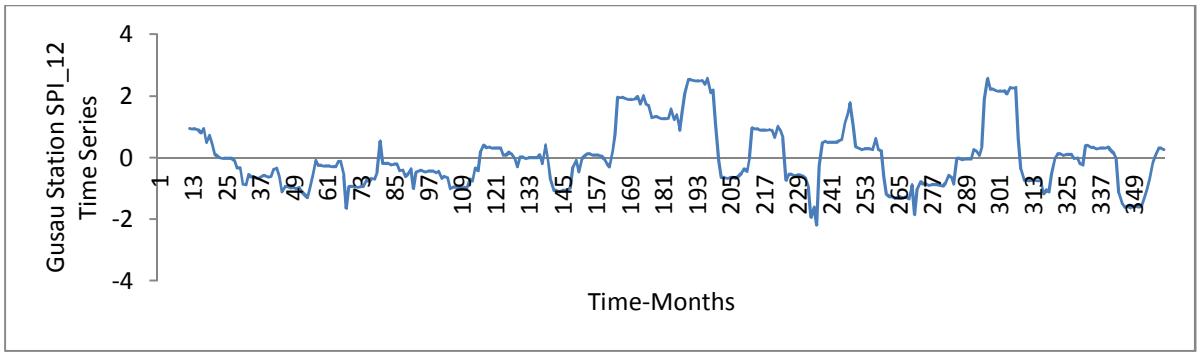
a. Gusau Station SPI_1 Time Series



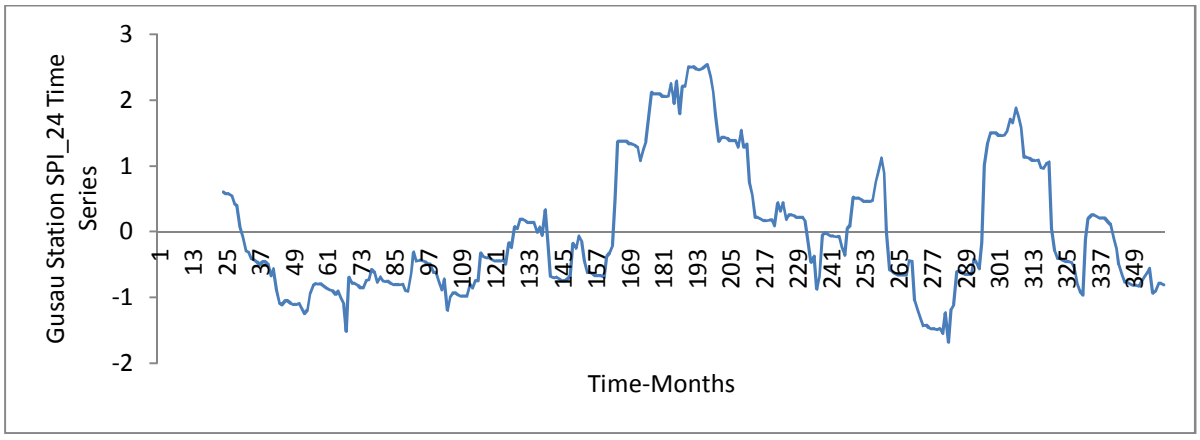
b. Gusau Station SPI_3 Time Series



c. Gusau Station SPI_6 Time Series

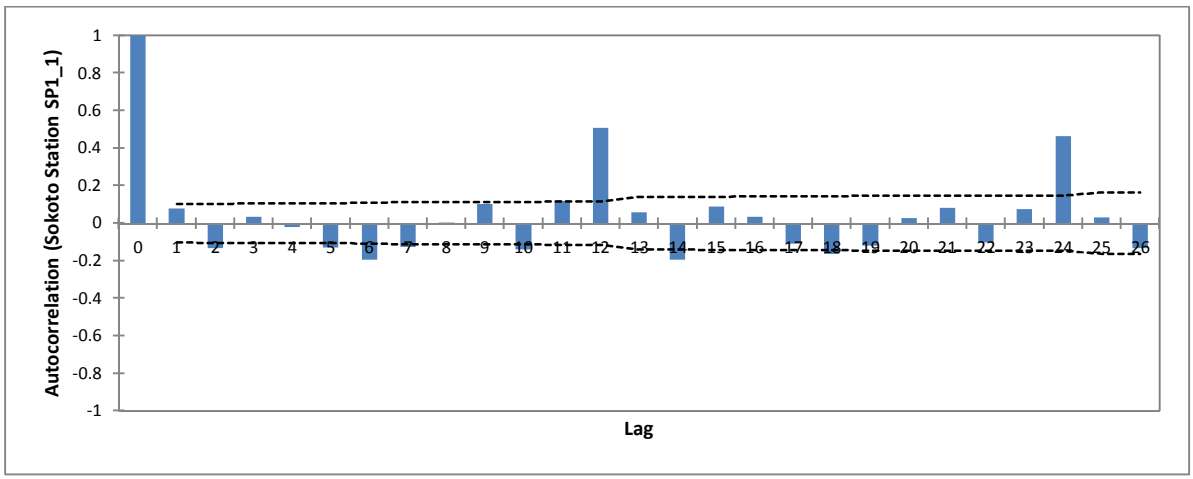


d. Gusau Station SPI_12 Time Series

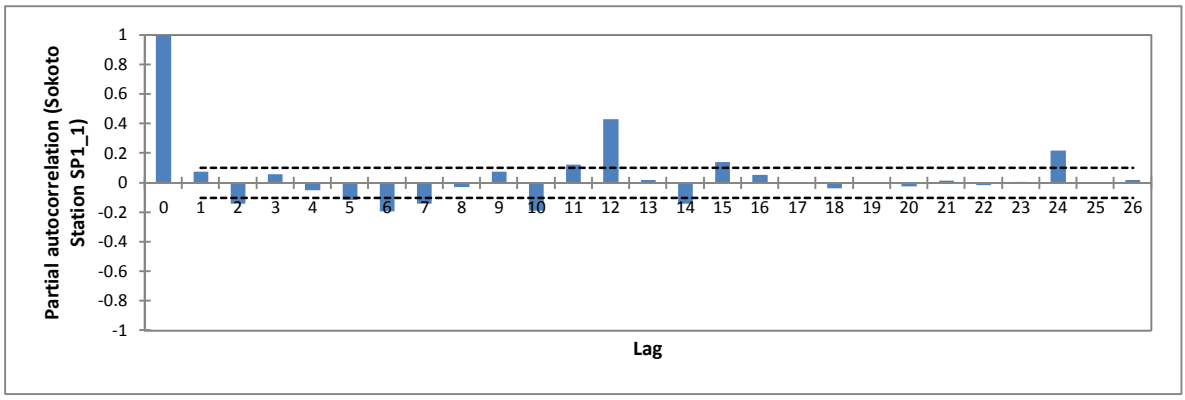


e. Gusau Station SPI_24 Time Series

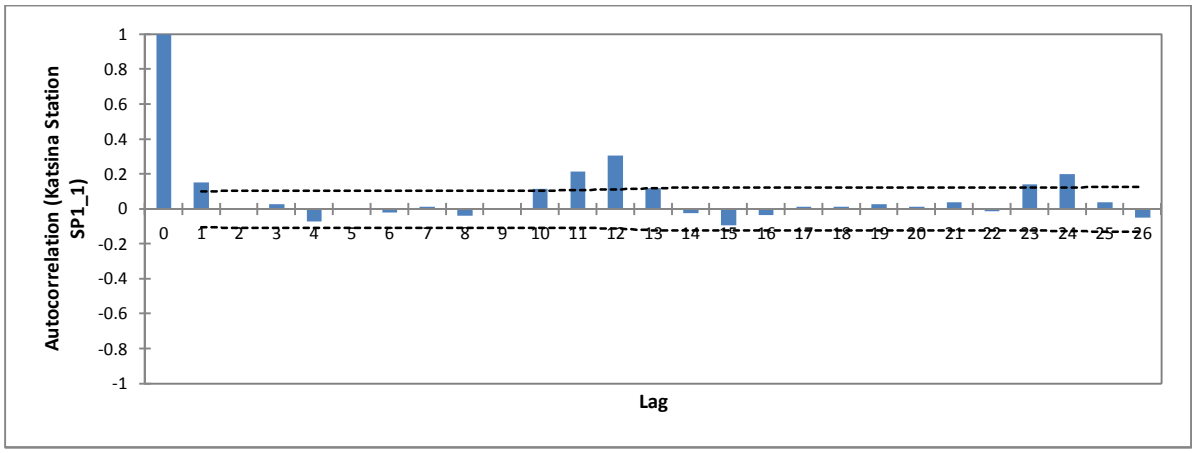
APPENDIX F: SPI_1 Autocorrelation Function (ACF) and Partial Autocorrelation Function (PACF



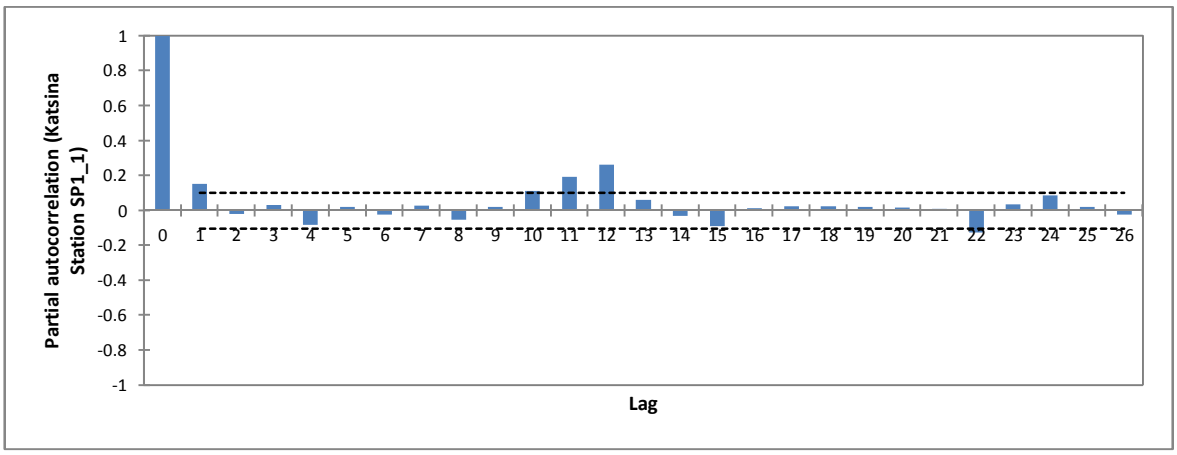
a. ACF plot for selecting relevant models for Sokoto Station SPI_1 series



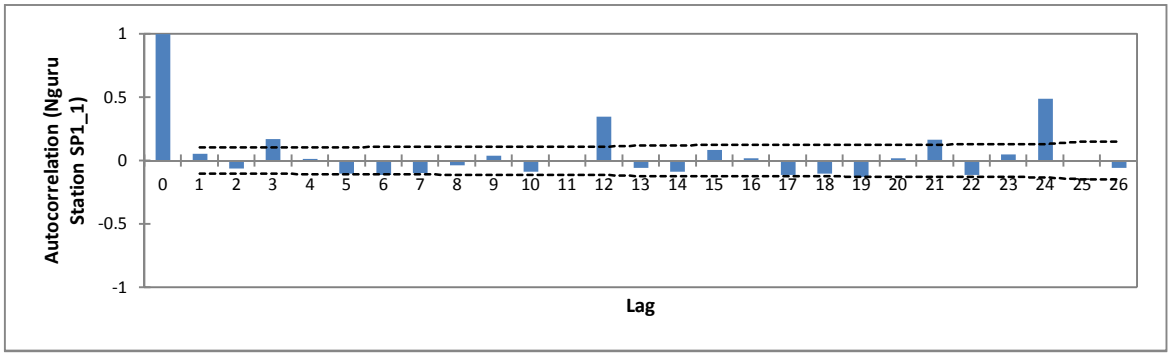
b. PACF plot for selecting relevant models for Sokoto Station SPI_1 series



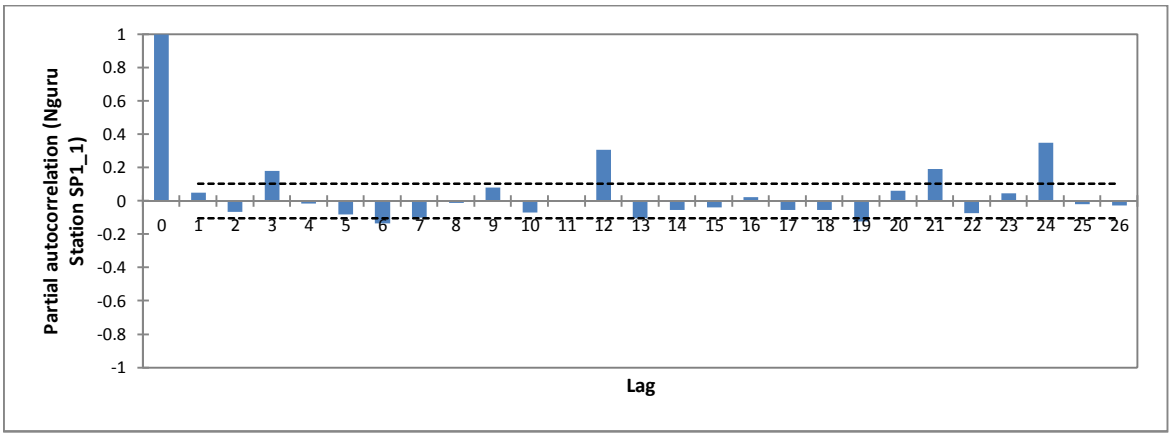
c. ACF plot for selecting relevant models for Katsina Station SPI_1 series



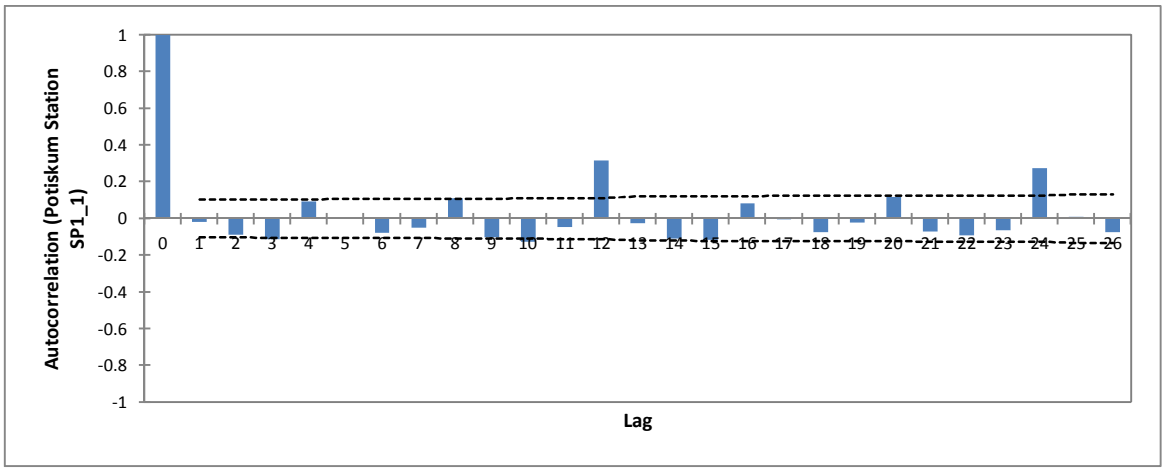
d. PACF plot for selecting relevant models for Katsina Station SPI_1 series



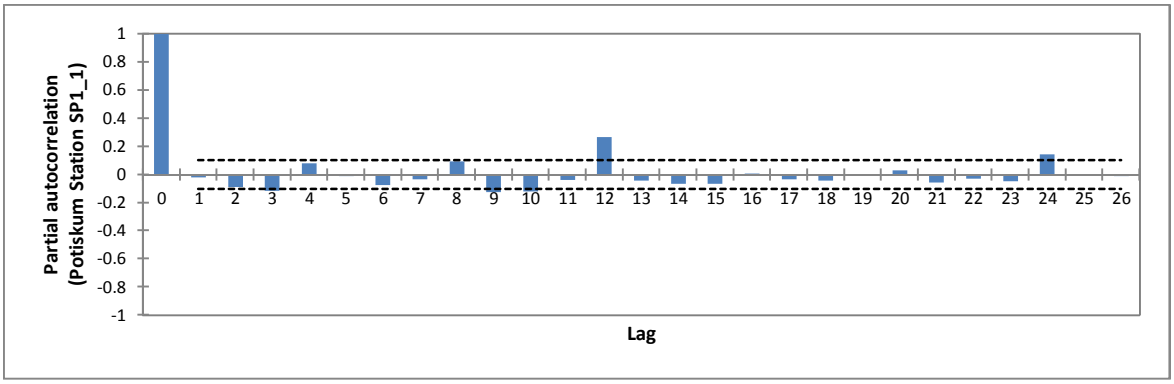
e. ACF plot for selecting relevant models for Nguru Station SPI_1 series



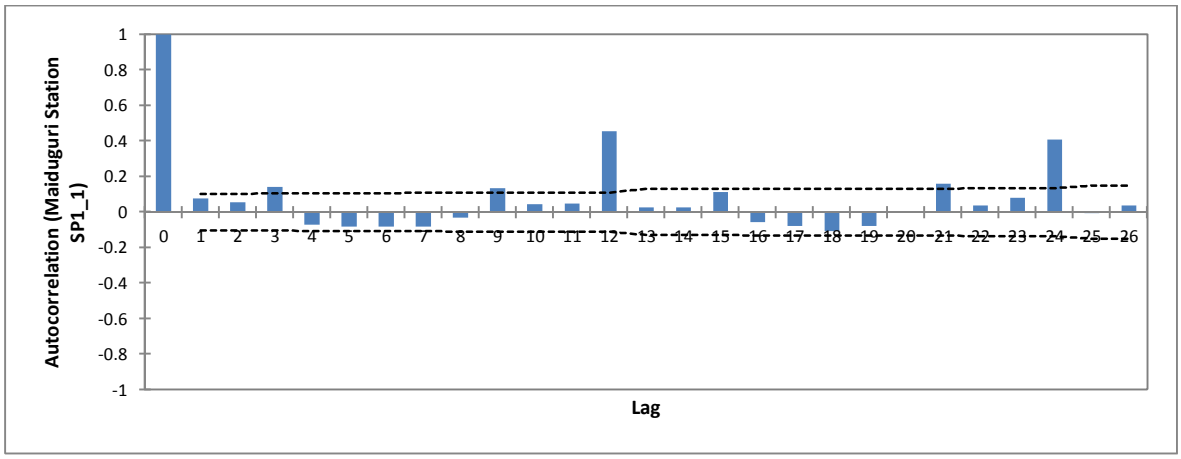
f. PACF plot for selecting relevant models for Nguru Station SPI_1 series



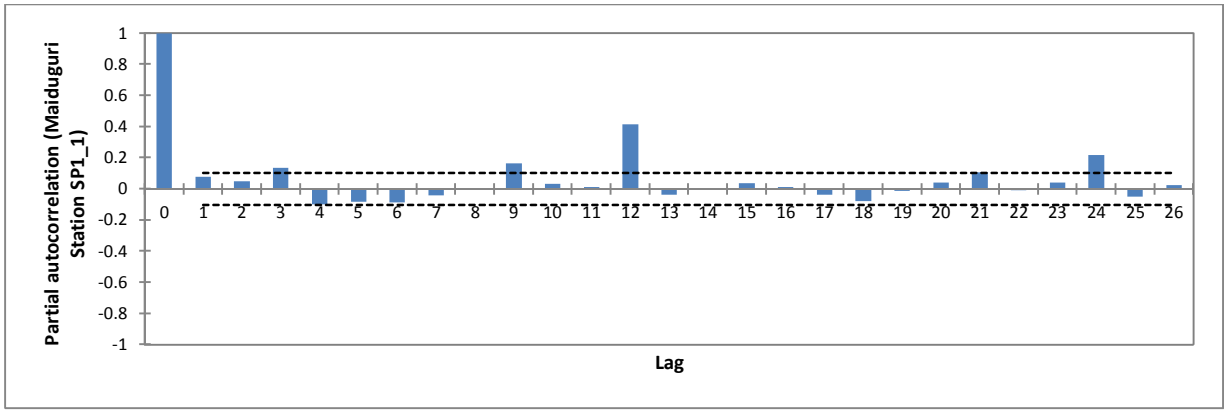
g. ACF plot for selecting relevant models for Potiskum Station SPI_1 series



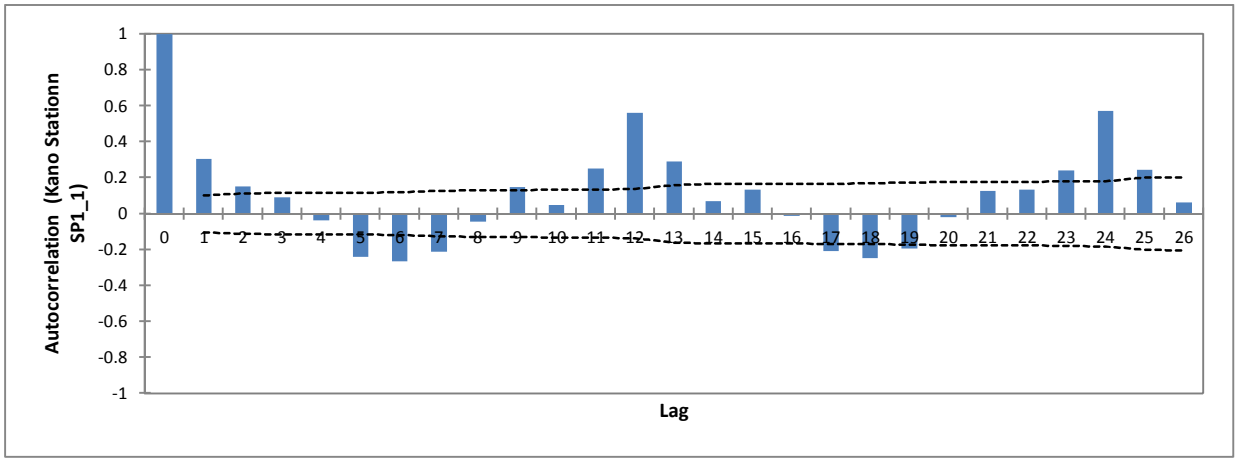
h. PACF plot for selecting relevant models for Potiskum Station SPI_1 series



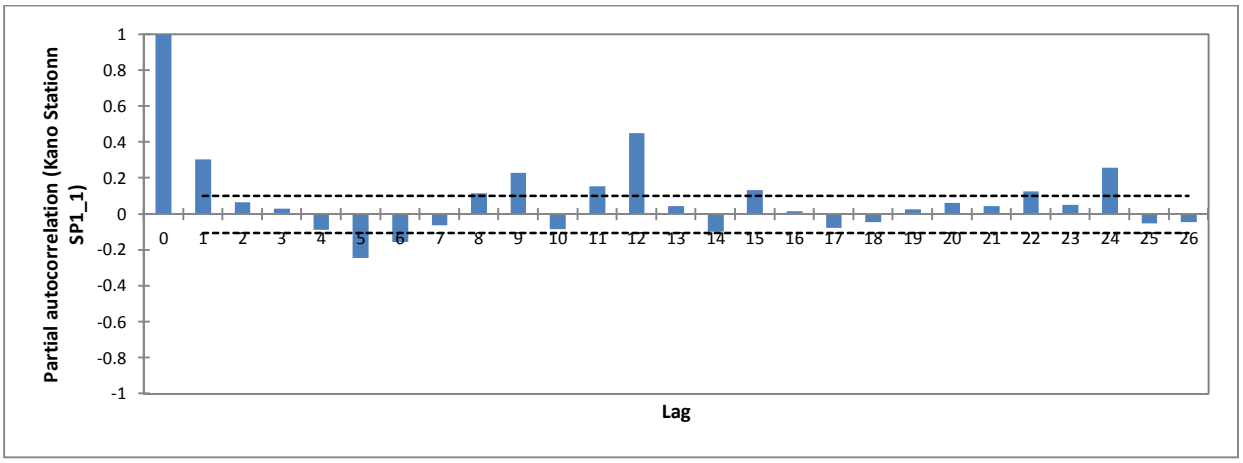
i. ACF plot for selecting relevant models for Maiduguri Station SPI_1 series



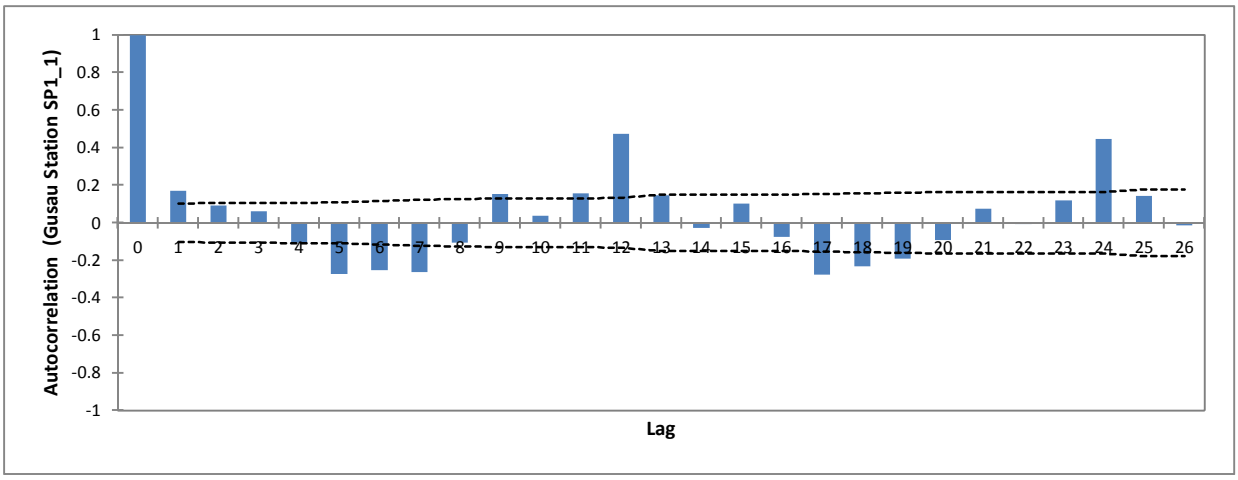
j. PACF plot for selecting relevant models for Maiduguri Station SPI_1 series



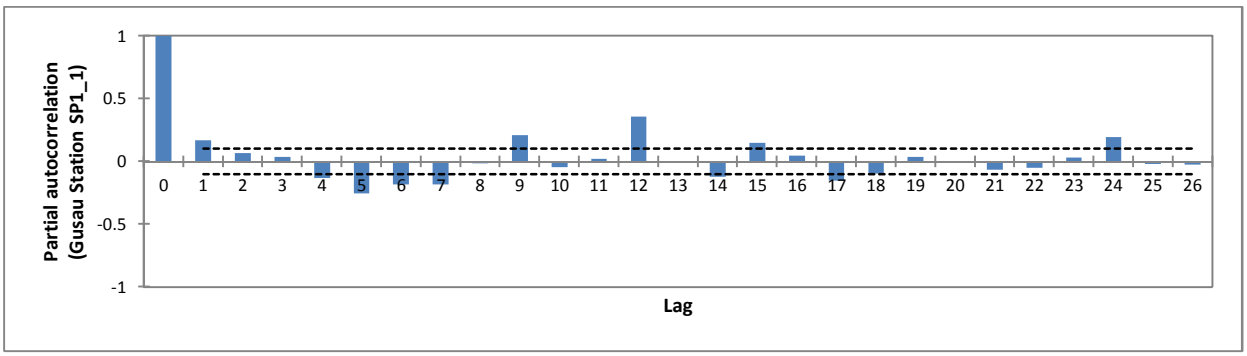
k. ACF plot for selecting relevant models for Kano Station SPI_1 series



l. PACF plot for selecting relevant models for Kano Station SPI_1 series



m. ACF plot for selecting relevant models for Gusau Station SPI_1 series



n. PACF plot for selecting relevant models for Gusau Station SPI_1 series

APPENDIX G: Results of SPI_1 Series SARIMA Models and Parameters

APPENDIX G 1: Results of NSSR SPI_1 SARIMA Model $(202)x(212)_{12}$

XLSTAT 2013.1.01 - ARIMA - on 3/23/2013 at 5:54:20 PM
Time series: Workbook = ARIMA.xlsm / Sheet = Arima / Range = Arima!$J$1:$J$361 /
360 rows and 1 column
Confidence intervals (%): 95
Center: No
Model parameters: p = 2 / d = 0 / q = 2 / P = 2 / D = 1 / Q = 2 / s = 12
Optimize: Likelihood (Convergence = 0.00001 / Iterations = 500)
Validation: 12
Prediction: 3
Confidence intervals (%): 95
Seed (random numbers): 123456789
Summary statistics:

Variable	Observations	Obs. with missing data	Obs. without missing data	Minimum	Maximum	Mean	Std. deviation
NSSR SP1_1	360	0	360	-2.740	2.400	0.325	0.896

Results of ARIMA modeling of the NSSR SP1_1 series:

Results after optimization (NSSR SP1_1):

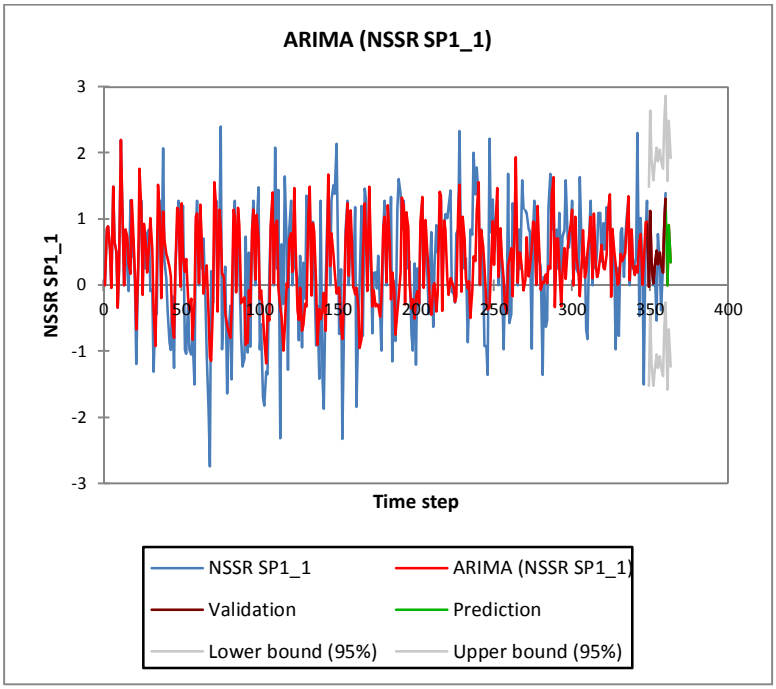
Goodness of fit statistics:

Observations	348.000
SSE	198.428
MAPE(Diff)	148.077
MAPE	113.651
WN Variance	0.591
WN Variance (estimate)	0.591
-2Log(Like.)	793.253
FPE	0.690
AIC	811.253
AICC	811.805
SBC	845.607

Model parameters:

Parameter	Value	Hessian standard error	Lower bound (95%)	Upper bound (95%)	Asympt. standard error	Lower bound (95%)	Upper bound (95%)
Constant	0.000	0.000	0.000	0.000	0.000	0.000	0.000

Parameter	Value	Hessian standard error	Lower bound (95%)	Upper bound (95%)	Asympt. standard error	Lower bound (95%)	Upper bound (95%)
AR(1)	0.027	0.127	-0.222	0.277	0.078	-0.126	0.181
AR(2)	-0.516	0.133	-0.777	-0.254	0.081	-0.675	-0.357
SAR(1)	-0.328	1.543	-3.353	2.697	0.078	-0.481	-0.175
SAR(2)	0.001	0.069	-0.134	0.137	0.082	-0.159	0.161
MA(1)	0.072	0.100	-0.124	0.269	0.070	-0.064	0.209
MA(2)	0.736	0.109	0.523	0.949	0.071	0.598	0.874
SMA(1)	-0.530	1.543	-3.554	2.494	0.076	-0.680	-0.381
SMA(2)	-0.281	1.327	-2.882	2.320	0.078	-0.434	-0.128



APPENDIX G 2: Result of Sokoto Station SPI_1 SARIMA Model $(011)x(011)_{12}$

XLSTAT 2013.1.01 - ARIMA - on 3/23/2013 at 5:40:21 PM
Time series: Workbook = ARIMA.xlsm / Sheet = Arima / Range = Arima!$I$1:$I$361 / 360 rows and 1 column
Confidence intervals (%): 95
Center: No
Model parameters: p = 0 / d = 1 / q = 1 / P = 0 / D = 1 / Q = 1 / s = 12
Optimize: Likelihood (Convergence = 0.00001 / Iterations = 500)
Validation: 12
Prediction: 3
Confidence intervals (%): 95
Seed (random numbers): 1503749048
Summary statistics:

Variable	Observations	Obs. with missing data	Obs. without missing data	Minimum	Maximum	Mean	Std. deviation
Sokoto Station SP1_1	360	0	360	-2.420	2.920	0.478	0.978

Results of ARIMA modeling of the Sokoto Station SP1_1 series:

Results after optimization (Sokoto Station SP1_1):

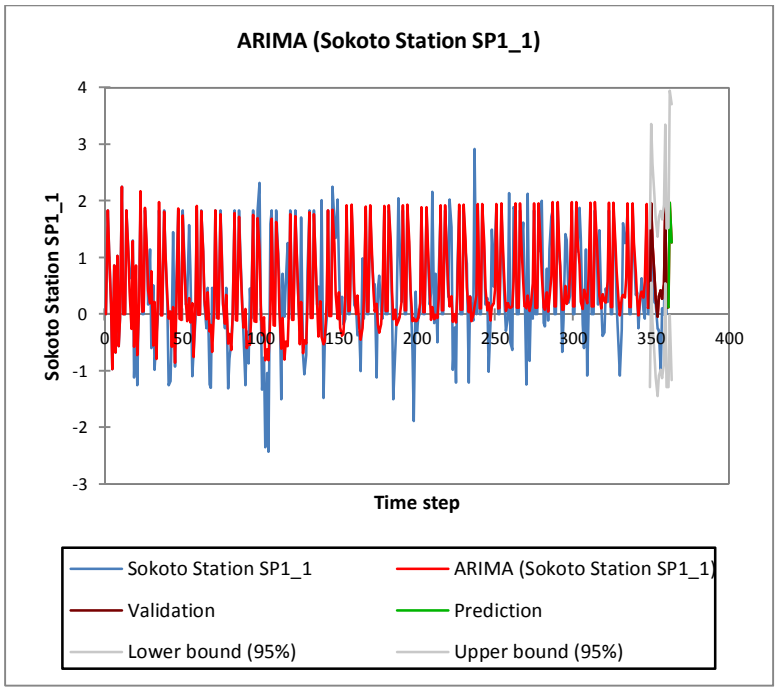
Goodness of fit statistics:

Observations	348.000
SSE	142.581
MAPE(Diff)	86.746
MAPE	101.166
WN Variance	0.426
WN Variance (estimate)	0.511
-2Log(Like.)	756.872
FPE	0.426
AIC	762.872
AICC	762.944
SBC	774.314

Model parameters:

Parameter	Value	Hessian standard error	Lower bound (95%)	Upper bound (95%)	Asympt. standard error	Lower bound (95%)	Upper bound (95%)
Constant	0.000	0.000	0.000	0.000	0.000	0.000	0.000

Parameter	Value	Hessian standard error	Lower bound (95%)	Upper bound (95%)	Asympt. standard error	Lower bound (95%)	Upper bound (95%)
MA(1)	-1.000	0.023	-1.046	-0.954	0.055	-1.107	-0.893
SMA(1)	-1.096	0.044	-1.182	-1.010	0.055	-1.203	-0.989



APPENDIX G 3: Result of Katsina Station SPI_1 SARIMA Model $(111)x(111)_{12}$

XLSTAT 2013.1.01 - ARIMA - on 3/23/2013 at 4:45:08 PM
Time series: Workbook = ARIMA.xlsm / Sheet = Arima / Range = Arima!$E$1:$E$361 / 360 rows and 1 column
Confidence intervals (%): 95
Center: No
Model parameters: p = 1 / d = 1 / q = 1 / P = 1 / D = 1 / Q = 1 / s = 12
Optimize: Likelihood (Convergence = 0.00001 / Iterations = 500)
Validation: 12
Prediction: 3
Confidence intervals (%): 95
Seed (random numbers): 123456789

Summary statistics

Summary statistics:

Variable	Observations	Obs. with missing data	Obs. without missing data	Minimum	Maximum	Mean	Std. deviation
Katsina Station SP1_1	360	0	360	-3.130	2.270	0.168	0.768

Results of ARIMA modeling of the Katsina Station SP1_1 series:

Results after optimization (Katsina Station SP1_1):

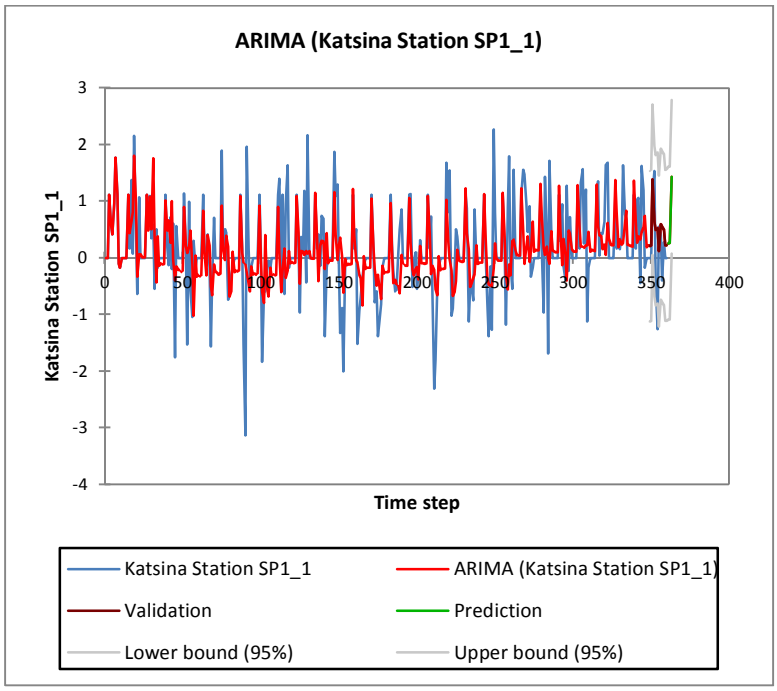
Goodness of fit statistics:

Observations	348.000
SSE	153.599
MAPE(Diff)	147.233
MAPE	117.106
WN Variance	0.459
WN Variance (estimate)	0.459
-2Log(Like.)	740.794
FPE	0.496
AIC	750.794
AICC	750.977
SBC	769.865

Model parameters:

Parameter	Value	Hessian standard error	Lower bound (95%)	Upper bound (95%)	Asympt. standard error	Lower bound (95%)	Upper bound (95%)
Constant	0.000	0.000	0.000	0.000	0.000	0.000	0.000

Parameter	Value	Hessian standard error	Lower bound (95%)	Upper bound (95%)	Asympt. standard error	Lower bound (95%)	Upper bound (95%)
AR(1)	0.063	0.057	-0.049	0.176	0.055	-0.045	0.171
SAR(1)	0.129	0.059	0.014	0.245	0.055	0.022	0.237
MA(1)	-1.037	0.018	-1.073	-1.001	0.057	-1.148	-0.925
SMA(1)	-0.942	0.064	-1.068	-0.816	0.053	-1.047	-0.838



APPENDIX G 4: Result of Nguru Station SPI_1 SARIMA Model $(011)x(011)_{12}$

XLSTAT 2013.1.01 - ARIMA - on 3/23/2013 at 5:15:52 PM
Time series: Workbook = ARIMA.xlsm / Sheet = Arima / Range = Arima!$G$1:$G$361 / 360 rows and 1 column
Confidence intervals (%): 95
Center: No
Model parameters: p = 0 / d = 1 / q = 1 / P = 0 / D = 1 / Q = 1 / s = 12
Optimize: Likelihood (Convergence = 0.00001 / Iterations = 500)
Validation: 12
Prediction: 3
Confidence intervals (%): 95
Seed (random numbers): 123456789



Summary statistics:

Variable	Observations	Obs. with missing data	Obs. without missing data	Minimum	Maximum	Mean	Std. deviation
Nguru Station SP1_1	360	0	360	-2.490	2.370	0.332	0.873

Results of ARIMA modeling of the Nguru Station SP1_1 series:
Results after optimization (Nguru Station SP1_1):

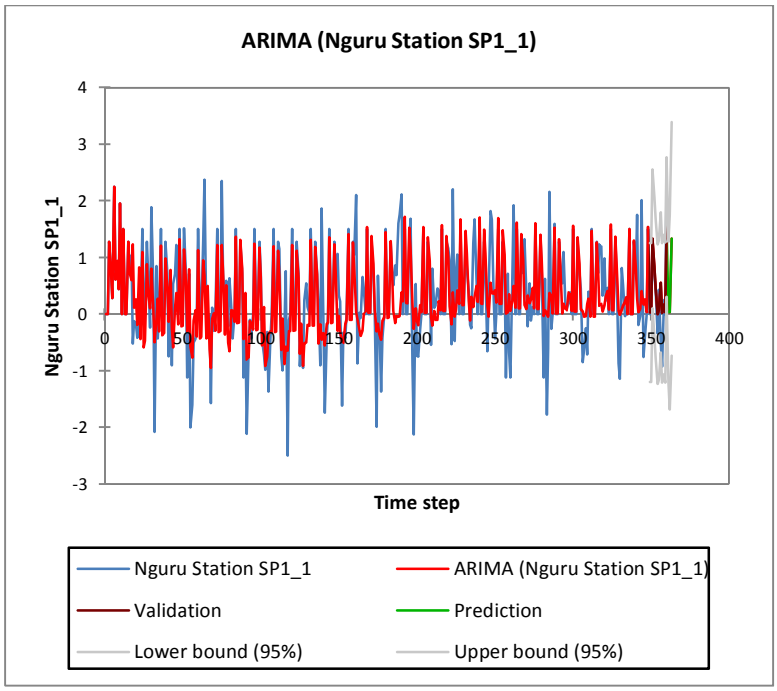
Goodness of fit statistics:

Observations	348.000
SSE	130.835
MAPE(Diff)	107.345
MAPE	109.642
WN Variance	0.391
WN Variance (estimate)	0.391
-2Log(Like.)	754.154
FPE	0.391
AIC	760.154
AICC	760.226
SBC	771.596

Model parameters:

Parameter	Value	Hessian standard error	Lower bound (95%)	Upper bound (95%)	Asympt. standard error	Lower bound (95%)	Upper bound (95%)
Constant	0.000	0.000	0.000	0.000	0.000	0.000	0.000

Parameter	Value	Hessian standard error	Lower bound (95%)	Upper bound (95%)	Asympt. standard error	Lower bound (95%)	Upper bound (95%)
MA(1)	-1.039	0.019	-1.077	-1.001	0.055	-1.146	-0.932
SMA(1)	-1.107	0.066	-1.237	-0.977	0.055	-1.214	-1.000



APPENDIX G 5: Result of Potiskum Station SPI_1 SARIMA Model $(011)x(011)_{12}$

XLSTAT 2013.1.01 - ARIMA - on 3/23/2013 at 5:32:50 PM
Time series: Workbook = ARIMA.xlsm / Sheet = Arima / Range = Arima!$H$1:$H$361 / 360 rows and 1 column
Confidence intervals (%): 95
Center: No
Model parameters: p = 0 / d = 1 / q = 1 / P = 0 / D = 1 / Q = 1 / s = 12
Optimize: Likelihood (Convergence = 0.00001 / Iterations = 500)
Validation: 12
Prediction: 3
Confidence intervals (%): 95
Seed (random numbers): 1326643119

Summary statistics

Summary statistics:

Variable	Observations	Obs. with missing data	Obs. without missing data	Minimum	Maximum	Mean	Std. deviation
Potiskum Station SP1_1	360	0	360	-2.210	2.990	0.276	0.885

Results of ARIMA modeling of the Potiskum Station SP1_1 series:

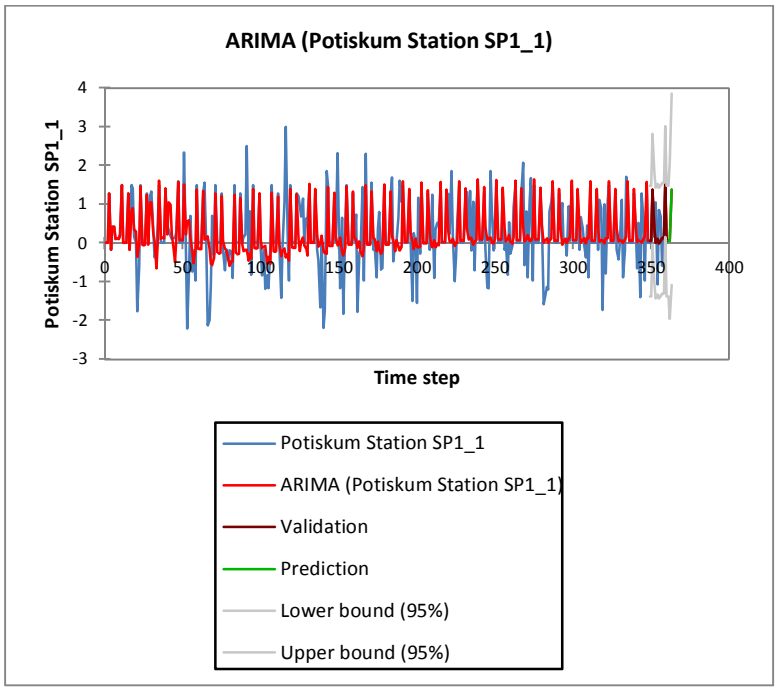
Results after optimization (Potiskum Station SP1_1):
Goodness of fit statistics:

Observations	348.000
SSE	177.945
MAPE(Diff)	122.867
MAPE	102.870
WN Variance	0.531
WN Variance (estimate)	0.531
-2Log(Like.)	789.257
FPE	0.531
AIC	795.257
AICC	795.329
SBC	806.699

Model parameters:

Parameter	Value	Hessian standard error	Lower bound (95%)	Upper bound (95%)	Asympt. standard error	Lower bound (95%)	Upper bound (95%)
Constant	0.000	0.000	0.000	0.000	0.000	0.000	0.000

Parameter	Value	Hessian standard error	Lower bound (95%)	Upper bound (95%)	Asympt. standard error	Lower bound (95%)	Upper bound (95%)
MA(1)	-1.000	0.026	-1.050	-0.950	0.055	-1.107	-0.893
SMA(1)	-1.000	0.055	-1.107	-0.893	0.055	-1.107	-0.893



APPENDIX G 6: Result of Maiduguri Station SPI_1 SARIMA Model $(111)x(111)_{12}$

XLSTAT 2013.1.01 - ARIMA - on 3/23/2013 at 5:11:31 PM
Time series: Workbook = ARIMA.xlsm / Sheet = Arima / Range = Arima!$F$1:$F$361 / 360 rows and 1 column
Confidence intervals (%): 95
Center: No
Model parameters: p = 1 / d = 1 / q = 1 / P = 1 / D = 1 / Q = 1 / s = 12
Optimize: Likelihood (Convergence = 0.00001 / Iterations = 500)
Validation: 12
Prediction: 3
Confidence intervals (%): 95
Seed (random numbers): 1236023973

Summary statistics

Summary statistics:

Variable	Observations	Obs. with missing data	Obs. without missing data	Minimum	Maximum	Mean	Std. deviation
Maiduguri Station SP1_1	360	0	360	-3.340	3.250	0.275	0.895

Results of ARIMA modeling of the Maiduguri Station SP1_1 series:

Results after optimization (Maiduguri Station SP1_1):

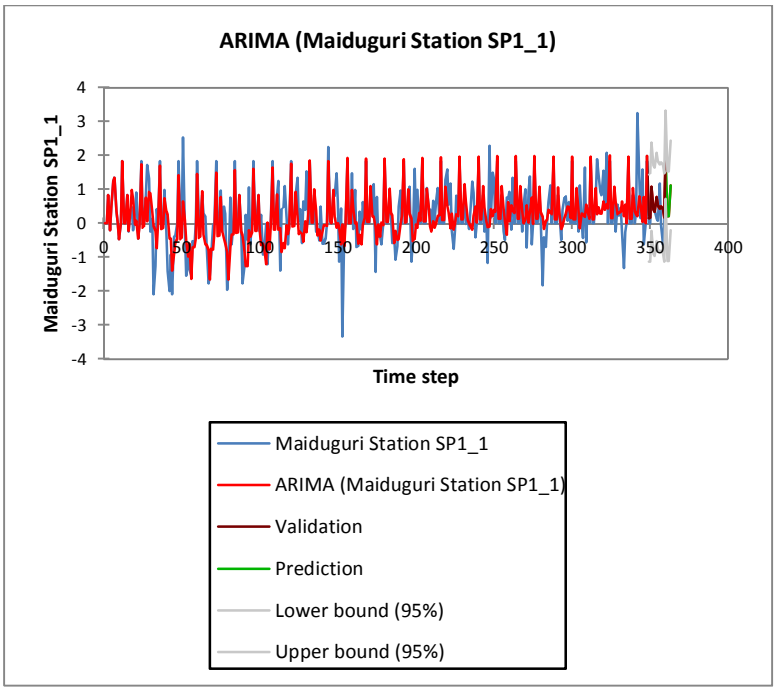
Goodness of fit statistics:

Observations	348.000
SSE	172.777
MAPE(Diff)	98.969
MAPE	167.825
WN Variance	0.516
WN Variance (estimate)	0.432
-2Log(Like.)	757.899
FPE	0.557
AIC	767.899
AICC	768.081
SBC	786.970

Model parameters:

Parameter	Value	Hessian standard error	Lower bound (95%)	Upper bound (95%)	Asympt. standard error	Lower bound (95%)	Upper bound (95%)
Constant	0.000	0.000	0.000	0.000	0.000	0.000	0.000

Parameter	Value	Hessian standard error	Lower bound (95%)	Upper bound (95%)	Asympt. standard error	Lower bound (95%)	Upper bound (95%)
AR(1)	0.154	0.055	0.046	0.261	0.046	0.063	0.244
SAR(1)	0.089	0.071	-0.049	0.228	0.055	-0.019	0.197
MA(1)	-1.000	0.051	-1.100	-0.900	0.053	-1.103	-0.897
SMA(1)	-0.915	0.045	-1.004	-0.827	0.052	-1.017	-0.814



APPENDIX G 7: Result of Kano Station SPI_1 SARIMA Model $(011)x(011)_{12}$

XLSTAT 2013.1.01 - ARIMA - on 3/23/2013 at 4:26:54 PM
Time series: Workbook = ARIMA.xlsm / Sheet = Arima / Range = Arima!$D$1:$D$361 / 360 rows and 1 column
Confidence intervals (%): 95
Center: No
Model parameters: p = 0 / d = 1 / q = 1 / P = 0 / D = 1 / Q = 1 / s = 12
Optimize: Likelihood (Convergence = 0.00001 / Iterations = 500)
Validation: 12
Prediction: 3
Confidence intervals (%): 95
Seed (random numbers): 123456789



Summary statistics:

Variable	Observations	Obs. with missing data	Obs. without missing data	Minimum	Maximum	Mean	Std. deviation
Kano Stationn SP1_1	360	0	360	-3.040	2.490	0.512	0.958

Results of ARIMA modeling of the Kano Stationn SP1_1 series:

Results after optimization (Kano Stationn SP1_1):

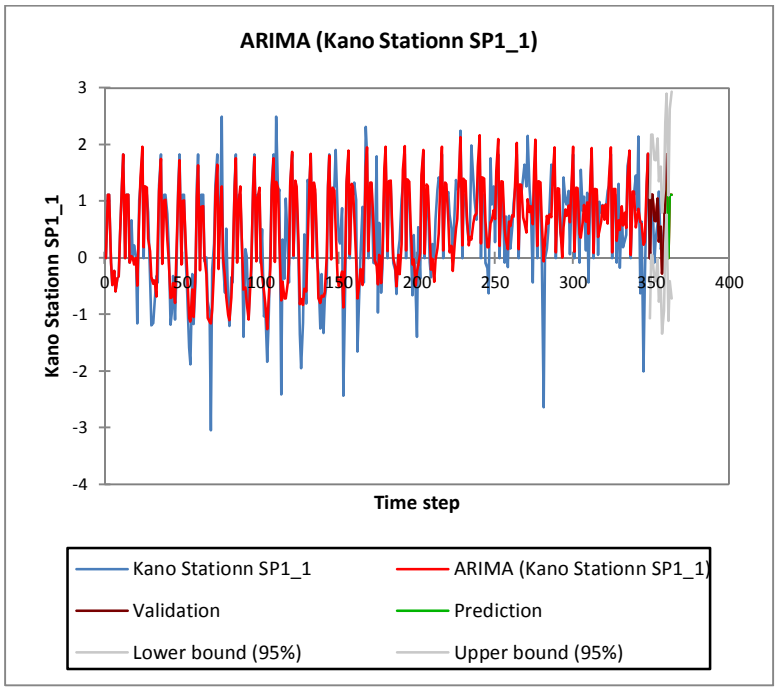
Goodness of fit statistics:

Observations	348.000
SSE	98.408
MAPE(Diff)	157.112
MAPE	118.826
WN Variance	0.294
WN Variance (estimate)	0.294
-2Log(Like.)	721.253
FPE	0.294
AIC	727.253
AICC	727.325
SBC	738.695

Model parameters:

Parameter	Value	Hessian standard error	Lower bound (95%)	Upper bound (95%)	Asympt. standard error	Lower bound (95%)	Upper bound (95%)
Constant	0.000	0.000	0.000	0.000	0.000	0.000	0.000

Parameter	Value	Hessian standard error	Lower bound (95%)	Upper bound (95%)	Asympt. standard error	Lower bound (95%)	Upper bound (95%)
MA(1)	-1.030	0.019	-1.067	-0.993	0.055	-1.137	-0.923
SMA(1)	-1.240	0.060	-1.357	-1.123	0.055	-1.347	-1.133



APPENDIX G 8: : Result of Gusau Station SPI_1 SARIMA Model $(011)x(011)_{12}$

XLSTAT 2013.1.01 - ARIMA - on 3/22/2013 at 9:14:29 PM
Time series: Workbook = ARIMA.xlsx / Sheet = Arima / Range = Arima!$C$1:$C$361 / 360 rows and 1 column
Confidence intervals (%): 95

Center: No
Model parameters: p = 0 / d = 1 / q = 1 / P = 0 / D = 1 / Q = 1 / s = 12
Optimize: Likelihood (Convergence = 0.00001 / Iterations = 500)
Validation: 12
Prediction: 3
Confidence intervals (%): 95
Seed (random numbers): 4346929

Summary statistics

Summary statistics:

Variable	Observations	Obs. with missing data	Obs. without missing data	Minimum	Maximum	Mean	Std. deviation
Gusau Station SP1_1	360	0	360	-3.080	2.560	0.516	1.024

Results of ARIMA modeling of the Gusau Station SP1_1 series:

Results after optimization (Gusau Station SP1_1):

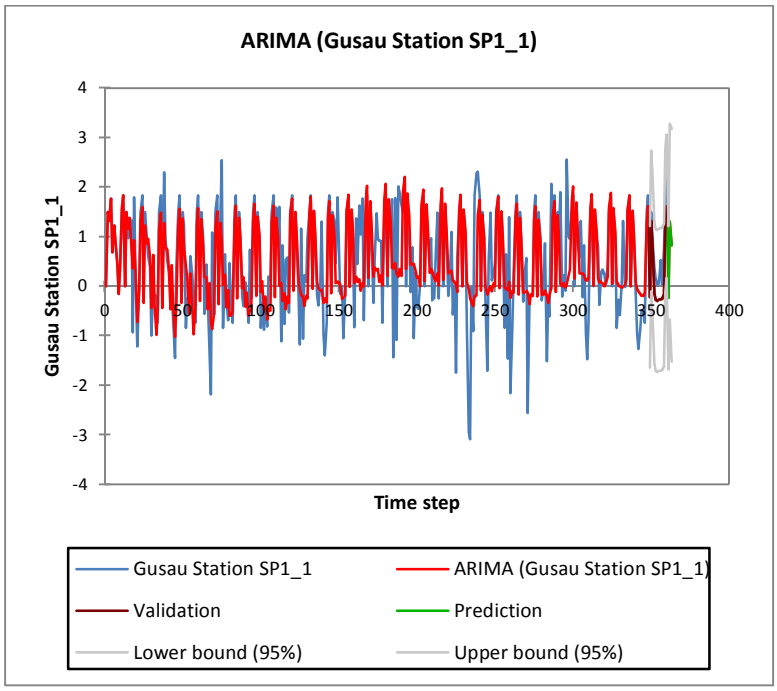
Goodness of fit statistics:

Observations	348.000
SSE	176.131
MAPE(Diff)	171.187
MAPE	87.232
WN Variance	0.526
WN Variance (estimate)	0.526
-2Log(Like.)	814.598
FPE	0.526
AIC	820.598
AICC	820.671
SBC	832.041

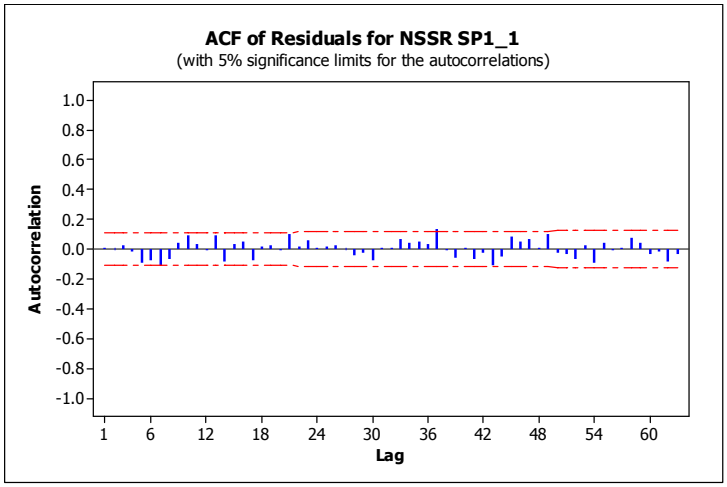
Model parameters:

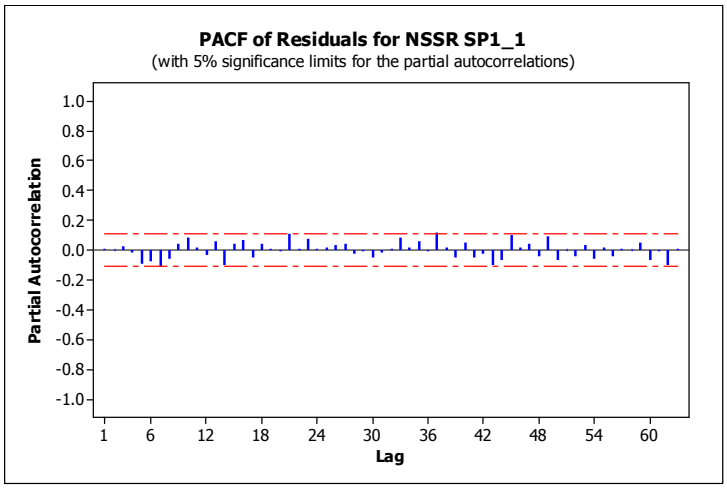
Parameter	Value	Hessian standard error	Lower bound (95%)	Upper bound (95%)	Asympt. standard error	Lower bound (95%)	Upper bound (95%)
Constant	0.000	0.000	0.000	0.000	0.000	0.000	0.000

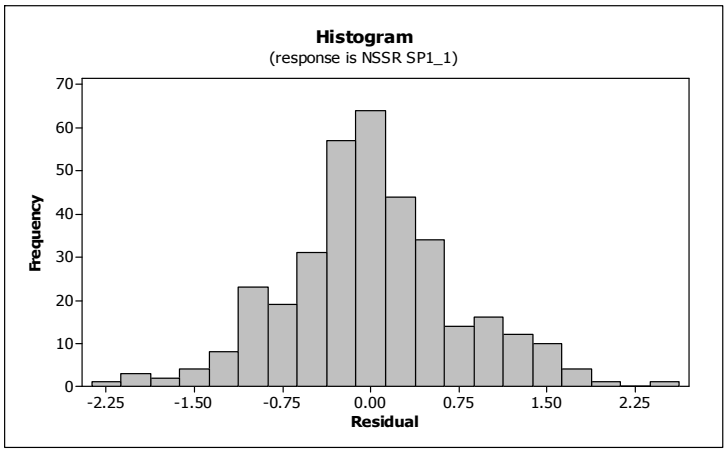
Parameter	Value	Hessian standard error	Lower bound (95%)	Upper bound (95%)	Asympt. standard error	Lower bound (95%)	Upper bound (95%)
MA(1)	-1.054	0.025	-1.102	-1.005	0.055	-1.161	-0.947
SMA(1)	-1.000	0.066	-1.129	-0.871	0.055	-1.107	-0.893

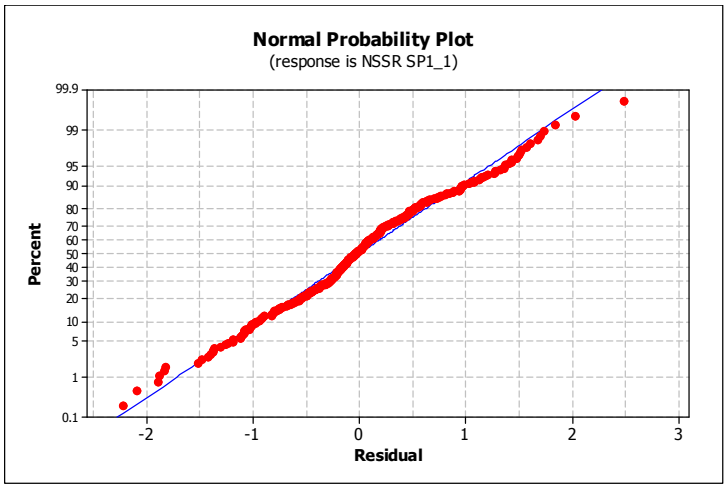


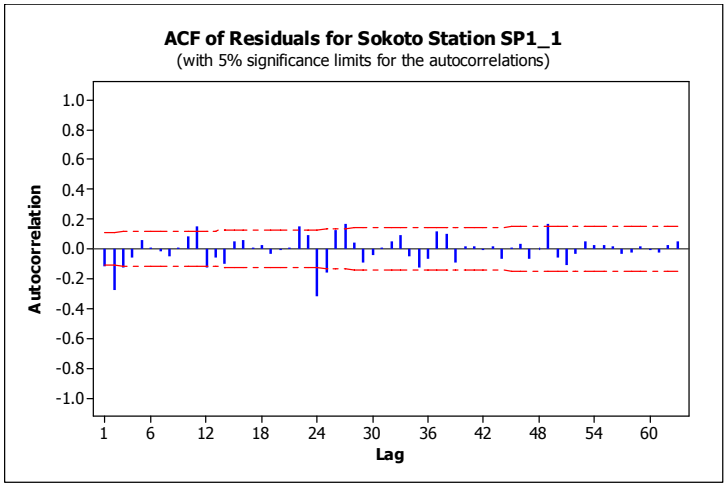
APPENDIX H: SPI_1 ACF & PACF OF RESIDUAL PLOTS, DISTRIBUTION HISTOGRAM AND NORMAL DISTRIBUTION PLOTS

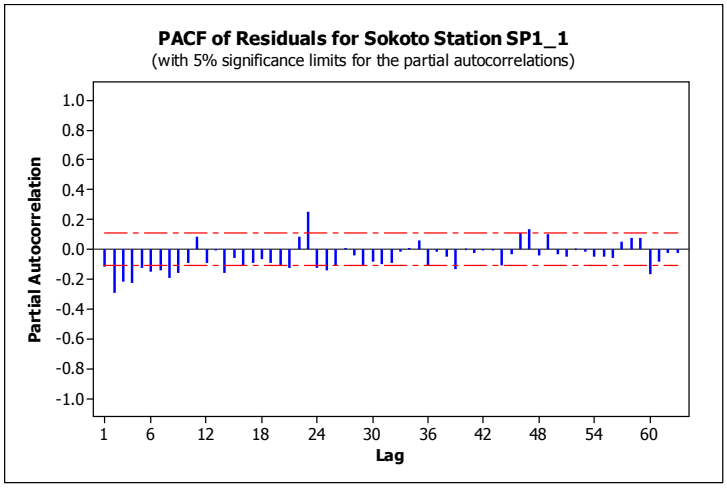


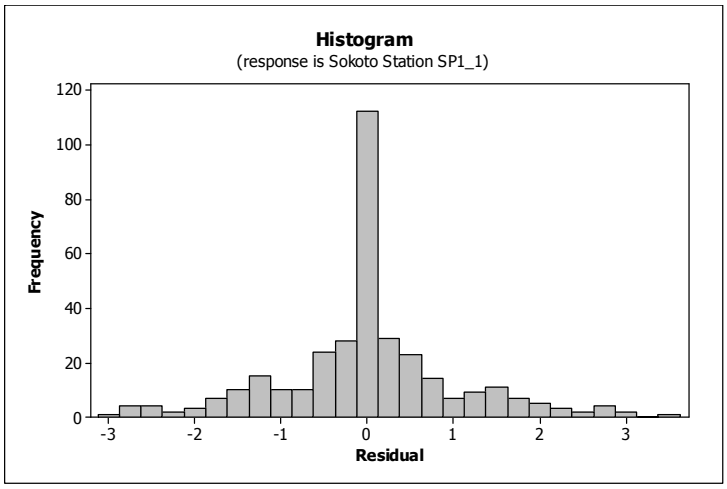


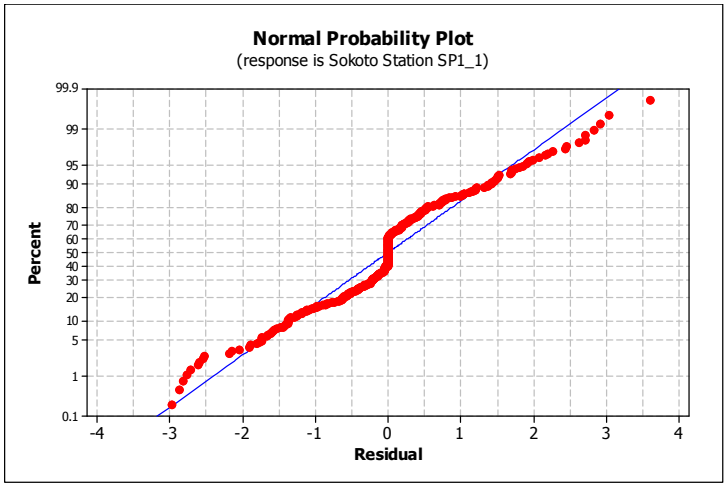


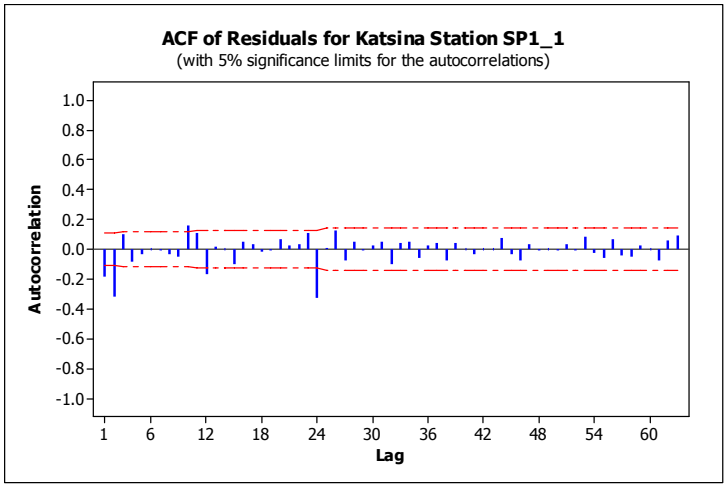

Normal Probability Plot
(response is NSSR SP1_1)
Percent
99.9
99
95
90
80
70
60
50
40
30
20
10
5
1
0.1
-2
-1
0
1
2
3
Residual

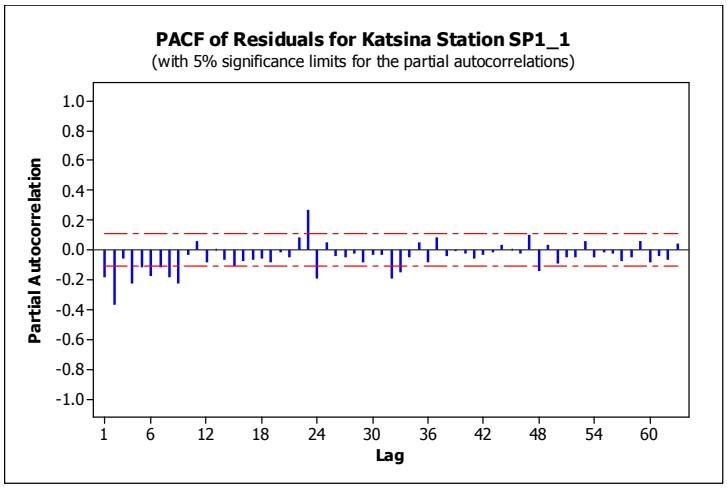

ACF of Residuals for Sokoto Station SP1_1
(with 5% significance limits for the autocorrelations)
Autocorrelation
1.0
0.8
0.6
0.4
0.2
0.0
-0.2
-0.4
-0.6
-0.8
-1.0
1
6
12
18
24
30
36
42
48
54
60
Lag

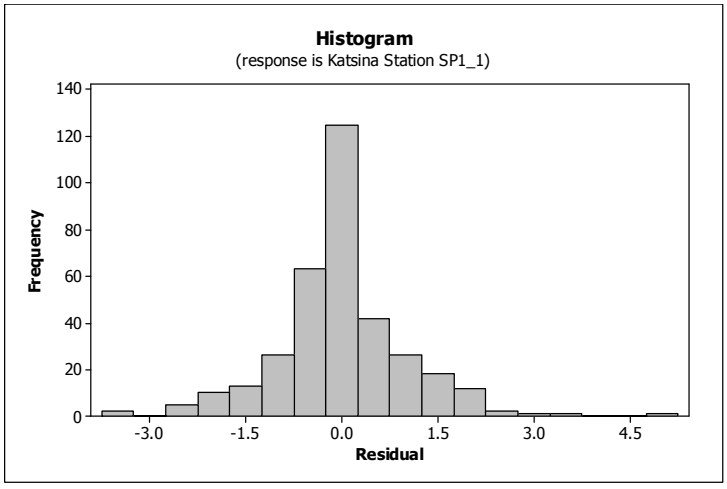

PACF of Residuals for Sokoto Station SP1_1
(with 5% significance limits for the partial autocorrelations)
Partial Autocorrelation
1.0
0.8
0.6
0.4
0.2
0.0
-0.2
-0.4
-0.6
-0.8
-1.0
1
6
12
18
24
30
36
42
48
54
60
Lag

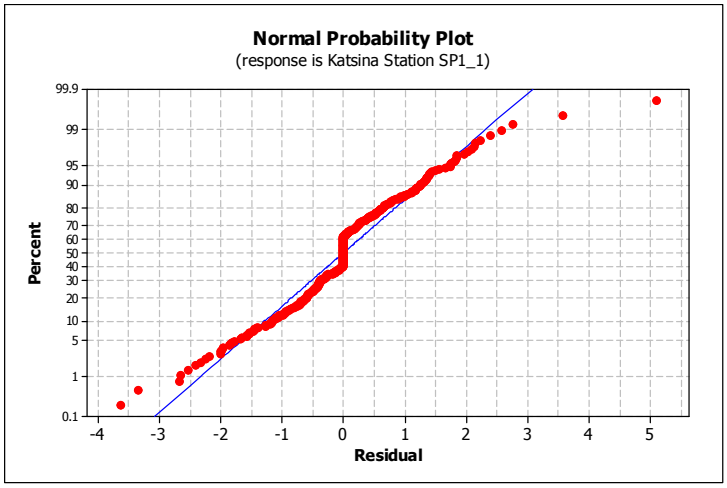

Histogram
(response is Sokoto Station SP1_1)
Frequency
Residual
120
100
80
60
40
20
0
-3
-2
-1
0
1
2
3

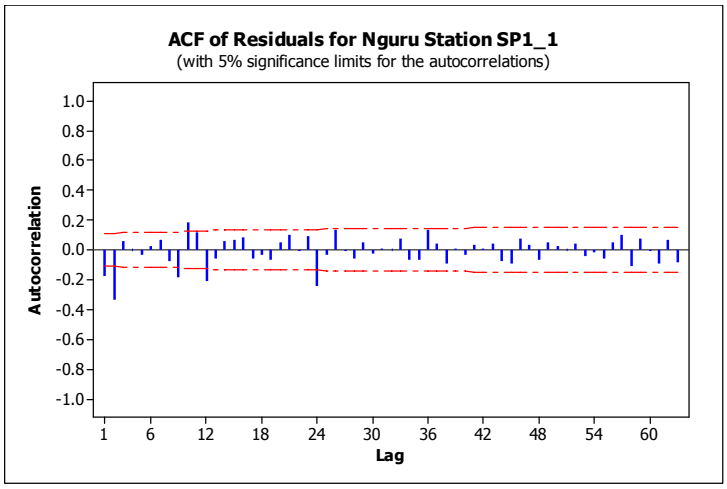

Normal Probability Plot
(response is Sokoto Station SP1_1)
Percent
Residual
99.9
99
95
90
80
70
60
50
40
30
20
10
5
1
0.1
-4
-3
-2
-1
0
1
2
3
4

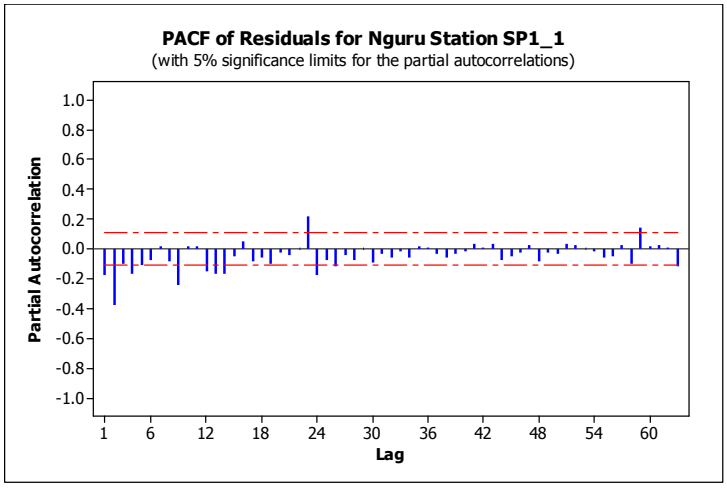

ACF of Residuals for Katsina Station SP1_1
(with 5% significance limits for the autocorrelations)
Autocorrelation
Lag
1.0
0.8
0.6
0.4
0.2
0.0
-0.2
-0.4
-0.6
-0.8
-1.0
1
6
12
18
24
30
36
42
48
54
60

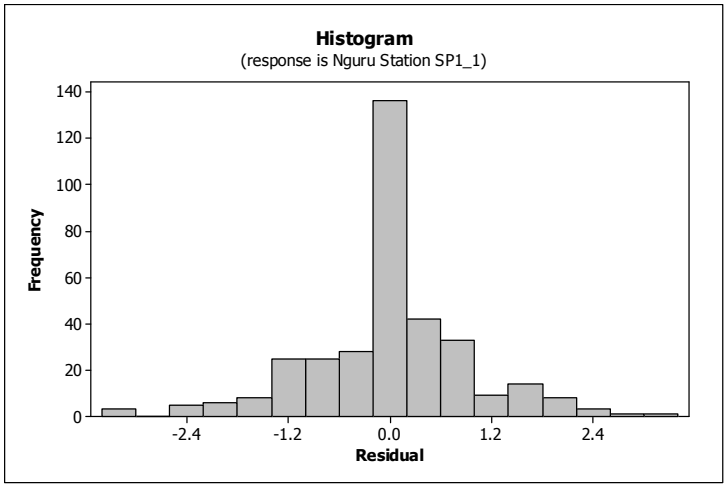

PACF of Residuals for Katsina Station SP1_1
(with 5% significance limits for the partial autocorrelations)
Partial Autocorrelation
1.0
0.8
0.6
0.4
0.2
0.0
-0.2
-0.4
-0.6
-0.8
-1.0
1
6
12
18
24
30
36
42
48
54
60
Lag

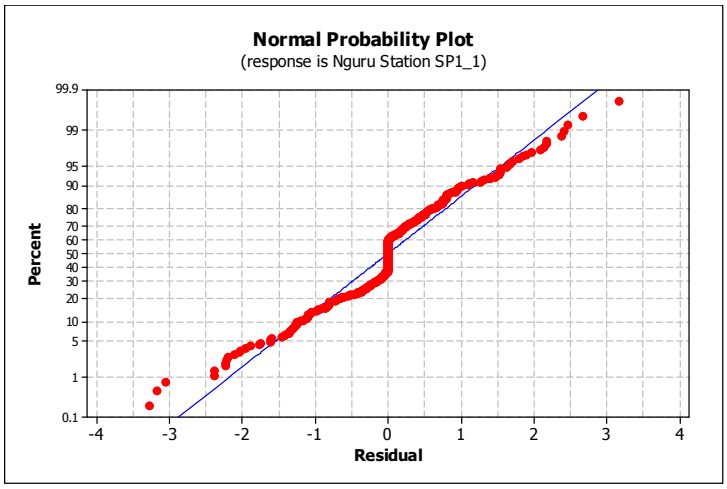

Histogram
(response is Katsina Station SP1_1)
Frequency
140
120
100
80
60
40
20
0
-3.0
-1.5
0.0
1.5
3.0
4.5
Residual

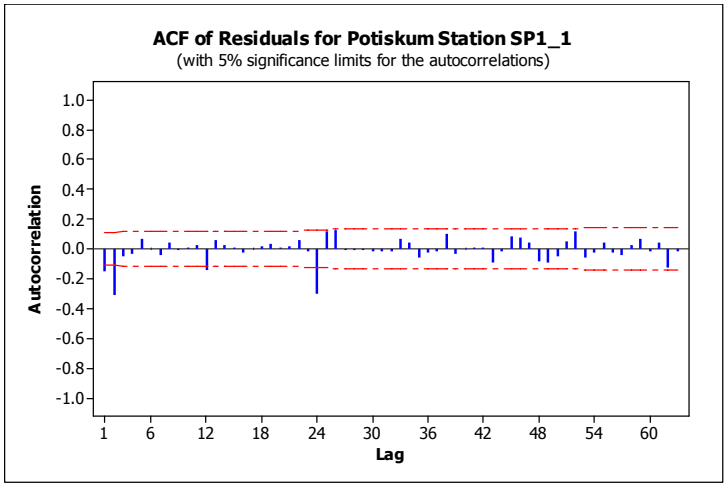

Normal Probability Plot
(response is Katsina Station SP1_1)
Percent
99.9
99
95
90
80
70
60
50
40
30
20
10
5
1
0.1
-4
-3
-2
-1
0
1
2
3
4
5
Residual

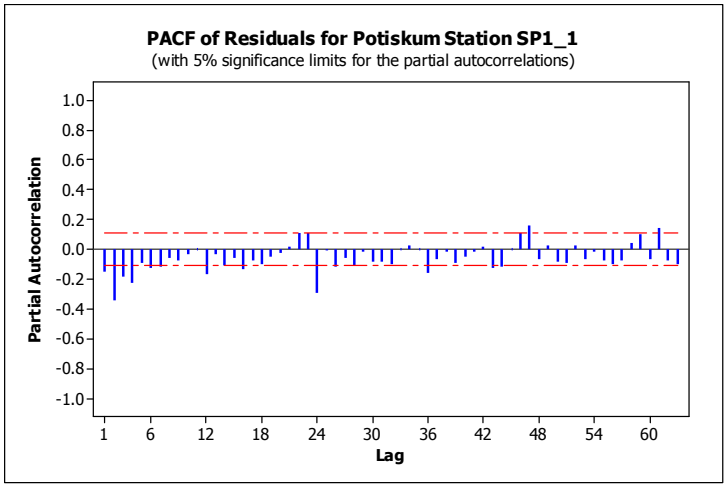

ACF of Residuals for Nguru Station SP1_1
(with 5% significance limits for the autocorrelations)
Autocorrelation
1.0
0.8
0.6
0.4
0.2
0.0
-0.2
-0.4
-0.6
-0.8
-1.0
1
6
12
18
24
30
36
42
48
54
60
Lag

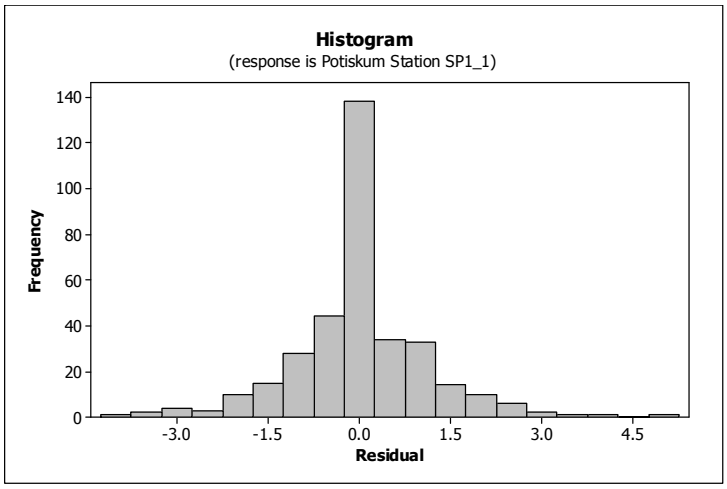

PACF of Residuals for Nguru Station SP1_1
(with 5% significance limits for the partial autocorrelations)
Partial Autocorrelation
1.0
0.8
0.6
0.4
0.2
0.0
-0.2
-0.4
-0.6
-0.8
-1.0
1
6
12
18
24
30
36
42
48
54
60
Lag

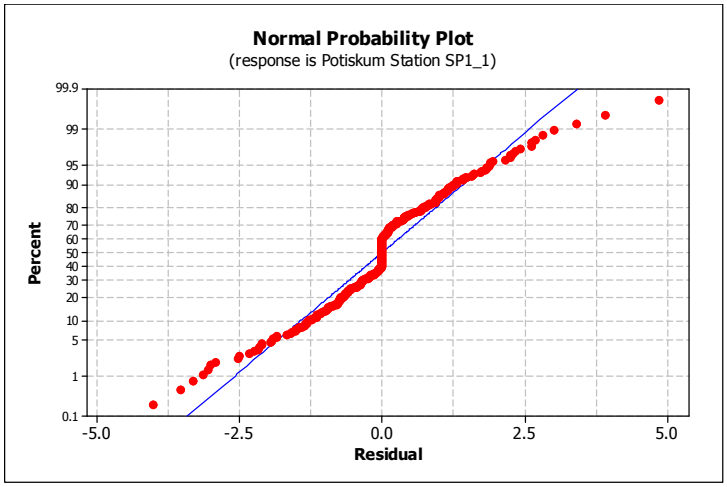

Histogram
(response is Nguru Station SP1_1)
Frequency
140
120
100
80
60
40
20
0
-2.4
-1.2
0.0
1.2
2.4
Residual

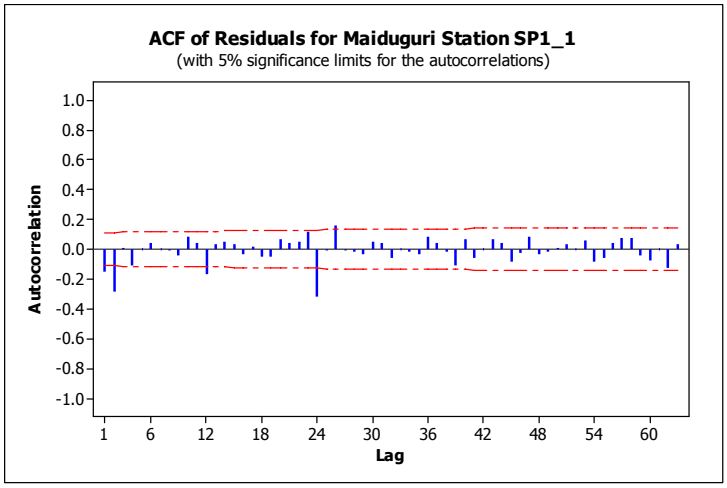

Normal Probability Plot
(response is Nguru Station SP1_1)
Percent
99.9
99
95
90
80
70
60
50
40
30
20
10
5
1
0.1
-4
-3
-2
-1
0
1
2
3
4
Residual

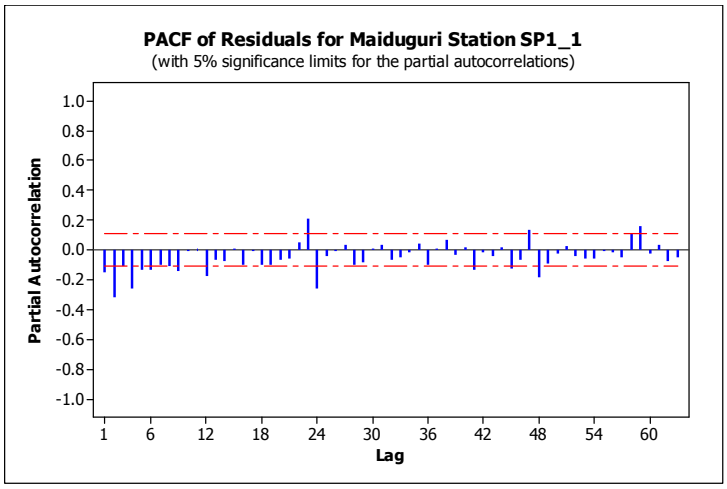

ACF of Residuals for Potiskum Station SP1_1
(with 5% significance limits for the autocorrelations)
Autocorrelation
1.0
0.8
0.6
0.4
0.2
0.0
-0.2
-0.4
-0.6
-0.8
-1.0
1
6
12
18
24
30
36
42
48
54
60
Lag

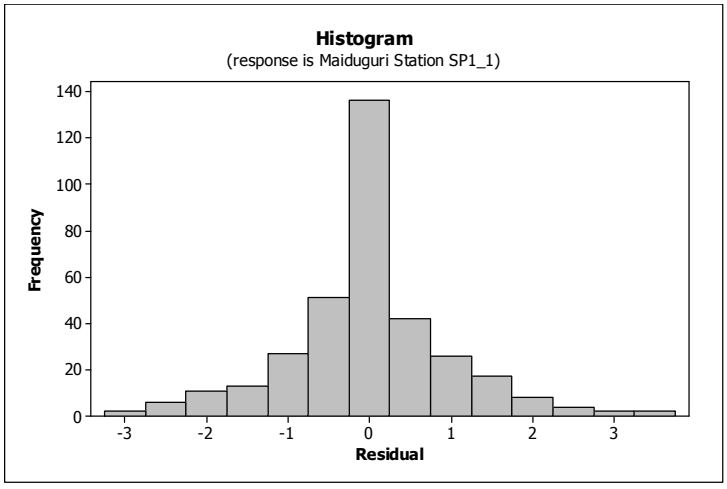

PACF of Residuals for Potiskum Station SP1_1
(with 5% significance limits for the partial autocorrelations)
Partial Autocorrelation
1.0
0.8
0.6
0.4
0.2
0.0
-0.2
-0.4
-0.6
-0.8
-1.0
1
6
12
18
24
30
36
42
48
54
60
Lag

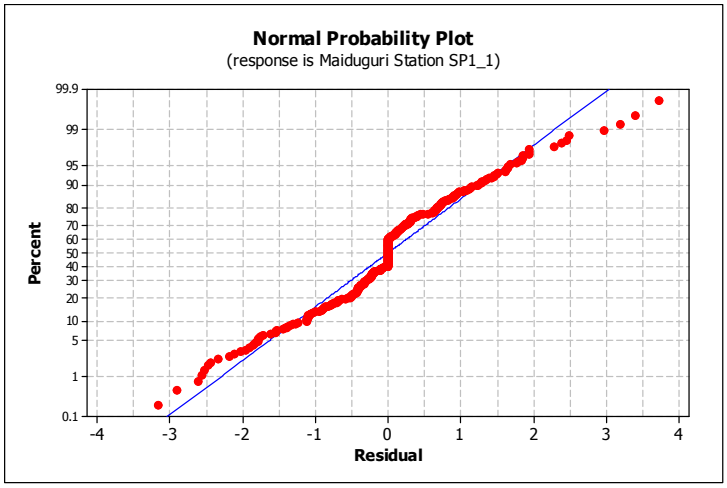

Histogram
(response is Potiskum Station SP1_1)
Frequency
Residual
140
120
100
80
60
40
20
0
-3.0
-1.5
0.0
1.5
3.0
4.5

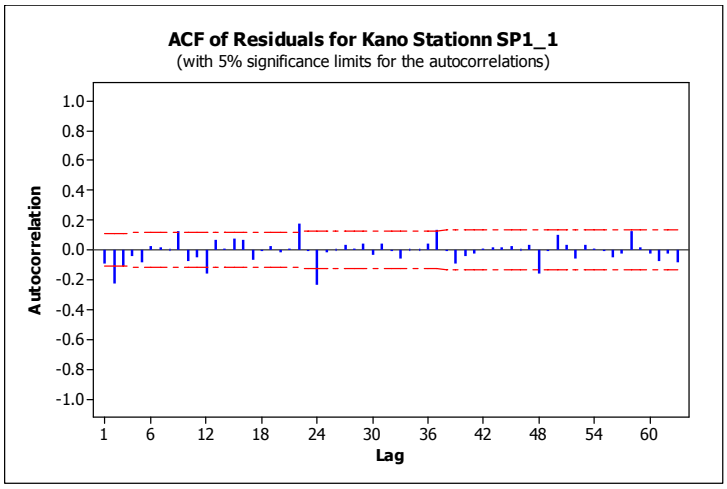

Normal Probability Plot
(response is Potiskum Station SP1_1)
Percent
Residual
99.9
99
95
90
80
70
60
50
40
30
20
10
5
1
0.1
-5.0
-2.5
0.0
2.5
5.0

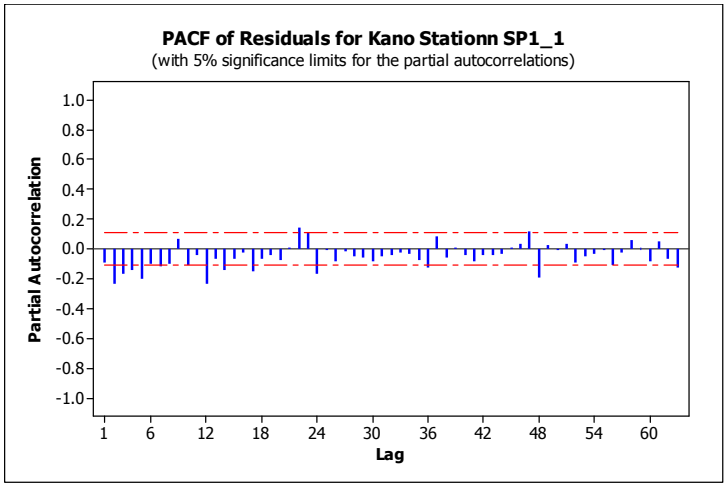

ACF of Residuals for Maiduguri Station SP1_1
(with 5% significance limits for the autocorrelations)
Autocorrelation
Lag
1.0
0.8
0.6
0.4
0.2
0.0
-0.2
-0.4
-0.6
-0.8
-1.0
1
6
12
18
24
30
36
42
48
54
60

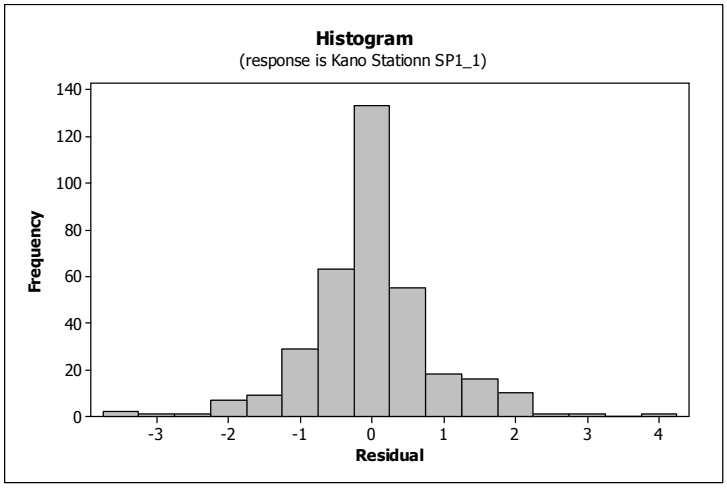

PACF of Residuals for Maiduguri Station SP1_1
(with 5% significance limits for the partial autocorrelations)
Partial Autocorrelation
1.0
0.8
0.6
0.4
0.2
0.0
-0.2
-0.4
-0.6
-0.8
-1.0
1
6
12
18
24
30
36
42
48
54
60
Lag

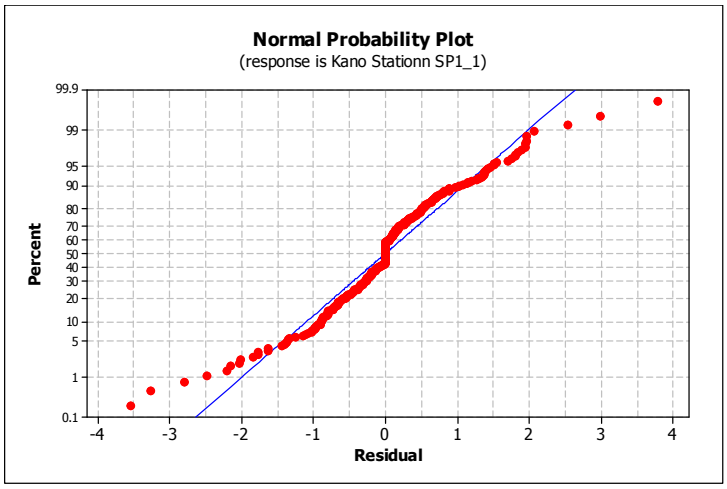

Histogram
(response is Maiduguri Station SP1_1)
Frequency
140
120
100
80
60
40
20
0
-3
-2
-1
0
1
2
3
Residual

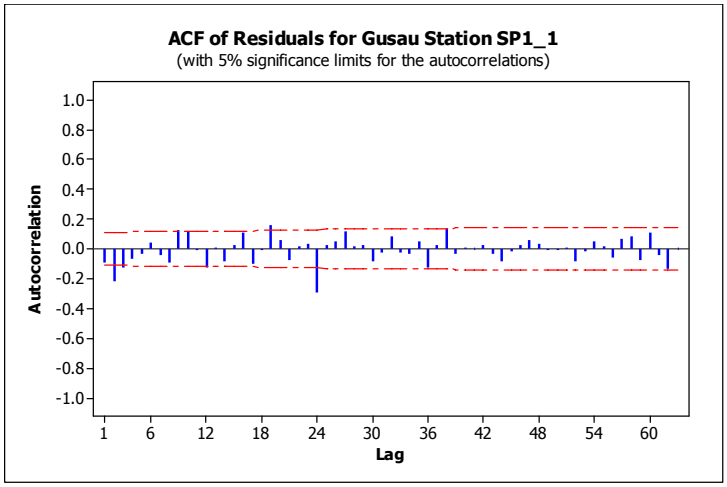

Normal Probability Plot
(response is Maiduguri Station SP1_1)
Percent
99.9
99
95
90
80
70
60
50
40
30
20
10
5
1
0.1
-4
-3
-2
-1
0
1
2
3
4
Residual

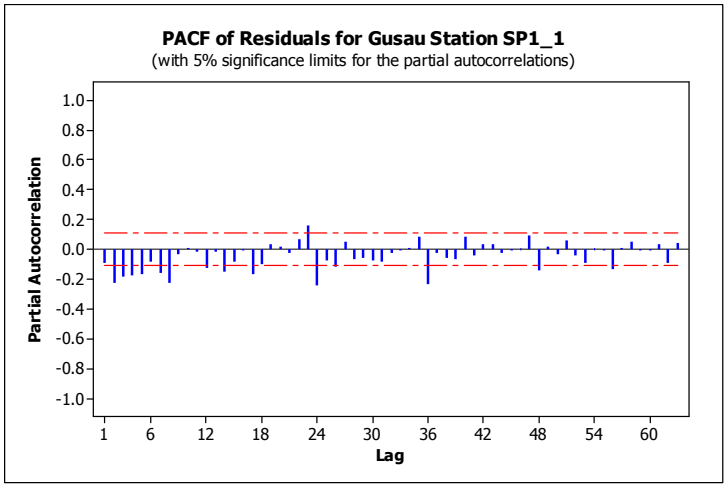

ACF of Residuals for Kano Stationn SP1_1
(with 5% significance limits for the autocorrelations)
Autocorrelation
1.0
0.8
0.6
0.4
0.2
0.0
-0.2
-0.4
-0.6
-0.8
-1.0
1
6
12
18
24
30
36
42
48
54
60
Lag

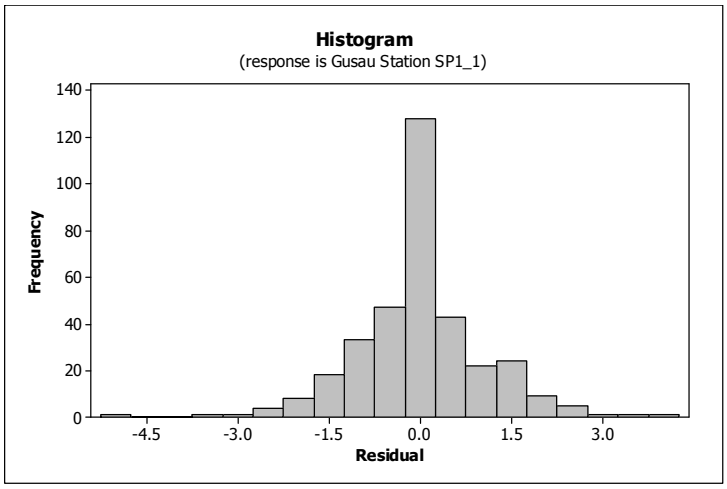

PACF of Residuals for Kano Stationn SP1_1
(with 5% significance limits for the partial autocorrelations)
Partial Autocorrelation
1.0
0.8
0.6
0.4
0.2
0.0
-0.2
-0.4
-0.6
-0.8
-1.0
1
6
12
18
24
30
36
42
48
54
60
Lag

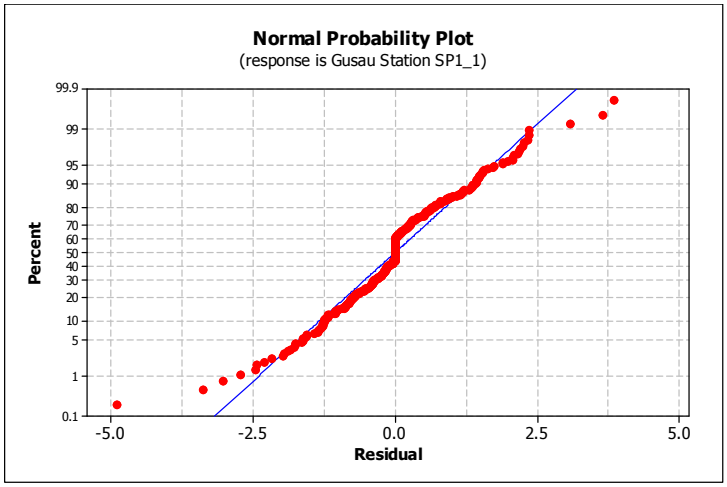

Histogram
(response is Kano Stationn SP1_1)
Frequency
140
120
100
80
60
40
20
0
-3
-2
-1
0
1
2
3
4
Residual


Normal Probability Plot
(response is Kano Stationn SP1_1)
Percent
99.9
99
95
90
80
70
60
50
40
30
20
10
5
1
0.1
-4
-3
-2
-1
0
1
2
3
4
Residual

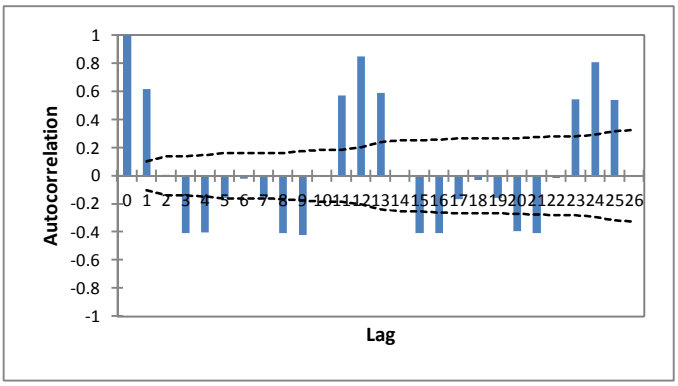

ACF of Residuals for Gusau Station SP1_1
(with 5% significance limits for the autocorrelations)
Autocorrelation
1.0
0.8
0.6
0.4
0.2
0.0
-0.2
-0.4
-0.6
-0.8
-1.0
1
6
12
18
24
30
36
42
48
54
60
Lag


PACF of Residuals for Gusau Station SP1_1
(with 5% significance limits for the partial autocorrelations)
Partial Autocorrelation
1.0
0.8
0.6
0.4
0.2
0.0
-0.2
-0.4
-0.6
-0.8
-1.0
1
6
12
18
24
30
36
42
48
54
60
Lag

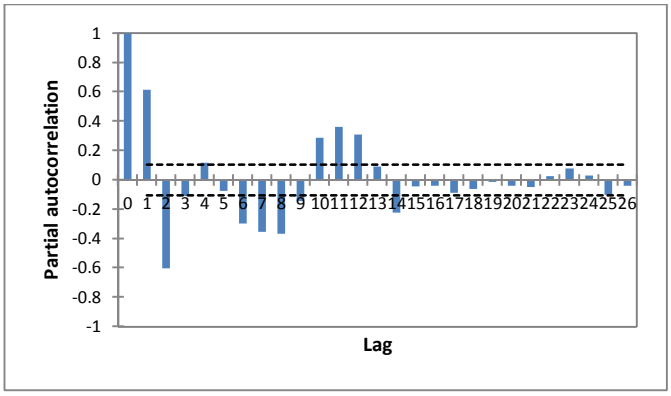

Histogram
(response is Gusau Station SP1_1)
Frequency
Residual
140
120
100
80
60
40
20
0
-4.5
-3.0
-1.5
0.0
1.5
3.0


Normal Probability Plot
(response is Gusau Station SP1_1)
Percent
Residual
99.9
99
95
90
80
70
60
50
40
30
20
10
5
1
0.1
-5.0
-2.5
0.0
2.5
5.0

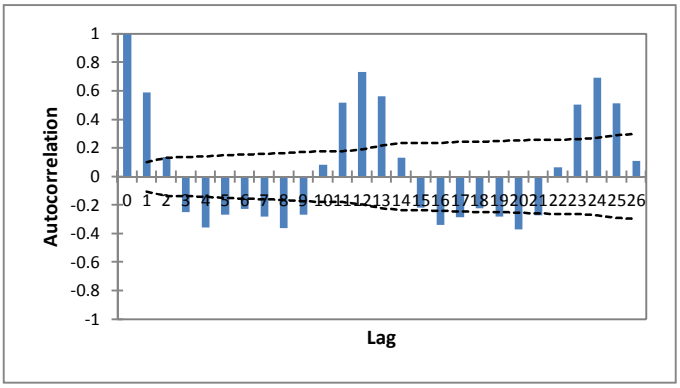
APPENDIX I: ACF and PACF plots for transformed temperature data



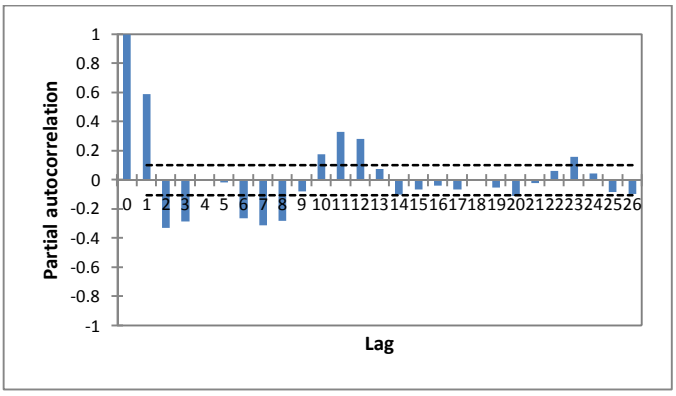
a. ACF plot for selecting relevant models for transformed Sokoto Station temperature series



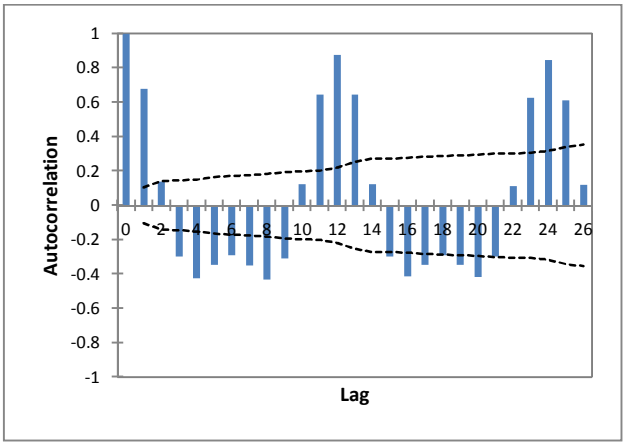
b. PACF plot for selecting relevant models for transformed Sokoto Station temperature series



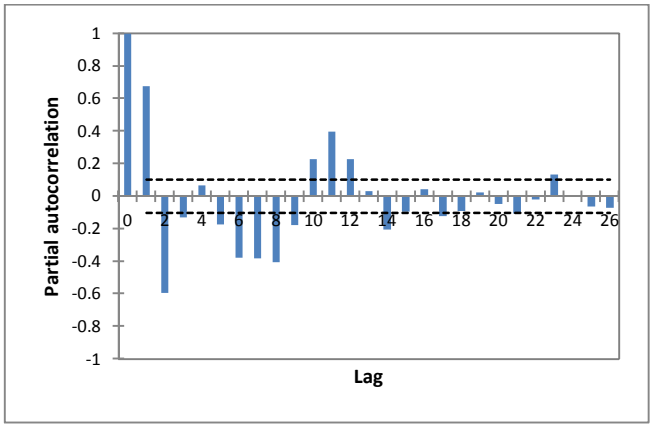
c. ACF plot for selecting relevant models for transformed Katsina Station temperature series



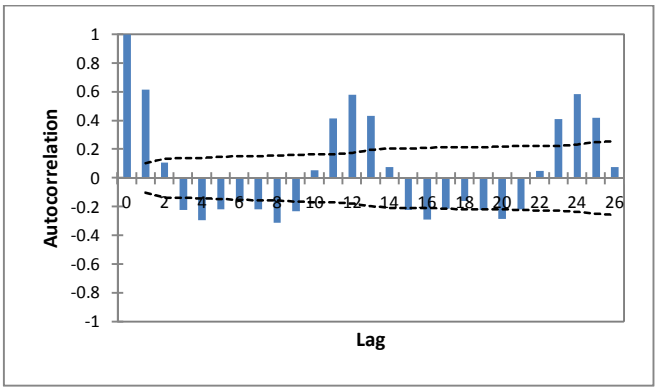
d. PACF plot for selecting relevant models for transformed Katsina Station temperature series



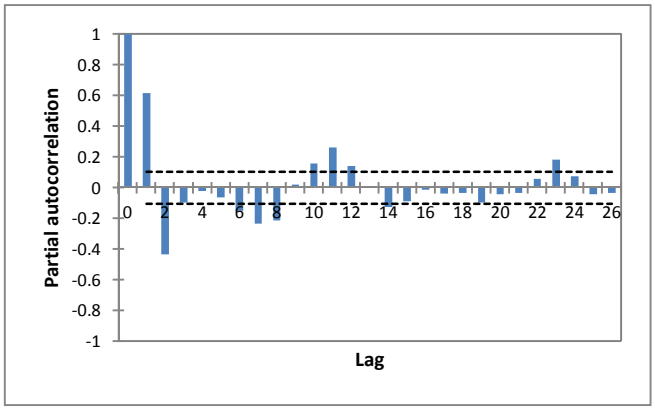
e. ACF plot for selecting relevant models for transformed Nguru Station temperature series



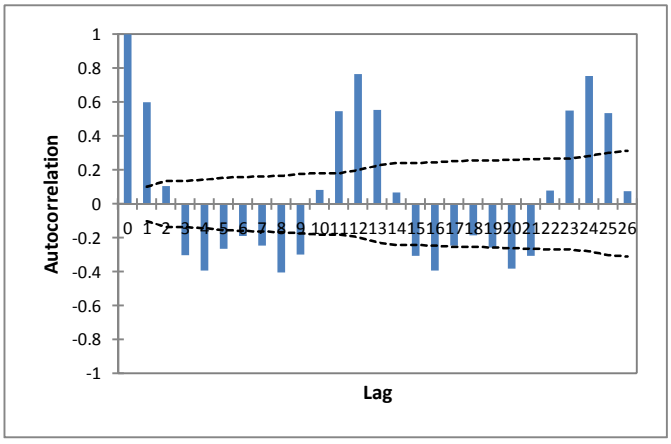
f. PACF plot for selecting relevant models for transformed Nguru Station temperature series



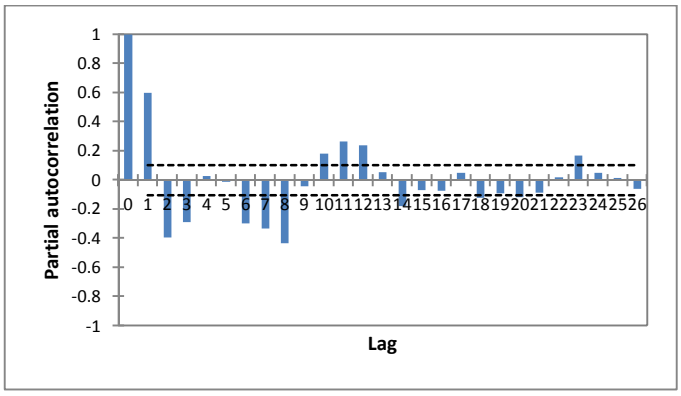
g. ACF plot for selecting relevant models for transformed Potiskum Station temperature series



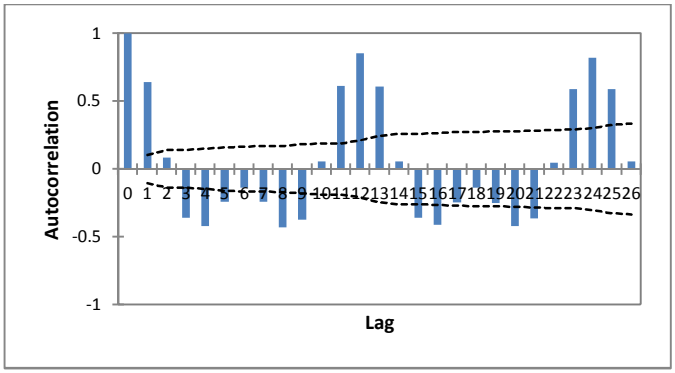
h. PACF plot for selecting relevant models for transformed Potiskum Station temperature series



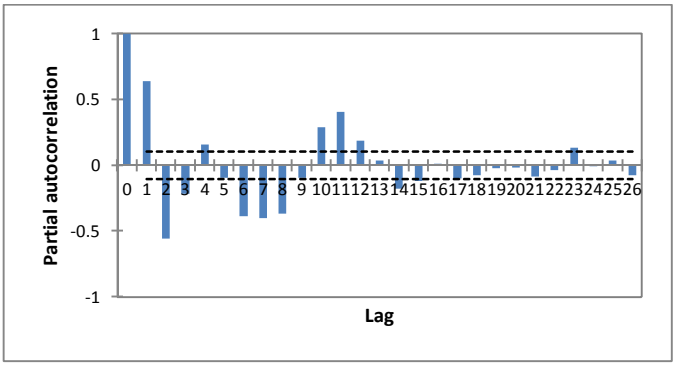
i. ACF plot for selecting relevant models for transformed Maiduguri Station temperature series



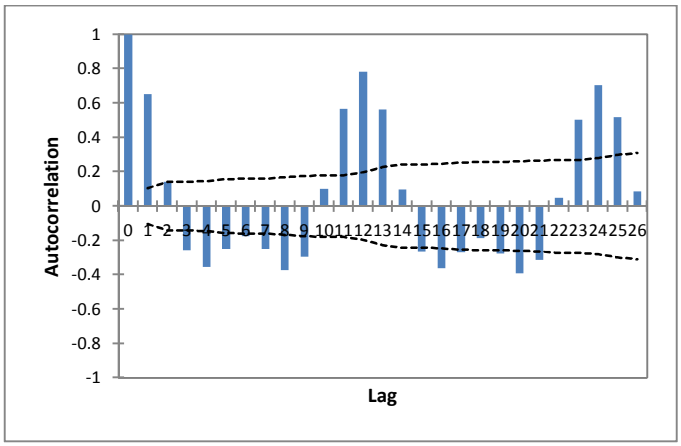
j. PACF plot for selecting relevant models for transformed Maiduguri Station temperature series



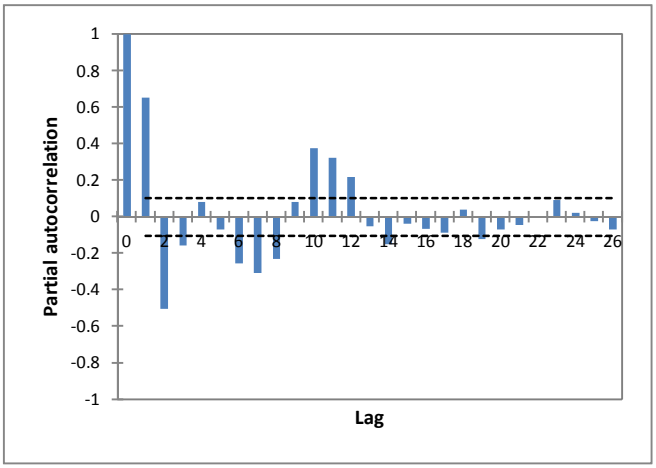
k. ACF plot for selecting relevant models for transformed Kano Station temperature series



l. PACF plot for selecting relevant models for transformed Kano Station temperature series



m. ACF plot for selecting relevant models for transformed Gusau Station temperature series



n. PACF plot for selecting relevant models for transformed Gusau Station temperature series

APPENDIX J:TEMPERATURE SERIES SARIMA MODELS AND PARAMETERS

APPENDIX J 1: Result of NSSR Temperature SARIMA Model $(211)x(211)_{12}$

XLSTAT 2013.1.01 - ARIMA - on 3/29/2013 at 3:36:36 PM
Time series: Workbook = ARIMA 4.xlsm / Sheet = Temp / Range = Temp!$L$1:$L$361 /
360 rows and 1 column
Confidence intervals (%): 95
Center: No
Model parameters: p = 2 / d = 1 / q = 1 / P = 2 / D = 1 / Q = 1 / s = 12
Optimize: Likelihood (Convergence = 0.00001 / Iterations = 500)
Validation: 12
Prediction: 3
Confidence intervals (%): 95
Seed (random numbers): 4289839



Summary statistics:

Variable	Observations	Obs. with missing data	Obs. without missing data	Minimum	Maximum	Mean	Std. deviation
Box-Cox(SSZ Region)	360	0	360	2.943	3.517	3.305	0.121

Results of ARIMA modeling of the Box-Cox(NSSR) series:
Results after optimization (Box-Cox(NSSR)):

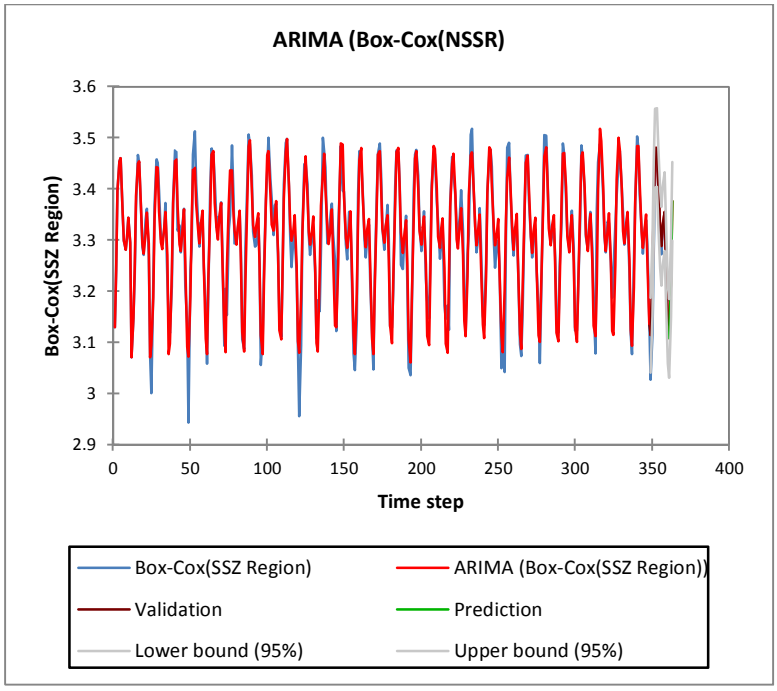
Goodness of fit statistics:

Observations	348.000
SSE	0.465
MAPE(Diff)	188.233
MAPE	0.786
WN Variance	0.001
WN Variance (estimate)	0.001
-2Log(Like.)	-1202.334
FPE	0.002
AIC	-1188.334
AICC	-1187.991
SBC	-1161.635

Model parameters:

Parameter	Value	Hessian standard error	Lower bound (95%)	Upper bound (95%)	Asympt. standard error	Lower bound (95%)	Upper bound (95%)
Constant	0.000	0.000	0.000	0.000	0.000	0.000	0.000

Parameter	Value	Hessian standard error	Lower bound (95%)	Upper bound (95%)	Asympt. standard error	Lower bound (95%)	Upper bound (95%)
AR(1)	0.212	0.048	0.117	0.306			
AR(2)	0.178	0.050	0.081	0.276			
SAR(1)	-0.038	0.046	-0.129	0.052			
SAR(2)	-0.012	0.048	-0.107	0.083			
MA(1)	-1.000	0.022	-1.043	-0.957			
SMA(1)	-1.000	0.066	-1.130	-0.870			



APPENDIX J 2: Result of Sokoto Temperature SARIMA Model $(211)x(211)_{12}$

XLSTAT 2013.1.01 - ARIMA - on 3/29/2013 at 4:48:40 PM
Time series: Workbook = ARIMA 4.xlsm / Sheet = Temp / Range = Temp!$N$1:$N$361 / 360 rows and 1 column
Confidence intervals (%): 95
Center: No
Model parameters: p = 2 / d = 1 / q = 1 / P = 2 / D = 1 / Q = 1 / s = 12
Optimize: Likelihood (Convergence = 0.00001 / Iterations = 500)
Validation: 12
Prediction: 3
Confidence intervals (%): 95
Seed (random numbers): 1218872228
Summary statistics:

Variable	Observations	Obs. with missing data	Obs. without missing data	Minimum	Maximum	Mean	Std. deviation
Log (Sokoto)	360	0	360	3.072	3.560	3.359	0.105

Results of ARIMA modeling of the Log (Sokoto) series:

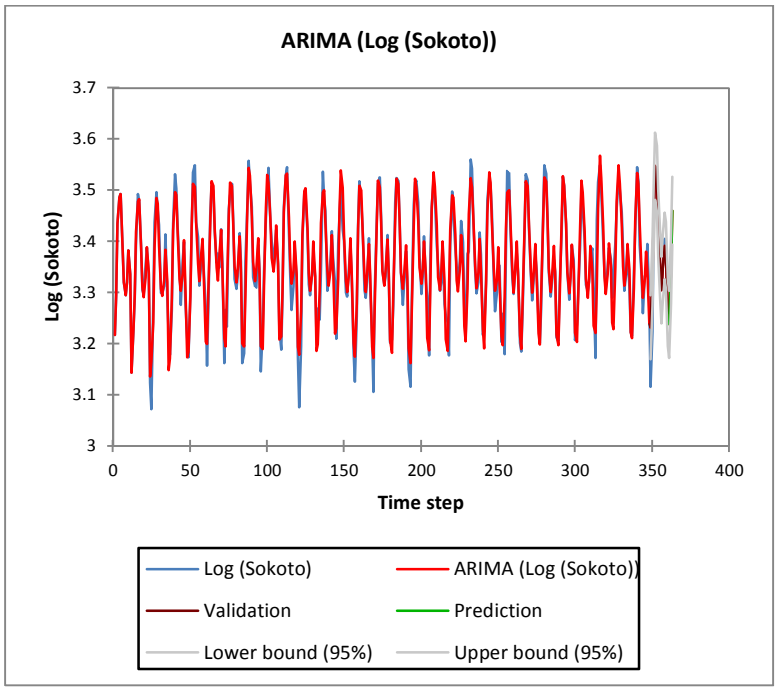
Results after optimization (Log (Sokoto)):
Goodness of fit statistics:

Observations	348.000
SSE	0.343
MAPE(Diff)	150.344
MAPE	0.681
WN Variance	0.001
WN Variance (estimate)	0.001
-2Log(Like.)	-1243.247
FPE	0.001
AIC	-1229.247
AICC	-1228.905
SBC	-1202.548

Model parameters:

Parameter	Value	Hessian standard error	Lower bound (95%)	Upper bound (95%)	Asympt. standard error	Lower bound (95%)	Upper bound (95%)
Constant	0.000	0.000	0.000	0.000	0.000	0.000	0.000

Parameter	Value	Hessian standard error	Lower bound (95%)	Upper bound (95%)	Asympt. standard error	Lower bound (95%)	Upper bound (95%)
AR(1)	0.207	0.062	0.085	0.329			
AR(2)	0.154	0.053	0.051	0.258			
SAR(1)	-0.015	0.075	-0.161	0.131			
SAR(2)	-0.076	0.070	-0.213	0.061			
MA(1)	-1.000	0.024	-1.046	-0.954			
SMA(1)	-1.133	0.058	-1.247	-1.019			



APPENDIX J 3: Result of Katsina Temperature SARIMA Model $(311)x(311)_{12}$

XLSTAT 2013.1.01 - ARIMA - on 3/29/2013 at 5:10:11 PM
Time series: Workbook = ARIMA 4.xlsm / Sheet = Temp / Range = Temp!$O$1:$O$361 / 360 rows and 1 column
Confidence intervals (%): 95
Center: No
Model parameters: p = 3 / d = 1 / q = 1 / P = 3 / D = 1 / Q = 1 / s = 12
Optimize: Likelihood (Convergence = 0.00001 / Iterations = 500)
Validation: 12
Prediction: 3
Confidence intervals (%): 95
Seed (random numbers): 123456789



Summary statistics:

Variable	Observations	Obs. with missing data	Obs. without missing data	Minimum	Maximum	Mean	Std. deviation
Log (Katsina Station Monthly Mean Temp.)	360	0	360	2.313	3.512	3.276	0.144

Results of ARIMA modeling of the Log (Katsina Station Monthly Mean Temp.) series:

Results after optimization (Log (Katsina Station Monthly Mean Temp.)):

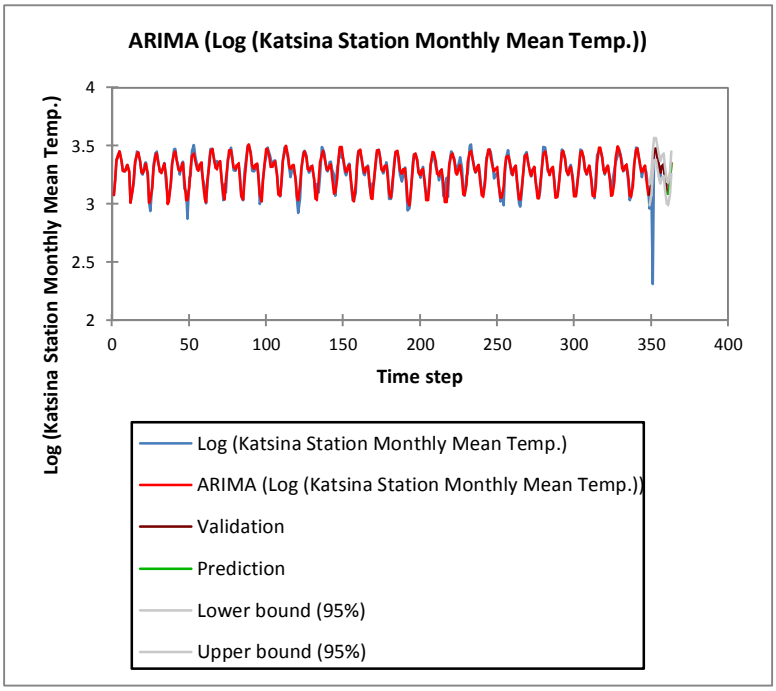
Goodness of fit statistics:

Observations	348.000
SSE	0.703
MAPE(Diff)	213.822
MAPE	0.977
WN Variance	0.002
WN Variance (estimate)	0.002
-2Log(Like.)	-1083.411
FPE	0.003
AIC	-1065.411
AICC	-1064.857
SBC	-1031.084

Model parameters:

Parameter	Value	Hessian standard error	Lower bound (95%)	Upper bound (95%)	Asympt. standard error	Lower bound (95%)	Upper bound (95%)
Constant	0.000	0.000	0.000	0.000	0.000	0.000	0.000

Parameter	Value	Hessian standard error	Lower bound (95%)	Upper bound (95%)	Asympt. standard error	Lower bound (95%)	Upper bound (95%)
AR(1)	0.159	0.058	0.046	0.273	0.059	0.044	0.275
AR(2)	0.151	0.059	0.035	0.266	0.055	0.042	0.259
AR(3)	0.055	0.059	-0.061	0.171	0.056	-0.055	0.165
SAR(1)	-0.016	0.064	-0.141	0.110	0.056	-0.126	0.095
SAR(2)	-0.076	0.059	-0.192	0.040	0.059	-0.192	0.039
SAR(3)	0.041	0.061	-0.078	0.160	0.059	-0.075	0.156
MA(1)	-0.961	0.033	-1.025	-0.897	0.027	-1.014	-0.908
SMA(1)	-0.947	0.060	-1.065	-0.829	0.027	-1.001	-0.894



APPENDIX J 4: Result of Nguru Temperature SARIMA Model $(211)x(211)_{12}$

XLSTAT 2013.1.01 - ARIMA - on 3/29/2013 at 5:30:13 PM
Time series: Workbook = ARIMA 4.xlsm / Sheet = Temp / Range = Temp!$P$1:$P$361 / 360 rows and 1 column
Confidence intervals (%): 95
Center: No
Model parameters: p = 2 / d = 1 / q = 1 / P = 2 / D = 1 / Q = 1 / s = 12
Optimize: Likelihood (Convergence = 0.00001 / Iterations = 500)
Validation: 1
Prediction: 3
Confidence intervals (%): 95
Seed (random numbers): 301629493

Summary statistics

Summary statistics:

Variable	Observations	Obs. with missing data	Obs. without missing data	Minimum	Maximum	Mean	Std. deviation
Log (Nguru Station Monthly Mean Temp.)	360	0	360	2.901	3.538	3.330	0.132

Results of ARIMA modeling of the Log (Nguru Station Monthly Mean Temp.) series:

Results after optimization (Log (Nguru Station Monthly Mean Temp.)):

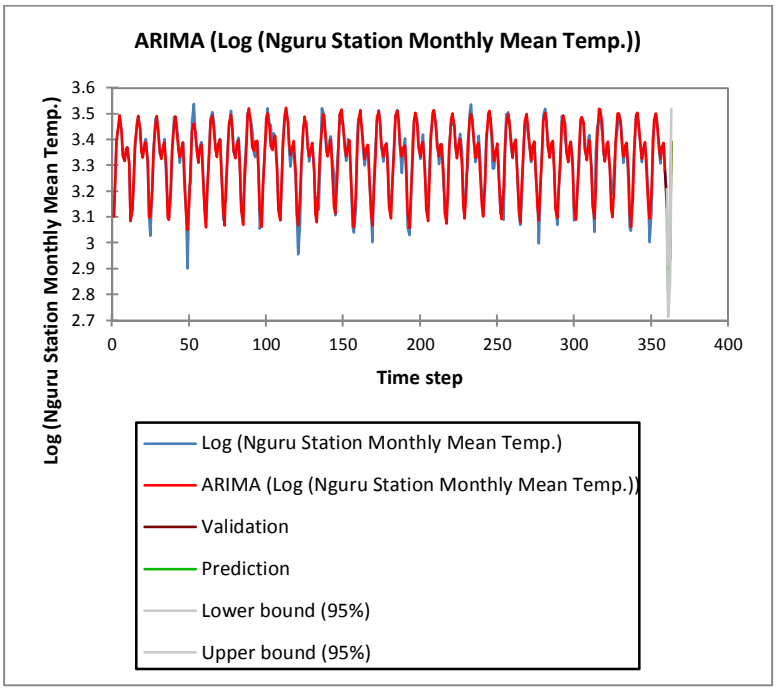
Goodness of fit statistics:

Observations	359.000
SSE	0.000
MAPE(Diff)	172.936
MAPE	0.783
WN Variance	0.000
WN Variance (estimate)	0.001
-2Log(Like.)	
FPE	0.002
AIC	-1228.400
AICC	-1228.069
SBC	-1201.475

Model parameters:

Parameter	Value	Hessian standard error	Lower bound (95%)	Upper bound (95%)	Asympt. standard error	Lower bound (95%)	Upper bound (95%)
Constant	0.000	0.000	0.000	0.000	0.000	0.000	0.000

Parameter	Value	Hessian standard error	Lower bound (95%)	Upper bound (95%)	Asympt. standard error	Lower bound (95%)	Upper bound (95%)
AR(1)	-0.895	0.040	-0.974	-0.816			
AR(2)	-0.450	0.034	-0.517	-0.383			
SAR(1)	0.887	0.044	0.799	0.974			
SAR(2)	0.836	0.040	0.758	0.914			
MA(1)	0.847	0.016	0.816	0.878			
SMA(1)	-0.318	0.047	-0.411	-0.225			



APPENDIX J 5: Result of Potiskum Temperature SARIMA Model $(211)x(211)_{12}$

XLSTAT 2013.1.01 - ARIMA - on 3/29/2013 at 8:28:57 PM
Time series: Workbook = ARIMA 4.xlsm / Sheet = Temp / Range = Temp!$Q$1:$Q$361 / 360 rows and 1 column
Confidence intervals (%): 95
Center: No
Model parameters: p = 2 / d = 1 / q = 1 / P = 2 / D = 1 / Q = 1 / s = 12
Optimize: Likelihood (Convergence = 0.00001 / Iterations = 500)
Validation: 12
Prediction: 3
Confidence intervals (%): 95
Seed (random numbers): 418075375
Summary statistics:

Variable	Observations	Obs. with missing data	Obs. without missing data	Minimum	Maximum	Mean	Std. deviation
Log Potiskum Station Monthly Mean Temp.)	360	0	360	2.438	3.525	3.287	0.153

Results of ARIMA modeling of the Log Potiskum Station Monthly Mean Temp.) series:

Results after optimization (Log Potiskum Station Monthly Mean Temp.)):

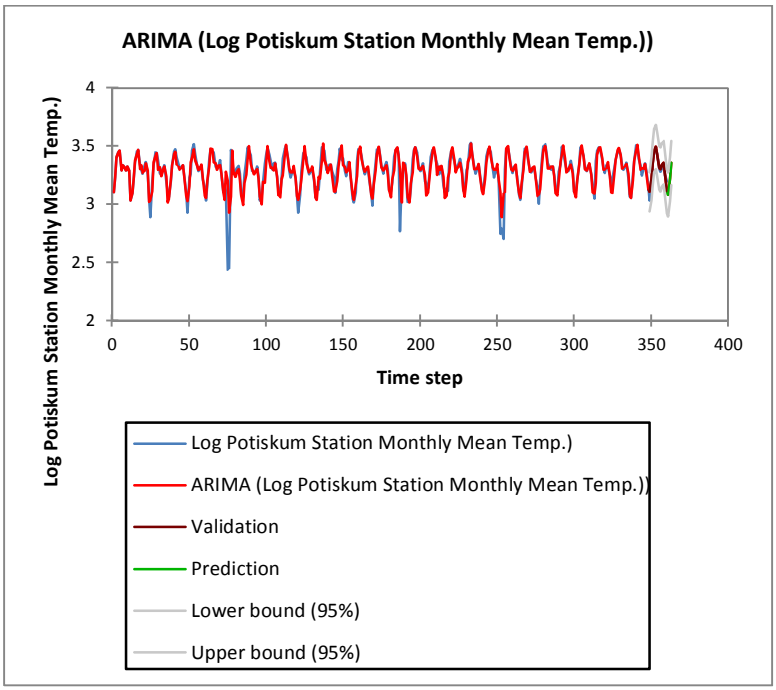
Goodness of fit statistics:

Observations	348.000
SSE	2.449
MAPE(Diff)	745.662
MAPE	1.408
WN Variance	0.007
WN Variance (estimate)	0.007
-2Log(Like.)	-647.111
FPE	0.009
AIC	-633.111
AICC	-632.769
SBC	-606.412

Model parameters:

Parameter	Value	Hessian standard error	Lower bound (95%)	Upper bound (95%)	Asympt. standard error	Lower bound (95%)	Upper bound (95%)
Constant	0.000	0.000	0.000	0.000	0.000	0.000	0.000

Parameter	Value	Hessian standard error	Lower bound (95%)	Upper bound (95%)	Asympt. standard error	Lower bound (95%)	Upper bound (95%)
AR(1)	0.503	0.048	0.408	0.598			
AR(2)	-0.126	0.061	-0.245	-0.006			
SAR(1)	-0.031	0.043	-0.116	0.053			
SAR(2)	0.034	0.050	-0.064	0.131			
MA(1)	-1.000	0.017	-1.034	-0.966			
SMA(1)	-1.000	0.094	-1.184	-0.816			



APPENDIX J 6: Result of Maiduguri Temperature SARIMA Model $(311)x(311)_{12}$

XLSTAT 2013.1.01 - ARIMA - on 3/29/2013 at 10:56:28 PM
Time series: Workbook = ARIMA 4.xlsm / Sheet = Temp / Range = Temp!$R$1:$R$361 / 360 rows and 1 column
Confidence intervals (%): 95
Center: No
Model parameters: p = 3 / d = 1 / q = 1 / P = 3 / D = 1 / Q = 1 / s = 12
Optimize: Likelihood (Convergence = 0.00001 / Iterations = 500)
Validation: 12
Prediction: 3
Confidence intervals (%): 95
Seed (random numbers): 460617218

Summary statistics:

Variable	Observations	Obs. with missing data	Obs. without missing data	Minimum	Maximum	Mean	Std. deviation
Log Maiduguri Station Monthly Mean Temp.)	360	0	360	2.634	3.552	3.315	0.138

Results of ARIMA modeling of the Log Maiduguri Station Monthly Mean Temp.) series:
Results of search for the best model:

p	q	P	Q	AICC
3	1	3	1	-817.140

The best model for the selected selection criterion is displayed in blue

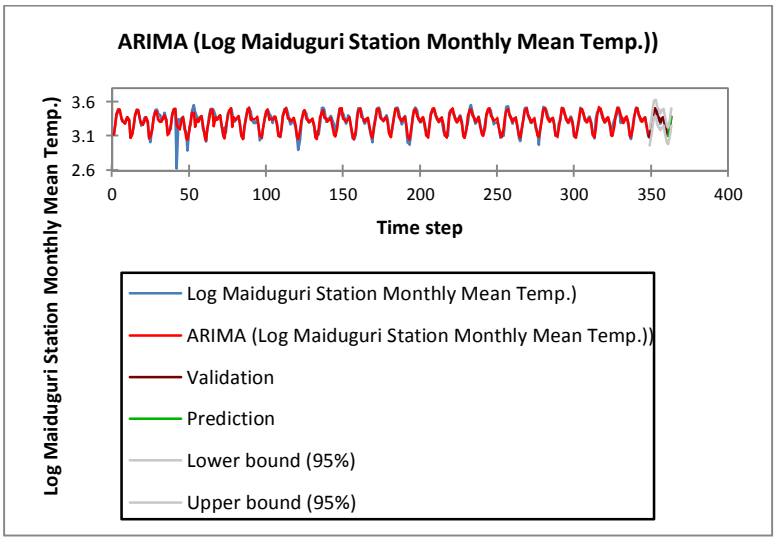
Results after optimization (Log Maiduguri Station Monthly Mean Temp.)):
Goodness of fit statistics:

Observations	348.000
SSE	1.268
MAPE(Diff)	483.030
MAPE	1.123
WN Variance	0.004
WN Variance (estimate)	0.004
-2Log(Like.)	-869.467
FPE	0.005
AIC	-851.467
AICC	-850.913
SBC	-817.140

Model parameters:

Parameter	Value	Hessian standard error	Lower bound (95%)	Upper bound (95%)	Asympt. standard error	Lower bound (95%)	Upper bound (95%)
Constant	0.000	0.000	0.000	0.000	0.000	0.000	0.000

Parameter	Value	Hessian standard error	Lower bound (95%)	Upper bound (95%)	Asympt. standard error	Lower bound (95%)	Upper bound (95%)
AR(1)	0.118	0.039	0.043	0.194			
AR(2)	0.119	0.031	0.058	0.181			
AR(3)	-0.010	0.042	-0.093	0.074			
SAR(1)	-0.029	0.040	-0.108	0.049			
SAR(2)	0.036	0.032	-0.027	0.098			
SAR(3)	0.091	0.040	0.012	0.169			
MA(1)	-1.000	0.013	-1.026	-0.974			
SMA(1)	-1.000	0.040	-1.079	-0.921			



APPENDIX J 7: Result of Kano Temperature SARIMA Model $(211)x(211)_{12}$

XLSTAT 2013.1.01 - ARIMA - on 3/29/2013 at 11:36:54 PM
Time series: Workbook = ARIMA 5.xlsm / Sheet = Temp / Range = Temp!$S$1:$S$361 / 360 rows and 1 column
Confidence intervals (%): 95
Center: No
Model parameters: p = 2 / d = 1 / q = 1 / P = 2 / D = 1 / Q = 1 / s = 12
Optimize: Likelihood (Convergence = 0.00001 / Iterations = 500)
Validation: 12
Prediction: 3
Confidence intervals (%): 95
Seed (random numbers): 4369856

Summary statistics

Summary statistics:

Variable	Observations	Obs. with missing data	Obs. without missing data	Minimum	Maximum	Mean	Std. deviation
Log Kano Station Monthly Mean Temp.)	360	0	360	2.859	3.501	3.281	0.128

Results of ARIMA modeling of the Log Kano Station Monthly Mean Temp.) series:

Results after optimization (Log Kano Station Monthly Mean Temp.)):

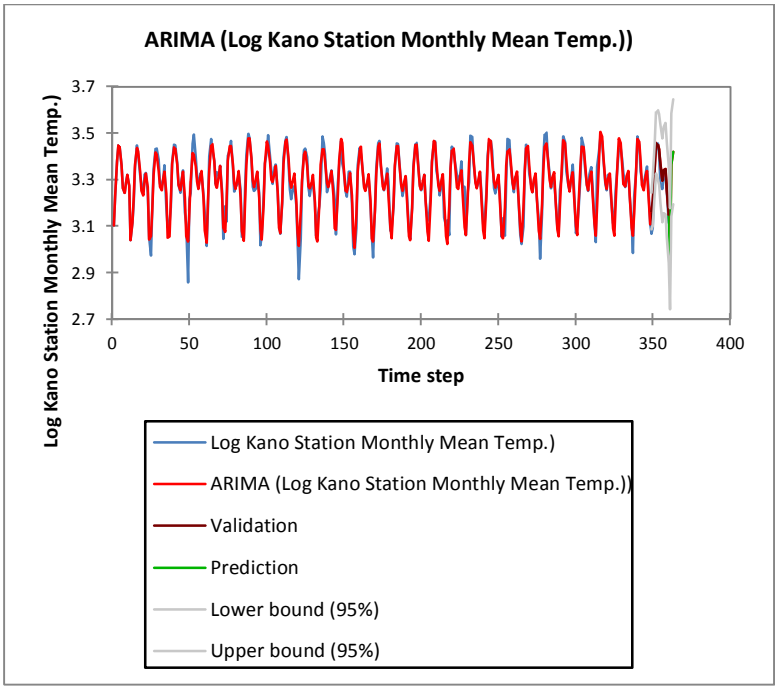
Goodness of fit statistics:

Observations	348.000
SSE	0.000
MAPE(Diff)	159.405
MAPE	0.838
WN Variance	0.000
WN Variance (estimate)	0.002
-2Log(Like.)	
FPE	0.002
AIC	-1128.158
AICC	-1127.479
SBC	-1090.017

Model parameters:

Parameter	Value	Hessian standard error	Lower bound (95%)	Upper bound (95%)	Asympt. standard error	Lower bound (95%)	Upper bound (95%)
Constant	0.000	0.000	0.000	0.000	0.000	0.000	0.000

Parameter	Value	Hessian standard error	Lower bound (95%)	Upper bound (95%)	Asympt. standard error	Lower bound (95%)	Upper bound (95%)
AR(1)	-0.788	0.048	-0.883	-0.693	0.057	-0.899	-0.676
AR(2)	-0.704	0.045	-0.792	-0.615	0.055	-0.812	-0.596
SAR(1)	-0.833	0.047	-0.926	-0.740	0.056	-0.943	-0.723
SAR(2)	0.174	0.050	0.076	0.272	0.057	0.063	0.285
MA(1)	0.695	0.025	0.645	0.745	0.013	0.669	0.721
SMA(1)	-0.342	0.104	-0.546	-0.139	0.001	-0.344	-0.340



APPENDIX J 8: Result of Gusau Temperature SARIMA Model $(211)x(211)_{12}$

XLSTAT 2013.1.01 - ARIMA - on 3/30/2013 at 2:12:28 PM
Time series: Workbook = ARIMA 5.xlsm / Sheet = Temp / Range = Temp!$T$1:$T$361 / 360 rows and 1 c
Confidence intervals (%): 95
Center: No
Model parameters: p = 2 / d = 1 / q = 1 / P = 2 / D = 1 / Q = 1 / s = 12
Optimize: Likelihood (Convergence = 0.00001 / Iterations = 500)
Validation: 12
Prediction: 3
Confidence intervals (%): 95
Seed (random numbers): 1229441156
Summary statistics:

Variable	Observations	Obs. with missing data	Obs. without missing data	Minimum	Maximum	Mean	Std. deviation
Log Gusau Station Monthly Mean Temp.)	360	0	360	2.907	3.495	3.280	0.105

Results of ARIMA modeling of the Log Gusau Station Monthly Mean Temp.) series:

Results after optimization (Log Gusau Station Monthly Mean Temp.)):

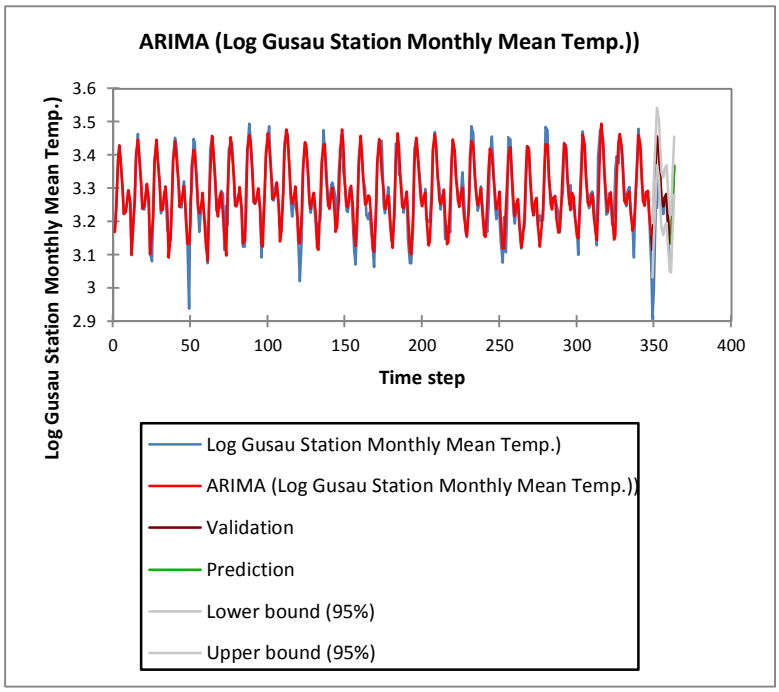
Goodness of fit statistics:

Observations	348.000
SSE	0.587
MAPE(Diff)	111.177
MAPE	0.858
WN Variance	0.002
WN Variance (estimate)	0.002
-2Log(Like.)	-1130.642
FPE	0.002
AIC	-1116.642
AICC	-1116.299
SBC	-1089.943

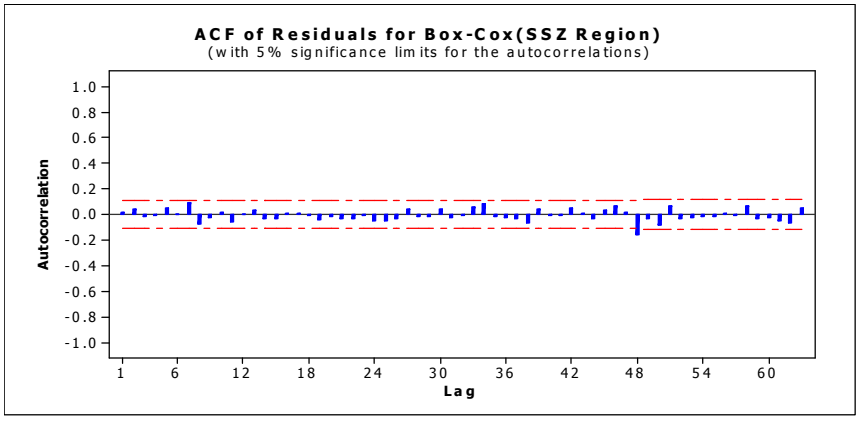
Model parameters:

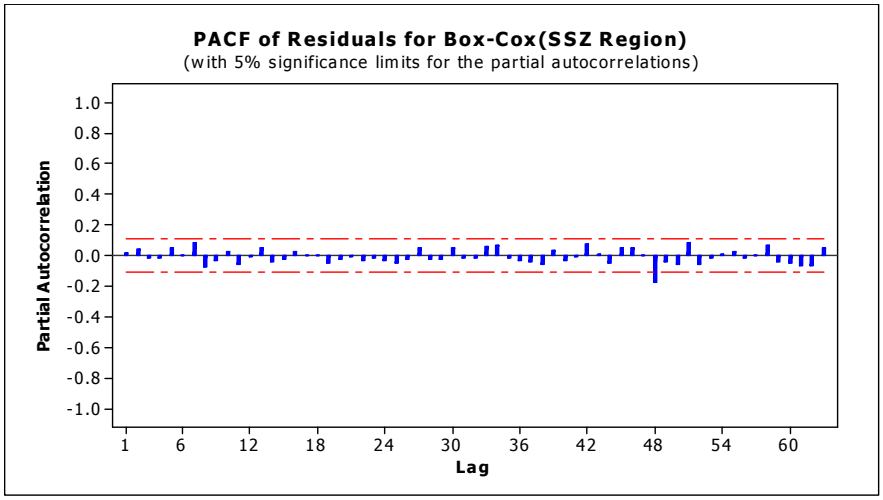
Parameter	Value	Hessian standard error	Lower bound (95%)	Upper bound (95%)	Asympt. standard error	Lower bound (95%)	Upper bound (95%)
Constant	0.000	0.000	0.000	0.000	0.000	0.000	0.000

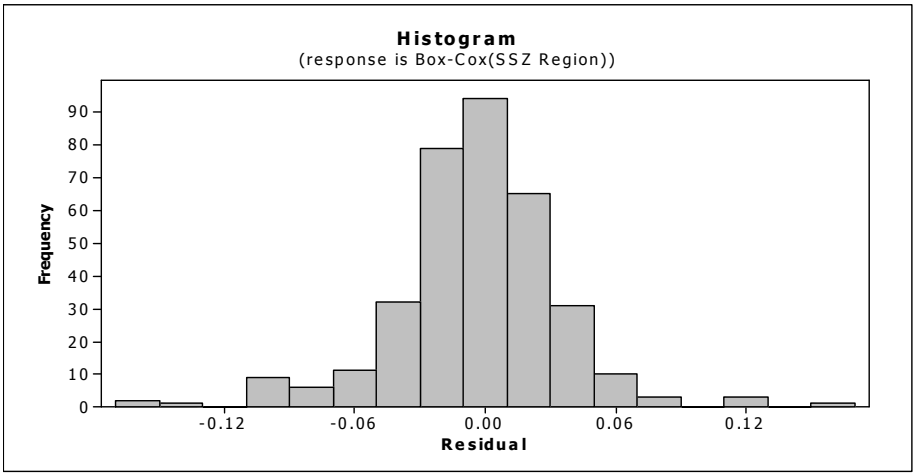
Parameter	Value	Hessian standard error	Lower bound (95%)	Upper bound (95%)	Asympt. standard error	Lower bound (95%)	Upper bound (95%)
AR(1)	0.292	0.061	0.173	0.411	0.043	0.209	0.375
AR(2)	0.054	0.072	-0.088	0.196	0.058	-0.060	0.168
SAR(1)	0.160	0.052	0.058	0.262	0.060	0.042	0.278
SAR(2)	0.027	0.085	-0.140	0.194	0.218	-0.399	0.453
MA(1)	-1.000	0.032	-1.064	-0.936	0.258	-1.505	-0.495
SMA(1)	-1.000	0.054	-1.107	-0.893	0.167	-1.326	-0.674

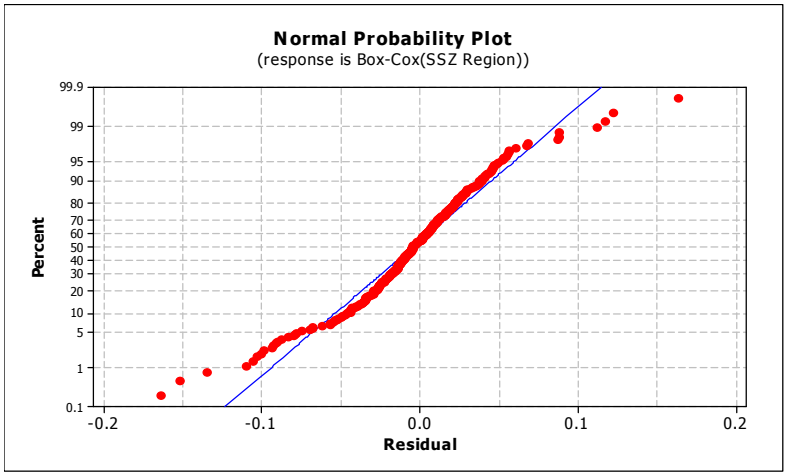


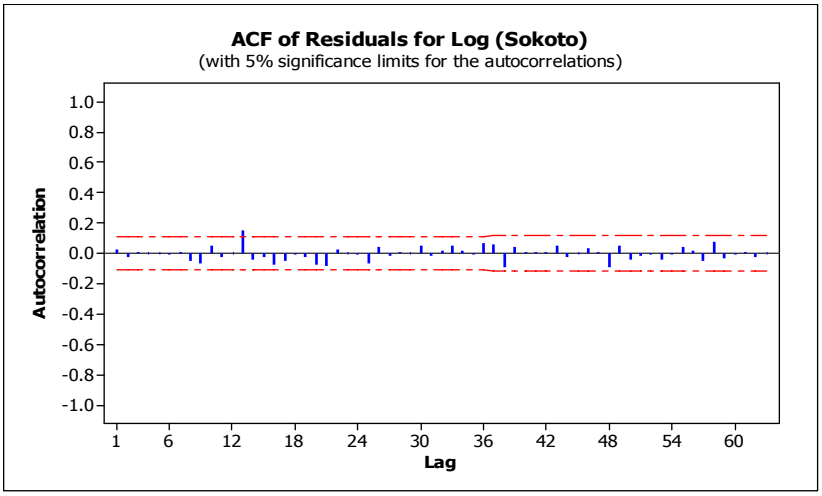
APPENDIX K: Temperature Model ACF & PACF of Residual Plots, Distribution Histogram And Normal Distribution Plots

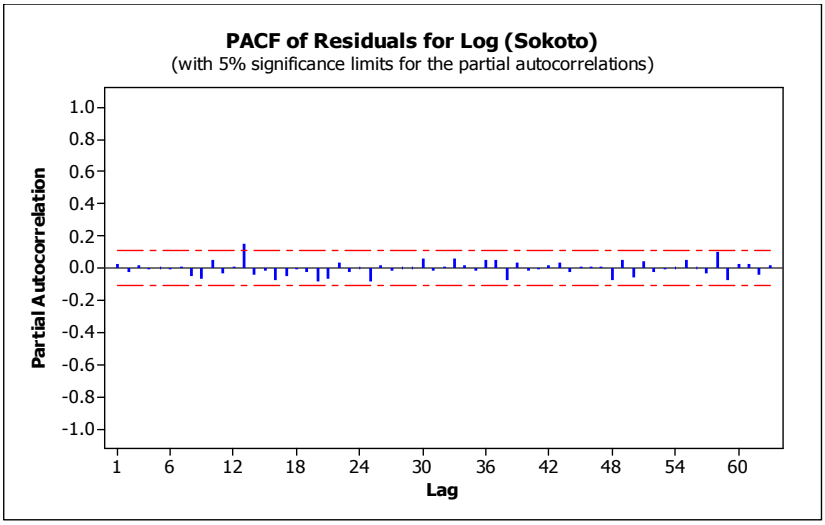


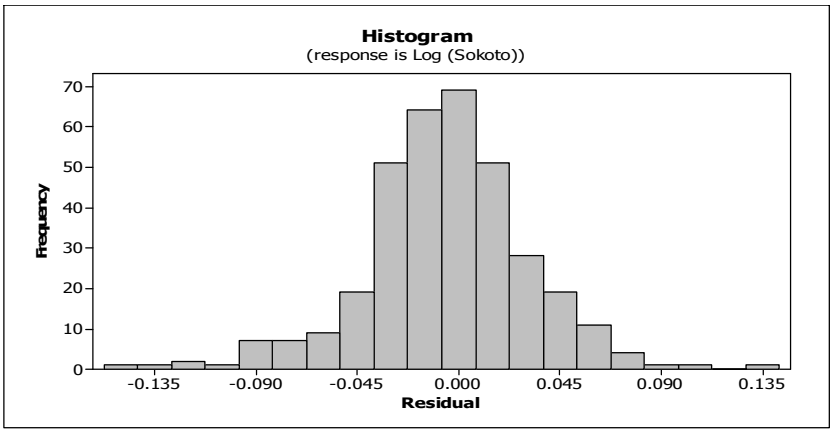


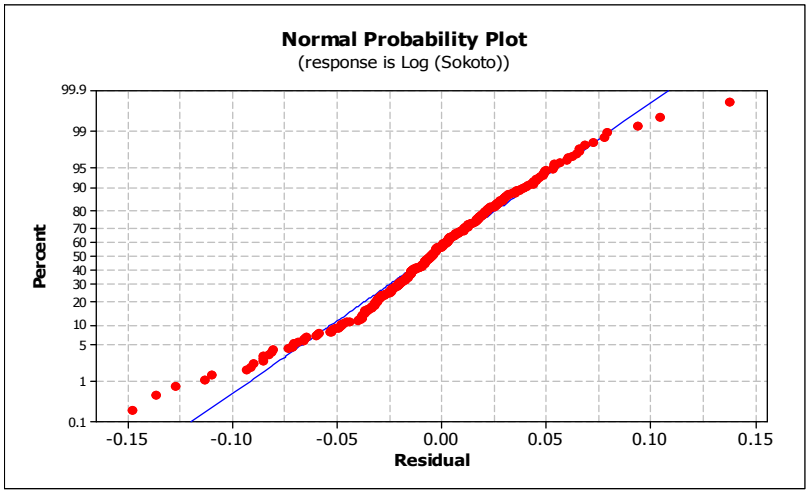


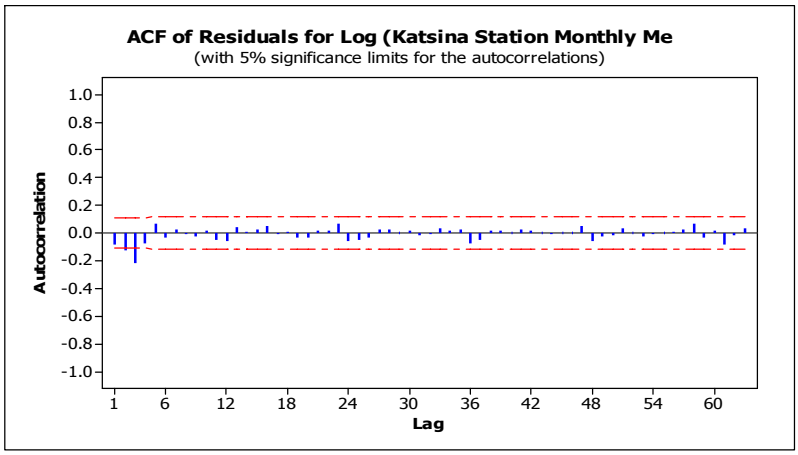

Normal Probability Plot
(response is Box-Cox(SSZ Region))
Percent
99.9
99
95
90
80
70
60
50
40
30
20
10
5
1
0.1
-0.2
-0.1
0.0
0.1
0.2
Residual

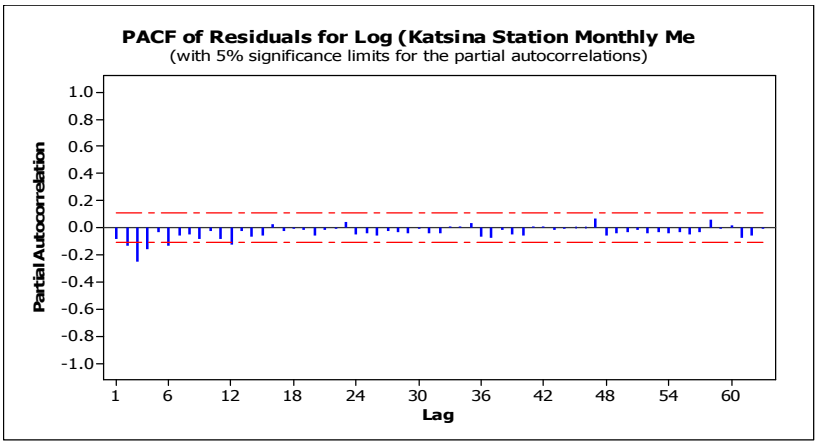

ACF of Residuals for Log (Sokoto)
(with 5% significance limits for the autocorrelations)
Autocorrelation
1.0
0.8
0.6
0.4
0.2
0.0
-0.2
-0.4
-0.6
-0.8
-1.0
1
6
12
18
24
30
36
42
48
54
60
Lag

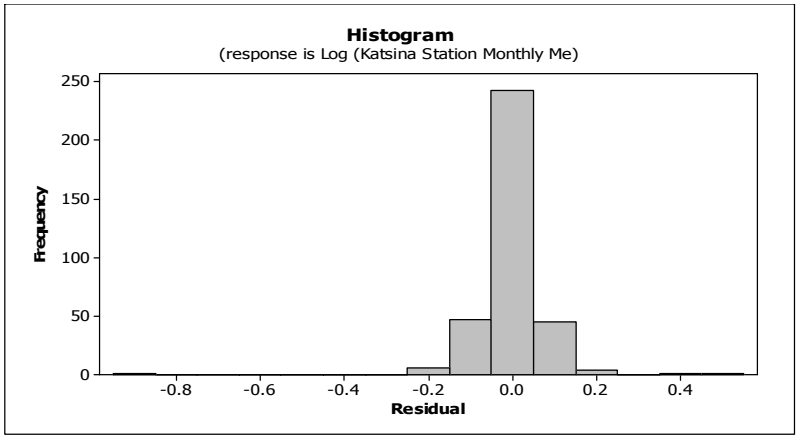

PACF of Residuals for Log (Sokoto)
(with 5% significance limits for the partial autocorrelations)
Partial Autocorrelation
1.0
0.8
0.6
0.4
0.2
0.0
-0.2
-0.4
-0.6
-0.8
-1.0
1
6
12
18
24
30
36
42
48
54
60
Lag

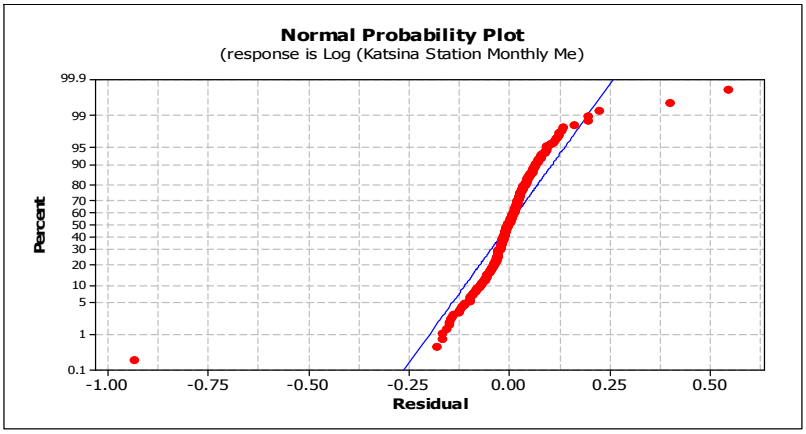

Histogram
(response is Log (Sokoto))
Frequency
Residual
70
60
50
40
30
20
10
0
-0.135
-0.090
-0.045
0.000
0.045
0.090
0.135


Normal Probability Plot
(response is Log (Sokoto))
Percent
Residual
99.9
99
95
90
80
70
60
50
40
30
20
10
5
1
0.1
-0.15
-0.10
-0.05
0.00
0.05
0.10
0.15

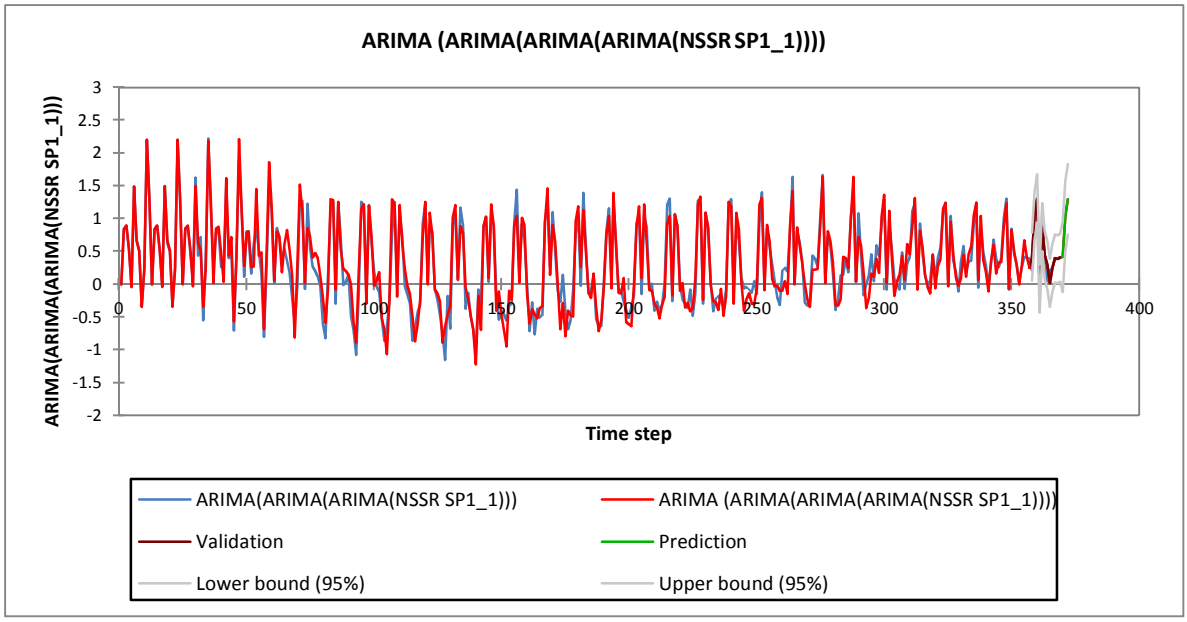

ACF of Residuals for Log (Katsina Station Monthly Me
(with 5% significance limits for the autocorrelations)
Autocorrelation
Lag
1.0
0.8
0.6
0.4
0.2
0.0
-0.2
-0.4
-0.6
-0.8
-1.0
1
6
12
18
24
30
36
42
48
54
60


PACF of Residuals for Log (Katsina Station Monthly Me
(with 5% significance limits for the partial autocorrelations)
Partial Autocorrelation
1.0
0.8
0.6
0.4
0.2
0.0
-0.2
-0.4
-0.6
-0.8
-1.0
1
6
12
18
24
30
36
42
48
54
60
Lag

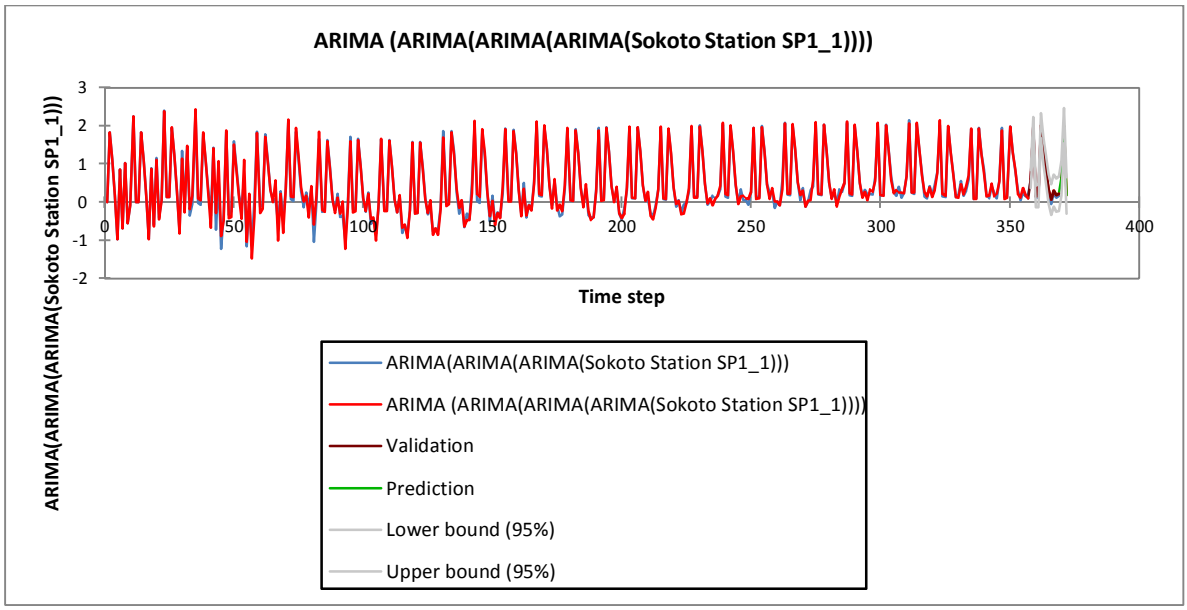

Histogram
(response is Log (Katsina Station Monthly Me)
Frequency
250
200
150
100
50
0
-0.8
-0.6
-0.4
-0.2
0.0
0.2
0.4
Residual


Normal Probability Plot
(response is Log (Katsina Station Monthly Me)
Percent
99.9
99
95
90
80
70
60
50
40
30
20
10
5
1
0.1
-1.00
-0.75
-0.50
-0.25
0.00
0.25
0.50
Residual

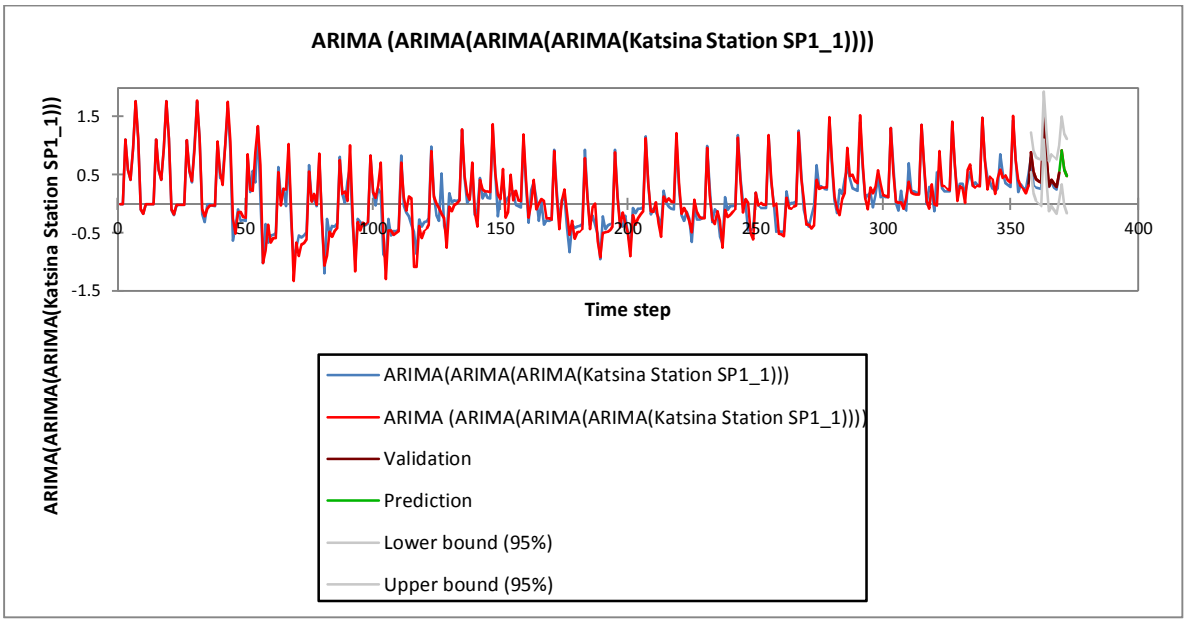
APPENDIX L: SPI Forecasts using Selected SPI_1Models



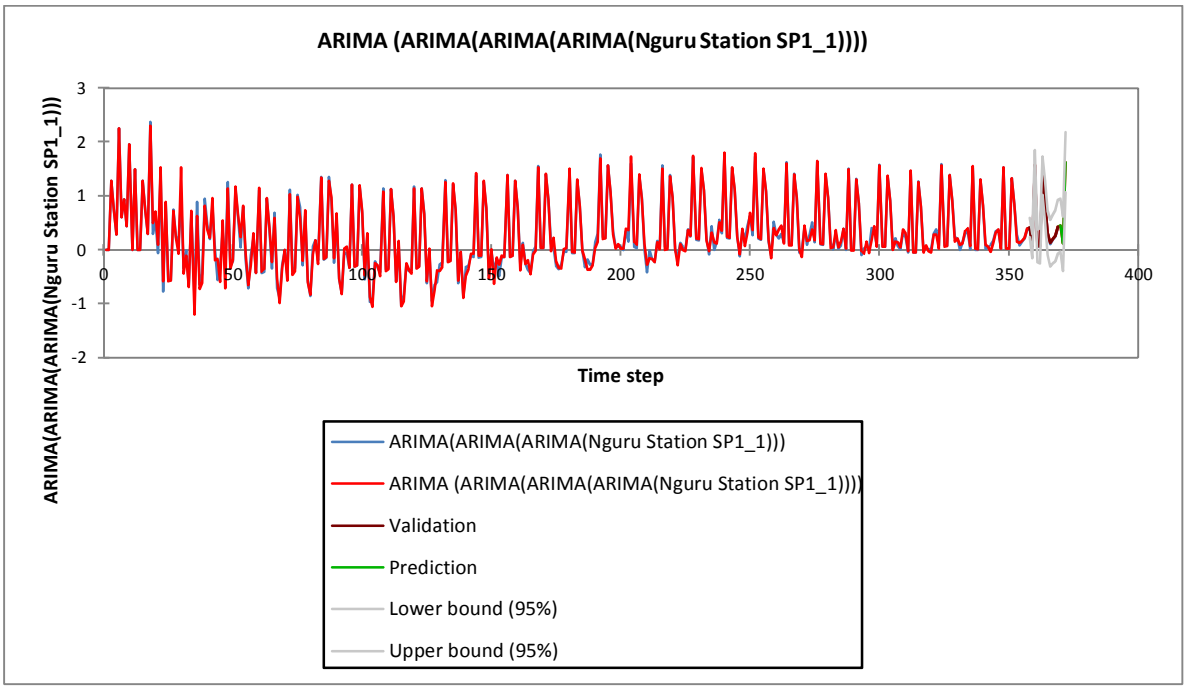
a: Comparison of computed NSSR SPI_1 with forecasted SPI_1 using SARIAM $(2,0,2)x(2,1,2)_{12}$



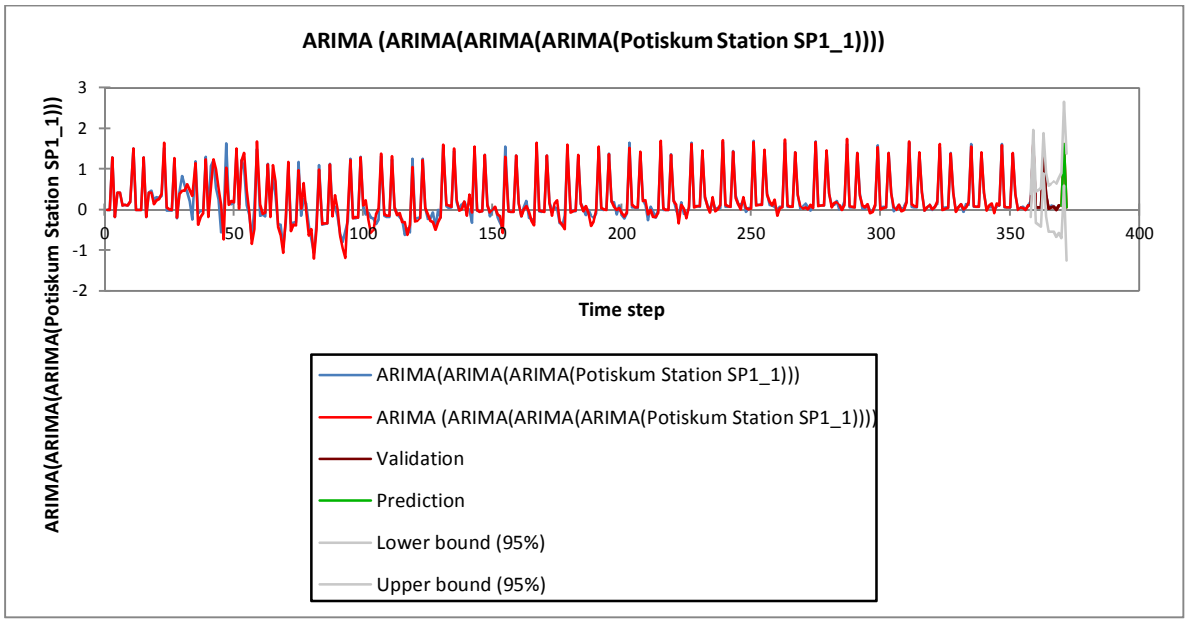
b: Comparison of computed Sokoto Station SPI_1 with forecasted SPI_1 using SARIMA $(0,1,1)x(0,1,1)_{12}$



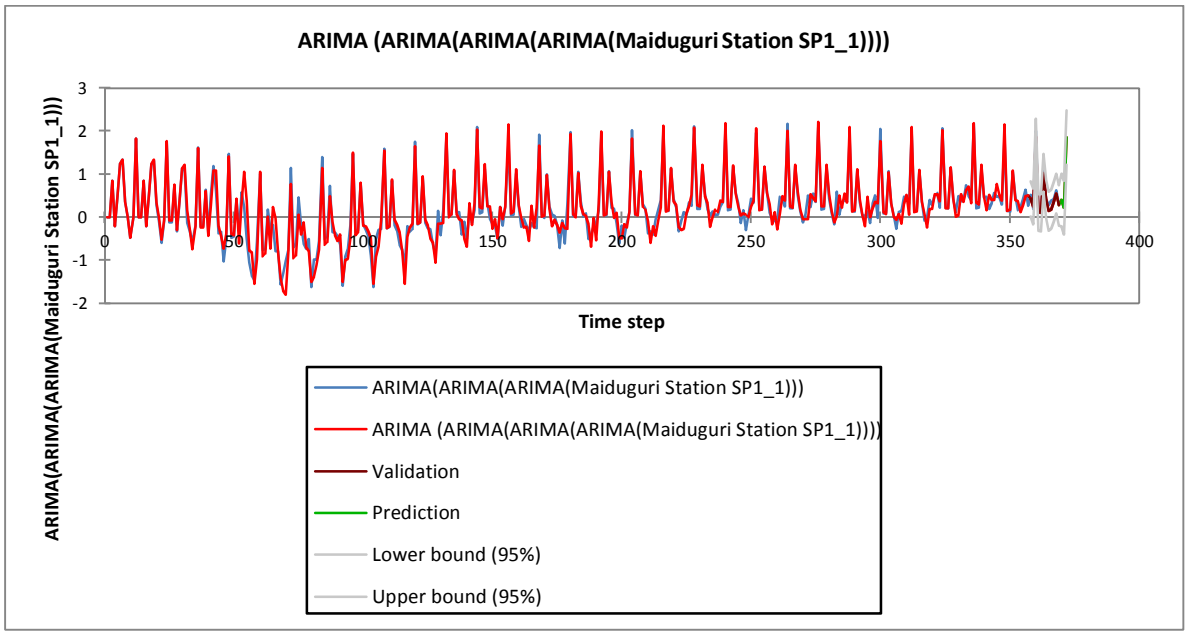
c: Comparison of computed Katsina Station SPI_1 with forecasted SPI_1 using SARIMA $(1,1,1)x(1,1,1)_{12}$



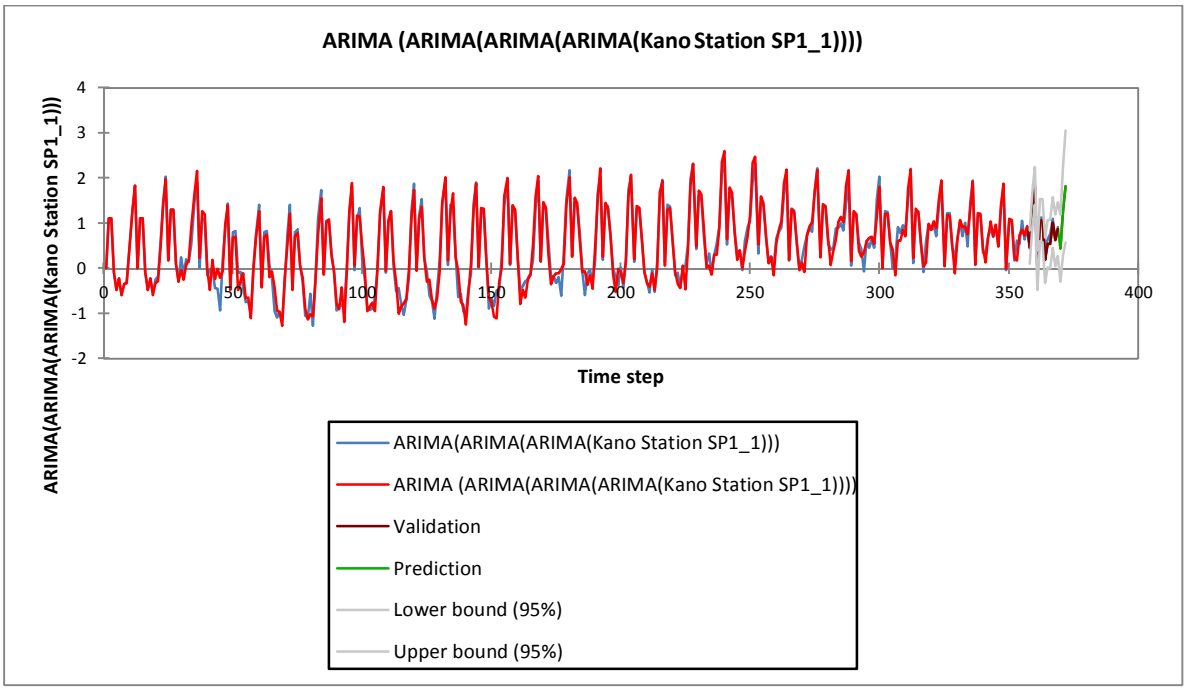
d: Comparison of computed Nguru Station SPI_1 with forecasted SPI_1 using SARIMA $(0,1,1)x(0,1,1)_{12}$



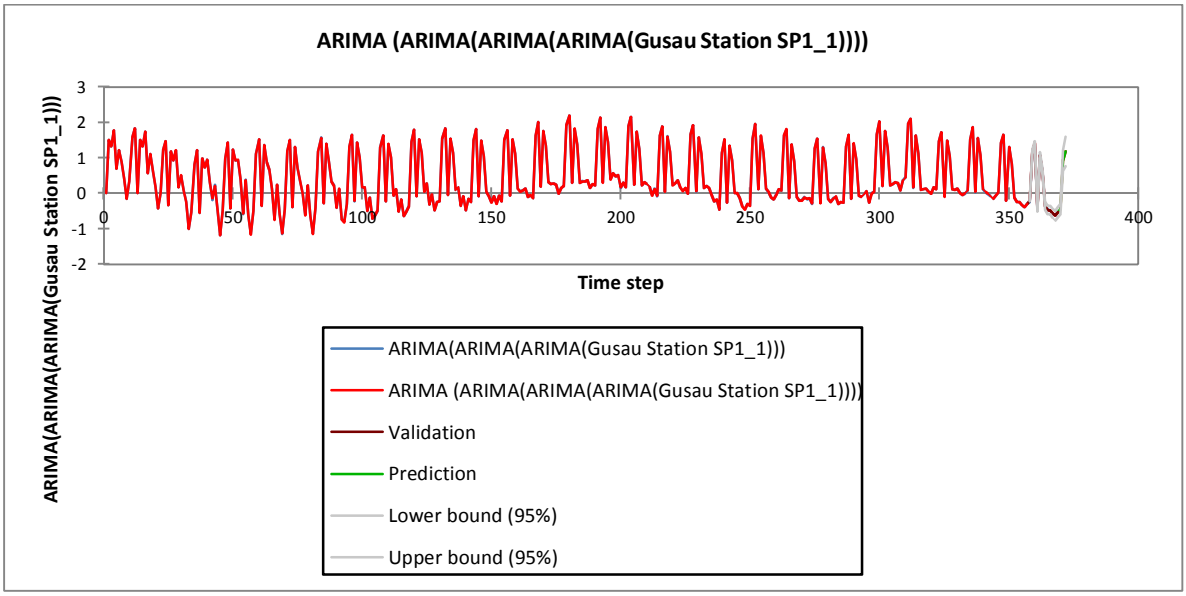
e. Comparison of computed Potiskum Station SPI_1 with forecasted SPI_1 using SARIMA $(0,1,1)x(0,1,1)_{12}$



f. Comparison of computed Maiduguri Station SPI_1 with forecasted SPI_1 using SARIMA $(1,1,1)x(1,1,1)_{12}$

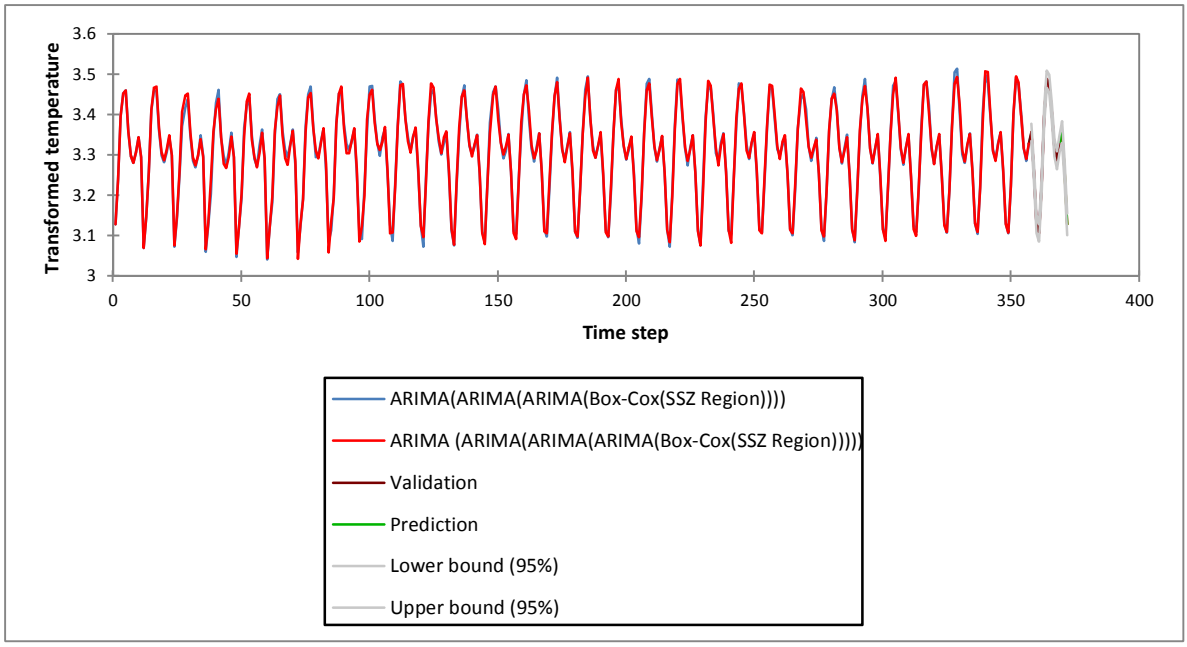


g. Comparison of computed Kano Station SPI_1 with forecasted SPI_1 using SARIMA $(0,1,1)x(0,1,1)_{12}$

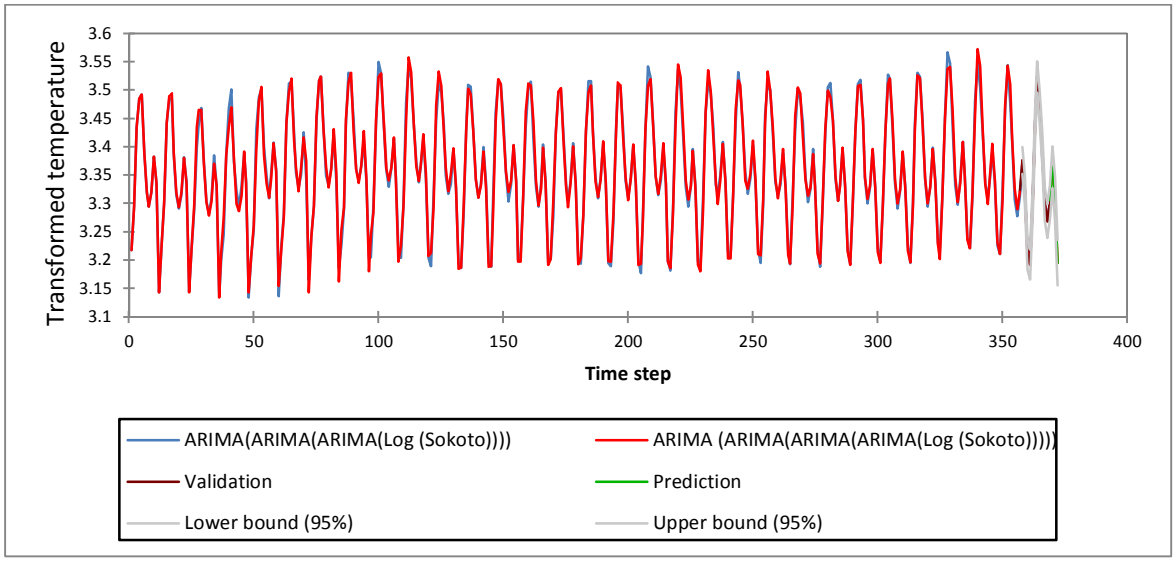


h. Comparison of computed Gusau Station SPI_1 with forecasted SPI_1 using SARIMA $(0,1,1)x(0,1,1)_{12}$

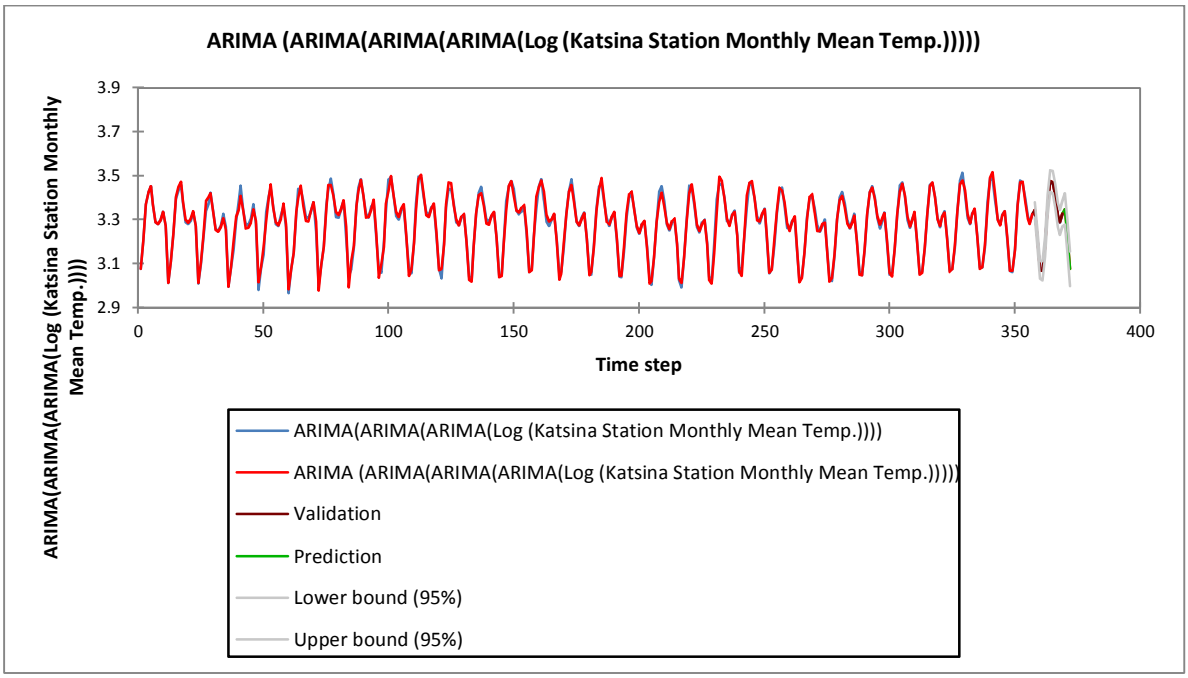
APPENDIX M: Temperature Forecasts using Selected Temperature Models



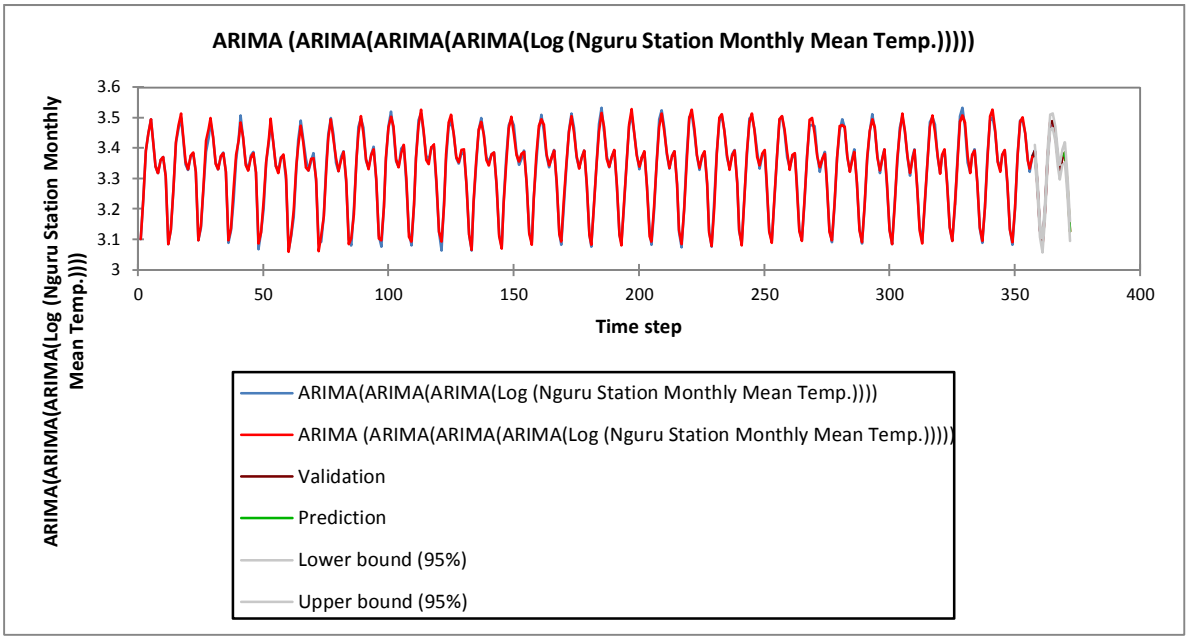
a: Comparison of NSSR Observed and predicted Transformed Temperature using SARIMA $(2,1,1)x(2,1,1)_{12}$



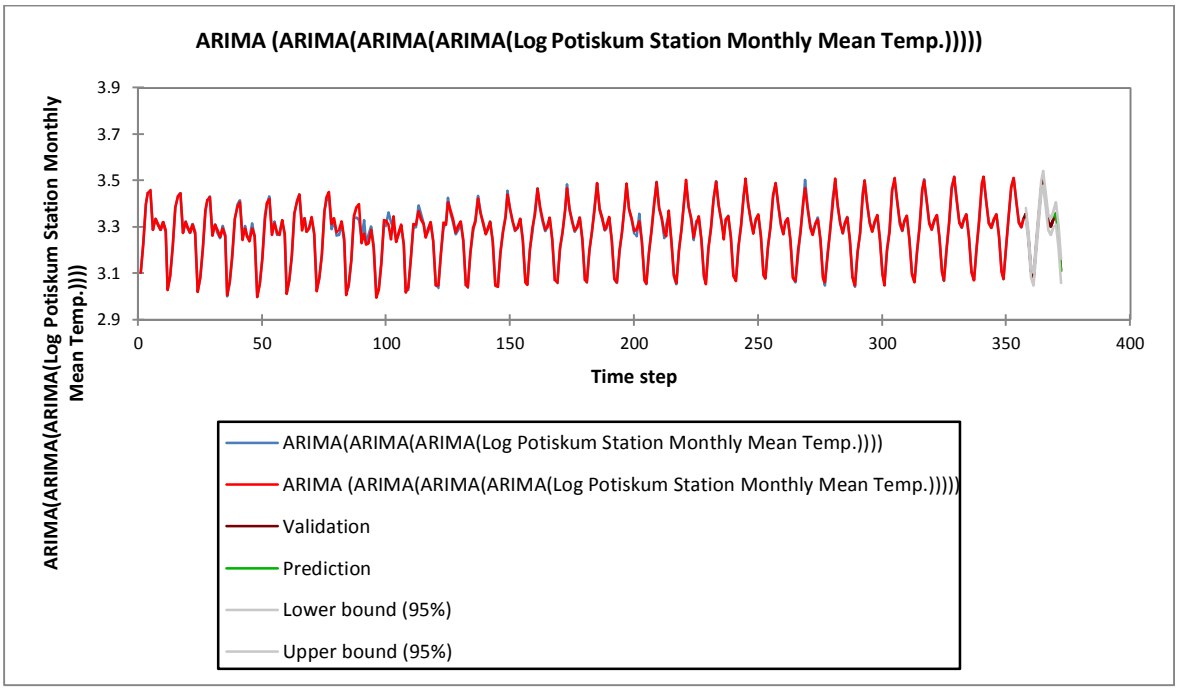
b: Comparison of Sokoto Station Observed and predicted Transformed Temperature using SARIMA $(2,1,1)x(2,1,1)_{12}$



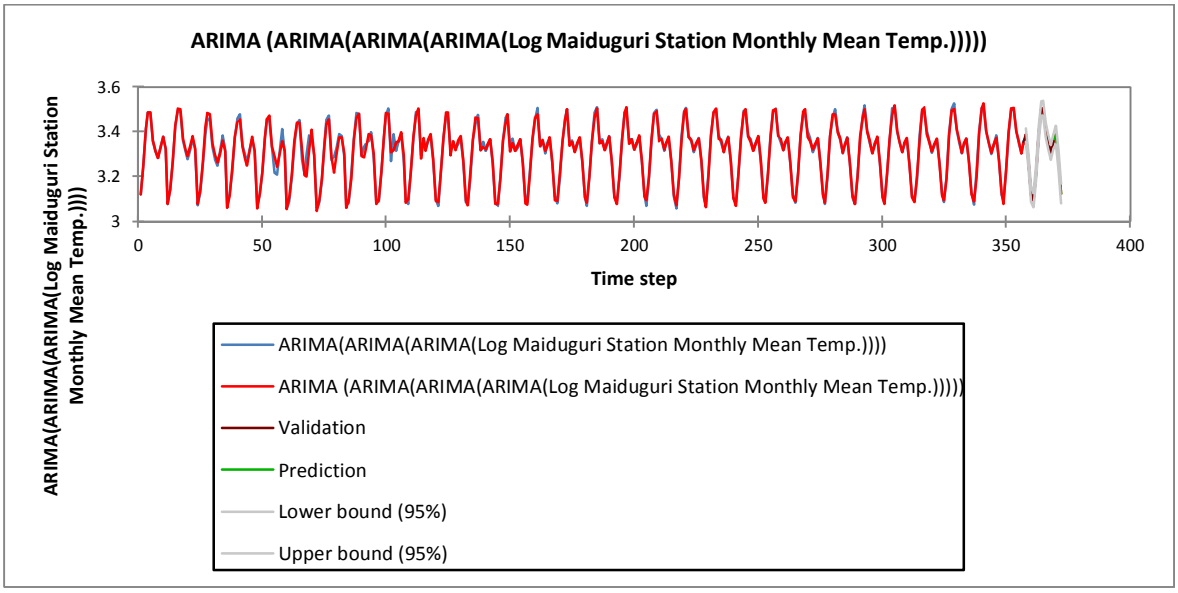
c: Comparison of Katsina Station Observed and predicted Transformed Temperature using SARIMA $(3,1,1)x(3,1,1)_{12}$



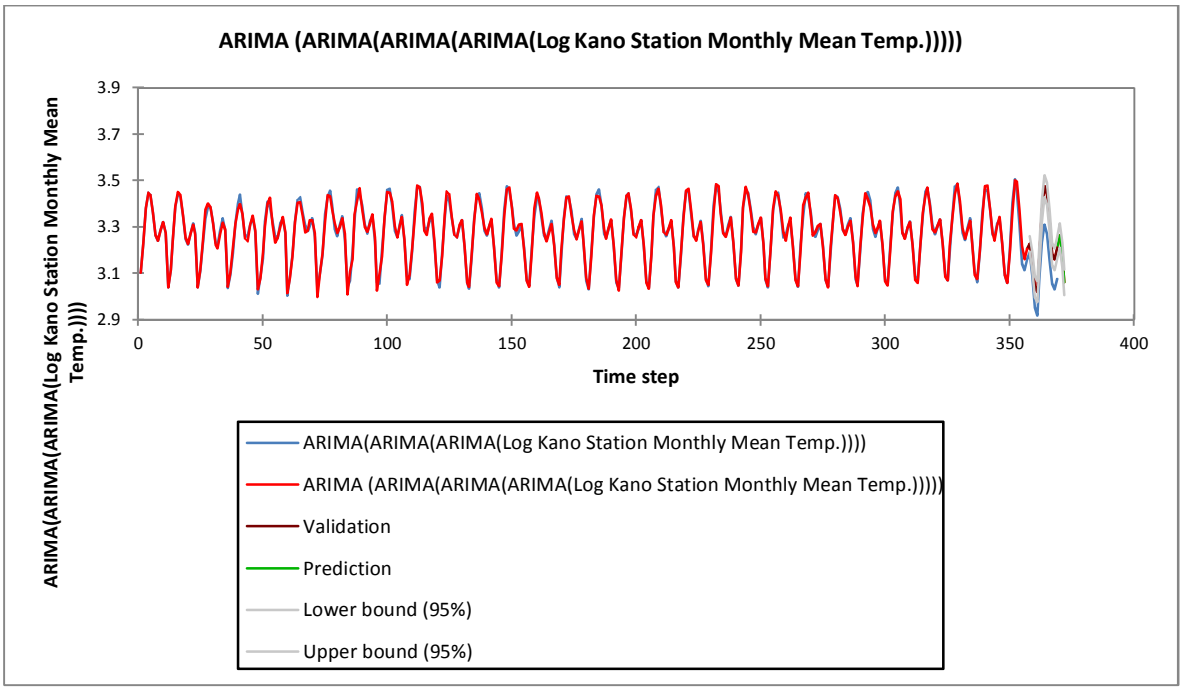
d: Comparison of Nguru Station Observed and predicted Transformed Temperature using SARIMA $(2,1,1)x(2,1,1)_{12}$



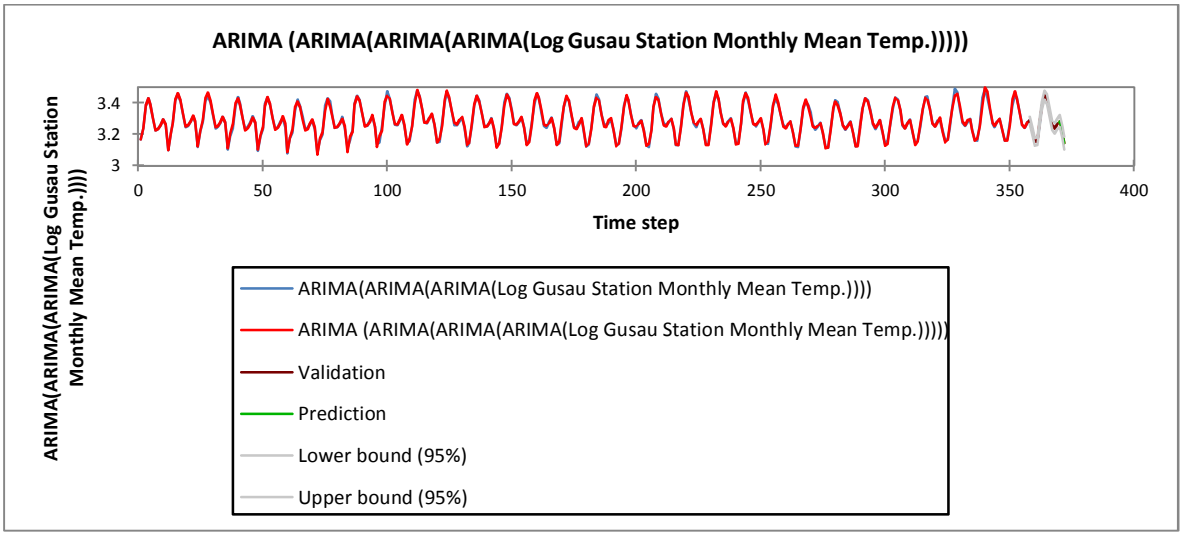
e: Comparison of Potiskum Station Observed and predicted Transformed Temperature using SARIMA $(2,1,1)x(2,1,1)_{12}$



f: Comparison of Maiduguri Observed and predicted Transformed Temperature using SARIMA $(3,1,1)x(3,1,1)_{12}$



g: Comparison of Kano Station Observed and predicted Transformed Temperature using SARIMA $(2,1,1)x(2,1,1)_{12}$



h: Comparison of Gusau Station Observed and predicted Transformed Temperature using SARIMA $(2,1,1)x(2,1,1)_{12}$